THEORETICAL ANALYSIS OF GAS EXCHANGE IN A LUNG MODEL

A Thesis submitted to

THE UNIVERSITY OF ASTON IN BIRMINGHAM

as Partial Requirement

for the Degree of

DOCTOR OF PHILOSOPHY

by

DAVID ANTHONY SCRIMSHIRE, BSc (hons)

May, 1973

SUMMARY

A mathematical model, derived from physiological data, is presented to represent gas exchange in the lung during steady state and, for the first time, unsteady state conditions. The model is used to simulate functional defects that can occur in the diseased lung. From a review of available literature four types of defect are recognised, namely, regional inequalities of ventilation, regional inequalities of blood flow, series inequalities and direct pulmonary blood shunts. The effects of changing minute volume, cardiac output and inspired oxygen concentration upon overall gas exchange are studied for each defect when oxygen uptake and carbon dioxide output are held constant at normal values in the steady state. The unsteady state condition is examined during the uptake and elimination of four hypothetical inert gases having differing blood solubilities.

The model is used to assess how well certain pulmonary function tests discriminate between the various defects considered, and from information gained a new protocol for defining lung function is proposed.

Utilising a more elaborate version of the model, the influence of nitrous oxide induction and excretion upon overall gas exchange is evaluated. The effect of blood recirculation time, minute volume, cardiac output, lung volume and inspired N_2O concentration upon arterial P_{O_2} and P_{CO_2} are examined during the unsteady state. The change in FRC occasioned when inspired and expired volumes are kept constant, are discussed as an alternative to the general case in which FRC is held constant and expired volume varied. A comparison between the model prediction of expired gas tensions with values obtained from three normal subjects during N_2O induction is also included.

CONTENTS

DECLARATION

No part of the work described in this thesis has been submitted in support of an application for another degree or qualification of this or any other University or other institute of learning.

No part of the work described in this thesis has been done in collaboration with any other person.

David A. Scrimshaw

ACKNOWLEDGMENTS

The Author expresses his sincere thanks to Mr.R.A.Etheridge* and Dr. P.J.Tomlin+ for their guidance and supervision, and to Prof. R.H.Thornley* and Prof.J.S.Robinson+ for permitting this work to be carried out in their respective departments. I am especially indebted to Prof.J.S.Robinson for taking over as supervisor during Dr.P.J.Tomlin's sabatical leave of absence.

The United Birmingham Hospitals Endowment Fund is thanked for providing personal financial support.

Finally, I must thank my wife Jennie for her patience and understanding throughout the project, and also for carrying out the bulk of the paper work and for typing the final manuscript.

---

*Dept.of Production Engineering, University of Aston in Birmingham.

+Dept.of Anaesthetics, University of Birmingham.

LIST OF FIGURES

CHAPTER 1

INTRODUCTION

Since the actual transfer mechanisms for gaseous species from the environment to the peripheral tissues are too complex to be easily grasped, respiratory physiologists have approximated these processes by conceptual models which are amenable to analytical investigation. The first such quantitative formulation was that of Bohr (9) who visualized the lungs as having only two compartments; a dead space and an alveolar space. The so called Bohr equation which is derived from this concept describes the movement of the respiratory gases into and out of the lung model, thereby defining alveolar ventilation. Improvements to this analysis followed, mainly in the field of aviation medicine (11, 51, 110) culminating in the comprehensive description of gas phase transport by Fenn et al. (40), from which the well known alveolar gas equations and alveolar ventilation equations stem.

The inherent assumption present in all the foregoing analyses is that of homogeneous alveolar gas composition. That this is not so in the actual lungs was realised by both Haldane (50) and Krogh and Lindhard (67), and was shown experimentally by Sonne (103) and Roelsen (88) who serially sampled aliquots of gas during a forced expiration. The authors explained these differences in expired gas composition as resulting from regional inhomogeneities in alveolar gas composition. These studies were followed by Rawerda's detailed work (82), which gave support to the concept of regional inhomogeneity and suggested that such differences in alveolar gas composition must arise from mismatching of regional ventilation and blood flow. The problem was therefore to predict this gas composition in an alveolus for any given ventilation and blood flow combination.

In 1949 two essentially similar solutions were advanced by Riley

and Cournand (84) and Rahn (81). Both methods made the same general statements, namely that in any respiratory element the exchange ratio of the alveolar gas must be equal to that of the blood, coupled with the assumption that alveolar gas and end capillary blood are in equilibrium. The analyses differed only in the form of presentation; Riley and Cournand utilising a four-quadrant diagram to contain the necessary characterisation of blood-gas exchange, whilst the Rahn procedure employed a blood nomogram for the same characterisation.

During the past 20 years, a number of improvements to these classical analyses have been proposed. The first introduced a correction which could be applied when an alveolus is inspiring gas through a dead space (89), and the second extends the original equations to allow for the inclusion of one or more soluble inert gases in the inspirate (38).

In addition, a variety of composite lung models have also been proposed in which the classical equations are applied to a number of functional units in which the mixed venous blood, as it returns from the body tissues, comes into equilibrium with air in the pulmonary alveoli. The composition of the mixed arterial blood in such models is calculated by summing the contributions from all of the units, each weighted by its perfusion. Similarly, the composition of the mixed alveolar gas is determined by weighting the contributions of each unit by the ventilation of that unit. In 1955 Farhi and Rahn (39) proposed such a model with, in effect, an infinite number of functional units. It was of course necessary to make an assumption as to the manner in which ventilation and blood flow were apportioned between the different units, and the authors utilised a frequency distribution which was log-normal in shape. At that time an exhaustive extrapolation of the model's characteristics was

virtually impossible due to the complexity of the calculations involved, hence it remained little more than a curiosity. With contemporary developments in digital computers and computing techniques, however, this drawback has been overcome and a number of authors have presented the results of investigations using similar models. Of these, probably the most notable is that of West (113), who quantified the effects of increasing the degree of derangement of ventilation or blood flow upon overall gas exchange by increasing the standard deviation of the assumed log-normal distribution whilst retaining constant the oxygen uptake and carbon dioxide output of the body.

Although the use of such models has considerably increased the understanding of pulmonary gas exchange, the Riley and Cournand equations (84) on which they are based are not without critisism. First, alveolar ventilation is not continuous, but cyclic. Second, the analysis assumes that there is no reservoir for gas within the lungs hence step changes in the inspired gas composition produce immediate changes in alveolar and arterial gas composition. The model is therefore limited to describing steady state conditions.

In order to overcome these critisisms, the present study replaces the classical model by one more closely based upon the actual form and function of the lungs as derived from physiological studies. By representing the bronchial tree as a number of well mixed compartments, and the continuous process of pulmonary gas exchange as an idealised sequence of gas volume movements, the derived analysis enables both steady state and, uniquely, unsteady state situations to be simulated. Specifically, the model will be used to investigate the effects of various lung defects upon overall gas exchange. On information gleaned from a survey of the literature, four separate types of defect will be considered,

namely, uneven regional inequalities of ventilation, uneven regional inequalities of blood flow, series inequalities and pulmonary blood shunts. Evidence will be presented to show that the use of the log-normal frequency distribution to describe regional inequalities in respiratory parameters is not supported by experimental observation, and as a result, new theoretical distributions will be introduced which enable independent regional distributions of ventilation or blood flow to be assessed. The discussion section is devoted to assessing how well various pulmonary function tests distinguish between lung defects. The tests are applied in turn to the model, which is used to simulate particular defects, and the closeness to which the test description accords with the actual simulated defect is taken as a measure of its effectiveness. From information gained in this study a new protocol for assessing pulmonary function is suggested. Finally, the uptake and elimination of nitrous oxide will be studied in a modified version of the model (95) which accounts for gas absorbtion by the lung parenchyma and the dynamic exchange of nitrogen and nitrous oxide at the body tissues.

CHAPTER 2

LUNG FORM AND FUNCTION

2.1 Pulmonary Structure

The lungs are composed of a branching system of airway tubes termed bronchi and bronchioles (Figure 1) and a spongy parenchyma consisting of the respiratory tissue in which gas exchange with the pulmonary capillaries takes place. The airways communicate with the environment via the nose or mouth which lead into the naso- and oro-pharynges, and then into the trachea. The latter bifurcates into the main bronchi which further divide into lobar bronchi that enter the five lobes. Each lobar bronchus continues to branch dichotomously for approximately twelve generations down to the terminal bronchioles (77). The terminal bronchioles further branch into three generations of respiratory bronchioles which lead into the alveolar ducts and sacs. Alveoli are laterally opposed to these elements; the surfaces of the alveolar ducts and sacs being completely alveolated, whereas those of the respiratory bronchioles only partially (Figure 2). The average geometric shape of an alveolus has been likened to an elliptic cone (108) with an average diameter of 200 μ. The total number of alveoli present in a healthy adult is of the order of 300×10^6 (107) which collectively provide for a total internal surface area of some 100 m^2 (114).

Each lung is enclosed in a serous sac, the pleura, one layer of which is closely adherent to the walls of the thorax and diaphragm (parietal); the other closely covers the lung (visceral). The pleura is a thin fibro-elastic membrane which forms two closed sacs, the right and the left, each invaginated by the lung. The two layers of the pleural sacs, moistened by serum, move easily upon one another with each respiration. The right lung is larger and broader than the left, due to the inclination of the heart to the left side; it is also shorter as a

result of the diaphragm's rising higher on the right side to accommodate the liver. It is divided by fissures into three lobes - superior, middle, and inferior. The left lung is smaller, narrower, and longer than the right. It is divided into two lobes - superior and inferior.

The mouth or nose, oro- or naso-pharynx, and trachea constitute the common pathway from environment to the commencement of the parallel lung divisions. Because of the relatively rigid properties of the bone which serves to support these structures this part of the airway system is relatively nondistendible during quiet breathing (104). From the trachea down to about the tenth generation of bronchi, the airways are lined with a mucous membrane and their walls consist of progressively decreasing amounts of smooth muscle and cartilage. The respiratory tissue in which all gas exchange occurs consists of respiratory bronchioles, alveolar ducts and sacs, alveoli and interalveolar septa. The septa between adjacent alveoli contain elastic fibres which support the thin walled respiratory bronchioles which would otherwise collapse during expiration (104), however, these elastic fibres are less rigid than the smooth muscle which supports the more proximal airways. The volumetric disposition of the various airways is shown diagramatically in Figure 3, and illustrates dramatically the preferential distribution of volume to the respiratory portion of the lungs.

The main source of blood for the lungs is the pulmonary artery which conveys venous blood from the systemic circulation to the alveolar capillaries. The pulmonary artery divides into right and left main branches and these in turn subdivide. These branches accompany the bronchi and bronchioles, and end in a plexus of capillaries around the alveoli. These networks, in turn, drain into the pulmonary venules which lie in the periphery of the lobules. The venules unite to form

veins which join to form the main pulmonary veins.

2.2 Mechanism of Breathing

The respiratory movements of inspiration and expiration produce mixing between inspired air and residual gas in the respiratory region. During normal breathing, expansion of the lung is caused by the upward and outward movement of the ribs and the flattening of the diaphragm. The expansion of the thoracic cavity lowers the pressure at the pleural surface of the lung relative to that in the surrounding atmosphere. This causes air to enter the lungs and they expand. During expiration, the inspiratory muscles relax and the intrapleural pressure becomes less negative. The elastic recoil of the lung tissue then raises the pressure at the mouth and reverses the direction of gas flow. The ventilatory pattern is approximately periodic in spontaneous breathing.

2.3 Regional Inequalities of Ventilation and Blood Flow

Although attention has been centred on the regular features of lung structure it is incorrect to imply that the respiratory portion of the whole organ may be considered as one unit. Actually, the bronchial tree is not symmetrical and the distance from the trachea to alveolated respiratory bronchioles is known to vary throughout the lungs (57). As a result the proportion of fresh gas reaching various alveolar regions must differ. In addition, the pressure-volume curve for the upright lung is not linear, in that the base of the lung expands more than the apex. This arises because the weight of the lung is supported partly by the chest wall and diaphragm hence the intrapleural pressure is less negative at the basal regions than at the apex (114). Again the result is an unequal distribution of inspired ventilation.

A similar pattern for regional blood flow has also been found in the upright lung but in this case the difference between apex and base is

approximately three times that for ventilation. The cause for this regional distribution of perfusion has been fully reviewed by West (112), but briefly the weight of the column of blood in the upright lung increases the perfusing pressure, and therefore the blood flow, down the lung. Summarising, we may say that the regional ventilation and blood flow in normal subjects is by no means uniform, however, it has been demonstrated elsewhere (111) that this regional inequality has little effect upon the overall efficiency of gas transport. As will be seen in Chapter 3 this situation can be greatly exaggerated in abnormal lungs and can result in a gross impairment of gas transport.

2.4 Gaseous Transport Across the Alveolar-Capillary Membrane

The exclusive function of the pulmonary system is to remove carbon dioxide from, and add oxygen to venous blood returning from the body tissues. This transfer to and fro across the alveolar membrane is achieved by passive physical diffusion; the gases moving in the direction of a decreasing concentration gradient. When a unit of blood enters an alveolar capillary a very rapid movement of gas occurs between it and the gases in the alveolus. In the case of an inert gas*, which is passing into the blood, it has been shown that the tension in the blood rises to the level of the alveoli within 20 msec. and thereafter remains virtually unchanged (30). For gases which react chemically with haemoglobin a similar initial rise in the blood tension occurs; however, it does not instantaneously reach the alveoli level. Instead, within about 10 msec., a state of dynamic equilibrium is attained in which the rate of gas transport across the alveolar membrane is balanced by the rate at which it combines with the blood (43).

---

*In the present context, the word inert refers to the fact that the gas does not react chemically with blood, and is therefore present only in physical solution.

Even for such gases, however, the tension in the blood leaving the capillaries is probably within a fraction of 1 mm Hg. of that in the alveolar gas.

2.5 Gas Exchange for Carbon Dioxide

Carbon dioxide is formed in the body tissues and thence passes by diffusion into the blood in the tissue capillaries. A small amount remains in simple solution in the plasma where it slowly hydrates to form carbonic acid; this dissociates into bicarbonate ions and hydrogen ions which displace sodium from combination with phosphate and protein in the plasma ($CO_2 + H_2O \rightleftharpoons H_2CO_3$; $H_2CO_3 \rightleftharpoons H^+ + HCO_3^-$; $H^+ = HCO_3^- + NaPr \rightleftharpoons HPr + Na^+ + HCO_3^-$). The majority of the carbon dioxide, however, diffuses from plasma into the red blood cells (erythrocytes) where the enzyme carbonic anhydrase catalyzes the formation of carbonic acid ($H_2O + CO_2 \rightleftharpoons H_2CO_3$). This results in an increase in hydrogen ions and favours the decomposition of oxyhaemoglobin ($HHbO_2 \rightleftharpoons HHb + O_2$) and the escape of oxygen to tissue cells. In as much as reduced haemoglobin is a weaker acid than is oxyhaemoglobin, this reaction, decreases the hydrogen ion concentration within the erythrocyte. A further decrease results from the reaction of carbonic acid with the potassium salts of haemoglobin ($KHb + H_2CO_3 \rightleftharpoons HHb + KHCO_3$). During these reactions the concentration of bicarbonate ions (HCO_3^-) within the erythrocytes increases; consequently these ions diffuse from erythrocytes into the plasma thus building up the sodium bicarbonate concentration in plasma. In compensation for the influx of these anions, chloride ions (Cl^-) diffuse from plasma into the erythrocytes; this adjustment is known as the chloride shift. Part of the carbon dioxide which enters the erythrocytes combines directly with haemoglobin to form carbamino haemoglobin ($HbNH_2 + CO_2 \rightleftharpoons HbNHCOOH \rightleftharpoons HbHNHCOO^- + H^+$). This reaction

occurs to an increasing extent as the oxyhaemoglobin gives up its oxygen to the tissues. In the alveolar capillaries reverse changes take place. These are initiated by both the fall in carbon dioxide tension which alters the position of equilibrium between dissolved carbon dioxide and carbonic acid, and the rise in the tension of oxygen which increases the concentration of oxyhaemoglobin.

Figure 4 shows the dissociation curve for carbon dioxide, in which the content of carbon dioxide, (measured in ml/100ml blood) is plotted against the carbon dioxide tension (measured in mm Hg.) at chemical equilibrium. Clearly, reduced blood at any given carbon dioxide tension binds appreciably more carbon dioxide than does oxygenated blood. This shift in the dissociation curve is called the "Haldane effect" and is due to the fact that reduced haemoglobin is a weaker acid than oxyhaemoglobin, and can thus assimilate greater numbers of hydrogen ions.

2.6 Gas Exchange for Oxygen

Oxygen is carried in the blood in two forms. Much the greater proportion is in reversible chemical combination with haemoglobin contained in the erythrocytes, while a smaller part is in simple solution in the plasma.

The molecule of haemoglobin consists of four heme groups, designated Hb_4, each capable of combining with one molecule of oxygen. According to Adair's intermediate compound hypothesis (1), the reversible reaction of the haemoglobin molecule takes place in four stages, through three compounds varying in composition between Hb_4 (fully reduced) and $Hb_4\ O_8$ (fully oxygenated). These reactions may be presented as follows

$$Hb_4 + O_2 \rightleftharpoons Hb_4\ O_2 \qquad \text{Equilibrium constant } K_1$$

$Hb_4O_2 + O_2 \rightleftharpoons Hb_4O_4$ Equilibrium constant K_2

$Hb_4O_4 + O_2 \rightleftharpoons Hb_4O_6$ Equilibrium constant K_3

$Hb_4O_6 + O_2 \rightleftharpoons Hb_4O_8$ Equilibrium constant K_4

By suitable manipulation of the above expressions, Roughton (90) has derived the following equation defining the per cent. saturation (oxygenation) of haemoglobin, y, in terms of the oxygen tension, P, and the equilibrium constants K_1, K_2, K_3, and K_4, viz.,

$$\frac{y}{100} = \frac{K_1P + 2K_1K_2P^2 + 3K_1K_2K_3P^3 + 4K_1K_2K_3K_4P^4}{4(1 + K_1P + K_1K_2P^2 + K_1K_2K_3P^3 + K_1K_2K_3K_4P^4)}$$

Clearly, the extent to which haemoglobin combines with oxygen depends upon the tension of oxygen in solution. When the tension is high, most or all of the haemoglobin is combined with oxygen; when the tension is low, little haemoglobin is combined with oxygen.

This relation between percentage saturation and oxygen tension is expressed in the oxygen dissociation curve, which is experimentally determined (Figure 5). The shape depends on the temperature and acidity of the blood, and there is variation between individuals. Increase of acidity, in particular, decreases the percentage saturation at a given oxygen tension; that is, decreases the affinity of the haemoglobin for oxygen. This tends to flatten the curve, an effect which results from interaction between the buffering groups within the haemoglobin molecule. Higher carbon dioxide tensions increase the acidity and hence have the same effect, as is shown by the family of curves at different carbon dioxide tensions (see insert in Figure 5). There is evidence (74) to support the contention that carbon dioxide has a specific effect on the oxygen dissociation curve due to its combination with haemoglobin to form carbamino compounds. Lastly, the

shape of the curve, as indicated by the size of the inflection at low oxygen tensions, may depend on the electrolyte composition of the blood.

2.7 Mathematical Descriptions of the Oxygen and Carbon Dioxide Dissociation Curves

Recently, Kelman has presented mathematical models to simulate both the carbon dioxide (61) and the oxygen (60) dissociation curves.

The carbon dioxide model first calculates the total carbon dioxide content of the plasma using the Henderson-Hasselbalch equation (52) and then converts this value into whole blood content by means of an experimentally determined ratio of total blood CO_2 content of erythrocytes to total CO_2 content of plasma (106). Temperature dependence is allowed for by means of the empirical relation of Austin et al. (4), and the effect of oxyhaemoglobin desaturation by adjustment of the CO_2 plasma to CO_2 erythrocytes ratio.

The oxygen dissociation curve model utilises a modification of the Roughton equation (page 11) for which values of the unknown coefficients (K_1, K_2, K_3 and K_4) are supplied by curve fitting by least-squares to the experimental data of Severinghaus (100). The shifts in the curve produced by changes in acidity, carbon dioxide tension, and temperature are simulated by adjusting the oxygen tension axis mathematically by the use of empirical factors (98).

Both models show excellent agreement with experimental observation and are incorporated unchanged in the analysis of gas exchange presented in this thesis.

CHAPTER 3

MODEL FORMULATION

The objective of this chapter is to describe a general physicomathematical model to represent pulmonary gas transport and exchange under a variety of steady-state and unsteady-state conditions. The system of equations thus derived will enable mean gas concentrations at different sites in the lungs to be predicted for each breathing cycle, and also determine overall gas exchange in terms of mean expired alveolar gas tensions and mean arterial blood composition.

3.1 Model Description

The airways and alveoli are represented in the model by a set of well-mixed compartments, with both series and parallel elements. A schematic diagram of the various compartments showing their spatial relationships is shown in Figure 6.

Three series elements have been included to reflect the morphometric division of the lungs into common upper airways, conducting airways and alveoli (94). The mathematical analysis describing the function of the model is formulated to ensure that some fresh gas reaches the alveolar regions so long as the tidal volume is greater than the volume of the upper airways compartment, thereby mimicking the actual behaviour of the lungs which have been shown to have alveolar ventilation at very low tidal volumes (12).

The parallel elements are included to represent the regional inhomogeneities in gas composition that must exist even in normal lungs as a result of variation in ventilation and blood flow to different alveolar populations.

Complete mixing of residual gas in the conducting airways with gas entering from the upper airways is assumed during inspiration. The

actual exchange of gases occurs between the variable volume alveolar compartments and the adjacent capillaries.

3.2 Assumptions and Simplifications

1.) Complete equilibrium is achieved between alveolar gas and end-capillary blood, and there is no membrane diffusion block. This supposition appears reasonable since there is no substantial evidence to indicate that any of the disease states considered in the present study cause significant changes in the diffusing capacity. It is felt that the observed decrease in D_{LCO} noted by some authors (3, 31, 78) in patients is primarily caused by the reduction in the effective functioning interface between ventilated alveoli and perfused capillaries, and not by any thickening of the pulmonary membrane, per se.

2.) Although the gas composition differs between model compartments, the composition within compartments is assumed to be homogeneous and mixing is instantaneous. This is obviously an inherent assumption of any analysis which attempts to represent the complex nature of gas transport in the bronchial tree by compartmental means. It has, however, been shown by Saidel et al. (92) that such an approach is a reasonable approximation to the continuous state, a fact borne out by more vigorous mathematical examination by Himmelblau and Bischoff (55).

3.) The composition of venous blood perfusing all alveolar regions is assumed to be constant. Although this seems well substantiated, the possibility of erythrocyte deformation and skimming within the small blood vessels must be borne in mind (14) as it is known to exist in other organs. If this occurs in the lungs, it would affect the oxygen and carbon dioxide contents of blood perfusing the alveolar capillaries as well as altering the shapes of the respective dissociation curves.

4.) The pre-inspiratory lung volume remains constant from breath to

breath. This assumption was necessary to define the volume expired from the alveolar compartments, and appears reasonable since the lungs return approximately to FRC after each breathing cycle during air breathing.

3.3 Derivation of Equations

All symbols used in deriving relationships will follow the Papperheimer nomenclature (79) with the following additions

V_D - volume of the common upper airway (as opposed to the total anatomical deadspace)

V_C - total volume of conducting airways

V_{AL} - total volume of the alveolar region

F_{CG} - fractional concentration for any gas G in the conducting airways

G - any gas species

Quantities suffixed with the symbol (i) will be taken as referring to the i^{th} compartment of the model, e.g. $V_{AL}(i)$ - volume of the i^{th} alveolar compartment. In addition, the suffix ' will be used to indicate a value resulting from the immediately preceding respiratory cycle, i.e. $F'_{AG}(i)$ - pre-inspiratory fractional concentration of gas G in the i^{th} alveolar compartment.

Considering any alveolar compartment during one respiratory cycle, the actual amount of gas species G exchanged with the capillary blood flow is given by

$$\Delta V_G = F_{IAG}(i)\, V_{IA}(i) + F'_{AG}(i)\, V_{AL}(i) - F_{AG}(i) \left\{ V_{AL}(i) + V_{EA}(i) \right\} \quad .. \; .. \; .. \; .. \; .. \; (1)$$

Where $F_{IAG}(i)$ is the fractional concentration of gas G being inspired into the i^{th} alveolar compartment,

$$F_{IAG}(i) = \frac{V_D \times \frac{V_{IA}(i)}{V_T} \times F'_{DG} + \left\{ V_T(i) - V_D \cdot \frac{V_{IA}(i)}{V_T} \right\} \times F_{IG} + V_C(i) \times F'_{CG}(i)}{V_{IA}(i) + V_C(i)} \quad \ldots\ldots\ldots\ldots (2)$$

The term $V_D \times \frac{V_{IA}(i)}{V_T}$ is the volume of upper airways gas inspired into the i^{th} alveolar compartment in one breath.

Applying the Fick principle to gas exchange in capillary blood; let $C_{\bar{V}G}$ represent contents of gas G (ml/ml blood) in venous blood, and $C_{aG}(i)$ represent contents in arterial blood. The amount of gas exchanged may therefore be expressed

$$\Delta V^*_G = \frac{\dot{Q}(i)}{f} \left\{ C_{\bar{V}G} - C_{aG}(i) \right\} \quad \ldots\ldots\ldots\ldots (3)$$

The term $\frac{\dot{Q}(i)}{f}$ is the volume of blood perfusing the i^{th} alveolar compartment during the period of one breathing cycle; ΔV^*_G being measured in ml. BTPS.

Assuming that no gas is absorbed or excreted by the lung tissue, then the alveoli and capillaries form a closed system where the net exchange of any gas species must be zero. Applying this fact to gas G we have

$$\Delta V_G + \Delta V^*_G = 0$$

Rearranging terms,

$$\Delta V_G = -\Delta V^*_G \quad \ldots\ldots\ldots\ldots (4)$$

This means that gas lost from capillary blood equals gas gained by the alveoli, and vice versa.

Applying equations (1) and (3) to oxygen and carbon dioxide exchange in the i^{th} alveolar compartment yields:

$$\Delta V_{O2} = F_{IAO2}(i) \times V_{IA}(i) + F'_{AO2}(i) \times V_{AL}(i) - F_{AO2}(i) \left\{ V_{AL}(i) + V_{EA}(i) \right\} \quad .. ..(5)$$

$$\Delta V^*_{O2} = \frac{\dot{Q}(i)}{100\ f} \left\{ C_{\bar{v}O2} - C_{aO2} \right\} \quad .. ..(6)$$

$$\Delta V_{CO2} = F_{IACO2}(i) \times V_{IA}(i) + F'_{ACO2}(i) \times V_{AL}(i) - F_{ACO2}(i) \left\{ V_{AL}(i) + V_{EA}(i) \right\} \quad .. ..(7)$$

$$\Delta V^*_{CO_2} = \frac{\dot{Q}(i)}{100f} \left\{ C_{\bar{v}CO_2} - C_{aCO_2}(i) \right\} .. ..(8)$$

Equations 6 and 8 are divided by a factor of 100 in order to express blood O_2 and CO_2 contents in the customary units of ml/100 ml. blood.

Thus far, the volume of gas expired from the i^{th} alveolar compartment, $V_{EA}(i)$ is not determined. Under normal conditions when atmospheric air is being breathed $V_{IA}(i)$ is sensibly equal to $V_{EA}(i)$, that is, inspired and expired volumes are equal. Unfortunately this simplifying assumption cannot be made during inert gas uptake and elimination as large volumes of the gas are being exchanged. It is therefore necessary to express $V_{EA}(i)$ in terms of the other variables and parameters before it can be included in the analysis.

Dividing equation 8 by equation 6, yields

$$\frac{\Delta V^*_{CO_2}}{\Delta V^*_{O_2}} = \frac{C_{\bar{v}CO_2} - C_{aCO_2}(i)}{C_{\bar{v}O_2} - C_{aO_2}(i)} \quad .. ..(9a)$$

It will be noted that the modulus of the term on the left hand side of the equation is the repiratory quotient, R, for the i^{th} blood compartment. We may therefore write the equation thus

$$R = \frac{C_{\bar{v}CO_2} - C_{aCO_2}(i)}{C_{\bar{v}O_2} - C_{aO_2}(i)} \quad .. ..(9)$$

Similarly, by dividing equation 7 by equation 5 we obtain,

$$R = \frac{F_{IACO_2}(i) \times V_{IA}(i) + F'_{ACO_2}(i) \times V_{AL}(i) - F_{ACO_2}(i) \left\{ V_{AL}(i) + V_{EA}(i) \right\}}{F_{IAO_2}(i) \times V_{IA}(i) + F'_{AO_2}(i) \times V_{AL}(i) - F_{AO_2}(i) \left\{ V_{AL}(i) + V_{EA}(i) \right\}} \quad .. \; .. \; .. \; .. \; .. \; (10)$$

Solving for $V_{EA}(i)$

$$V_{EA}(i) = \frac{V_{IA}(i)\left\{F_{IACO_2}(i) - R.F_{IAO_2}(i)\right\} + V_{AL}(i)\left\{F'_{ACO_2}(i) - F_{ACO_2}(i) + R.F_{AO_2}(i) - R.F'_{AO_2}(i)\right\}}{F_{ACO_2}(i) - R.F_{AO_2}(i)}$$

$$.. \; .. \; .. \; .. \; .. \; (11)$$

where R has the value given in equation 9 as blood R must equal gas R.

By multiplying both numerator and denominator of the above equation by $(P_{Bar} - 47)$ it is possible to express $V_{EA}(i)$ in terms of dry gas tensions, thus

$$V_{EA}(i) = \frac{V_{IA}(i)\left\{P_{IACO_2}(i) - R.P_{IAO_2}(i)\right\} + V_{AL}(i)\left\{P'_{ACO_2}(i) - P_{ACO_2}(i) + R.P_{AO_2}(i) - R.P'_{AO_2}(i)\right\}}{P_{ACO_2}(i) - R.P_{AO_2}(i)}$$

$$.. \; .. \; .. \; .. \; .. \; (12)$$

Having defined $V_{EA}(i)$, a system of equations may now be derived which determine the unknown gas tensions, $P_{AO_2}(i)$, $P_{ACO_2}(i)$, $P_{AN_2}(i)$ and $P_{AG}(i)$ for the given conditions.

Writing equation 4 for oxygen

$$\Delta V_{O_2} = -\Delta V^*_{O_2}$$

Substituting for ΔV_{O_2} and $\Delta V^*_{O_2}$ from equations 5 and 6 respectively we have

$$F_{IAO_2}(i) \times V_{IA}(i) + F'_{AO_2}(i) \times V_{AL}(i) - F_{AO_2}(i) \left\{ V_{AL}(i) + V_{EA}(i) \right\}$$

$$= \frac{\dot{Q}(i)}{100f} \left\{ C_{aO_2}(i) - C_{\bar{v}O_2} \right\} \quad .. \; .. \; .. \; .. \; .. \; (13)$$

Inserting the expression for $V_{EA}(i)$ from equation 11 and simplifying,

$$F_{IACO_2}(i).\ V_{IA}(i) + F'_{ACO_2}(i)\ .\ V_{AL}(i)$$

$$= \frac{F_{ACO_2}(i)}{F_{AO_2}(i)} \left[F_{IAO_2}(i)\ .\ V_{IA}(i) + F'_{AO_2}(i)\ .\ V_{AL}(i) + \frac{\dot{Q}}{100f} \left\{ C_{\bar{v}CO_2} - C_{aCO_2}(i) \right\} \right]$$

$$- \frac{R.\dot{Q}(i)}{100f} \left\{ C_{\bar{v}O_2} - C_{aO_2}(i) \right\} \qquad \ldots\ \ldots\ \ldots\ \ldots\ \ldots\ (14)$$

Again multiplying throughout by $(P_{Bar} - 47)$ to express gaseous composition in terms of dry gas tension we have

$$P_{IACO_2}(i)\ .\ V_{IA}(i) + P'_{ACO_2}(i)\ .\ V_{AL}(i)$$

$$= \frac{P_{ACO_2}(i)}{P_{AO_2}(i)} \left[P_{IAO_2}(i)\ .\ V_{IA}(i) + P'_{AO_2}(i)\ .\ V_{AL}(i) + \frac{\dot{Q}(P_{Bar} - 47)}{100\ f} \left\{ C_{\bar{v}O_2} - C_{aO_2}(i) \right\} \right]$$

$$- \frac{R.\dot{Q}(i)}{100f}\ .\ (P_{Bar} - 47)\ .\ \left\{ C_{\bar{v}O_2} - C_{aO_2}(i) \right\} \qquad \ldots\ \ldots\ \ldots\ \ldots\ \ldots\ (15)$$

Applying equation 4 to nitrogen exchange

$$\Delta V_{N_2} = -\Delta V^*_{N_2} \qquad \ldots\ \ldots\ \ldots\ \ldots\ \ldots\ (16)$$

ΔV_{N_2} may be obtained from the general expression given in equation 2 thus

$$\Delta V_{N_2} = F_{IAN_2}(i) \times V_{IA}(i) + F'_{AN_2}(i) \times V_{AL}(i) - F_{AN_2}(i) \left\{ V_{AL}(i) + V_{EA}(i) \right\}$$

$$\ldots\ \ldots\ \ldots\ \ldots\ \ldots\ (17)$$

Considering nitrogen exchange in the blood,

$$\Delta V^*_{N_2} = \frac{\dot{Q}\ (i)}{f} \left\{ C_{\bar{v}N2} - C_{aN_2}(i) \right\}$$

Defining λ_{N_2} as the Ostwald Solubility Coefficient for nitrogen,

$$\Delta V^*_{N_2} = \frac{\lambda_{N_2}}{760} \cdot \frac{\dot{Q}(i)}{f} \left\{ P_{\bar{v}N_2} - P_{aN_2}(i) \right\}$$

Since complete equilibration is assumed between alveolar gas and arterial blood, $P_{aN_2}(i)$ equals $P_{AN_2}(i)$, hence

$$\Delta V^*_{N_2} = \frac{\lambda_{N_2}}{760} \cdot \frac{\dot{Q}(i)}{f} \left\{ P_{\bar{v}N_2} - P_{AN_2}(i) \right\} \quad .. .. (18)$$

Equating 17 and 18 as in equation 16 and multiplying through by $(P_{Bar} - 47)$ gives

$$P_{IAN_2}(i) \times V_{IA}(i) + P'_{AN_2} \cdot V_{AL}(i) - P_{AN_2}(i) \cdot \left\{ V_{AL}(i) + V_{EA}(i) \right\}$$

$$= \frac{\lambda_{N_2} \times \dot{Q}(i)}{760\, f} \cdot (P_{Bar} - 47) \cdot \left\{ P_{\bar{v}N_2} - P_{AN_2}(i) \right\} \quad .. .. (19)$$

Solving for $P_{AN_2}(i)$

$$P_{AN_2}(i) = \frac{V_{IA}(i) \cdot P_{IAN_2}(i) + V_{AL}(i) \cdot P'_{AN_2}(i) + \frac{\lambda_{N_2} \cdot \dot{Q}(i)}{760\, f} \cdot (P_{Bar} - 47) \cdot P_{\bar{v}N_2}}{V_{AL}(i) + V_{EA}(i) + \frac{\lambda_{N_2}}{760} \cdot \frac{\dot{Q}(i)}{f} \cdot (P_{Bar} - 47)}$$

$$.. .. .. (20)$$

Similarly, an expression may be derived for any inert gas, G, thus

$$P_{AG}(i) = \frac{V_{IA}(i) \cdot P_{IAG}(i) + V_{AL}(i) \cdot P'_{AG}(i) + \frac{\lambda_G \cdot \dot{Q}(i)}{760 f} (P_{Bar} - 47) \cdot P_{\bar{v}G}}{V_{AL}(i) + V_{EA}(i) + \frac{\lambda_G}{760} \cdot \frac{\dot{Q}(i)}{f} (P_{Bar} - 47)}$$

$$.. .. .. (21)$$

Since the pressure in the alveoli is atmospheric during spontaneous breathing,

$$P_{Bar} = P_{AO_2}(i) + P_{ACO_2}(i) + P_{AN_2}(i) + P_{AG}(i) + 47$$

$$.. .. .. (22)$$

3.4 Solution of Equations

Four equations have now been derived (i.e. 15, 20, 21 and 22) defining the exchange of all the gases present in any alveolar compartment.

A cursory inspection of these equations reveals six unknowns viz; $P_{AO_2}(i)$, $P_{ACO_2}(i)$, $P_{AN_2}(i)$, $P_{AG}(i)$, $C_{aO_2}(i)$ and $C_{aCO_2}(i)$, hence they cannot be solved in their present form. It is therefore necessary to express $P_{AO_2}(i)$ and $P_{ACO_2}(i)$ in terms of $C_{aO_2}(i)$ and $C_{aCO_2}(i)$.

The quantitative relationship between oxygen tension and blood content depends upon several factors. In any individual, however, the values of such parameters as haemoglobin concentration, body temperature, and so on, may be considered to be invarient, and under these circumstances the blood oxygen content may be considered to be a function solely of oxygen and carbon dioxide tensions. The input values for the Kelman algorithm (60) for describing the oxygen and carbon dioxide tensions are blood pH, and temperature. The value of pH corresponding to any given carbon dioxide tension is obtained from the equation $pH=8.4169-0.63494 \times \log P_{CO_2}$, which is derived from a "least squares" fit to the data of Siggard-Anderson (102). The output from the Kelman algorithm is haemoglobin saturation, which is itself a function of pH. A reiterative approach is therefore necessary to determine the true saturation for given oxygen and carbon dioxide tensions. It has, however, been shown that only one iteration is in fact required (62). From this value of saturation, total blood oxygen content can be determined by the following expression

$$O_2\text{content} = 1.39 \times Hb \times sat/100 + \lambda O_2 \times \frac{P_{O_2}}{760}$$

where λO_2 is the solubility of oxygen in blood at 37°C. The coefficient 1,39 is the number of grammes of oxygen which combine with one gramme of haemoglobin. This value has been chosen in preference to the more conventional 1.34 (22), in view of recent work which suggests that the

molecular weight of human haemoglobin is 64,458 (59).

The blood carbon dioxide content may be expressed in terms of cabon dioxide tension in an analogous manner by the use of the second Kelman algorithm, which describes the carbon dioxide dissociation curve. The inputs to the algorithm are carbon dioxide tension, haemoglobin saturation, haematocrit and temperature, and pH; which may again be expressed explicitly as functions of oxygen and carbon dioxide tensions.

Having reduced the number of unknowns in the four exchange equations to $P_{AO_2}(i)$, $P_{ACO_2}(i)$, $P_{AN_2}(i)$ and $P_{AG}(i)$, a unique solution is now possible. Unfortunately, the complex inter-relationships between oxygen and carbon dioxide blood contents and corresponding gas tensions precludes a simple algebraic approach, hence resort is made to a numerical method. The technique employed first solves equation 15 for $P_{ACO_2}(i)$ by progressive bisection (68) with a fixed value of $P_{AO_2}(i)$. Equations 20 and 21 are next evaluated for $P_{AN_2}(i)$ and $P_{AG}(i)$, which are then substituted into equation 22 for appraisal. If this equation is not satisfied to within a specified tolerance, a re-estimation of $P_{AO_2}(i)$ is made, again by the use of the bisection technique. The entire process is reiterated until values for all the unknowns have been found.

3.5 The Composite Model

By applying this analysis to all alveolar compartments simultaneously, it is possible to calculate overall gas exchange for the model. The data on the respective ventilation and blood flow for each compartment are derived in the main from theoretical distributions to be defined in the next chapter.

Mean expired gas tensions are calculated by weighting the alveolar gas tensions in each compartment after gas exchange by their respective expired volumes. For any gas species X, this is expressed

$$\bar{P}_{EAX} = \frac{\sum_{i=1}^{i=n} P_{AX}(i) \cdot V_{EA}(i)}{\sum_{i=1}^{i=n} V_{EA}(i)} \quad .. .. (23)$$

Mixed arterial blood oxygen and carbon dioxide tensions are calculated by firstly weighting the O_2 and CO_2 blood contents associated with each of the alveolar compartments by the respective blood flows, and the deriving the mean arterial contents thus

$$\bar{C}_{aO_2} = \frac{\sum_{i=1}^{i=n} C_{aO_2}(i) \cdot \dot{Q}(i)}{\sum_{i=1}^{i=n} \dot{Q}(i)} \quad .. .. (24)$$

$$\bar{C}_{aCO_2} = \frac{\sum_{i=1}^{i=n} C_{aCO_2}(i) \cdot \dot{Q}(i)}{\sum_{i=1}^{i=n} \dot{Q}(i)} \quad .. .. (25)$$

These values for mean blood contents are then converted into gas tensions by use of the Kelman algorithms mentioned earlier.

Since inert gases are assumed to obey Henry's Law, then their mean arterial partial pressures are defined as

$$P_{aG} = \frac{\sum_{i=1}^{i=n} P_{AG}(i) \cdot \dot{Q}(i)}{\sum_{i=1}^{i=n} \dot{Q}(i)} \quad .. .. (26)$$

The gas tensions obtaining in each of the conducting airway compartments after expiration are determined by assuming complete mixing of the residual gas in these compartments with gas being excreted from the adjacent alveolar compartments. For any gas species X this is expressed for the i^{th} compartment.

$$P_{CX}(i) = \frac{P_{AX}(i) \cdot V_{EA}(i) + P'_{CX}(i) \cdot V_C(i)}{V_{EA}(i) + V_C(i)} \quad \ldots\ldots\ldots\ldots\ldots (27)$$

Finally, the gas tensions in the upper airways at the end of expiration are calculated by weighting the gas tension in each of the conducting airways (equation 26 above) by the volume being expired from that compartment thus

$$P_{DX} = \frac{\sum_{i=1}^{i=n} P_{CX}(i) \cdot V_{EA}(i)}{\sum_{i=1}^{i=n} V_{EA}(i)} \quad \ldots\ldots\ldots\ldots\ldots (28)$$

3.6 Modes of Model Operation

The model in its present form can be used to solve two basic types of problem. First, by defining the composition of inspired gas, minute volume, cardiac output, oxygen consumption and carbon dioxide output, the model can be used to investigate the effects of a given distribution of ventilation and/or blood flow upon gas exchange in the steady state. Second, if the steady state conditions are known, the model is such that for the first time investigations can be made into the time course changes in gas exchange when some "step change" is made to, say, inspired gas composition.

Considering the first type of problem, the adopted procedure initially assumes values for all constituent tensions in the model compartments and in mixed venous blood. One complete breathing cycle is then simulated and results in new values for the alveolar gas tensions. Overall gas exchange is then computed and the new value for arterial blood composition is found. A re-estimation of mixed venous P_{O_2} and P_{CO_2} is then made by subtracting the given oxygen uptake from, and adding the

carbon dioxide to, the arterial blood composition. As nitrogen is neither used or excreted by the body, its mixed venous tension is assumed equal to its new arterial tension. Using these newly calculated values as initial conditions another breathing cycle is now simulated.

The above procedure is reiterated until gas compositions do not fluctuate from one breath to another, at which time steady state conditions have been established.

In the second type of problem, the steady state values obtained from a procedure such as described above are assumed as initial conditions for alveolar gas tensions, and mixed venous blood gas tensions. A step change is then made to the inspired gas composition as would occur, for example, in anaesthesia, and the transient changes in alveolar and arterial gas tensions are monitored as breathing proceeds.

Obviously manual computation of the foregoing analysis would prove to be extremely labourious, hence the entire sequence of operations has been mechanised in the form of a FORTRAN program. A simplified flowchart is shown in Figure 7.

CHAPTER 4

FUNCTIONAL DEFECTS OF THE LUNG

This chapter deals with the manner in which chronic lung disease interferes with normal lung function. Although no exhaustive review of pulmonary pathology is intended, an attempt will be made to separate out the main types of functional defects that occur in the various disease states so that their influence upon overall gas exchange may be assessed subsequently by use of the proposed model.

Three classifications will be presented, namely, regional inequalities, series inequalities, and direct pulmonary blood shunts. The first group will be further divided into regional inequalities of ventilation and regional inequalities of blood flow. Obviously, any attempt to classify chronic lung diseases in this way is in a sense idealistic, since the majority of diseases manifest more than one of the functional defects listed. Nevertheless, the study of lung models embodying each of the defects during the steady state and unsteady state will illustrate how each particular defect reduces the efficiency of gas transport and exchange, and may help in pinpointing the predominant disturbance in any given subject.

4.1 Regional Inequalities

In many forms of pulmonary disease the pattern of regional ventilation and blood flow distributions may be greatly altered from the normal.

If blood vessels are destroyed selectively as in the granulomatoses and collagen diseases the alveolar capillary blood supply must be redistributed, or reduced, or interrupted completely (7). Progressive non-perfusion of the upper parts of the lung may also occur in normal subjects exposed to high acceleration forces (112), during pressure

ventilation (114) or in anaesthesia (114).

The most frequently occuring chronic lung diseases, however, are those in which normal structure of the airways is disrupted. The result may well be a simple mechanical block of both inspiration and expiration, or more importantly an increase beyond normal in the size of airspaces distal to the terminal bronchioles, either from dilation or from destruction of their walls. The primary examples of such lesions are the group of obstructive diseases known as emphysema which exist in a number of forms usually classified on morphological grounds, (see Table 1). It is well known that the occurence of pulmonary emphysema, in all its forms, is frequently observed to be irregular in lungs examined at autopsy (8,42). Even in severe cases where the disease is generalised, destruction is often more extensive in some lobes or segments than in others. Significant regional differences in pulmonary vasculature may also be demonstrated in subjects who appear to have generalised pulmonary emphysema.(44).

Investigations using x^{133} as a tracer gas have also shown very considerable regional abnormalities of function in vivo, as revealed by impairment of both ventilation and perfusion, in numerous subjects diagnosed as having pulmonary emphysema. In certain subjects it is clearly demonstrable that most of the tidal volume and the blood flow is going to zones, or possibly lobes, of the lung in which the structure is relatively preserved, but which represent only a small fraction of the total lung volume (8). In this circumstance it might be conjectured that little ventilation-perfusion abnormality exists, although gas exchange would be effectively limited to one lobe of the lung. However, the fact that ventilation and blood flow are regionally reduced in the same direction does not necessarily imply that they are both affected to the same degree. In addition it must be realised that the

volume of the lung tissue scanned by the scintilation counters is composed of units which must be behaving very differently, and the region cannot be regarded as a uniform field.

The existence of marked regional differences in ventilation in subjects with chronic pulmonary emphysema have been demonstrated by Briscoe and Cournand (13) using an indirect method (29) for interpreting the data obtained from helium washout tests in terms of two or more groups of alveoli; the so called "fast" and "slow" spaces. By use of a graphical technique (14) to determine the maximum fraction of cardiac output which could perfuse the slow spaces whilst being compatible with observed arterial oxygen saturation, the same authors were able to estimate the blood flow associated with each of the alveolar groups. The results obtained indicate that in an "average case" of emphysema, 66 per cent. of the lung volume was ventilated by 10 per cent. of the alveolar ventilation and perfused by 52 per cent. of the cardiac output (16).

More recently, new mathematical methods for computing inverse La Place transforms have enabled the work of Briscoe and Cournand to be extended to a lung with an infinite number of alveolar groups thereby providing a continuous distribution of the respiratory parameters. The techniques have been applied to both normal and abnormal subjects, and continuous distributions of both ventilation (70) and pulmonary blood flow (70) have been determined. These results establish that in normal subjects most of the effective ventilation and most of the blood flow are evenly distributed to the largest part of the lung volume. In subjects with emphysema, blood flow is again found to be distributed fairly uniformly with respect to lung volume, however, only a small fraction of the ventilation corresponds to the greatest part of blood flow and lung volume, hence most of the ventilation is ineffective. It may therefore

be concluded that the predominant disturbance, in subjects with emphysema, lies in the relatioship between ventilation and lung volume rather than between lung volume and blood flow.

Previous work concerned with the study of regional inequalities upon overall gas exchange has invariably assumed that the variation in ventilation and blood flow in the lungs is such that the pattern of ventilation-perfusion ratios so produced is compatible with a log normal frequency distribution. The concept was first introduced by Rahn (81) who showed that an $(A - a)D_{O2}$ of 8 mm Hg would be developed in a lung if the standard deviation of the distribution was log 1.3. A later extension by Farhi and Rahn (39) demonstrated that progressively larger $(A - a)D_{O2}$ values would result if the range of ventilation-perfusion ratios was widened by increasing the standard deviation. Similar studies have been presented more recently by Kelman (63) and West (113). The former study confirmed the earlier findings of higher $(A - a)D_{O2}$ values when the range of $\dot{V}_{IA}/\dot{Q}$ ratios is increased, and also defined the concomitant changes in P_{aCO2} and P_{aN_2}. The latter study, by assuming a fixed body metabolism was able to simulate the changes in mixed venous blood gases in the steady state and to show that the output of carbon dioxide was affected nearly as much as the uptake of oxygen by inequalities in regional $\dot{V}_{IA}/\dot{Q}$ ratios. This fact had not been previously realised due to the assumption of a "normal" venous blood composition in the lung models. Although West (113) in fact used a log normal distribution of ventilation per unit volume with constant blood flow per unit volume to generate data, he observed that "an unexpected finding was that the impairment of gas exchange resulting from ventilation inequalities was identical to that found with perfusion inequalities" and attributed this to being "a feature of log normal distributions". This "feature" may easily be appreciated by referring to Figure 8, in which data generated

from log normal distributions of ventilation and blood flow for a six compartment lung model is shown. Clearly, there is little difference in the $\dot{V}_{IA}/\dot{Q}$ ratios generated for the majority of compartments regardless of whether an uneven distribution of ventilation or blood flow is assumed. The only major differences in $\dot{V}_{IA}/\dot{Q}$ ratios are in the two compartments at the extreme ends of the range, but as these compartments are so poorly perfused their influence on mixed arterial blood gas content is negligible. Obviously, the differences between the $\dot{V}_{IA}/\dot{Q}$ ratios generated from the distributions will decrease as the number of compartments increase, hence log normal distributions of ventilation or blood flow are unsuitable for investigating the effects of independent changes in the regional distribution of either parameter.

Although the distribution of ventilation with respect to lung volume has been shown to approximate to a log normal distribution with small standard deviation in normal subjects (13,70), there is no evidence to support the contention that a log normal distribution with a large standard deviation represents the conditions obtaining in an emphysematious lung. Briscoe and Cournand (16) offer two main reasons why the nitrogen washout curves obtained from subjects with emphysema are not compatible with such distributions of ventilation. Firstly, too great a proportion of lung volume is too poorly ventilated, so that the frequency distribution curve would have to be very much skewed with its peak well to one side, or else it must have more than one peak. Secondly, in nitrogen washout data collected by the best possible technique, the washout from the poorly ventilated regions of the lung fits one exponent within experimental error, indicating that these regions are remarkably homogeneous in most cases (35). Again, the inference is that the distribution of ventilation with respect to lung volume is highly skewed in subjects with emphysema.

If pulmonary function is to be studied under the various pathological conditions described above, a more satisfactory regional distribution of the respiratory parameters must be postulated which more closely accords with the pattern observed clinically. A simple working assumption is that the parameter under consideration; be it ventilation or perfusion; follows a geometric progression. For example, a lung model considered to consist of ten <u>equal volume</u> alveolar compartments with an uneven distribution of ventilation and an even distribution of blood flow might be proposed as follows*

Compartment Number, N	1	2	3	4	5	6	7	8	9	10
Ventilation $\dot{V}_{IA}$	1.000	1.682	2.828	4.756	8.000	13.45	22.62	38.05	64.00	107.6
Blood flow, $\dot{Q}$	1	1	1	1	1	1	1	1	1	1

The numbers in the lower rows represent the magnitudes of ventilation and blood flows to the various alveolar compartments with reference to compartment number one. Taking the alveolar ventilation to be 5 litres/min, the pulmonary blood flow 5 litres/min and the breathing frequency 10 breaths/min, then the <u>volumes</u> of gas and blood coming into contact with each compartment per breath are as given below

N	1	2	3	4	5	6	7	8	9	10
$\dot{V}_{IA}$	1.893	3.185	5.356	9.008	15.15	25.48	42.85	72.06	121.2	203.8
$\dot{Q}$	50.0	50.0	50.0	50.0	50.0	50.0	50.0	50.0	50.0	50.0
$\dot{V}_{IA}/\dot{Q}$	.0379	.0637	.1071	.1802	.3030	.5096	.8570	1.441	2.424	4.076

If we lump compartments 1 to 6 and 7 to 10 together, then the above

*all figures quoted have been rounded up for brevity.

figures indicated that 60 per cent. of the volume of the lung model is ventilated by some 12 per cent. of the inspired ventilation and perfused by 60 per cent. of the pulmonary blood flow. These results are reminiscent of the figures of Briscoe and Cournand quoted earlier (see page 28) for an average case of emphysema. It would therefore appear that the proposed distribution, embodying uneven ventilation and even blood flow, represents a good approximation to the regional inequalities found in this disease.

The situation existing in the disease states in which blood flow is disrupted are unfortunately impossible to verify at the present time, as no suitable physiological data is available for comparison. In the absence of such concrete data it is permissible to assume that a pattern of regional inequality similar to that proposed for ventilation exists in these cases. For the same degree of inequality as previously adopted for the uneven ventilation distribution, the following uneven distribution of blood flow and even distribution of ventilation may be generated

Compartment Number, N	1	2	3	4	5	6	7	8	9	10
Ventilation V_{IA}	1	1	1	1	1	1	1	1	1	1
Blood flow, $\dot{Q}$	1.000	1.682	2.828	4.756	8.000	13.45	22.62	38.05	64.00	107.6

Again, assuming an alveolar ventilation of 5 litres/min, a pulmonary blood flow of 5 litres/min and a breathing frequency of 10 breaths/min, the volumes of gas and blood entering each compartment per breath may be computed thus

N	1	2	3	4	5	6	7	8	9	10
$\dot{V}_{IA}$	50.0	50.0	50.0	50.0	50.0	50.0	50.0	50.0	50.0	50.0
$\dot{Q}$	1.893	3.185	5.356	9.008	15.15	25.48	42.85	72,06	121.2	203.8
$\dot{V}_{IA}/\dot{Q}$	26.40	15.70	9.335	5.551	3.300	1.962	1.167	.6938	.4126	.2453

In general the relative magnitude of ventilation or blood flow to any alveolar compartment, N, may be expressed as $A^{(N-1)b}$. Clearly, the range of magnitudes of ventilation or blood flow will depend upon the terms A and b, and upon the total number of compartments. In the present context A is always equal to 1.0 and N to 10, hence the range of the respective distributions is entirely determined by the value assigned to b (for the examples given above, b was equal to 0.75). The choice of ten compartments was a result of a compromise between a realistic representation of a continuous distribution of ventilation or blood flow to the functional lung units and the time taken to run the computer programs. Moreover, it has been demonstrated elsewhere (113) that very little change in accuracy occurs in models of the type described in this thesis on increasing the number of compartments above ten.

To generate data for a lung model having an uneven distribution of ventilation and an even distribution of blood flow, a particular value must be assigned to parameter b so that values for compartmental ventilations may be calculated, and b for the blood flow data in set equal to zero to produce identical blood flows for each compartment. Likewise, an uneven distribution of blood flow and an even distribution of ventilation may be generated by interchanging the assigned values of b. The two separate distributions thus formed will be said to possess the same degree of inequality; that is, the range of compartmental ventilations in the former distribution is equal to the range of compartmental blood flows in the latter.

Figure 9 shows the ranges of $\dot{V}_{IA}/\dot{Q}$ ratios generated for a ten compartment model as the degree of inequality (i.e.parameter b) of uneven distributions of ventilation and even distributions of blood flow, and uneven distributions of blood flow and even distributions of ventilation, is increased. Note that the relative increase in $\dot{V}_{IA}/\dot{Q}$ ratios over the

range is identical for distributions having uneven ventilation and distributions having uneven blood flow with the same value of parameter b. For example, with b equal to 1.0 there is a five hundred fold increase in the $\dot{V}_{IA}/\dot{Q}$ ratios for both distributions. Although the relative changes in $\dot{V}_{IA}/\dot{Q}$ ratios are equal for uneven distributions of ventilation and even distributions of blood flow, and uneven distributions of blood flow and even distributions of ventilation, generated with the same value of 'b' it can be seen that the distributions embodying uneven ventilation consistently have lower $\dot{V}_{IA}/\dot{Q}$ ratios than the corresponding distributions having uneven blood flow. It will also be noted that this difference between the two types of distribution becomes more marked as the degree of inequality increases.

4.2 Series Inequalities

As inspired gas progresses down the bronchial tree, the linear velocity diminishes as the accumulative cross-sectional area of the air passages increase, until at or about the level of the first order alveolar duct the forward velocity becomes so small that gaseous diffusion takes over as the major force affecting molecular movement towards the periphery.

Evidence for this change in the mode of gaseous transport is available from both experimental and theoretical observations. Altschuler et al. (2) using aerosol droplets of 0.5μ diameter, which may be regarded as infinitely large molecules and therefore non-diffusible, concluded that direct ventilatory exchange in normal subjects amounts to less than one third of the tidal volume, and affects less than one-tenth of FRC. From the studies of Weibel and Gomez (108), it is apparent that in the conductive system of the normal lungs, from trachea down to the smaller bronchioles, a simple relationship exists between average diameter and the generation of branching. The relationship no longer

holds, however, for the respiratory bronchioles and alveolar ducts, which have much greater diameters than expected. The above authors take this fact to indicate that at these levels the phenomenon of molecular diffusion rather than mass movement of air dominate the gas transport. Looked at another way; a tidal volume of 500ml inspired into a lung having an FRC of 2.4 litres would produce an average volume change in the entire respiratory system of about ±10 per cent., that is 2400 ± 250ml. Considering an alveolus to be a sphere; a 10 per cent. volume change corresponds to an alteration of only 2.15 per cent. in the alveolar diameter hence the air in the alveoli must be practically stationary during the normal breathing cycle, and air exchange can only occur by diffusion. Moreover, the volume of the airways down to the alveolar ducts as calculated from morphometric data (107), is much larger than the average tidal volume, therefore gas molecules can only be transported to and from the alveolo-capillary membrane by diffusion.

During the normal respiratory cycle in healthy lungs the anatomical level at which the inspired gas and the residual gas have their boundary is about the first order alveolar duct, from which interface there remains a distance of about 2mm to be covered for gas mixing to be complete in the terminal unit (107). In emphysematous lungs, the normal structure of airways distal to the terminal respiratory bronchioles is disrupted. Figure 10 shows a terminal unit in which there is disruption of the second and third order respiratory bronchioles with the formation of a dilated space. This is an example of centrilobular emphysema (53,27). The effect of such a structure on ventilatory efficiency may be estimated provided a few assumptions are made (56). The diameter of the dilation is about 2mm and if fifty per cent. of the terminal ventilatory units are involved in the destructive process, this means that the total volume of all the dilations is about 560ml (assuming a figure of 28,000 for the

total number of ventilatory units). To this must be added about 150 ml of airways dead space (22) making a total of 710 ml. An inspirate of 500 ml into this system would bring the interface between inspired air and residual gas somewhere within the dilation. In order to mix with gas in the preserved alveoli the inspirate must diffuse out of the dilation and into the alveolar ducts, a distance of 7mm with the constriction caused by the relatively narrow openings to the alveolar ducts. Centrilobular emphysema thus presents a considerable obstruction to diffusive gas mixing, vida infra.

A similar difficulty in ventilation is encountered in pan-acinar emphysema, as shown in Figure 11. This illustrates a complex "inseries" dilation with no normal alveolar structures remaining (c.f. the terminal ventilatory unit in the normal lung, Figure 12). The interface is again established within the dilation, however, the linear distance over which diffusion must occur is greater than in the previous case and may be over 10mm (27). Thus, gas mixing will be impaired even more than in centrilobular emphysema.

In order to assess the magnitude of alveolar hypoventilation caused by the above lesions, it is necessary to estimate the speed with which diffusion equilibrium is achieved. Although there is general agreement that gas mixing occurs by diffusion, a great deal of controversy exists as to the rate of the process. In 1946 Rauwerda (82) made the first calculation of the time for diffusion in normal lungs by the analysis of two models; a cylinder and a cone with a globular end. In each case the system was closed, and the distance for diffusion was 7mm, a distance identical to that from the beginning of a respiratory bronchiole to a terminal alveolus according to the data of Weibel (107). The author found that diffusion was more rapid in the cone than in the cylinder, and in each case was extremely rapid; equilibrium being attained in less than

half a second. Rauwerda's findings were generally accepted until Cumming et al.(26) criticised the models on which the calculations had been made on the grounds that they were closed at both ends, whereas the terminal airways of the lungs are open proximally. They proposed instead a larger right circular cone, having a length for diffusion of 2.1cm, and found that an appreciable diffusion gradient persisted in this model for five seconds or more after an interface between inspired air and residual gas was established 2mm from the distal end. Whilst the critisism of Rauwerda's models by Cumming et al. is perfectly valid, their own work in turn is open to critisism on the grounds that the proposed right circular cone model does not realistically represent the structural form of the airways. Using a dichotomously branched model of the human lung, La Force et al. (69) showed that if an interface between a volume of inspired oxygen and residual gas was established at the terminal bronchioles, oxygen concentration in the terminal alveoli would rise to a plateau value in 2 seconds, and would be maintained for fifty seconds. Further, if the interface was assumed to be in the alveolar ducts, the plateau would be attained in one second. More recently, the model of La Force has also been questioned, and by using a structurally similar model Cumming and co-workers (28) have investigated the effects of two basically different boundary conditions upon the speed of diffusion equilibrium. In the first, an interface between inspired and residual gas was instituted at two volumes within the lung, and in the second the interface was allowed to move in and out of the lung whilst diffusion continued. The two boundary conditions were shown to give rise to entirely different results in respect of both the time course of diffusive mixing and the concentration gradients in the alveolar gas. Specifically, the results obtained with the moving boundary condition indicated that diffusion

equilibrium might not be attained during a normal breathing cycle, and the authors concluded that series or "stratified" inequality of gas concentrations probably exists even in healthy lungs.

Accepting that a mild form of stratified inhomogeneity exists in healthy lungs it is of interest to speculate upon its possible exaggeration in pulmonary disease. If we represent a normal bronchial tree as in Figure 12 A with cones distally for the acini, then the dilations of centrilobular emphysema will be as shown in Figure 12 B. In this case 50 per cent. of the lung volume has dilations. Obviously, such a condition, although arising from a form of stratified inhomogeneity, would behave functionally as a lung having a regional inequality of ventilation as discussed earlier. What is probably of greater importance is the significance of widely distributed centrilobular emphysema of apparently minor degree (56). In this case (Figure 12 C) all the respiratory bronchioles have a dilation on them but the total amount involved may only be ten per cent. of the total volume. If the lung volume were 5,000 ml at FRC*, the dilations would add up to 500ml. During inspiration in such a lung, the gas would not reach the alveolar ducts and a gross disturbance in the normally rapid diffusion mixing would occur, resulting in severe hypoventilation of the intact alveoli distal to the dilations. The lung shown in Figure 12 C would therefore behave functionally as a single unit having a low $\dot{V}_{IA}/\dot{Q}$ ratio.

The predominance of low $\dot{V}_{IA}/\dot{Q}$ regions in many cases of emphysema have been established experimentally by Hilton (54) and more recently by Bates et al. (6). The latter authors explain their inability to demonstrate high $\dot{V}_{IA}/\dot{Q}$ regions in any of their emphysematous subjects by

---

*A typical value for patients suffering from this disease (5).

arguing that high $\dot{V}_{IA}/\dot{Q}$ alveoli must exist, but their volume representation is small. A more plausible explanation might be that the high $\dot{V}_{IA}/\dot{Q}$ regions in widespread emphysema are essentially zones through which air is passing on its way to low $\dot{V}_{IA}/\dot{Q}$ regions. One might visualise high $\dot{V}_{IA}/\dot{Q}$ regions as being the more proximal respiratory bronchioles and part of the dilation shown in Figure 12 C, and the low $\dot{V}_{IA}/\dot{Q}$ regions as the terminal alveoli which are receiving the bulk of the capillary blood flow. The overall effects upon gas exchange of such a respiratory defect would clearly differ from those produced by a lung having a regional maldistribution of ventilation and therefore merits separate consideration.

In order to simulate a series inequality, use is made of the model structure outlined in the previous chapter. Part of the conducting airways compartment is assumed to represent the abnormal dilations, and by altering the volume of this compartment it is possible to increase or decrease the influence of the dilation. As the diffusion limitation has the effect of reducing the flow of gas into and out of the alveoli, an additional factor, F, is introduced which defines the fraction of tidal volume which actually enters the alveolar compartment. The term V_{IA} in the derived system of equations therefore becomes $F.V_{IA}$, where $0 \leq F \leq 1$. When F equals zero, no gas reaches the alveoli, and when F equals unity all the inspired gas reaches the alveoli.

4.3 Pulmonary Blood Shunts

In normal subjects there are contributions to the arterial blood which have bypassed ventilated areas of the lungs and have therefore taken no part in gas exchange. Such phenomena are referred to as pulmonary shunts and may be classified into two groups. First, shunts in which blood from the pulmonary arteries bypasses the pulmonary capillaries and enters the pulmonary veins. Functionally the effect is

to add amounts of systemic venous blood directly to arterial blood, hence this group is usually termed venous to arterial shunt. Second, anatomical shunts in which blood flow from the systemic arteries bypasses the pulmonary capillary bed and reaches the pulmonary veins. These include part of the bronchial venous blood which finds its way into the pulmonary veins and thence into the systemic arterial stream (77), and Thebesian veins which drain from the myocardium direct into the left side of the heart (83). Values between 0 and 5 per cent. of the cardiac output have been reported for these combined contributions in normals (41, 91,114).

Although pulmonary shunts have negligible effect upon overall pulmonary function in normal subjects, considerable disfunction may result under certain pathological circumstances. In patients with congenital heart disease; in whom blood flow in the pulmonary arteries is reduced or absent, increased pulmonary collateral flow may be considerable. Venous-to-arterial shunting in patients with pulmonary arterio-venous fistulas is the cause of the worst examples of venous admixture, and may carry more than 50 per cent. of the cardiac output (45). Abnormal channels connecting the portal system to the pulmonary veins may develop in some patients with cirrhosis of the liver (18), and appear functionally as venous to arterial shunts. Increased shunting of bronchial arterial blood bypassing the bronchial capillary bed is most striking in patients with bronchiectasis (71,24,46). The nature of the pulmonary infection appears unimportant, and it is thought that new blood vessel formation in the inflammatory tissue surrounding the lesions is responsible for the increased flow. The increased pulmonary collateral flow, sometimes observed in patients with tuberculosis (41) or carcinoma of the bronchus (24), is probably due to this mechanism (76).

In addition to the above abnormal conditions responsible for

pulmonary blood shunts, normal lungs may also develop increased venous to arterial shunts during sustained artificial pressure ventilation or shallow spontaneous breathing (75). These responses have been observed in anaesthetised dog and man, and in awake man (17), and have been attributed to microatelectasis; that is collapse of alveoli on a random topological basis.

Qualitatively, it is obvious that pulmonary blood shunts, arising from whatever cause, must reduce the overall efficiency of gas exchange in the lungs and result in arterial blood gas tensions which are closer to those of mixed venous blood that would otherwise be the case. Quantitatively, the effect is easily simulated by splitting the blood entering the lungs along the pulmonary artery into two separate streams. Part of the total cardiac output bypassing the alveolar compartments of the model completely, the remainder coming into contact with the alveolar compartments as before, the two streams then reunite to form mixed arterial blood. The amount of blood taking no part in gas exchamge; expressed as a percentage of cardiac output, will be referred to as the pulmonary blood shunt(see Figure 13).

It should be noted that an inherent assumption in the above modification to the model is that the composition of venous blood added directly to the arterial stream is of homogeneous composition. It must, however, be borne in mind that even for the conditions prevailing in the lungs of normal subjects, venous composition may vary considerably, the oxygen content of blood flow in the Thebesian veins for instance being very low and therefore causing appreciable falls in arterial oxygen tension out of proportion with its actual perfusion. In fact, it was thought by Cole and Bishop (21) that the Thebesian veins constitute the major part of the venous admixture in healthy man. The assumption of

homogeneous venous composition used in the analysis is nevertheless thought to be a good approximation to the situation existing in lungs with large amounts of shunt since the diseases causing these shunts are predominantly of a direct venous-to-arterial nature.

CHAPTER 5

REGIONAL INEQUALITIES

The existence of predominantly ventilatory or blood flow defects in certain types of lung disease were discussed in the previous chapter, and theoretical distributions embodying uneven regional ventilation and even blood flow, and uneven regional blood flow and even ventilation, were postulated to quantitatively describe pulmonary function under these circumstances. The present chapter is devoted to investigating the effects of such inequalities upon overall gas exchange during steady state and unsteady state conditions. In particular, the steady state arterial P_{O_2} and P_{CO_2}, venous P_{O_2} and P_{CO_2}, $(A - a)D_{O_2}$ and $(A - a)D_{CO_2}$ existing in lung models having uneven distributions of ventilation and even distributions of blood flow will be compared and contrasted with lung models having uneven distributions of blood flow and even distributions of ventilation when the degree of inequality of the uneven parameters is identical. The effects of differing levels of minute volume, pulmonary blood flow and inspired oxygen concentration will also be assessed. Unsteady state gas exchange will be studied during the uptake and elimination of hypothetical inert gases of various blood solubilities; the time course changes in arterial P_{O_2} and P_{CO_2}, $(A - a)D_{O_2}$, $(A - a)D_{CO_2}$, the overall rates of uptake and elimination of the inert gases being used for comparison in these cases.

5.1 Model Configuration

As it is intended to concentrate attention on regional inequalities of ventilation and blood flow, the generalised model formulated in Chapter 3 will be simplified by omitting the two series compartments comprising the upper airways and conducting airways. Equation 2 is therefore deleted from the system of equations and $F_{IAG}(i)$, the fractional

concentration of any gas G being inspired into the i^{th} alveolar compartment, takes the inspirate value for all compartments. For simulations of steady state gas exchange, the mixed venous blood composition will be determined by the reiterative technique described earlier, and for unsteady state gas exchange the venous composition will be held at a previously determined steady state value.

5.2 Steady State Gas Exchange

5.2.1 Effect of Increasing the Degree of Regional Inequality

Figure 14 shows the arterial P_{O_2} and P_{CO_2} values obtaining in lung models having uneven distributions of ventilation and even distributions of blood flow, and uneven distributions of blood flow and even distributions of ventilation, when the degree of the inequality is increased. In all cases, the body uptake of oxygen and output of carbon dioxide were held constant at 250 ml/min and 200 ml/min respectively and the alveolar ventilation and pulmonary blood flow were 5 litres/min, breathing frequency being at a rate of 12 breaths/min. For both ventilatory and blood flow inequalities the P_{aO_2} and P_{aCO_2} curves have the same shape. There is a continual fall in P_{aO_2} as the degree of inequality increases, however, the fall is steepest over the intermediate range (b = 0.25 to b = 0.75). P_{aCO_2} is little affected by small degrees of inequality (b 0.5), but a progressive increase is evident as the inequality becomes more marked.

Comparing the behaviour of lung models having uneven distributions of ventilation and even distributions of blood flow with lung models having uneven distributions of blood flow and even distributions of ventilation, it can be seen that for any given degree of inequality (parameter b identical for both uneven distributions) lung models having blood flow defects are more effective at oxygenating arterial blood than

are lung models having ventilatory defects, whereas the converse is true for carbon dioxide removal; where lung models with ventilatory defects fare better than lung models with blood flow defects.

The accompanying changes in mixed venous P_{O_2} and P_{CO_2} as a function of the degree of regional inequality are shown in Figure 15. Since pulmonary blood flow is fixed, the difference between arterial and mixed venous gas tensions represents the constant arterio-venous oxygen and carbon dioxide differences of 5 ml/100 ml and 4 ml/100 ml respectively. The relatively large differences between P_{aO_2} and $P_{\bar{v}O_2}$ for small degrees of inequality are a reflection of the sigmoid shape of the haemoglobin dissociation curve. The more linear carbon dioxide dissociation curve results in a nearly constant difference between arterial and mixed venous P_{CO_2}.

The reasons for the observed differences between lung models having ventilatory and blood flow defects may best be explained by considering regional gas exchange in each of their alveolar compartments. Figure 16 shows the oxygen and carbon dioxide contents of capillary blood draining from the ten compartments of a lung model having an uneven distribution of ventilation and an even distribution of blood flow, and a lung model having an uneven distribution of blood flow and an even distribution of ventilation. The degree of inequality for both uneven distributions is the same, parameter b being equal to 1.0. Similar patterns exist for the entire range of values of parameter b, the only difference being in the range of $\dot{V}_{IA}/\dot{Q}$ values encountered. Circles are used to indicate contents associated with an uneven distribution of ventilation, and squares to indicate contents associated with an uneven distribution of blood flow. In both cases, the open symbols refer to oxygen contents and the closed symbols to carbon dioxide contents; the smooth curves drawn through the points being referred to as O_2 or CO_2

content lines. The numbers adjacent to the symbols indicate the volume of blood perfusing that alveolar compartment in one breath.

Generally, the O_2 content line displays an increasing upward slope from low $\dot{V}_{IA}/\dot{Q}$ ratios up to a $\dot{V}_{IA}/\dot{Q}$ ratio of approximately 0.6, after which point little increase in O_2 content occurs over the remainder of the range. The CO_2 content line commences as a gentle slope downwards at low $\dot{V}_{IA}/\dot{Q}$ ratios, however, the slope rapidly becomes steeper over the ranges of $\dot{V}_{IA}/\dot{Q}$ ratios 0.2 to 1.3 after which it remains almost linear.

Considering oxygen exchange first, it can be seen that compartments with low $\dot{V}_{IA}/\dot{Q}$ ratios will have a greater influence upon mixed arterial blood than will compartments with high $\dot{V}_{IA}/\dot{Q}$ ratios providing that the amounts of blood contributed by the compartments are equal. This is because there is little increase in the oxygen content of the blood draining from compartments with $\dot{V}_{IA}/\dot{Q}$ ratios in excess of 0.6 due to the near saturation of haemoglobin. Thus in the case of the model having a ventilatory defect, the compartments with $\dot{V}_{IA}/\dot{Q}$ ratios greater than o.6 cannot make up the deficit of oxygen content incurred by blood draining from the compartments with very low $\dot{V}_{IA}/\dot{Q}$ ratios. In the situation shown in Figure 16, the oxygen content in blood draining from compartments having $\dot{V}_{IA}/\dot{Q}$ ratios of less than 0.6 is 14.647 ml/100 ml for the lung having the ventilatory defect, and 16.020 ml/100 ml for the lung having the blood flow defect. Comparable figures for compartments with $\dot{V}_{IA}/\dot{Q}$ ratios greater than 0.6 for both lungs are 20.253 ml/100 ml and 20.220 ml/100 ml respectively.

Whereas arterial oxygen content is mainly dependent upon the presence of low $\dot{V}_{IA}/\dot{Q}$ ratio compartments, arterial carbon dioxide content is more influenced by high $\dot{V}_{IA}/\dot{Q}$ ratio compartments. This being so, it

is at first sight surprising to find that P_{aCO_2} is greater in the lung model having a blood flow defect as the majority of its compartments have $\dot{V}_{IA}/\dot{Q}$ ratios greater than 0.2, and are therefore endowed with low end capillary CO_2 contents. Closer scrutiny of the uneven blood flow distribution, however, reveals that these compartments are poorly perfused with blood, and are therefore unable to make up for the high CO_2 content contributed by the two compartments with the lowest $\dot{V}_{IA}/\dot{Q}$ ratios which receive 75 per cent. of the total pulmonary blood flow. Although the lung with an uneven distribution of ventilation has more compartments with low $\dot{V}_{IA}/\dot{Q}$ ratios, the CO_2 content remains almost constant for $\dot{V}_{IA}/\dot{Q}$ ratios of less than 0.2, hence no additional penalty is paid by the low $\dot{V}_{IA}/\dot{Q}$ ratio compartments. The remaining compartments with $\dot{V}_{IA}/\dot{Q}$ ratios greater than 0.2 are able to reduce considerably the mixed arterial CO_2 content because of their relatively high blood flows.

5.2.2 Effect of Increasing Minute Volume

The effect of increasing the minute volume to lung models having uneven distributions of ventilation and even distributions of blood flow, and uneven distributions of blood flow and even distributions of ventilation, is shown in Figure 17; the pulmonary blood flow and breathing frequency were retained constant at 5 litres/min and 12 breaths/min throughout. The degree of inequality for both uneven distributions was fairly severe, parameter b being equal to 1.0, which at a normal value of minute volume (5 litres/min) results in a P_{aO_2} and P_{aCO_2} of 40.5 mm Hg and 39.7 mm Hg for a lung model with a ventilatory defect and 49.5 mm Hg and 51.5 mm Hg for a lung model with a blood flow defect.

As the minute volume increases, there is a dramatic rise in arterial P_{O_2}, in the lung model having uneven distribution of blood flow, amounting to a total increase of 58.0 mm Hg from a minute volume of 5 litres/min to 15 litres/min.

By contrast, the increase in arterial P_{O_2} for the lung model having an uneven distribution of ventilation is negligible, amounting to only 1.25 mm Hg over the same range of minute volumes. Significant falls in arterial P_{CO_2} are recorded for lung models with both ventilatory and blood flow defects; on increasing the minute volume from 5 litre/min to 15 litre/min there is a decrease of 24.0 mm Hg in the lung model having a ventilatory defect and a decrease of 32.0 mm Hg in the lung model having a blood flow defect. Note in particular, that the difference in P_{aCO_2} between the lung models with ventilatory defects and lung models with blood flow defects diminishes as the minute volume increases.

The above changes in P_{aO_2} and P_{aCO_2} observed as minute volume is increased, arise for two reasons. Firstly, the increase in minute volume results in a proportional increase in the ventilation to each alveolar compartment of the lung models causing a rise in the compartments' $\dot{V}_{IA}/\dot{Q}$ ratio. Secondly, the mixed venous blood composition perfusing the lung models changes due to the new gas exchange conditions prevailing. Figure 18 illustrates these changes graphically for the lung models having ventilatory and blood flow defects shown in Figure 17 when the minute volume is increased from 5 litre/min to 12.5 litre/min. The shift to the right of all alveolar compartments is seen to affect the CO_2 content lines in a different manner to the O_2 content lines. In the case of the CO_2 content lines; although the position of the curves for lung models having ventilatory and blood flow defects are changed, their relative shape is altered only slightly, hence similar changes in P_{aCO_2} are to be expected from both distributions. The decreased difference in P_{aCO_2} between the two lung models results from the lowering of $P_{\bar{v}CO_2}$, which in turn causes the CO_2 content lines to virtually superimpose; thereby reducing the influence of the lowest $\dot{V}_{IA}/\dot{Q}$ ratio compartment in the lung model having a blood flow defect. It is this compartment that

was primarily responsible for causing the higher P_{aCO_2} values observed at lower minute volumes.

The O_2 content lines, in contrast, suffer both a displacement to the right, and a change in shape relative to one another. As all compartments in the lung model having an uneven distribution of blood flow are receiving a reasonable ventilation at the lower minute volumes, since the distribution of ventilation is uniform, any increase in overall ventilation tends to move the positions of the alveolar compartments to the flat portion of the O_2 content lines. For a lung model having an uneven distribution of ventilation, the change in shape is not so drastic because of the presence of the poorly ventilated compartments. Even with a substantial increase in minute volume these compartments still have very low $\dot{V}_{IA}/\dot{Q}$ ratios, and therefore low end capillary oxygen contents; the majority of the additional ventilation being diverted to the already well ventilated compartments. For example, the two alveolar compartments with the lowest $\dot{V}_{IA}/\dot{Q}$ ratios have ventilations of 0.4073 ml/breath and 0.8146 ml/breath at a minute volume of 5 litres/min, and even with a minute volume of 12.5 litres/min they only increase to 1.0183 ml/breath and 2.0365 ml/breath respectively. As a result, a significant number of compartments remain on the early part of the O_2 content line, and because they are well perfused with blood, the tendency is to lower the mean arterial saturation.

The accompanying changes in $(A - a)D_{O_2}$ and $(A - a)D_{CO_2}$ as minute volume is increased are shown in Figure 19 for lung models having both ventilatory and blood flow defects and clearly reflect the changes in regional gas exchange discussed above. For the lung model having an uneven distribution of ventilation and an even distribution of blood flow, $(A - a)D_{O_2}$ increases as minute volume increases; indicating that the majority of the additional gas inspired is ineffective in raising the oxygen content of arterial blood. In the lung model having an uneven

distribution of blood flow and an even distribution of ventilation there is a fall in $(A - a)D_{O_2}$ of approximately 35.0 mm Hg when the minute volume is increased from 5 litres/min to 15 litres/min, the corresponding change in P_{aO_2} being 58.0 mm Hg. As the fall in $(A - a)DO_2$ is less than the rise in P_{aO_2} this implys that some of the increased ventilation is ineffective, however, in comparison to the lung model having an uneven distribution of ventilation the inefficiency is small. A perusal of Figure 18 shows that the portion of minute volume "wasted" in both cases can be attributed to the ventilation of alveolar compartments already on the flat lart of the O_2 content line. The percentage is obviously greater for the lung model having an uneven distribution of ventilation, as such compartments receive most of the ventilation even at the lower minute volumes. Falls in $(A - a)D_{CO_2}$ are recorded in lung models having both ventilatory and blood flow defects, however a slightly greater fall is noted for the lung model having the blood flow defect. Again, the changes can be explained in terms of the content lines, carbon dioxide content being affected marginally more by changes in minute volume in the lung model having an uneven blood flow distribution than in the lung model having an uneven distribution of ventilation (see Figure 18).

5.2.3 Effect of Increasing Pulmonary Blood Flow

The changes in arterial P_{O_2} and P_{CO_2} as pulmonary blood flow is increased to lung models having uneven distributions of ventilation and even distributions of blood flow, and even distributions of ventilation and uneven distributions of blood flow are shown in Figure 20. It can be seen that the rise in P_{aO_2} is much smaller in the lung model having a blood flow defect as pulmonary blood flow is increased; compared to the rise observed with an equivalent increase in minute volume, however, the rise in P_{aO_2} in the lung having a ventilatory defect is larger. Changes

in P_{aCO_2} are smaller for both lung models than those occuring with the same increases in minute volume.

The reasons for these results lies in the interaction of two phenomena associated with increases in pulmonary blood flow, namely, the lowering of the $\dot{V}_{IA}/\dot{Q}$ ratios of all alveolar compartments and the gains and falls in $P_{\bar{v}O_2}$ and $P_{\bar{v}CO_2}$ resulting from the smaller amounts of oxygen removed from, and carbon dioxide added to, each unit volume of blood perfusing the body tissues at the higher blood flows. From Figure 21 it can be seen that a greater gain in $P_{\bar{v}O_2}$ is made in the lung model having an uneven distribution of ventilation than in the lung model having an uneven distribution of blood flow. Both gains, however, are accompanied by a shift to the left of the O_2 content line, thereby effectively lowering the end capillary content of oxygen draining from each alveolar compartment. The falls in $P_{\bar{v}CO_2}$ are approximately equal for both lung models having uneven distributions of ventilation and uneven blood flow, but there is little change in P_{aCO2} in both cases because of the shift to the left of the alveolar compartments on the CO_2 content line. It will be noted that all but three of the alveolar compartments of the lung model having an uneven distribution of ventilation lie on the horizontal part of the CO_2 content line at a pulmonary blood flow of 12.5 litre/min, implying that very little reduction is to be expected in P_{aCO_2} by further increases in overall blood flow; a fact borne out by the trend shown in Figure 20.

5.2.4 Effect of Increasing Inspired Oxygen Concentration

Increasing the inspired concentration of oxygen is often resorted to in extreme cases of respiratory insufficiency in order to correct hypoxemia. Figure 22 shows the arterial PO_2 values resulting from different levels of inspired oxygen concentration in a homogeneous lung

model and in lung models with increasing degrees of ventilatory and blood flow inequalities. For a homogeneous lung model, P_{aO_2} is directly related to the inspired oxygen concentration; that is a twofold increase in F_{IO_2} will result in a doubling of P_{aO_2}. The rise with increasing F_{IO_2} in lung models having uneven distributions of blood flow and even distributions of ventilation is only slightly less than that for a homogeneous lung model even when the degree of inequality is large. Although lung models having an uneven distributions of ventilation and even distributions of blood flow behave in the same general manner when the degree of inequality is small, the rise in P_{aO_2} is much slower when the inequality is more marked. It will be noted that when F_{IO_2} is equal to 100 per cent., all lung models have a correspondingly high P_{aO_2} regardless of the type or degree of their inequality.

Again, the difference in behaviour of lung models having uneven distributions of ventilation and even distributions of blood flow and uneven distributions of blood flow and even distributions of ventilation may best be explained by referring to the O_2 and CO_2 content lines (Figure 23). In both the cases shown, the degree of inequality was the same, parameter b being equal to 1.0. When F_{IO_2} is increased to 40 per cent. the blood leaving all alveolar compartments with $\dot{V}_{IA}/\dot{Q}$ ratios greater than 0.2 is completely saturated. Compartments with $\dot{V}_{IA}/\dot{Q}$ ratios of less than 0.004, in contrast, still remain unsaturated even when F_{IO_2} is 80 per cent. For a lung model having an uneven distribution of ventilation, more alveolar compartments are present with low $\dot{V}_{IA}/\dot{Q}$ ratios than is the case for a lung model having the same inequality of blood flow. In the example cited in Figure 23, all compartments in the lung model having an uneven distribution of blood flow have $\dot{V}_{IA}/\dot{Q}$ ratios greater than 0.2, and complete saturation of blood leaving each compartment is achieved by increasing F_{IO_2} to 40 per cent. The lung model having an uneven

distribution of ventilation, however, has half of its compartments with $\dot{V}_{IA}/\dot{Q}$ ratios of less than 0.2, and one third with $\dot{V}_{IA}/\dot{Q}$ ratios less than 0.004, and it is blood draining from these latter alveolar compartments that is responsible for the slow rise in P_{aO_2} as F_{IO_2} is increased.

5.3 Unsteady State Gas Exchange

Because of the complex interactions of variables in the unsteady state, consideration will first be given to the homogeneous lung in which all alveolar compartments receive identical ventilation and blood flow. Having examined this simple case, attention will then be switched to models which have regional inequalities of ventilation or blood flow. The behaviour of the homogeneous lung will also serve as a standard by which the changes in arterial and alveolar gas compositions in models having any type of functional defect may be compared during inert gas uptake and elimination.

5.3.1 Gas Exchange During Inert Gas Uptake in a Homgeneous Lung

In a homogeneous lung breathing 5 litre/min at 12 breaths/min, and being perfused with a pulmonary blood flow of 5 litre/min, 20.83 ml of oxygen are removed from, and 16.67 ml of carbon dioxide are added to alveolar gas each breath when breathing air. These conditions result in steady state arterial oxygen, carbon dioxide and nitrogen tensions of 115.5 mm Hg, 28.8 mm Hg and 568.7 mm Hg respectively (see Figure 14). If the nitrogen of the inspirate is replaced by a soluble inert gas the steady state is upset and the tensions of all the gases present in the lung model alter as breathing proceeds. The resulting changes in arterial P_{O_2} and P_{CO_2} over thirty breaths are shown in Figure 24 for four hypothetical inert gases with partition coefficients of 0.01, 0.1, 1.0 and 10.0. For inert gases with partition coefficients of 0.1, 1.0 and 10.0, P_{aO_2} increases with breath number and the rate of increase is clearly related to the inert

gas solubility; the higher the solubility, the greater the gain in P_{aO_2}. The rise over thirty breaths being 304 mm Hg, 116 mm Hg and 8 mm Hg respectively for each of the gases. A similar pattern of behaviour is observed for P_{aCO_2}, but the changes are far less marked. For example, the rise in P_{aCO_2} over thirty breaths is only 8 mm Hg for the highest solubility inert gas, which is only about 2.6 per cent. of the accompanying rise in P_{aO_2}. Increases with inert gases of lower solubility are proportionately smaller. There is a small but mathematically demonstrable decrease in P_{aO_2} and P_{aCO_2} when nitrogen is replaced by an inert gas with a partition coefficient of 0.01, the falls are however less than 1.0 mm Hg over the thirty breaths.

The rise in oxygen and carbon dioxide tensions are primarily due to the uptake of inert gas by capillary blood, which causes a decrease in the lung volume at full inspiration. Consequently, the amounts of oxygen and carbon dioxide represent a higher fraction of the total volume and the tensions of the two gases rise. In addition, as the lungs are assumed to return to FRC after expiration, less gas is expired to the environment because of the uptake of the inert gas and hence the quantity of oxygen and carbon dioxide remaining in the lungs is greater than during steady state air breathing. Both the "concentration" effect due to the inert gas uptake and the concomitant decrease in expired volume act in unison and cause the observed increase in oxygen and carbon dioxide tensions.

Figure 25 shows how the rate of uptake of the inert gases by capillary blood varies with breath number. It can be seen that all gases tend toward a pseudo steady state in which the uptake of gas remains constant from breath to breath. At this point the net amount of gas entering the lungs in one breath is equal to the net amount leaving the lungs via the capillary blood in one breath. Expressed mathematically,

the pseudo steady state exists when

$$V_{IA} \cdot F_{IA} - V_{EA} \cdot F_{AG} = \frac{\dot{Q} \lambda_G}{f.760} \cdot P_{aG} \qquad \ldots\ldots\ldots\ldots\ldots (29)$$

Bearing in mind that the rate of uptake of the inert gas tends to a plateau it is surprising to note from Figure 24 that P_{aO_2} continues to increase over the thirty breaths in all cases. In order to explain this result it is necessary to consider the dynamic changes in the tensions of all gases present in the lungs during the uptake period. Nitrogen, being the most abundant gas in the lungs initially, and having the lowest blood solubility (0.01277) is most affected by the uptake of the inert gas during the first few breaths because it can only be resorbed into the blood at a very slow rate. Now as breathing proceeds the nitrogen is gradually washed out of the lungs and oxygen becomes the most abundant gas. Because P_{O_2} was initially high (P_{aO_2} = 115.5 mm Hg when breathing air in the steady state), and therefore on the flat portion of the haemoglobin dissociation curve, additional oxygen can only be carried in simple solution in blood. As the partition coefficient for oxygen is low (λ_{O_2} = 0.023), oxygen behaves very much as a low solubility inert gas under these conditions. The net result is that as nitrogen is removed, the concentration effect is gradually passed on to oxygen and therefore its arterial tension continues to rise even though the rate of uptake of the inert gas itself does not increase.

It is of interest to note the difference in behaviour of oxygen and carbon dioxide during the period of inert gas uptake. Oxygen, being relatively insoluble because of the complete saturation of haemoglobin, can only enter the capillary blood in small amounts, hence the alveolar oxygen tension rises. The transfer of carbon dioxide, by contrast, is not so affected because the ability of the blood to chemically

carry the gas is not limited in the same manner as oxygen hence its dissociation curve is relatively steep. Any rise in the tension of carbon dioxide in the lungs therefore results in an increase in blood carbon dioxide content; thus offsetting any concentration effect. This means that during inert gas uptake a greater increase in arterial blood carbon dioxide content is to be expected in comparison to the slight increase in oxygen content, implying a fall in the respiratory exchange ratio. Figure 26 has been produced from the output of the model and clearly illustrates this point during the uptake of inert gases with solubility partition coefficients of 0.1, 1.0 and 10.0, however, a minute rise in respiratory quotient is recorded for the lowest solubility inert gas.

The apparent non-conformity of the lowest solubility inert gas to the general pattern observed during uptake can be explained by reconsidering the cause of the concentration effect. During steady state air breathing, nitrogen is neither used nor produced by the body tissues hence its net flux from lungs to blood is zero. When nitrogen is replaced in the inspirate by an inert soluble gas the nitrogen in the lungs will be depleted by the ventilation, and nitrogen from mixed venous blood will flow into the alveoli due to the partial pressure difference produced. For the higher solubility inert gases this evolution of nitrogen is negligible when compared to their own uptake rate, hence the concentration effect occurs. If the inert gas replacing nitrogen has a solubility less than that of nitrogen, then an interesting situation arises in which the uptake of the inert gas is now less than the output of nitrogen. In the case of the lowest solubility inert gas considered; its partition coefficient is in fact lower than that of N_2. A small dilution of alveolar gases would therefore be expected, together with a small fall in the respiratory quotient due to the reversal of

inert gas flows.

5.3.2 Steady State Effects of Breathing Inert Gases in a Homogeneous Lung

If a mixture of 21 per cent oxygen and 79 per cent. inert gas is breathed for sufficient time, the nitrogen dissolved in the body tissues will eventually be replaced by the inert gas, and the inert gas uptake will fall to zero, resulting in new steady state conditions. The gas tensions existing in the alveolar compartments, arterial blood and mixed venous blood of a homogeneous lung model breathing such mixtures may be predicted by adopting a reiterative procedure similar to that described earlier for air breathing. In the present instance nitrogen is replaced in the inspirate by the particular inert gas, and the mixed venous tension of the inert gas is determined in the same manner as described for nitrogen; that is by assuming that the tissue uptake of the gas is zero after each iteration. The results obtained for the four hypothetical inert gases indicate that the steady state gas tensions associated with homogeneous lungs are independent of the inert gas solubilities provided that the overall ventilation, pulmonary blood flow, oxygen consumption and carbon dioxide output are equal.

In the homogeneous lung, all alveolar compartments are identical and may therefore be considered as a single functional unit. As such, it is clear that in a steady state condition, in which the uptake of the inert gas is zero, the only gases being exchanged are oxygen and carbon dioxide. Considering the oxygen exchange equations (i.e.equations 5 and 6 in chapter 3), and dropping the subscript (i) since we are now only dealing with one alveolar compartment, F'_{AO_2} must equal F_{AO_2} because alveolar oxygen concentration must be constant from breath to breath in the steady state.

Rewriting these equations we obtain

$$\Delta V_{O_2} = F_{IO_2} \cdot V_{IA} - F_{AO_2} \cdot V_{EA} \qquad \ldots\ldots\ldots\ldots (30)$$

$$\Delta V^*_{O_2} = \frac{\dot{Q}}{100f} \cdot (C_{\bar{v}O_2} - C_{aO_2}) \qquad \ldots\ldots\ldots\ldots (31)$$

Equating (30) and (31) as before and solving for F_{AO_2}

$$F_{AO_2} = \frac{F_{IO_2} \cdot V_{IA} + \frac{\dot{Q}}{100f} (C_{aO_2} - C_{\bar{v}O_2})}{V_{EA}} \qquad \ldots\ldots\ldots\ldots (32)$$

Multiplying through by $(P_{Bar} - 47)$ to express the gas concentrations as partial pressures

$$P_{AO_2} = \frac{P_{IO_2} \cdot V_{IA} + \frac{\dot{Q} \cdot (P_{Bar} - 47)}{100f} (C_{aO_2} - C_{\bar{v}O_2})}{V_{EA}} \qquad \ldots\ldots\ldots (33)$$

Now, as the homogeneous lung is considered to contain only one functional alveolar compartment, that compartment must be responsible for exchanging all the oxygen and carbon dioxide required by the body metabolism. The expired alveolar volume, V_{EA}, must therefore equal the inspired volume, V_{IA}, minus the volume of oxygen removed, ΔV_{O_2}, plus the volume of carbon dioxide added, ΔV_{CO_2}, that is

$$V_{EA} = V_{IA} - \Delta V_{O2} + \Delta V_{CO_2} \qquad \ldots\ldots\ldots\ldots (34)$$

Substituting for V_{EA} in equation (33) gives

$$P_{AO_2} = \frac{P_{IO_2} \cdot V_{IA} + \frac{\dot{Q} \cdot (P_{Bar} - 47)}{100f} (C_{AO_2} - C_{\bar{v}O_2})}{V_{IA} - V_{O_2} + V_{CO_2}} \qquad \ldots\ldots\ldots (35)$$

By similar manipulation the following expression may be derived for P_{ACO_2}

$$P_{ACO_2} = \frac{\dot{Q}\,(P_{Bar} - 47)}{100f} \quad \frac{(C_{ACO_2} - C\bar{}_{\bar{v}CO_2})}{V_{IA} - V_{O_2} + V_{CO_2}} \qquad \ldots\ldots\ldots\ldots\ldots (36)$$

Note that the term $P_{ICO_2}.V_{IA}$ does not appear above because the inspired carbon dioxide tension is assumed to be zero. Examination of equations 6 and 7 reveal that both P_{AO_2} and P_{ACO_2} are soley functions of V_{IA} and $\dot{Q}$. The remaining terms are either constants, viz., f, $(P_{Bar} - 47)$, ΔV_{O_2} and ΔV_{CO_2}, or functions of P_{AO_2} and P_{ACO_2}, viz. C_{aO_2}, C_{aCO_2}, $C\bar{}_{\bar{v}O_2}$ and $C\bar{}_{\bar{v}CO_2}$. As the overall ventilation and blood flows are identical for all the inert gas mixtures then the steady state oxygen and carbon dioxide tensions must be the same irrespective of the inert gas solubility.

5.3.3 Inert Gas Elimination in Homogeneous Lungs

On switching back to air breathing after attaining a steady state with a 21 per cent. oxygen, 79 per cent. inert gas mixture, the inert gas is excreted into the alveolar spaces and dilutes all gases present. Figure 27 shows the changes in arterial P_{O_2} and P_{CO_2} occuring in a homogeneous lung model during the first thirty breaths of inert gas elimination. The falls in arterial P_{O_2} recorded are some three to four times smaller than the corresponding rises in arterial P_{O_2} during the uptake period, however, the falls in arterial P_{CO_2} are of the same order as the rises in arterial P_{CO_2} during uptake. Again, the largest changes in arterial tensions are associated with the higher solubility gases and a reversal pattern is evident for the lowest solubility gas ($\lambda = 0.01$); P_{aO2} and P_{aCO_2} increasing as the inert gas is excreted in this case.

The relatively modest falls in arterial P_{O_2} during the elimination

of the inert gases is primarily due to the rapid wash in of nitrogen which constitutes the bulk of the inspirate and is therefore most affected by changes due to dilution. It can be seen from Figure 28 that the time course changes in the rate of inert gas excretion, and alveolar nitrogen tension, follow an identical pattern, and both reach a pseudo steady state at the same time. Considering the highest solubility inert gas, both curves attain a plateau after approximately ten breaths, hence no further changes in alveolar gas tensions would be anticipated. This prediction is borne out by inspecting Figure 27 where the falls in P_{aO_2} and P_{aCO_2} are seen to level out after ten breaths. A similar relationship holds for the other inert gases, however, the time at which the dilution effect ceases increasing occurs progressively later for the lower solubility gases.

Additionally, the decrease in P_{aO_2} during the elimination period is also affected by the characteristic shape of the haemoglobin dissociation curve (see Figure 5). When P_{O_2} falls to values below 90 mm Hg, the slope of the curve increases until at about 50 mm Hg the steep portion of the curve is reached. A comparison of the changes in P_{O_2} during the uptake and elimination of the highest solubility inert gas (Table 2) shows that the effects of concentration and dilution are approximately equal until breath four after which the divergence occurs. The change in behaviour is seen to commence when the P_{O_2} falls below 66.8 mm Hg during elimination, that is, the point at which the slope of the dissociation curve begins to increase. The divergence becomes more marked after breath seven; at which time the P_{O_2} has fallen to values on the steep portion of the curve. The lungs therefore react to the dilution of alveolar oxygen tension by decreasing the amount of oxygen transferred to capillary blood, however, as the haemoglobin dissociation curve is steep at lower P_{O_2} values, large decreases in blood oxygen content produce

only small falls in P_{O_2}. The accompanying changes in C_{aO_2} during the uptake and elimination of the inert gases are shown in Figure 29 and illustrates the compensatory falls in blood oxygen content during elimination. It should be noted, however, that the mechanism is only evident to any great extent for the highest solubility gas, hence the rapid washin of nitrogen must be the predominant factor causing the modest fall in arterial P_{O_2} during inert gas elimination.

As the inert gases are excreted into the lungs they must dilute all gas species present in proportion to their relative abundance. Considering carbon dioxide first, any fall in its alveolar tension due to dilution is immediately countered by a rise in carbon dioxide output from the capillary blood tending to restore the alveolar tension to its initial steady state value. For oxygen, however, no such compensating mechanism exists, as gas transfer is always from the alveolar spaces into capillary blood, that is, P_{AO_2} is always greater than $P_{\bar{v}O_2}$ in all instances. The result is therefore a slight fall in P_{ACO_2}, a relatively large fall in P_{AO_2}, and a progressive rise in the repiratory quotient (see Figure 30).

5.3.4 Inert Gas Uptake in Inhomogeneous Lungs

In the homogeneous lung the extent to which P_{aO_2} and P_{aCO_2} change when nitrogen is being replaced by an inert gas has been shown to depend soley upon the solubility of the eluting gas; overall ventilation and blood flow remaining constant. In the non-homogeneous lung, the changes in P_{aO_2} and P_{aCO_2} will depend not only upon the inert gas solubility but also on the regional ventilation and blood flow associated with each of its alveolar compartments. Figure 31 shows the changes in arterial P_{O_2} and P_{CO_2} over the first thirty breaths of inert gas uptake in two such lung models; one having an uneven distribution of ventilation and an even

distribution of blood flow, and the other an uneven distribution of blood flow and an even distribution of ventilation. In both cases the degree of inequality was fairly severe, parameter b being equal to 1.0. Again, four hypothetical inert gases are used in turn to replace the nitrogen of the inspirate; their solubility coefficients being 0.01, 0.1, 1.0 and 10.0.

The increase in arterial P_{O_2} during uptake of the inert gases having solubility coefficients of 10.0, 1.0 and 0.1 are extremely small in comparison to those observed in homogeneous lungs. A greater rise is recorded in lung models having uneven distributions of blood flow, however, than in lung models having uneven distributions of ventilation for the same inert gas. In contrast, the changes in P_{aCO_2} are of the same order as observed in homogeneous lungs, with larger increases associated with lung models having uneven distributions of blood flow. Again, small falls in P_{aO_2} and P_{aCO_2} are observed with the inert gas of lowest solubility ($\lambda = 0.01$).

Considering the uptake of the inert gas of solubility 10.0 for illustration purposes, it can be seen from Figures 32a and 32b that the concentration effect produces more marked increases in the end capillary oxygen contents of blood draining from compartments having $\dot{V}_{IA}/\dot{Q}$ ratios in the range 0.2 to 2.0 as breathing proceeds. Clearly, the increases are greater in the lung model having an uneven distribution of blood flow and an even distribution of ventilation, and, in addition, it will be noted that the compartments in which the greatest increase in oxygen content takes place are also those receiving the highest blood flow. The greater rise in P_{aO_2} in this model is therefore not surprising.

The increase in end capillary carbon dioxide content during the uptake of the inert gas extends over a larger range of $\dot{V}_{IA}/\dot{Q}$ ratios than for oxygen (0.2 to 10.0). The relatively larger increase in P_{aCO_2} in

a lung model having an uneven distribution of blood flow as breathing proceeds is explained by the rise of carbon dioxide content in end capillary blood draining from the lower $\dot{V}_{IA}/\dot{Q}$ ratio compartments which receive the bulk of the pulmonary blood flow. The corresponding increases in the lung model having an uneven distribution of ventilation have a lesser effect upon P_{aCO_2} because of their smaller perfusion.

Smaller, but similar, changes in regional O_2 and CO_2 contents are observed in both lung models during the uptake of inert gases of 1.0 and 0.1, and minute falls in O_2 and CO_2 contents are observed during the induction of the lowest solubility gas ($\lambda = 0.01$) for the reasons detailed previously.

During the uptake of all the inert gases changes occur in $(A - a)D_{O_2}$ and $(A - a)D_{CO_2}$, however, the changes associated with the lower solubility species are insignificant in comparison to the gases having solubilities of 1.0 and 10.0 (see Figure 33). For this reason, the discussion will be limited to the high solubility gases, however, the arguments apply equally to the lower solubility gases. Any increase in $(A -)D_{O_2}$ or $(A - a)D_{CO_2}$ implys that a disproportionate amount of alveolar gas is being expired from compartments which are relatively under perfused, hence the observed changes occuring during inert gas uptake must result from exaggerations of the steady state conditions prevailing in the lung models.

Figures 34a and 34b show the oxygen and carbon dioxide tensions existing in each alveolar compartment of the two lung models at breaths 0, 10, 20 and 30 of the uptake period. As breathing proceeds the uptake of the inert gas tends to concentrate all the components of alveolar gas and hence their respective partial pressures. The effect is more marked, however, in compartments having $\dot{V}_{IA}/\dot{Q}$ ratios between 0.4

and 10.0. Considering the changes in regional oxygen tension first, it can be seen that the greatest increase in P_{O_2} in the lung model having an uneven distribution of ventilation occurs in those compartments receiving the bulk of the ventilation. In contrast, the larger proportion of the blood flow is perfusing alveolar compartments in which the oxygen tension hardly increases at all, hence expired alveolar gas will refelct the high oxygen tensions existing in the under perfused compartments, and the mixed arterial blood will reflect the low oxygen tensions existing in the better perfused compartments. The result is therefore a large $(A - a)D_{O_2}$, which increases with time due to the continuing rise in P_{O_2} in the well ventilated alveolar compartments. Although a similar situation exists in the lung model having an uneven distribution of blood flow, it is seen from Figure 34b that the oxygen tensions in compartments with low $\dot{V}_{IA}/\dot{Q}$ ratios do increase to some extent as breathing proceeds and also the rise in oxygen tension in the poorly perfused compartments is smaller than in the lung model having an uneven distribution of ventilation. Both these factors act to limit the differential increase in expired alveolar and mixed arterial oxygen tensions as breathing of the inert gas mixture proceeds, hence a smaller rise in $(A - a)D_{O_2}$ occurs.

The small fall in $(A - a)D_{CO_2}$ in the lung model having an uneven distribution of ventilation during the uptake of the inert gas of blood solubility 10.0 noted in Figure 33 is explained again by the disproportionate amounts of ventilation coming from compartments with $\dot{V}_{IA}/\dot{Q}$ ratios greater than 0.4. The effect is to weight the expired alveolar gas with a high P_{CO_2} which is not reciprocated by an increase in arterial P_{CO_2} since most of the blood flow is perfusing alveolar compartments in which the carbon dioxide tension increases by only a small amount. The situation is therefore one in which the carbon dioxide tension in expired

alveolar gas, weighted by the high P_{CO_2} existing in the higher $\dot{V}_{IA}/\dot{Q}$ ratio compartments, is less than the CO_2 tension in mixed arterial blood, hence the $(A - a)D_{CO_2}$ falls as breathing proceeds. The rise in $(A - a)D_{CO_2}$ in the lung model having an uneven distribution of blood flow is a result of the increase in carbon dioxide tension in the three well perfused compartments which tends to increase P_{aCO_2} without affecting expired alveolar gas to the same extent.

5.3.5 Steady State Effects of Breathing Inert Gases in Inhomogeneous Lungs

Figure 35 shows the arterial P_{O_2} and P_{CO_2} values obtaining in lung models having uneven distributions of ventilation and even distributions of blood flow, and uneven distributions of blood flow and even distributions of ventilation, during the steady state when breathing mixtures of 21 per cent. oxygen and 79 per cent. inert gases of differing solubilities (λ = 0.01, 0.1, 1.0 and 10.0). Although the characteristic differences in P_{aO_2} and P_{aCO_2} between the two distributions observed during air breathing are retained when nitrogen is replaced by the various inert gases, the resulting P_{aO_2} and P_{aCO_2} values are seen to rise as the solubility of the gases increases.

Essentially, the increases in the arterial gas tensions are due to alterations in regional P_{O_2} and P_{CO_2} caused by the exchange of the inert gases. Even though the net exchange of these gaseous species is zero in the steady state, inert gas must enter the capillary from compartments in which P_{AG} is greater than $P_{\bar{v}G}$ and be excreted from capillary blood in compartments in which P_{AG} is less than $P_{\bar{v}G}$. This gives rise to a continual circulation of the inert gases out of the blood for compartments having lower $\dot{V}_{IA}/\dot{Q}$ ratios and into the blood for compartments having higher $\dot{V}_{IA}/\dot{Q}$ ratios. The amounts of the inert gas thus exchanged will depend upon its blood solubility; larger volumes being

uptaken or excreted where the solubility is high.

In discussing unsteady state gas exchange in the homogeneous lung, it was demonstrated that the uptake of an inert gas gives rise to a concentration effect on oxygen and carbon dioxide, whilst inert gas excretion results in a dilution effect. In the present instance, both mechanisms are occuring simultaneously on a regional basis in each of the lung models, however, as the alveolo-venous pressure difference in all alveolar compartments is small when compared to the gradients existing in the unsteady state, there is relatively little increase in P_{aO_2} and P_{aCO_2} when the solubility of the inert gas is increased. Moreover, as a dilution effect also occurs in some alveolar compartments (that is, those in which P_{AG} is less than $P_{\bar{v}G}$) this must tend to offset the gains in P_{aO_2} and P_{aCO_2} made in compartments where a concentration effect is operating. The fact that net increases in P_{aO_2} and P_{aCO_2} do occur indicates that a greater proportion of the pulmonary blood flow must be perfusing compartments in which P_{AG} is greater than $P_{\bar{v}G}$ in both models.

5.3.6 Inert Gas Elimination in Inhomogeneous Lungs

The changes in arterial P_{O_2} and P_{CO_2} in lung models having uneven distributions of ventilation and even distributions of blood flow, and uneven distributions of blood flow and even distributions of ventilation, during inert gas elimination are shown in Figure 36. The eluting gas is air and the degree of inequality is identical to that assumed for the models in the uptake study, parameter b being equal to 1.0. The gas tensions existing in each of the alveolar compartments and in mixed venous blood prior to the elimination period were obtained from the steady state results detailed in the previous section.

A comparison of the falls in P_{aO_2} and P_{aCO_2} occuring during inert

gas elimination with the rises occuring during uptake, reveals that greater changes occur during the elimination period, with the largest changes again being associated with the lung models having uneven distributions of blood flow.

The reasons for the differences between the two distributions during elimination may be appreciated by referring to Figures 37a and 37b; where the O_2 and CO_2 content lines are shown for the steady state conditions and after thirty breaths of air. The steady state conditions assumed were those obtained when the models were respiring a mixture of 21 per cent. oxygen and 79 per cent. inert gas of blood solubility 10.0. As for the discussion concerned with the uptake of inert gases, similar changes were observed for the lower solubility gases; the highest solubility gas merely being used as a prototype in this context.

Inspection of the O_2 content lines for both distributions, reveals that almost identical falls in oxygen contents are recorded for compartments having $\dot{V}_{IA}/\dot{Q}$ ratios greater than 0.2; compartments with $\dot{V}_{IA}/\dot{Q}$ ratios between 5 and 100 included in the model having the uneven distribution of blood flow have little influence upon overall P_{aO_2} because of their extremely small perfusions (less than 3.1 per cent. of total pulmonary blood flow.) Now, changes in arterial oxygen content must be weighted in favour of those compartments which have the highest blood flows. Clearly, the model having an uneven distribution of blood flow has the most marked falls in oxygen content in the compartments receiving the bulk of the perfusion, whereas the model having an uneven distribution of ventilation has equal perfusions of all compartments. The former model would therefore be expected to display larger falls in mixed arterial contents, and hence P_{aO_2}, during inert gas elimination.

From the CO_2 content lines shown in Figure 37b, it is clear that

the greater falls in carbon dioxide content have occured in the lung model having an uneven distribution of blood flow in comparison to the falls in the model having an uneven distribution of ventilation during the elimination period. The fact that only minor reductions in carbon dioxide contents occur in the three highest $\dot{V}_{IA}/\dot{Q}$ ratio compartments of the model having an uneven distribution of blood flow are inconsequential because of their low perfusion.

CHAPTER 6

SERIES INEQUALITIES

In discussing the possible existence of a series inequality of ventilation in cases of widely distributed emphysema, two important features of this type of abnormality were noted. First, there are increases in the volume of the airways distal to the terminal bronchioles. Taken in the context of the proposed lung model, this feature is equivalent to an enlarged conducting airways compartment. Second, gaseous mixing by molecular diffusion within the terminal airways appeared incomplete during the period of a normal breathing cycle, hence alveolar hypoventilation must ensue. As detailed in Chapter 4, such a condition may be simulated by decreasing the fraction of gas reaching the alveolar compartments from the conducting airways compartments.

The present chapter is primarily concerned with quantifying the effects of both these features upon overall gas exchange during the steady state and unsteady state. Specifically, the effect of differing levels of minute volume, pulmonary blood flow and breathing frequency will be investigated, together with the changes in arterial P_{O_2} when F_{IO_2} is increased above normal for the steady state. The time course changes in arterial P_{O_2} and P_{CO_2} will be monitored during the uptake and elimination of hypothetical inert gases for the unsteady state.

6.1 Model Configuration

In order to reduce the number of variables involved, no regional differences in ventilation or blood flow will be assumed. In addition, as the upper airways compartment serves only to decrease the volume of gas entering the conducting airways compartment by a fixed amount on each breath, it too will be omitted. The model will therefore consist of a single alveolar compartment inspiring gas from the environment through a conducting airways compartment.

6.2 Steady State Gas Exchange

6.2.1 Effect of Increasing the Degree of Series Inequality

Figure 38 shows the changes in arterial P_{O_2} and P_{CO_2} occuring as the series inequality is increased in lung models having different conducting airways compartment volumes during steady state air breathing. Body tissue uptake of oxygen and output of carbon dioxide were held constant at 250 ml/min and 200 ml/min throughout, and the minute volume and pulmonary blood flow were 5 litre/min respectively, breathing frequency being at a rate of 12 breaths per minute.

The characteristic feature that emerges from the results is that arterial P_{CO_2} is affected nearly as much as arterial P_{O_2} when the series inequality becomes more marked. For example, a decrease of 50 per cent. from unity in the fraction of tidal volume* reaching the alveolar compartment from the conducting airways, results in a fall in arterial P_{O_2} of 32 mm Hg and a rise in arterial P_{CO_2} of 25 mm Hg when the volume of the conducting airways is 1,000 ml. It should be noted that the absolute values of P_{aO_2} are lower, and P_{aCO_2} higher, in the lung models having larger conducting airways for the same degree of series inequality.

Two factors are primarily responsible for determining the above steady state arterial oxygen and carbon dioxide tensions in lung models having series inequalities. First, the interposition of the conducting airways compartment between inspired air and alveolar air in the lung model, serves to decrease the oxygen tension and increase the carbon dioxide tension of gas entering the alveolar compartment. This

---

* In the present context, minute volume is defined as the flow rate of air into the conducting airways per minute, and not the flow rate of air into the alveolar compartment as in the previous chapter.

contamination of the inspirate results from the fact that the conducting airways act as a reservoir through which alveolar gas must pass on route to the environment during expiration, hence the composition of gas in this region must reflect both environmental and alveolar air. Second, as the degree of series inequality becomes more marked, the $\dot{V}_{IA}/\dot{Q}$ ratio of the alveolar compartment decreases because it is now receiving a physically smaller volume of gas.

Although it is intuitively obvious that both the above factors will tend to reduce arterial P_{O_2}, and increase arterial P_{CO_2}, the latter clearly has the greater influence in determining the manner in which arterial P_{O_2} and P_{CO_2} change when the degree of inequality increases, as a comparison of the curves resulting from models having finite conducting airways volumes, with the model having a negligible conducting airways volume illustrates (Figure 38). It is clear that the shape of all the curves is identical, and the volume of the conducting airways compartment only alters the absolute values of P_{aO_2} and P_{aCO_2} for any given degree of series inequality.

The reason for the existence of different P_{O_2} and P_{CO_2} values in alveolar compartments having the same degree of inequality (i.e.the same $\dot{V}_{IA}/\dot{Q}$ ratio), but differing conducting airways volumes, may best be appreciated by considering the changes in gas tensions in the lung models during the first half of the breathing cycle. During inspiration, the oxygen and carbon dioxide tensions in the conducting airways are determined by the ratio of inspired volume to the volume of the conducting airways compartment. If the ratio is low, the resulting gas composition will be weighted towards that present in the conducting airways prior to inspiration. Conversely, if the ratio is high, then the gas composition will be weighted in favour of environmental gas. Higher P_{O_2}

and lower P_{CO_2} values will, therefore, be produced in conducting airways having smaller volumes during inspiration, and as this gas forms the inspirate for the alveolar compartment, alveolar P_{O_2} and P_{CO_2} must also be affected. As we are dealing with a steady state condition, the simplified equations defining alveolar P_{O_2} and P_{CO_2} derived in Chapter 5 may be utilised to assess the resulting changes in these gas tensions (i.e. equations 35 and 36). Rewriting these equations, but replacing the terms P_{IO_2} and P_{ICO_2} by P_{IAO_2} and P_{IACO_2} respectively to distinguish between gas being inspired from the environment, and gas being inspired from the conducting airways, we obtain

$$P_{AO_2} = \frac{P_{IAO_2} \cdot V_{IA} + \frac{\dot{Q}\,(P_{Bar} - 47)}{100f}\,(C_{AO_2} - C_{\bar{v}O_2})}{V_{IA} - \Delta V_{O_2} + \Delta V_{CO_2}} \quad \ldots\ldots\ldots\ldots (37)$$

$$P_{ACO_2} = \frac{P_{IACO_2} \cdot V_{IA} + \frac{\dot{Q}\,(P_{Bar} - 47)}{100f}\,(C_{ACO_2} - C_{\bar{v}CO_2})}{V_{IA} - \Delta V_{O_2} + \Delta V_{CO_2}} \quad \ldots\ldots\ldots\ldots (38)$$

Obviously, any increase in P_{IAO_2} will produce a higher P_{AO_2}, and any decrease in P_{IACO_2} will produce an equivalently lower P_{ACO_2}. The observed differences in alveolar, and hence arterial, P_{O_2} and P_{CO_2} in lung models having the same degree of series inequality and differing conducting airways compartment volumes are therefore to be expected.

The accompanying changes in mixed venous P_{O_2} and P_{CO_2} are shown in Figure 39. It can be seen that as the degree of series inequality increases, there is initially very little change in mixed venous P_{O_2}, whereas the venous P_{CO_2} climbs rapidly. Moreover, mixed venous P_{O_2} is higher in lung models having lower arterial P_{O_2} values for the

smaller degrees of series inequality. This unexpected finding can be attributed to the changes in oxygen tension which occur when the oxygen content remains nearly constant (actually, the venous oxygen content is slightly greater for the lung models having smaller conducting airways) but the carbon dioxide tension is lowered; the so-called "Bohr effect".

6.2.2 Effect of Increasing Minute Volume

The effect of increasing minute volume to a lung model having a conducting airways compartment volume of 500 ml, and a series inequality such that only 40 per cent. of the gas inspired into the conducting airways actually enters the alveolar compartment, is shown in Figure 40. As the minute volume increases, dramatic changes occur in both arterial P_{O_2} and P_{CO_2}. For example, the P_{aO_2} and P_{aCO_2} values of 50 mm Hg and 81 mm Hg recorded at a minute volume of 5 litre/min are altered to the more normal values of 100 mm Hg and 40 mm Hg when the minute volume is doubled.

Somewhat surprising changes are seen in venous P_{O_2} when the minute volume is raised (Figure 41). For increases in minute volume between 5 litre/min and 7.5 litre/min, appreciable gains are made in $P_{\bar{v}O_2}$, however, further increases paradoxically result in falls in $P_{\bar{v}O_2}$ although the venous blood oxygen content continues to rise. Again, this unexpected finding can be attributed to the Bohr effect; that is, the falls in $P_{\bar{v}CO_2}$ cause the oxygen dissociation curve to shift to the left, hence the gains in arterial oxygen content are not reflected by concomitant increases in $P_{\bar{v}O_2}$.

6.2.3 Effect of Increasing Pulmonary Blood Flow

Increases in pulmonary blood flow are seen to produce only modest rises in arterial P_{O_2} and only marginally greater falls in arterial P_{CO_2} (Figure 42); similar insignificant changes being observed

in mixed venous gas tensions (Figure 43). The structural configuration of the lung model is identical with that investigated in the previous section with regard to both conducting airways volume and degree of series inequality. Minute volume and breathing frequency were held constant at 5 litre/min and 12 breaths per minute throughout. The changes observed were very similar to those found for regional inequalities and are attributed to the same causes. Any gains in venous P_{O_2} and falls in venous P_{CO_2} resulting from the increased systemic blood flow being counteracted by the lowering of the $\dot{V}_{IA}/\dot{Q}$ ratios of the alveolar compartments, hence there is very little improvement in the arterial levels of P_{O_2} or P_{CO_2}.

6.2.4 Effect of Increasing Breathing Frequency

Figure 44 shows the effect on arterial P_{O_2} and P_{CO_2} of varying the frequency of breathing whilst retaining constant the minute volume and pulmonary blood flow at 5 litre/min respectively in two lung models, one having a fairly mild, and the other a more severe, degree of series inequality. In both models the volume of the conducting airways compartment was 500 ml.

It was stated when discussing the effect of increasing the series inequality that the composition of the conducting airways gas (i.e. inspired alveolar gas) was dependent upon the ratio of inspired volume to the volume of the conducting airways. The results obtained for the lung model having the less marked degree of series inequality (80 per cent. of the tidal volume entering the alveolar compartment), tends to conform to this pattern, in that increasing the frequency of breathing decreases the volume of gas being inspired into the conducting airways per breath, and hence reduces the ratio. No changes occur in the $\dot{V}_{IA}/\dot{Q}$ ratio of the alveolar compartment since increasing the frequency

of breathing reduces the volume of blood perfusing the alveolar compartment per breath in the same proportion as the inspired volume, hence the observed changes in P_{aO_2} and P_{aCO_2} are entirely due to the influence of the conducting airways compartment.

The changes in arterial P_{O_2} and P_{CO_2} in the lung model having the more marked degree of series inequality (40 per cent. of tidal volume entering the alveolar compartment) do not at first sight appear to wholly concurr with the above results, in that increasing the frequency of breathing above 10 breaths/min causes the P_{aO_2} to rise and P_{aCO_2} to fall. It should, however, be borne in mind that as the frequency of breathing increases, there is less contamination of conducting airways gas by alveolar air because smaller volumes of inspired gas reach the alveolar compartment, and hence proportionally smaller volumes of alveolar air are expired into the conducting airways. As a result the pre-inspiratory* levels of P_{O_2} and P_{CO_2} in the conducting airways are closer to those existing prior to the expiration of alveolar air, and gas inspired from the environment is therefore able to raise P_{O_2}, and lower P_{CO_2}, in the conducting airways to a greater extent on the following breath. The composition of inspired alveolar gas is hence improved (i.e.higher P_{O_2} and lower P_{CO_2}) and a concomitant rise in P_{aO_2} and fall in P_{aCO_2} results.

6.2.5 Effect of Increasing Inspired Oxygen Concentration

Figure 45 shows that rapid gains are made in arterial P_{O_2} when the inspired oxygen concentration is increased in models with both small degrees of series inequality (i.e. 80 per cent. of inspired volume entering alveoli) and large degrees of series inequality (i.e. 40 per

---

*i.e. the condition of the conducting airways after alveolar air has been expired, completely mixed, and an equal volume of the resulting gas excreted to the environment.

cent of inspired volume entering alveoli).

This result is hardly surprising in view of previous work (see page 52), which has shown that so long as an alveolar compartment has a $\dot{V}_{IA}/\dot{Q}$ ratio greater than 0.2, complete saturation of haemoglobin will be accomplished on increasing the F_{IO_2} to 40 per cent.

6.3 Unsteady State Gas Exchange

The uptake and elimination of the same hypothetical inert gases considered in the previous chapter (λ = 0.01, 0.1, 1.0 and 10.0) will be used to study the behaviour of lungs having series inequalities during the unsteady state. Only one particular model will actually be presented, however, previous work has indicated that its response during the unsteady stste is typical of a whole spectrum of models embodying series inequalities. It has an alveolar compartment volume of 2,400 ml, a conducting airways compartment volume of 500 ml, and a degree of series inequality such that only 40 per cent. of the minute volume reaches the alveolar regions. Inspection of Figures 38 and 39 show that during steady state air breathing, the model's arterial P_{O_2} and P_{CO_2} are 49.6 mm Hg and 80.8 mm Hg, and the venous P_{O_2} and P_{CO_2} are 33.2 mm Hg and 83.8 mm Hg, with a minute volume of 5 litre/min, pulmonary blood flow 5 litre/min and breathing frequency 12 breaths/min.

6.3.1 Inert Gas Uptake

Figure 46 shows the changes in arterial P_{O_2} and P_{CO_2} occuring in the model after the steady state is upset by replacing the normal (air) inspirate of 21 per cent. oxygen, 79 per cent. nitrogen by a mixture of 21 per cent. oxygen and 79 per cent. inert gases of differing blood solubilities. In many respects the curves are reminiscent of those obtained for homogeneous lungs (see Figure 24), however, two important differences should be noted. First, the increases in arterial P_{O_2} are

some five to ten times less, and the increases in arterial P_{CO_2} three to four times greater, in the present model having a series inequality than in the homogeneous lung model. Second, whereas arterial P_{O_2} always increases to a greater extent than arterial P_{CO_2} in the homogeneous lung, and indeed in lungs having regional inequalities; this is not invariably the case with the series inequality model. An examination of Figure 46 reveals that during the uptake of the inert gas of blood solubility 0.1, relatively greater changes occur in arterial P_{aCO_2} than in P_{aO_2} throughout the thirty breaths simulated. For the two higher solubility gases (λ_G= 1.0 and 10.0), the pattern is not so uniform; changes in arterial P_{CO_2} being greater than arterial P_{O_2} during the initial stages of inert gas uptake, but arterial P_{O_2} increasing to a greater extent subsequently.

Because of the alveolar hypoventilation in lung models having series inequalities, less inert gas enters the arterial blood from the airspaces in a given time compared to a homogeneous lung. This is clearly evident from an examination of Figure 47; where the uptake of all the inert gases in the present model are shown. A diminution in the concentration effect upon oxygen and carbon dioxide must therefore follow, since the major factor causing the phenomenon is the uptake rate of the inert gas. In addition, the low alveolar ventilations must result in correspondingly low expired volumes; a feature that is exaggerated by the net uptake of the inert gases. Nitrogen will therefore be retained in the alveolar compartments to a greater extent and act as a passive "filler" gas effectively reducing the increase in oxygen tension. This reduction in expired alveolar volume also explains why arterial P_{CO_2} rises more appreciably in models having series inequalities, even though the concentration effect is reduced, by causing carbon dioxide retention in the alveolar spaces.

An interesting feature to emerge from the results, is the relative changes in arterial P_{O_2} and P_{CO_2} as breathing of the inert gases proceeds. When discussing the role of the concentration effect upon arterial P_{O_2} and P_{CO_2} in the homogeneous lung (page 55), the relatively greater increases in P_{O_2} observed were attributed to the slope of the haemoglobin dissociation curve. In the cases studied at that time, the steady state P_{O_2} values* corresponded to the "flat" portion of the dissociation curve, hence little further oxygen could be absorbed into the capillary blood, and the P_{O_2} increased. The arterial P_{CO_2}, by contrast, showed only a small change since additional carbon dioxide is easily absorbed into the blood because of the steep slope of its dissociation curve. In the series inequality model under consideration here, the arterial P_{O_2} attained when breathing air in the steady-state is only 49.7 mm Hg; a value corresponding to the steep portion of the haemoglobin dissociation curve. Now it transpires that the slope of the carbon dioxide dissociation curve is in fact less then that of the haemoglobin dissociation curve for the range of oxygen and carbon dioxide tension encountered during the uptake of the inert gas having a blood solubility of 0.1. Oxygen is therefore more "chemically soluble" in blood than carbon dioxide, hence the concentration effect will affect carbon dioxide to a greater extent in this situation. Examination of the rate of increase of arterial P_{O_2} and P_{CO_2} during the uptake of the higher solubility gases shows that the rate of increase of P_{aCO_2} exceeds that of P_{aO_2} until breath twenty for the gas having a solubility of 1.0, and breath ten for the gas having a solubility of 10.0. In both instances, the arterial P_{O_2} and P_{CO_2} at which the change occurs are

---

*i.e. the P_{O_2} values existing in the model prior to the onset of inert gas breathing.

approximately the same * and represent those points on the respective dissociation curves at which the slopes are equal. For all P_{O_2} values below this point carbon dioxide is less chemically soluble than oxygen (i.e. its dissociation curve is flatter) and is therefore concentrated to a greater extent. At higher P_{O_2} and P_{CO_2} values, oxygen is less chemically soluble than carbon dioxide and there is a reversal in behaviour, oxygen now being concentrated more than carbon dioxide.

6.3.2 Steady State Inert Gas Breathing

On completely replacing nitrogen in the model by an alternative inert gas, no change in the arterial P_{O_2} or P_{CO_2} occurs regardless of the blood solubility of the gas. A full discussion has already been given to this topic in Chapter 5, where it was demonstrated mathematically that provided a lung model consisted of only one functional alveolar compartment the steady state arterial gas tensions would be independent of the solubility of the inert gas.

6.3.3 Inert Gas Elimination

Figure 48 shows the changes occuring in the arterial P_{O_2} and P_{CO_2} of lung models with series inequalities, which, having reached a steady state condition with 21 per cent. oxygen, 79 per cent. inert gas mixtures, are switched back to air breathing. The blood solubilities of the inert gas present in the steady state are again 0.01, 0.1, 1.0 and 10.0 respectively.

During the elimination of the inert gases having blood solubilities of 0.1 and 1.0, arterial P_{O_2} decreases to a greater extent than arterial

---

*P_{aO_2} = 62.7 mm Hg and P_{aCO_2} = 93.8 mm Hg with λ= 1.0;
P_{aO_2} = 63.4 mm Hg and P_{aCO_2} = 94.8 mm Hg with λ= 10.0

P_{CO_2}, however, the situation is reversed for the highest solubility gas (λ_G= 10.0), where arterial P_{CO_2} is seen to decrease more than arterial P_{O_2}. The excretion of the inert gases into the alveolar compartments serves to dilute both oxygen and carbon dioxide as breathing proceeds; the amount by which the tension of each gas is reduced being a function of both the flow rate of the inert gas from the capillaries, and the chemical solubility of oxygen and carbon dioxide in blood. Obviously, the higher the inert gas solubility, the greater will be the flow rate during elimination, resulting in a more marked dilution effect. At the very low oxygen tensions reached during the elimination of the highest solubility gas, the haemoglobin dissociation curve is <u>steeper</u> than the carbon dioxide dissociation curve, that is, it is chemically more soluble. P_{O_2} is therefore affected to a <u>lesser</u> degree than P_{CO_2} by the dilution effect since it is more easily absorbed in blood, and as a result arterial P_{CO_2} <u>decreases</u> more than arterial P_{O_2}. For the elimination of the lower solubility inert gases the slope of the carbon dioxide dissociation curve is always greater than that of the haemoglobin dissociation curve, hence arterial P_{CO_2} is less affected by dilution than arterial P_{O_2}.

An interesting finding was that arterial P_{O_2} fell <u>below</u> the venous level after eight breaths during the elimination of the highest solubility gas. Further examination of the arterial oxygen content, however, revealed that C_{aO_2} did <u>not</u> in fact decrease below $C_{\bar{v}O_2}$, but fell steadily from the steady state level over the first fifteen breaths and then remained at an almost constant value some 0.2 ml/100 ml above the venous point. The continuing fall in arterial P_{O_2} is therefore attributed to the Bohr effect which results from the concomitant falls in arterial P_{CO_2}.

CHAPTER 7

PULMONARY BLOOD SHUNTS

Although the occurence of diseases actually causing increases above normal in the amounts of venous blood being shunted directly into the arterial stream is comparitively rare, the phenomenon itself is of considerable clinical importance as it may manifest itself in patients having normal lungs under specific conditions. The purpose of the present chapter is therefore to assess the effects of increases in pulmonary shunt upon steady state arterial and venous P_{O_2} and P_{CO_2} when breathing air, and to investigate the resulting changes in these variables when minute volume, cardiac output and inspired oxygen concentration are increased. The unsteady state will be studied in a similar manner to that adopted for the other functional defects, namely, by monitoring the changes in arterial and expired alveolar P_{O_2} and P_{CO_2} during the uptake and elimination of a number of hypothetical inert gases.

7.1 Model Configuration

As the parameter under consideration in the present chapter is pulmonary shunt, regional differences in ventilation and perfusion will be ignored, as will series inequalities, hence the model will consist of a single alveolar compartment being directly ventilated from the environment. The pulmonary shunt is simulated by allowing various percentages of cardiac output to bypass the alveolar compartment in the manner detailed in Chapter 4.

7.2 Steady State Gas Exchange

7.2.1 Effect of Increased Pulmonary Shunt

Figure 49 shows the steady state arterial P_{O_2} and P_{CO_2} values existing in lung models as the percentage of pulmonary shunt is increased. In all cases the minute volume was 5 litre/min, the cardiac output

5 litre/min and the breathing frequency of 12 breaths/min, and an oxygen consumption of 250 ml/min and a carbon dioxide output of 200 ml/min were assumed. It can be seen that the precipitous fall in arterial P_{O_2} is not reciprocated by an accompanying rise in arterial P_{CO_2}. For example, when the percentage of shunt is increased from zero (homogeneous lung) to 40 per cent., the arterial P_{O_2} changes from 115.5 mm Hg to 43.0 mm Hg, a fall of 72.5 mm Hg, whilst the arterial P_{CO_2} increases by a mere 2 mm Hg.

Only that part of the cardiac output that perfuses the alveolar compartment; the so-called capillary blood flow; can exchange gas with the environment. It must therefore be responsible for adding <u>all</u> the oxygen and removing <u>all</u> the carbon dioxide demanded by body tissue metabolism. The blood flow bypassing the alveolar compartment through the shunt takes no part in gas exchange hence the mixed arterial blood contents are determined soley by the capillary blood flow. It is therefore to be expected that as the percentage of shunt increases, the carbon dioxide content of arterial blood will rise, and the oxygen content fall, by amounts whose <u>ratio</u> must equal the respiratory quotient; 0.8 in the present instance. Table 3; which lists the end capillary contents, mixed arterial contents and mixed venous contents of oxygen and carbon dioxide for various percentages of pulmonary shunt, confirms this fact and in addition shows that very little change occurs in the end capillary contents as the amount of shunt increases. In view of the reduction in capillary blood flow, and therefore the increase in the $\dot{V}_{IA}/\dot{Q}$ ratio, of the alveolar compartment an improvement in the end capillary gas contents might have been anticipated. That this did not materialise is explained by the deterioration of oxygen and carbon dioxide levels in mixed venous blood. It can be seen (Table 3) that they too change in a ratio equal to the respiratory quotient as the shunt increases, and always reflect the fixed arterio-venous carbon dioxide and oxygen differences of 4 ml/100 ml

and 5 ml/100 ml respectively.

The gross differences in the behaviour of arterial P_{O_2} and P_{CO_2} as the percentage of shunt increases as a result of the very different shapes of the respective dissociation curves. For oxygen, small falls in content are accompanied by very large falls in partial pressure, whereas the shape of the carbon dioxide dissociation curve represents an almost "one-to-one" relationship between blood content and partial pressure, hence only modest increases in arterial P_{CO_2} occur. In addition, as the arterial blood becomes more desaturated, the carbon dioxide dissociation curve is shifted to the right (Haldane effect) therefore the potentially higher carbon dioxide tensions are also reduced to an extent by this mechanism.

The simultaneous changes occuring in mixed venous P_{O_2} and P_{CO_2} as the percentage of pulmonary shunt increases are shown in Figure 50. Again, the falls in oxygen tension are more severe than the increases in carbon dioxide tension, however, they are of a lesser order than the falls in arterial P_{O_2} because the venous oxygen contents correspond to the steeper portion of the haemoglobin dissociation curve.

7.2.2 Effects of Increasing Minute Volume

Figure 51 shows the steady state arterial P_{O_2} and P_{CO_2} values obtaining in a lung model having a 40 per cent. blood shunt at different levels of minute volume. Throughout, the cardiac output and breathing frequency were 5 litre/min and 12 breaths/min, and the body uptake of oxygen and output of carbon dioxide remained at their normal values of 250 ml/min and 200 ml/min respectively.

It can be seen that although arterial P_{CO_2} falls with increases in ventilation, arterial P_{O_2} also <u>falls</u> even though its arterial content shows a small rise. Again, this paradoxical fall in arterial P_{O_2} can

be explained by the interaction of the haemoglobin and carbon dioxide dissociation curves.

Increasing the minute volume produces almost equal changes in alveolar (and therefore end capillary) oxygen and carbon dioxide tensions; P_{O_2} rising and P_{CO_2} falling. However, as haemoglobin is virtually saturated with oxygen at the partial pressures encountered, end capillary oxygen content increases by only very small amounts in comparison to the large falls in carbon dioxide content. As a result, the arterial oxygen content remains almost constant as minute volume increases, but appreciable falls are recorded for carbon dioxide. The observed fall in arterial P_{O_2} is a consequence of the shift to the left of the haemoglobin dissociation curve produced by the reduction in arterial P_{CO_2} (Bohr effect); the near constant oxygen contents being now associated with lower partial pressures.

Figure 52 shows the corresponding changes in mixed venous P_{O_2} and P_{CO_2} as minute volume increases. Again the paradoxical fall in oxygen tension is explained in terms of the Bohr effect, brought about by the falls in $P_{\bar{v}CO_2}$.

7.2.3 Effect of Increasing Cardiac Output

Figures 53 and 54 show how steady state arterial and mixed venous P_{O_2} and P_{CO_2} values change as the cardiac output is increased to a lung model identical to the one studied above. In the present instance, minute volume is held constant at 5 litre/min, the other parameters remaining at their previous values. As the cardiac output is raised, useful gains are made in both arterial and mixed venous P_{O_2} but little improvement is evident for carbon dioxide. For example, a twofold increase in cardiac output from 5 litre/min to 15 litre/min results in increases of 10.5 mm Hg and 11.0 mm Hg in P_{aO_2} and $P_{\bar{v}O_2}$ respectively,

whilst the corresponding decreases in P_{aCO_2} and $P_{\bar{v}CO_2}$ are only 0.5 mm Hg and 2 mm Hg respectively.

Reiterating the earlier finding, any increase in cardiac output results in a reduction in the amount of oxygen removed from, and carbon dioxide added to, each unit volume of arterial blood, whilst simultaneously lowering the $\dot{V}_{IA}/\dot{Q}$ ratios in the lungs. In the present instance the potential improvements in venous P_{CO_2} are counteracted by an increase in end capillary carbon dioxide content thus the mixed arterial P_{CO_2} remains virtually constant as cardiac output increases. For oxygen, however, the decrease in $\dot{V}_{IA}/\dot{Q}$ ratio of the alveolar compartment results only in a minute fall in end capillary contents, hence full advantage is taken of the rise in mixed venous oxygen content, and arterial P_{O_2} improves.

7.2.4 Effect of Increasing Inspired Oxygen Concentration

An examination of Figure 49 reveals that the presence of pulmonary shunts primarily affects arterial P_{O_2} whilst arterial P_{CO_2} is hardly altered from normal. It is therefore tempting to suggest that this defect might be remedied by increasing the inspired oxygen concentration. Further reflection, however, shows that such a manoeuvre could not improve arterial P_{O_2} to any extent since the haemoglobin contained in the erythrocytes of capillary blood draining from the alveolar compartment is fully saturated with oxygen when breathing air. Further increases in P_{IO_2} would therefore only serve to increase the small proportion of oxygen carried in simple solution in blood plasma. Figure 55 confirms this argument, and also illustrates that even when the amount of shunt is small (i.e.20 per cent.) no improvements in P_{aO_2} occur on increasing the inspired oxygen concentration.

7.3 Unsteady State Gas Exchange

7.3.1 Inert Gas Uptake

Figure 56 shows the changes occuring in arterial P_{O_2} and P_{CO_2} in a lung model having a 40 per cent. pulmonary blood shunt when air is replaced as the inspirate by mixtures of 21 per cent. oxygen and 79 per cent. inert gases of differing blood solubilities (λ = .01, .1, 1 and 10). Although the increase in the arterial gas tensions are small in comparison to those observed with the other functional defects, it is interesting to note that arterial P_{CO_2} is affected to a greater extent than arterial P_{O_2} during the period of inert gas uptake regardless of the blood solubility of the particular gas. This feature has been found in lung models having a wide range of pulmonary shunts and appears to be an inherent characteristic of this functional defect.*

The changes in P_{O_2} and P_{CO_2} during the unsteady state have been fully discussed in a previous chapter (i.e.chapter 5), but briefly, the net uptake of the inert gases causes oxygen and carbon dioxide to assume higher fractions of alveolar gas, hence their partial pressures increase. Consequently, the contents of oxygen and carbon dioxide in end capillary blood rise, but because of the different "chemical solubilities" of the two gases (i.e.the shape of their dissociation curves) a greater increase in carbon dioxide content occurs. Now, in the present situation, mixed arterial blood composition is determined not only by the end capillary contents, but also by the contribution of blood flowing through the shunt. However, as the composition of the latter is assumed to remain constant at the steady state level, the observed changes in arterial blood must result entirely from the changes in end capillary composition. Since the end capillary carbon dioxide content increases to a greater extent than that of oxygen, since haemoglobin is fully saturated, it causes a greater change in mixed arterial contents which produces an equivalent

*Unpublished work (Scrimshire)

rise in arterial P_{CO_2}.

Although the small increase in end capillary oxygen content can only change the content of mixed arterial blood by a minute amount, P_{aO_2} still shows an appreciable increase as inert gas breathing proceeds. This is more astonishing since the haemoglobin dissociation curve is steep at the oxygen levels encountered in arterial blood, hence very little change in oxygen tension is expected. The observed increases in arterial P_{O_2} can therefore only be attributed to the Bohr effect caused by the rise in carbon dioxide tension. The nearly equal oxygen contents will therefore be associated with higher partial pressures because of the shift of the haemoglobin dissociation curve to the right.

7.3.2 Steady State Inert Gas Breathing

As we are again dealing with a single alveolar compartment model no changes in the arterial or venous P_{O_2} and P_{CO_2} occur when nitrogen is completely replaced by an other inert gas. The steady state conditions existing in a lung model having a 40 per cent. shunt during air breathing therefore also represent the conditions when the model is respiring a 21 per cent. oxygen, 79 per cent. inert gas mixture, and will be used as initial conditions for the following section.

7.3.3 Inert Gas Elimination

Figure 57 shows how arterial P_{O_2} and P_{CO_2} change as various inert gases are eliminated from venous blood into a lung model having a 40 per cent. pulmonary shunt. It can be seen that for the lower solubility gases (λ = .01, .1 and 1) arterial P_{CO_2} falls to a greater extent than arterial P_{O_2} over the thirty breaths simulated. For the highest solubility gas (λ = 10) a reversal in this pattern is seen after breath thirteen where arterial P_{O_2} decreases more than in arterial P_{CO_2}.

The falls in arterial P_{O_2} and P_{CO_2} during the elimination

period are a result of the dilution of alveolar P_{O_2} and P_{CO_2} by the excretion of the inert gases from capillary blood. The relatively greater changes in arterial P_{CO_2} for the lower solubility gases arise for the same reasons as discussed for uptake, namely, that end capillary carbon dioxide contents are affected to a greater extent than oxygen contents by changes in alveolar tensions. The change in the behaviour observed for the highest solubility gas is attributed to the very low P_{O_2} values reached in the alveolar compartment, and therefore in end capillary blood, as elimination proceeds. Such oxygen tensions correspond to the steep portion of the haemoglobin dissociation curve, hence the rate at which oxygen content falls now exceeds that of carbon dioxide. As a result, the decreases in arterial P_{O_2} exceed those in arterial P_{CO_2}.

CHAPTER 8

DISCUSSION

Numerous papers have been published concerned with assessing pulmonary defects either by direct measurement of alveolar and arterial gas tensions or indirectly by the use of scematised models for the interpretation of data. Few of the proposed tests, however, appear to have undergone any vigorous verification. Instead, they are usually held as adequate until new data with which they are not compatible becomes available, at which time they are discarded.

The model proposed in this thesis provides a unique opportunity for checking the degree of discrimination of such tests. By arranging for a specific functional defect to be simulated, the tests can be applied to the model in turn, and the closeness with which the derived descriptions of the defects accord with that actually existing in the model may be taken as a measure of the effectiveness of the individual tests.

8.1 Alveolar - arterial O_2 Difference

As the alveolar membrane causes no appreciable barrier to oxygen transfer in the majority of lung diseases (92) the observed difference between oxygen tension in the mixed alveolar gas and in arterial (pulmonary venous) blood flow must arise from inequalities in pulmonary ventilation and/or blood flow.

Inspection of Figure 58, in which the $(A - a)D_{O_2}$ values existing in models having (a) uneven regional ventilation, (b) uneven regional blood flow, (c) series inequalities and (d) blood shunts, shows that essentially similar results are obtained in each case; $(A - a)D_{O_2}$ increasing as the respective degrees of inequality become more marked.

The alveolar - arterial O_2 difference is usually explained by

the fact that the alveolar regions having high $\dot{V}_{IA}/\dot{Q}$ ratios must contribute more to ventilation than to blood flow, the opposite being true for alveolar regions having low $\dot{V}_{IA}/\dot{Q}$ ratios (114). Since the gas content of the former is high in oxygen, whilst that of the latter is low it follows that the mixed alveolar gas tensions must be higher than that of the arterial blood. This difference is increased by the non-linear shape of the haemoglobin dissociation curve (77). Although this explanation appears to fit the regional inequalities models quite well, in that both distributions contain compartments with high and low $\dot{V}_{IA}/\dot{Q}$ ratios, it is not immediately obvious why a large $(A - a)D_{O_2}$ materialises in models having series inequalities since they contain only one alveolar compartment which by definition has a low $\dot{V}_{IA}/\dot{Q}$ ratio. This anomaly is easily reconciled by considering the form of the series inequality model (see figure below). As expired alveolar gas is defined as that gas leaving the conducting airways compartment, it must

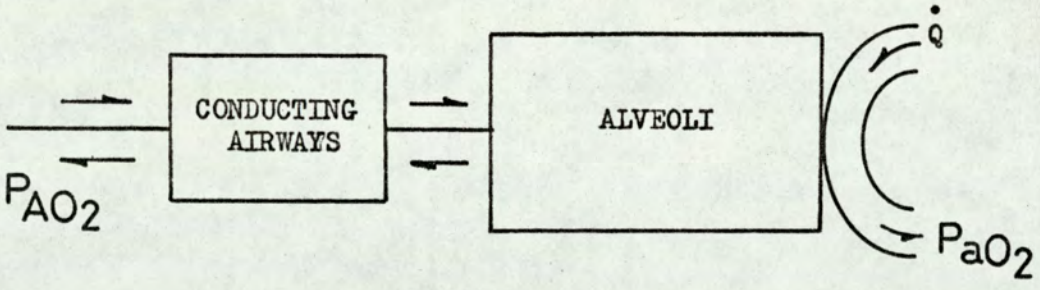

have a higher P_{O_2} than that existing in arterial blood since the conducting airways contain a high proportion of fresh inspired gas which is thoroughly mixed with alveolar air before expiration. The defect therefore behaves as a high $\dot{V}_{IA}/\dot{Q}$ ratio as far as the gas phase is concerned, and as a low $\dot{V}_{IA}/\dot{Q}$ ratio for the blood phase. As a result, $(A - a)D_{O_2}$ can exist in a lung having a series inequality in much the same way as in lungs having regional inequalities.

The observed rise in $(A - a)D_{O_2}$ in models having increasing amounts

of blood shunt is not surprising since the defect is equivalent to a two-compartment model with an uneven distribution of ventilation; one compartment having a moderately high $\dot{V}_{IA}/\dot{Q}$ ratio and the other a $\dot{V}_{IA}/\dot{Q}$ ratio of zero. As the amount of shunt increases, arterial oxygen tension is lowered by the addition of venous blood, and mixed expired alveolar oxygen tension rises slightly because of the increase in the alveolar compartment's $\dot{V}_{IA}/\dot{Q}$ ratio. The latter factor, however, has been shown to be small (see Chapter 7), hence the arterial contamination by venous blood must be primarily responsible for the rise in $(A - a)D_{O_2}$.

Increasing minute volume was shown to affect $(A - a)D_{O_2}$ in models having fairly severe regional inequalities in Chapter 4. These results are reproduced in Figure 59 together with corresponding data derived from models having series inequalities and pulmonary shunts. The degree of inequality in the former model was such that only 40 per cent. of the tidal volume actually entered the alveolar compartment per breath, and the latter model had 40 per cent. of cardiac output shunted directly into the arterial stream. It can be seen that in general increasing the minute volume increases the $(A - a)D_{O_2}$ in the models having either regional inequalities of ventilation or direct pulmonary blood shunts, whereas a decrease in $(A - a)D_{O_2}$ is noted in models having either regional inequalities of blood flow or series defects. Although the examples cited refer to only one "degree of inequality" similar changes are found over the whole spectrum.

Because of the difficulty of keeping minute volume constant at various levels whilst steady state conditions are obtained, especially in subjects suffering from chronic lung diseases, the above manoeuvre would prove difficult in practice. However, as an increased minute volume serves to add more oxygen to the lungs, the simple act of increasing F_{IO_2}

might produce similar effects and would be easier to perform under controlled conditions. Figure 60 shows the resulting $(A - a)D_{O_2}$ values in the same models as used previously (Figure 59), and clearly confirms this expectation, indeed, the differences between the various functional defects are considerably magnified.

By the use of theoretical calculations, Farhi and Rahn (39) showed that if the $(A - a)D_{O_2}$ breathing air is due to pulmonary blood shunt, an increase in inspired oxygen concentration should rapidly raise the O_2 difference. Inspection of the relationship between $(A - a)D_{O_2}$ and F_{IO_2} obtained from the models having an uneven distribution of ventilation (Figure 60), however, reveals that an almost equal rise in $(A - a)D_{O_2}$ occurs in this model as in the model having a true pulmonary shunt. It is therefore concluded that in the measurement of $(A - a)D_{O_2}$ at F_{IO_2} values of less than 80 per cent. would be unable to distinguish between true shunts and uneven regional distributions of ventilation, if the degree of the inequality is fairly severe.

Since the major inequality in healthy upright lungs lies in the relationship between regional blood flow and lung volume (112), the results would indicate that when F_{IO_2} is increased in normals, a small rise in $(A - a)D_{O_2}$ would occur inintially, however, further increases in F_{IO_2} would result in a fall in $(A - a)D_{O_2}$. This finding concurrs with the data of Cole and Bishop (21) who obtained an increase in the oxygen difference when P_{IO_2} was raised to 291 mm Hg and a subsequent fall when further increments in inspired oxygen were made.

8.2 Alveolar - arterial C_{O_2} Difference

When considering the cause of $(A - a)D_{O_2}$ it was stated that in a non-homogeneous lung, the mixed expired alveolar gas, being weighted in favour of elements having a high $\dot{V}_{IA}/\dot{Q}$ ratio and a high P_{O_2}, will have an

elevated oxygen tension, while the arterial blood will have a decreased oxygen tension because of the influence of low $\dot{V}_{IA}/\dot{Q}$ elements contributing poorly oxygenated blood. A similar reasoning may be applied to carbon dioxide and leads to the conclusion that the mixed expired alveolar gas will exhibit a lower CO_2 tension than the arterial blood. This is confirmed by Figures 61 (a), (b), (c) and (d), which show how $(A - a)D_{O_2}$ changes as the respective degrees of inequality in the four models discussed previously are increased.

Both the well established maxim that pulmonary shunts have almost no effect upon $(A - a)D_{CO_2}$, and the statement that an increase in the CO_2 difference is mainly a reflection of the effects of elements at the high end of the $\dot{V}_{IA}/\dot{Q}$ spectrum in lungs having regional inequalities appears to be substantiated by these findings (Figures 61d, 61a and 61b). It should, however, be noted that high $(A - a)D_{CO_2}$ values are also associated with models having series inequalities (Figure 61c), therefore the interpretation of experimental data should be made with reservations.

8.3 Alveolar - arterial N_2 Difference

The concept of the development of an $(A - a)D_{N_2}$ in non-homogeneous lungs was first introduced by Canfield and Rahn (20), but as no reliable methods for measuring blood nitrogen tension were available at the time the test was not applied to man. The authors did show, however, that the existence of an $(A - a)D_{N_2}$ must be due primarily to the existence of alveoli with low $\dot{V}_{IA}/\dot{Q}$ ratios (see Figure 2 ref,101). Subsequent developments using a modified Van Slyke apparatus (65) and the substitution of the urine-mean alveolar nitrogen for the $(A - a)D_{N_2}$ (66), has seen the measurement more widely applied, and several groups of workers have reported figures for the N_2 difference in normal man. The data vary from an average of 3 mm Hg (15) to 9.4 mm Hg (37). It is of interest

to note that both the above papers found no significant differences between urine and blood P_{N_2}. Greater nitrogen differences have been found in patients diagnosed as suffering from emphysema. Klocke and Rahn (66) report differences ranging from 14 mm Hg to 30 mm Hg, and Briscoe and Gurtner (15) found an average $(A - a)D_{N_2}$ of 20 mm Hg.

The $(A - a)D_{N_2}$ existing in the four models are shown in Figures 62 (a), (b) and (c) no difference, of course, being evident for the model having a pulmonary shunt since arterial and venous P_{N_2} are identical. Since very little increase in the N_2 difference is noted in the model having a series inequality, it may be stated that the large $(A - a)D_{N_2}$ values reported for subjects with emphysema must result from regional inequalities. This finding does not, however, distinguish between ventilatory or blood flow defects, but merely indicates that both distributions contain alveolar compartments with low $\dot{V}_{IA}/\dot{Q}$ ratios.

8.4 The O_2 - CO_2 Diagram of Riley and Cournand

In addition to defining the basic relationships between ventilation-perfusion ratios and gas tensions, the fundamental work of Riley and Cournand (84) also provided a means of describing lung function in terms of a three-compartment model. The analysis separates the effects of $\dot{V}_{IA}/\dot{Q}$ variance by equating the P_{CO_2} decrease in hyperventilated alveoli to an additional "dead space", while the effects of the hyperperfused alveoli are estimated in terms of the true "venous admixture" (i.e.pulmonary shunt) which would lower the P_{O_2} to the value actually measured in arterial blood. By applying this analysis in turn to the models embodying each of the functional defects it is possible to define the indices of "alveolar dead space" and "venous admixture" as the respective degrees of inequality increase. The results are shown in Figures 63 (a), (b), (c) and (d), and refer to models having uneven regional ventilation, uneven blood flow,

series inequalities and pulmonary blood shunts respectively.

It might at first seem surprising that an appreciable increase in alveolar dead space is evident for the model having various amounts of pulmonary shunt. It must be remembered, however, that the venous blood composition, from which the "ideal" point is calculated, is taken from the actual model. As the mixed venous P_{CO_2} increases with greater amounts of shunt, the "ideal" P_{CO_2} value must also increase, hence the alveolar dead space rises. Taking a numerical example; when the amount of shunt is equivalent to 10 per cent. of the cardiac output, the mixed expired P_{CO_2} obtaining in the model is 28.9 mm Hg, and the calculated "ideal" P_{CO_2} is 29.566. Alveolar dead space, as calculated from the equation $V_D/V_T = 1 - (P_{EACO_2}/P_{iCO_2})$, is then 2.26 per cent. On increasing the shunt to 60 per cent., the mixed expired P_{CO_2} alters by less than 0.08 per cent. whereas the "ideal" P_{CO_2} changes to 37.7 mm Hg and causes the alveolar dead space to increase to 23.3 per cent.

The observed increase in venous admixture noted in the model having series inequalities is explained by the marked fall in venous oxygen content which is not reciprocated by an accompanying fall in the "ideal" arterial oxygen contents. Again, taking an example, when the series inequality is such that 80 per cent. of the tidal volume enters the alveoli, the arterial and venous oxygen contents are 20.02 ml/100 ml, and 15.02 ml/100 ml respectively, and the calculated "ideal" arterial contents are 20.4 ml/100 ml. Venous admixture, as calculated from the equation $Q_S/Q_T = (C_{iO_2} - C_{aO_2})/(C_{iO_2} - C_{\bar{v}O_2})$, is therefore 7.1 per cent. When the series inequality is intensified such that only 40 per cent. of the tidal volume enters the alveoli, the arterial and venous contents alter to 15.6 ml/100 ml and 10.6 ml/100 ml respectively, however, the "ideal" arterial contents fall by only 0.7 ml/100 ml. The numerator

of the Q_S/Q_T equation therefore increases to a much greater extent than the denominator, hence the venous admixture rises.

Lung models having uneven regional distributions of ventilation are seen to behave very differently from models having uneven regional distributions of blood flow. As the respective degrees of inequality increase, the venous admixture is seen to increase to a greater extent than the alveolar dead space in the former models, whereas in the latter, the increase in both indices is sensibly equal, however, for small degrees of inequality the alveolar dead space does exceed venous admixture.

These findings clash with those of West (113) who concluded that venous admixture is always more than twice as large as alveolar dead space whether the ventilation-perfusion inequality is caused by uneven ventilation or blood flow. The basis for this erronious concept has been dealt with in Chapter 4; where a more detailed scrutiny of the log normal distributions of ventilation and blood flow assumed by West was given. At that time it was shown that both distributions were virtually identical and were, in essence, distributions of $\dot{V}_{IA}/\dot{Q}$ ratios and not separate ventilation or blood flow distributions as such. The author's conclusions are therefore not surprising and are easily reconciled with our own.

Only two previous studies appear to have dealt explicitly with independent variation of ventilation and blood flow. Riley and Permitt (86), utilising the "four quadrant" diagram (85), investigated the changes in alveolar dead space and venous admixture in a two-compartment lung model as the ratio of amount of ventilation to blood flow going to the compartments was increased. They found that when ventilation was unevenly distributed, the venous admixture was large but there was little increase in alveolar dead space, whereas an unevenly distributed blood flow gave rise to a large alveolar dead space but did not produce a correspondingly

large venous admixture (see Figures 6 and 8 in ref. 86). The authors went on to suggest that when alveolar dead space and venous admixture are both large there must be a joint uneven distribution of ventilation and blood flow. It must be remembered, however, that the indices were calculated from the results obtained from a two-compartment model which can by no means be considered to be equivalent to the continuous distributions of ventilation and blood flow presented in this thesis. Moreover, it has been shown elsewhere (113) that lung models having only a few functional compartments (i.e.less than 8) give unreliable results; a fact borne out by my own investigations* which also demonstrated that such models tended to italicise the features of particular distributions in an unrealistic manner. In addition, the Riley and Permitt analysis assumed that mixed venous return remained constant, no matter what level of arterial oxygen or carbon dioxide content was prevailing, hence the results would also be distorted by this assumption.

A two-compartment model was also proposed by Suwa and Bendixon (105), and differed from the previous model only in that the conversion of carbon dioxide tension to partial pressure was achieved by assuming a linear dissociation curve of the form $C_{CO_2} = kP_{CO_2} + m$, instead of using tabulated values. As the authors studied "physiological dead space" and not alveolar dead space, a direct comparison of their results with my own is impossible. It is, however, of interest to note that the results do agree, at least quantitatively, that the dead space effect (alveolar or physiological) increases when either ventilation or blood flow inequalities become more marked, and that the greatest increase is in lungs having an uneven blood flow. This is attributed to use of P_{aCO_2}

---

*Scrimshire, unpublished work.

by the authors, to calculate their dead space index, thus effectively including the dead space effect of shunting as part of the alveolar dead space.

In conclusion, it must be emphasised that in their original paper, Riley and Cournand did not claim to describe the true lung, but attempted to visualise the effects of an uneven distribution of ventilation-perfusion ratios. The major critisism of the work does not lie in its method of representation of pulmonary defects, therefore, but rather in its assumption that gas exchange inefficiency arises exclusively as a result of regional inequalities. Quite clearly, from Figures 63c and 63d, large alveolar dead space and venous admixture indices can result from both series inequalities and pulmonary blood shunts, as well as from uneven regional distributions of ventilation and blood flow.

8.5 The CO_2 - N_2 Relationship

In the Riley and Cournand analysis, the ventilation-perfusion ratio line is one in which the P_{CO_2} of an alveolar compartment is described as a function of its P_{O_2}. An alternative representation of the same relationship has been proposed by Rahn and Farhi (81), which replaces the reference axis by P_{N_2} instead of P_{O_2}. The resulting graph is known as the CO_2 - N_2 diagram.

By utilising the CO_2 - N_2 diagram, together with direct measurements of alveolar and arterial P_{N_2} and P_{CO_2}, Farhi (36) has suggested that pulmonary function could be described in terms of a two-compartment analogue. The method plots the position of the alveolar point A, and the arterial point a, on the CO_2 - N_2 diagram (see Figure 64). The two points are then joined by a straight line which intersects the ventilation-perfusion ratio line at L and M. The latter points have two interesting properties. First, they are on the ventilation-perfusion

ratio line, and therefore indicate gas composition that may be found in alveoli. Second, when gas or blood with their specific P_{CO_2} and P_{N_2} are mixed in the appropriate proportions, both a and A may be obtained.* A conceptual lung model may therefore be postulated, represented by the points L and M, which explains the observed alveolar and arterial P_{N_2} and P_{CO_2} in terms of two homogeneous groups of alveoli. The $\dot{V}_{IA}/\dot{Q}$ ratio for each group may be read directly on the ventilation-perfusion ratio line, and the ratio in which ventilation and perfusion are distributed are defined as

$$\frac{\dot{Q}_L}{\dot{Q}_M} = \frac{P_{mCO_2} - P_{aCO_2}}{P_{aCO_2} - P_{LCO_2}} \qquad \text{and} \qquad \frac{\dot{V}_L}{\dot{V}_M} = \frac{P_{mCO_2} - P_{ACO_2}}{P_{ACO_2} - P_{LCO_2}}$$

As the analysis is specifically designed to assess regional distributions of ventilation and blood flow, it will not be applied to the models embodying series inequalities or pulmonary shunts, however, this inherent assumption must be borne in mind. Table 4a summarises the results obtained from models having uneven regional ventilation, and models having uneven regional blood flow, for three degrees of inequality (i.e. parameter b = 0.5, 1.0 and 1.5). The various points required for drawing the ventilation-perfusion ratio line were obtained from the P_{CO_2} and P_{N_2} data output from the computer program for each of the ten alveolar compartments of the models.

By lumping together compartments in the actual models to produce two composite compartments, a comparison with the results derived from the analysis of Farhi is possible. This has been done in Table 4b, and shows that there is excellent agreement between the predicted and actual

---

* For a more detailed explanation, see P.184 in "Advances in Respiratory Physiology" ed. C.G.Caro.

distributions.

8.6 Nitrogen Decay Curves

The pulmonary function tests reviewed so far have two features in common, namely, they are all applied under steady state conditions and they all attempt to describe ventilatory and blood flow defects simultaneously. A second group of tests, specifically aimed at describing the distribution of ventilation in the lungs, rely on the interpretation of curves showing the pattern with which the nitrogen contained in the lungs is eliminated whilst breathing specific gas mixtures.

Although many such tests have been proposed (23),(87),(10), the present discussion will be limited to examining the "nitrogen decay curve", proposed by Cumming (25) since it represents the only attempt at classifying ventilatory defects into regional and series inequalities. Very simply, the technique plots out the volume of nitrogen remaining in one litre of lung volume against the turnover volume, which is defined as the summed tidal volume divided by FRC.

The nitrogen decay curves produced from lung models having uneven regional distributions of ventilation, and models having series inequalities, are shown in Figures 65a and 65b, together with the decay curves for a homogeneous lung of the same dimensions. In both cases 100 per cent. oxygen was the eluting gas. Clearly, both types of defect cause the curve to be displaced to the right. In addition, it will be noted that models having regional inequalities produce decay curves characterised by a slight curvature, whereas the curves resulting from models having series inequalities are straight.

For the interpretation of data from nitrogen decay curves, Cumming (25) made two statements: First; if the line is displaced to the right and is straight it must have been produced by a "stratified" or

series defect. Second; if the line is displaced to the right and has curvature, it must have resulted from a regional defect. The author also stated that the curvature would increase as the regional inequality became more severe. Certainly the results concurr with the above in general terms, however, it will be noted that the final statement concerning curvature is not upheld, in that increasing the degree of regional inequality of ventilation reduced slightly the curvature of the decay curve (c.f. curves with parameter b equal to 0.5 and 1.0).

In light of this result, the interpretation of nitrogen decay curves in patients with chronic bronchitis by Cumming et al. (27) might be brought into question. Figure 66 reproduces these data for the first five turnover volumes and clearly illustrates that appreciable curvature is present in all curves. Since similar curvature has been found in the decay curves derived from models having regional inequalities of ventilation (see Figure 65b), the patients studied could have had this defect predominating rather than the series inequality stated by the authors. It is not the intention to say that this was in fact the case, but to demonstrate that the decay curves might just as easily have originated from lungs having regional inequalities of a fairly severe nature.

We therefore conclude that the interpretation of nitrogen decay curves should be reassessed in light of the finding that increased regional inequalities of ventilation do not produce increased curvature.

8.7 Implications of Findings

Having reviewed the more important pulmonary function tests the conclusion has been reached that no one test can distinguish between the various functional defects that can occur in human lungs. It is therefore logical to enquire whether a combination of the tests might

provide a more satisfactory degree of assessment.

Since the nitrogen decay curve is only responsive to ventilatory defects, it provides an ideal first step in detecting the predominant inequality in a given lung. If the curve is displaced significantly to the right of the line of perfect mixing, or displays an increase in curvature, then it may be construed that the defect present is essentially of a ventilatory nature. On the other hand, if the curve falls within the"normal"range (27), the defect must be confined to the pulmonary blood flow.

Assuming that the defect is found to be ventilatory, two options are open. First, $(A - a)D_{O_2}$ could be measured at different levels of F_{IO_2}, as marked degrees of regional ventilation inequalities are known to give rise to large $(A - a)D_{O_2}$ values, whereas a decrease is observed if the defect is due to a series inequality (see Figures 58a and 58c). Although this manoeuvre is no doubt the easiest to perform, it was noted in Chapter 5 (Figure 22) that when the degree of regional ventilation inequality is mild, arterial P_{O_2} rises rapidly, with increases in F_{IO_2}, hence a large $(a - a)D_{O_2}$ will not invariably result from the presence of this defect. Second, the analysis of Riley and Cournand could be applied by simultaneously measuring arterial and alveolar P_{O_2} and P_{CO_2}. From these values, C_{aO_2} and C_{aCO_2} are found by the use of computer produced tables, and by measuring the oxygen uptake and carbon dioxide output over a period of some minutes, venous O_2 and CO_2 contents (and hence $P_{\bar{v}O_2}$ and $P_{\bar{v}CO_2}$) can be determined. The "ideal" P_{O_2} and P_{CO_2} values are now calculated as detailed previously and the indices of alveolar dead space and venous admixture defined. From Figure 63a it is established that a lung having a regional inequality of ventilation <u>always</u> displays a venous admixture which is larger than the corresponding

alveolar dead space, whereas the converse is true for lungs having series inequalities (Figure 63c). A comparison of the indices calculated from the experimental results would therefore show which defect predominates.

If the results of the nitrogen decay curve indicate normal ventilation, the defect must be due to the pulmonary blood flow. From Figure 60 it is clear that the simple act of increasing F_{IO_2} and measuring the resulting steady state $(A - a)D_{O_2}$ will determine whether the defect is due to an uneven regional distribution of blood flow, or a true pulmonary shunt. In the former case little change would be observed in the O_2 difference as F_{IO2} is increased, whereas a rapid rise would occur in the latter.

The above protocol is summerised in Figure 67.

CHAPTER 9

NITROUS OXIDE EXCHANGE

Although considerable attention has been given to the mathematical description of inert gas exchange in man, notably in the work of Kety (64) and Eger (32, 33, 34), the analyses have limited themselves to examining only the alveolar tensions of the inert gas. Moreover, the representation of the lungs as a single compartment continuous flow model, precludes any quantitative estimation of the effects of functional defects upon overall gas exchange during the unsteady state. Similar critisisms may also be applied to the electrical analogue models of Mapleson (72, 73), and Severinghaus (99).

More recently, Farhi and Olszowka (38), have introduced extensions to the Riley and Cournand (84) analysis of pulmonary gas exchange to include one or more soluble inert gases to be present in the lungs in addition to the normal respiratory gases O_2, CO_2 and N_2. The derived equations enable all constituent gas tensions within an alveolus, or a homogeneous lung, to be defined for a given ventilation-perfusion ratio. As pointed out by the authors, the equations are only strictly true for steady state conditions in which the uptake of the inert gas is zero, however, the equations remain approximately correct so long as changes in alveolar gas composition are slow.

Unfortunately, such conditions do not exist within the lungs during the initial stages of uptake and elimination of inert gases when the blood solubility of the gases is high. Severinghaus (97) has noted that the uptake of nitrous oxide is usually in excess of 100 ml/min for the first two hours during anaesthesia, and similar figures have been reported during nitrous oxide excretion (47). It would therefore appear invalid to use the Farhi and Olszowka analysis to describe pulmonary

gas exchange under these conditions.

The model presented in Chapter 3 suffers from none of the above defects, however, the assumption of a constant composition for mixed venous blood in the unsteady state is an obvious limitation. Clearly, after a certain interval, equal to the recirculation time of the blood, changes must occur in venous composition due to the dynamics of inert gas exchange at the body tissues, and because of the alterations in arterial P_{O_2} and P_{CO_2} caused by the concentration and dilution effects. In addition, as many of the inert gases are highly soluble in living tissue, the assumption that all the inert gas leaving the gas phase flows into the blood phase may be in error because of absorbtion by lung substance. Before any detailed study of the overall effects of nitrous oxide exchange can be undertaken it will therefore be necessary to extend the model formulated in Chapter 3 to account for these factors.

9.1 Modifications to Model

9.1.1 Lung Tissue Uptake

The term ΔV_G, defining the amount of any inert gas leaving the blood phase per breath, has so far been assumed equal to ΔV_G^*, the amount entering the blood phase. If, however, some inert gas is absorbed by the lung tissue, this relationship no longer holds and ΔV_G will exceed ΔV_G^* by an amount equal to that entering the tissue phase. The true relationship is therefore

$$\Delta V_G = -\left\{\Delta V_G^* + \Delta V_G^{LT}\right\} \qquad \text{.. .. .. (39)}$$

where ΔV_G^{LT} is the amount of inert gas entering the lung tissue per breath, and ΔV_G is defined as previously (i.e.equation 11, chapter 3)

$$\Delta V_G = \frac{P_{IAG}(i)\, V_{IA}(i) + P'_{AG}(i)\, V_{AL}(i) - P_{AG}(i)\left\{V_{AL}(i) + V_{EA}(i)\right\}}{(P_{Bar} - 47)} \qquad \text{.. .. .. (40)}$$

Similarly, the term ΔV_G^* is as previously defined

$$\Delta V_G^* = \frac{\lambda_G}{760} \cdot \frac{\dot{Q}(i)}{f} \left\{ P_{\bar{v}G} - P_{AG}(i) \right\} \quad \ldots\ldots\ldots\ldots\ldots (41)$$

The amount of inert gas transferred from gas phase to tissue phase in the i^{th} alveolar compartment given by

$$\Delta V_G^{LT} = \frac{\lambda_{LTG}}{760} \cdot V_{LT}(i) \left\{ P'_{AG}(i) - P_{AG}(i) \right\} \quad \ldots\ldots\ldots\ldots\ldots (42)$$

where λ_{LTG} is the tissue/gas partition coefficient at 37°C for gas G, and $V_{LT}(i)$ is the volume of lung tissue associated with the i^{th} alveolar compartment.

Substituting for ΔV_G, ΔV_G^* and ΔV_G^{LT} from equations 40, 41 and 42 in equation 39, and solving for $P_{AG}(i)$ yields

$$P_{AG}(i) = \frac{V_{IA}(i)P_{IAG}(i) + V_{AL}(i)P'_{AG}(i) + \frac{\lambda_G \cdot \dot{Q}(i) \cdot P_{DRY} \cdot P_{\bar{v}G}}{760.f} + V_{LT}(i) \cdot \lambda_{LTG} \cdot P_{DRY} \cdot P'_{AG}(i)}{V_{AL}(i) + V_{EA}(i) + \frac{\lambda_G \cdot \dot{Q}(i) \cdot P_{DRY}}{760.f} + \frac{\lambda_{LTG} \cdot V_{LT}(i) \cdot P_{DRY}}{760}}$$

$$\ldots\ldots\ldots\ldots\ldots (43)$$

The above equation now replaces equation 21 given in Chapter 3, thus accounting for lung tissue uptake and, of course, elimination. It should be noted that the effect of this additional factor is to increase the net uptake of the inert gas, and reduce P_{AG} during uptake and vice versa, during elimination.

9.1.2 Gas Exchange at the Body Tissues

An exact mathematical description of the various types of tissues present in the body would prove intractable. In an attempt to quantify

their behaviour, with respect to inert gas uptake and excretion, many authors (49, 93, 80) have suggested a classification system which separates the continuum into more managable units. The division of the body tissues into groups defined by common characteristics of perfusion and tissue/blood partition coefficients has previously been presented by Hunter (58), and more recently by Eiger (33). This approach will be adopted in the present study where four tissue groups will be distinguished: a vessel rich group (VRG), a muscle group (MG), a fat group (FG) and a vessel poor group (VPG). The values defining the allocation of systemic blood flow to each group, their volume, and the respective tissue/blood partition coefficients for nitrous oxide (the inert gas under consideration) are taken directly from Eiger's paper (33) and are listed in Table 5 along with equivalent partition coefficients for nitrogen (96).

Considering any tissue group, t, during one respiratory cycle, the amount of any inert gas species, G, exchanged with the perfusing blood flow is given by

$$\Delta V(t) = V'_G(t) - V_{TIS}(t) \cdot \lambda_{TBG}(t) \cdot C_{\bar{v}G}(t) \qquad \ldots\ldots\ldots\ldots\ldots (44)$$

where $\Delta V(t)$ is the amount of gas G exchanged by tissue group t during one respiratory cycle; $V'_G(t)$ is the volume of gas G in tissue group t at the start of the respiratory cycle; $V_{TIS}(t)$ is the volume of tissue group; $\lambda_{TBG}(t)$ is the tissue-blood partition coefficient for gas G at the assumed body temperature of 37°C for tissue group t; and $C_{\bar{v}G}(t)$ is the content of gas G in blood draining from tissue group t.

Similarly, the amount of any inert gas species, G, exchanged with tissue group t by the blood flow in one respiratory cycle is given by

$$\Delta V^*(t) = \frac{\dot{Q}(t)}{f} \cdot \left\{ \bar{C}_{aG} - C_{\bar{v}G}(t) \right\} \qquad \ldots\ldots\ldots\ldots\ldots (45)$$

where $\Delta V^*(t)$ is the amount of gas G exchanged by the blood perfusing tissue group t during one respiratory cycle; $\dot{Q}(t)/f$ is the volume of blood perfusing tissue group t in one respiratory cycle; and $\bar{C}_{aG}$ is the mean arterial content of gas G arriving at the body tissues. For any inert gas species

$$\bar{C}_{aG} = \frac{\bar{P}_{aG} \cdot \lambda_G \cdot \dot{Q}}{760f} \qquad \text{.. .. .. (46)}$$

As perfusing blood and tissue groups form a closed system with zero net exchange for any inert gas species

$$\Delta V^*(t) = -\Delta V(t) \qquad \text{.. .. .. (47)}$$

Substituting for $\Delta V^*(t)$ from equation 45 and for $\Delta V(t)$ from equation 44 in equation 47 yields

$$\frac{\dot{Q}(t)}{f} \cdot \left\{ \bar{C}_{aG} - C_{\bar{v}G}(t) \right\} = V_{TIS}(t) \cdot \lambda_{TBG}(t) \cdot C_{\bar{v}G}(t) - V'_G(t) \qquad \text{.. .. .. (48)}$$

Solving for $C_{\bar{v}G}(t)$

$$C_{\bar{v}G}(t) = \frac{\frac{\dot{Q}(t)}{f} \cdot \bar{C}_{aG} + V'_G(t)}{\frac{\dot{Q}(t)}{f} + V_{TIS}(t) \cdot \lambda_{TBG}(t)} \qquad \text{.. .. .. (49)}$$

Substitute for $C_{\bar{v}G}(t)$ in equation 45 from equation 49 and simplify

$$\Delta V^*(t) = \frac{\frac{\dot{Q}(t)}{f} \cdot \bar{C}_{aG} \cdot V_{TIS}(t) \cdot \lambda_{TBG}(t) - \frac{\dot{Q}(t)}{f} \cdot V'_G(t)}{\frac{\dot{Q}(t)}{f} + V_{TIS}(t) \cdot \lambda_{TBG}(t)} \qquad \text{.. .. .. (50)}$$

Equation 50 now defines the amount of any inert gas, G, transferred <u>from</u> the perfusing blood <u>to</u> any tissue group t during the

course of one respiratory cycle.

Before adding equation 50 to the existing model, two further problems must be overcome. Firstly, the initial amounts of the inert gases (nitrogen and nitrous oxide in the present context) in each of the four tissue groups must be defined, and secondly, a method of introducing the recirculation lag has to be found.

At equilibrium $\Delta V^*(t)$ equals zero, that is, there is no further exchange of inert gases with the body tissues. Equating equation 50 to zero gives

$$\dot{V}_G'(t) = C_{aG} \cdot V_{TIS}(t) \cdot \lambda_{TBG} \qquad \ldots\ldots\ldots\ldots\ldots (51)$$

Equation 51 now gives the volume of any inert gas species in any tissue group during steady state conditions for a specific arterial content of the gas.

The composition of mixed venous blood draining from the body tissues during either uptake or elimination of nitrous oxide is calculated by summating the values of $V_G^*(t)$ for each tissue group and then subtracting the sum from the mean arterial content.

$$C_{\bar{v}G} = \bar{C}_{aG} - \sum_{t=1}^{t=4} \Delta V_G^*(t) \qquad \ldots\ldots\ldots\ldots\ldots (52)$$

The gas tensions in venous blood are given by

$$P_{\bar{v}G} = \frac{C_{\bar{v}G} \cdot 760f}{\lambda_G \cdot \dot{Q}} \qquad \ldots\ldots\ldots\ldots\ldots (53)$$

Equation 50 is applied after each breath in the unsteady state, and thence by applying equation 52 and equation 53 the mixed venous gas tensions for nitrogen and nitrous oxide are determined.

In order to simulate the recirculation lag, use is made of the computer memory which is used to store the values of $P_{\bar{v}N_2}$ and $P_{\bar{v}N_2O}$; and

also $P_{\bar{v}O_2}$ and $P_{\bar{v}CO_2}$ which are determined at the same time by assuming that oxygen consumption and carbon dioxide output remain constant. After a preset number of breaths, equal to the recirculation time divided by the breathing frequency, the values for venous gas tensions are replaced by the values calculated at breath one, and on the following breath they are replaced by the values calculated at breath two, and so on. In this manner the dynamic changes in venous blood composition caused by the exchange of gases at the body tissues are simulated by a simple finite state approach.

9.2 Nitrous Oxide Uptake and Elimination in Homogeneous Lungs

9.2.1 Effect of Differing Recirculation Times

Figure 68 shows how different recirculation times affect the arterial P_{O_2} and P_{CO_2} in a homogeneous lung model during the first fifty breaths of a gas mixture of 21 per cent. oxygen and 79 per cent. nitrous oxide. In all cases the minute volume was assumed to be 5 litre/min, the cardiac output 5 litre/min, and the breathing frequency 12 breaths/min. Both oxygen uptake and carbon dioxide output were assumed to remain at their normal steady state values of 250 ml/min and 200 ml/min throughout the unsteady state.

The concentration effect upon oxygen is seen to pass through a well defined maximum, the value of which is directly related to the particular recirculation time assumed. With a recirculation time of 5 seconds, for example, a maximum arterial P_{O_2} of 143,7 mm Hg is reached after twenty one breaths, compared to a maximum of 157.8 mm Hg after twenty six breaths when the recirculation time is increased to 80 seconds. The concomitant increases in arterial P_{CO_2}, by contrast, reach maximum values much later in the uptake period. For example, with a recirculation time of 20 seconds, the maximum arterial P_{CO_2} of

34.0 mm Hg is reached after 37 breaths of the nitrous oxide-oxygen mixture.

If we compare the rate of nitrous oxide uptake with the simultaneous changes in arterial P_{O_2} and P_{CO_2} (Figure 69) it will be noted that neither the maximum arterial P_{O_2} nor the maximum arterial P_{CO_2} value coincide with each other or with the peak in nitrous oxide uptake. The amount to which arterial P_{O_2} and P_{CO_2} rise during inert gas uptake have been fully discussed in earlier chapters; where it was explained that the differential increases were solely a function of the "chemical solubilities" of the two gases. It was also demonstrated that both oxygen and carbon dioxide tensions continue to increase even when the inert gas uptake had reached a plateau, and this was ascribed to the continuing washout of nitrogen which acts as a passive "filler" gas effectively limiting the concentration of alveolar gases. Similarly, in the present instance, the continuing rise in arterial P_{O_2} in the face of a falling nitrous oxide uptake is also explained by the progressive washout of nitrogen. Arterial P_{CO_2}, however, continues to rise for a considerable period after the arterial peak. Essentially, the reason for this anomaly lies in the fact that considerably greater amounts of carbon dioxide enter the blood stream during the period of rapid nitrous oxide uptake than is the case for oxygen. For example, at breath fifteen the rise in oxygen content is less than 0.1 ml/100 ml, compared to a rise of 2.0 ml/100 ml for carbon dioxide. As a result, venous carbon dioxide content increases considerably and causes the persistence of a higher than normal arterial P_{CO_2}. The greater rise in arterial P_{CO_2} recorded for lower recirculation times is explained by the fact that venous blood with a higher carbon dioxide content is returned to the lungs whilst the nitrous oxide uptake, and hence the concentration effect, is still high. These simultaneously occuring

factors cause a greater rise with the lower recirculation times. The subsequent fall in arterial P_{CO_2} in all cases is brought about by the gradual removal of this additional carbon dioxide as the nitrous oxide uptake, and hence the concentration effect, diminishes with time.

The influence of recirculation time upon arterial P_{O_2} and P_{CO_2} during nitrous oxide elimination is shown in Figure 70. For all curves it was assumed that equilibrium conditions had been obtained with the inspired gas mixture of 21 per cent, oxygen, 79 per cent. nitrous oxide before switching back to air breathing. The nitrogen content in all tissue groups was therefore zero and the nitrous oxide contents, calculated from equation 51, were 2,227.2 ml, 13,058.6 ml, 11,678.9 ml and 4,377.4 ml in the VRG, MG, FG and VPG tissue compartments respectively. As recirculation time increases a lower minimum value for arterial P_{O_2} is attained and the position of the point is shifted to the right. The time course changes in arterial P_{CO_2} are protracted in comparison to arterial P_{O_2}, minimum values being reached much later in the elimination period. Again, lower minimum values are associated with the longer recirculation times.

Much of what has been said with respect to recirculation time for nitrous oxide uptake applies equally to elimination. One important point to note is that the relatively smaller changes in both arterial P_{O_2} and P_{CO_2} during the elimination period result from the more rapid rate of nitrogen washin compared to the rate of washout during uptake. Nitrogen therefore reassumes the role of the filler gas earlier, and is hence most affected by changes due to dilution. This corrects a previously held view (95) that the phenomenon resulted from the relatively less efficient transport of nitrous oxide during elimination compared to uptake.

9.2.2 Effect of Inspired Nitrous Oxide Concentration

The effect of differing inspired concentrations of nitrous oxide upon arterial P_{O_2} and P_{CO_2} is shown in Figure 71, and the subsequent changes during elimination after attaining a steady state with the given mixture, are shown in Figure 72. In all cases, the inspired oxygen concentration was held constant at 21 per cent., nitrogen constituting the residual gas.

Increasing the inspired concentration of nitrous oxide results in a progressive increase in the maximum arterial P_{O_2} and P_{CO_2} values reached during uptake. During the subsequent elimination, the lowest minimum values are likewise associated with steady state mixtures having the highest nitrous oxide concentration. It is of particular interest to note that no discontinuity in the behaviour of arterial P_{O_2} or P_{CO_2} occured when F_{IN_2O} was increased to 79 per cent., a finding that conflicts with the work of Farhi and Olszowka (38) who predicted large changes in arterial gas tensions when nitrogen is completely replaced by nitrous oxide. The authors assumed, however, that all alveolar nitrogen was removed before the nitrous oxide was inspired which obviously does not occur in the actual lungs nor in the model. This is an inherent limitation of all analyses based on the Riley and Cournand model (84).

9.2.3 Effect of Changes in FRC

The effect of different lung sizes on arterial P_{O_2} and P_{CO_2} during nitrous oxide (79 per cent.) uptake is shown in Figure 73. For the larger lungs, the peak values of both arterial P_{O_2} and P_{CO_2} are delayed and their actual values are reduced.

With larger FRC's the proportional changes in alveolar volume due to the uptake of nitrous oxide are smaller, hence the concentration effect upon oxygen and carbon dioxide tensions is less than in lungs of

smaller size. The delay in reaching the peak values is caused by the extra amounts of nitrous oxide required to be inspired into the larger lungs before the alveolar P_{N_2O} is raised to the level where maximum uptake occurs.

Equivalent changes are observed in lungs of different size during nitrous oxide elimination.

9.2.4 Effect of Minute Volume

The changes in arterial P_{O_2} and P_{CO_2} during nitrous oxide (79 per cent.) uptake at three levels of minute volume are shown in Figure 74. It should be explained that the steady state conditions prior to induction were also attained at the particular levels of minute volume shown, hence the only "step change" occuring is in the inspired gas composition. It can be seen that the transient changes in arterial P_{O_2} and P_{CO_2} are less marked at high minute volumes, and the peaks are reached earlier.

Now, increasing the minute volume also increases the alveolar volume. For example, the assumed FRC of 2,400 ml is increased by 17.36 per cent. on each inspiration when ventilated with a minute volume of 5 litre/min, and by 52.08 per cent. when the minute volume is raised to 15 litre/min. It has been shown in the previous section that smaller changes occur in alveolar P_{O_2} and P_{CO_2} in lungs with larger FRC's, hence the "effective" increase in lung volume brought about by the higher minute volumes partly explains the lower arterial P_{O_2} and P_{CO_2} values observed in the present case. In addition, the maximum rate of nitrous oxide uptake occurs earlier with higher minute volumes, and since alveolar nitrogen is washed out at approximately the same rate, any decrease in nitrous oxide uptake results in a fall in the concentration effect. Both arterial P_{O_2} and P_{CO_2} therefore begin to return to their steady state levels earlier with high minute volumes.

9.2.5 Effect of Cardiac Output

Figure 75 shows that the concentration effect is more marked for both arterial P_{O_2} and P_{CO_2} during nitrous oxide uptake at higher cardiac outputs in the same lung. This is to be expected, as the concentration effect is directly related to the rate of nitrous oxide uptake, which is itself functionally linked to cardiac output.

For the present investigation, a recirculation time of 20 seconds was assumed for all the cardiac outputs (i.e. $\dot{Q}$ = 5. 10 and 15 litre/min), but clearly a relationship must exist between recirculation time and cardiac output, with shorter recirculation times being linked with higher systemic blood flows, and vice versa. In view of this fact it is interesting to combine Figure 68; in which the isolated effects of recirculation times upon arterial P_{O_2} and P_{CO_2} were shown, with Figure 75. In qualitative terms, it can be seen that the reduction in the rise of both arterial P_{O_2} and P_{CO_2} caused by short recirculation times would be somewhat offset by the accompanying higher cardiac outputs that will tend to increase the gas tensions. The interaction of both mechanisms would therefore be to reduce the range of arterial P_{O_2} and P_{CO_2} values in subjects with different cardiac outputs during nitrous oxide induction.

9.3 Discussion

Having studied the response of the homogeneous lung during nitrous oxide exchange, it seems logical to enquire how the various functional defects alter the overall changes in arterial P_{O_2} and P_{CO_2} during uptake and elimination.

Figure 76 shows how arterial P_{O_2} and P_{CO_2} change during the uptake and elimination of nitrous oxide in lung models having either an uneven distribution of ventilation or an uneven distribution of blood flow when the degree of inequality is fairly severe (i.e.parameter b = 1.0).

In many respects the curves reflect the findings, in that, for inert gases of intermediate solubilities, the changes in both arterial P_{O_2} and P_{CO_2} are greater in lung models having an uneven blood flow than in models having the same degree of ventilation inequality. The increases in arterial P_{O_2} and P_{CO_2} observed in the model having an uneven distribution of blood flow, however, were larger than previously predicted and are attributed to the increase in venous levels of oxygen and carbon dioxide occuring in the present simulations.

One of the basic assumptions made in formulating the model was that the alveoli always return to the same pre-inspiratory volume after each breathing cycle. If, instead, it is arranged to keep both inspired and expired volumes equal, then a prediction of the equivalent change in FRC that would occur under these circumstances is possible.

Figure 77a shows a set of such results obtained during nitrous oxide uptake (21 per cent. O_2, 79 per cent. N_2O) in a homogeneous lung. The total decrease in FRC over the period monitored, is 1865.3 ml. Although such a large fall in lung volume in reality appears extremely unlikely, some decrease is to be expected due to the normal respiratory pattern of inspiring and expiring nearly equal volumes of gas when breathing ambient air. An experimental result during nitrous oxide uptake would therefore be likely to lie between the two extremes of constant FRC with variable expired volume, and variable FRC with constant expired volume. This may in part explain the observed fall in FRC noted by Shah et al. (101), however, it does not rule out the possibility of an increase in stretch receptor activity suggested by the authors.

By arranging for inspired and expired volumes to be equal during nitrous oxide elimination, a prediction of the equivalent changes in FRC can be made as during the uptake phase. Figure 77b shows these

changes, and indicates that if the condition of equal inspired and expired volumes is met, then a total increase of 1515.6 ml in FRC would occur over twenty breaths. This predicted rise in FRC is of particular interest during the early stages of nitrous oxide elimination as the conditions existing at this time represent a subject in deep anaesthesia. Under such conditions, Widdicombe (109) has shown that the stretch reflexes are extremely weak in man; a view substantiated by the earlier findings of Campbell et al. (19) who studied the responses of anaesthetised patients to expiratory resistance. It can therefore be assumed that some increase in total lung volume is likely due to the lack of any automatic responses necessary to return FRC to its steady state value.

Thus far, all data concerning regional ventilation and blood flow in the model has been generated from theoretical distributions, however, Scrimshire and Tomlin (95) previously utilised the experimentally obtained values of West (111), who described respiratory function in the lungs of erect man in terms of nine horizontal slices from apex to base. By reading this data into the computer simulation model at execution time, together with the appropriate values for minute volume, breathing frequency, cardiac output and so on, it is possible to compare the model simulation of gas exchange directly with that observed in human subjects. Figure 78 shows such a test in which computed values of expired alveolar P_{O_2} and P_{CO_2} are compared with the pooled results from three sets of experiments during nitrous oxide uptake in man.

The subjects were seated with a nose clip applied and breathed through a 3-way valve; one outlet of which was open to room air and the other to an anaesthetic bag supplied with a 21 per cent. O_2, 79 per cent. N_2O mixture. For approximately 10 minutes the subjects breathed air, in order to attain steady state conditions, after which they switched to

breathing from the bag for a further 18 breaths. Expired oxygen and carbon dioxide concentrations were monitored continuously with a Mass Spectrometer (Atlas MS 4) in the manner previously described by Shah et al. (101).

The small divergence between the model prediction and the experimental results occuring after 12 breaths was attributed to the fact that at this point the subjects found it increasingly difficult to keep tidal volume constant with the clouding of consciousness that this high concentration of nitrous oxide produced. The resulting decrease in alveolar ventilation would therefore be expected to reduce the rate of nitrous oxide uptake, and hence the oxygen 'concentration' effect.

The small predicted rise in alveolar carbon dioxide tension did not occur, although previously published data has indicated a slight increase during induction in one of the subjects (Figure 4, Ref. 101).

It may be concluded from these results that the model affords a reasonable representation of the lung exchanging gases during non-steady state conditions, and may therefore be usefully employed in investigating the effects of variation in a number of parameters during inert gas uptake and elimination.

CHAPTER 10

CONCLUSION

Although the proposed model, in common with all previous models, is an approximation to the actual lungs it has been found sufficiently accurate to enable a direct comparison with experimental results to be made (95). Quite obviously, any analogue which duplicates all facets of pulmonary form and function must be a replica of the living system itself, and such a model would be too complicated for practical purposes.

Of particular value and interest in the present context is the use of the model to investigate the lungs in the diseased state. By partitioning the more common diseases into four groups having common functional defects, it has been possible to define the characteristic levels of arterial and venous P_{O_2} and P_{CO_2} for each defect in the steady state, and the changes occuring in these variables in the unsteady state. The results obtained showed good agreement with current knowledge of respiration physiology, and a number of previously observed phenomena occuring during the unsteady state have been given a more vigorous quantitative explanation.

The extension of the model to include gas exchange in the body tissues has enabled a comprehensive study of pulmonary gas tensions during nitrous oxide induction and elimination to be made. Specifically, the effects of systemic blood recirculation time, minute volume, cardiac output, lung volume and inspired F_{IN_2O} are quantified, and an explanation for the observed changes in FRC during anaesthesia is postulated.

CHAPTER 11

FUTURE WORK

An obvious area of future work must be the application of the proposed protocol of pulmonary function tests to groups of normal and abnormal subjects. In the latter case it will be of particular interest to define the predominant functional defects present in various obstructive lung diseases.

Having defined the type of functional defect existing in a particular patient's lungs, a further question which must be considered is whether it is possible to assess the degree of inequality present. In principle, the problem is readily soluble. The patient is studied in the steady state condition, breathing atmospheric air and measurements made of oxygen consumption, carbon dioxide output, minute volume, breathing frequency, cardiac output, haemoglobin concentration, metabolic acid-base state and body temperature.* This information is then fed into the model and the steady state arterial P_{O_2} and P_{CO_2} values that would correspond to a number of degrees of inequality are computed. A comparison of the patient's actual arterial blood composition with these data should then reveal the particular degree of inequality obtaining in his lungs.

The mathematical model in its present form predicts the alveolar and arterial gas tensions for one complete breathing cycle. It is possible, however, to modify the computational procedure to follow the continuous changes in gas tensions throughout the breathing cycle without altering the model structure. Here, the volumes of gas and blood entering and leaving the model would be defined over some small

---

*The latter three parameters are required as input data for the Kelman alogorithms.

time interval instead of over the complete breathing cycle, and gas exchange between alveolar air and capillary blood would take place at the end of each such interval. Figure 79 shows the results of applying this procedure to a homogeneous lung consisting of an upper airways compartment, a single conducting airways compartment, and a single alveolar compartment. Although this simple version has limited application, a more complex multi-compartment model could be used to investigate the effects of differing flow patterns upon overall gas exchange. In addition, by omitting the assumtion that the pressure in the alveoli is atmospheric, the combined effects of given flow and pressure wave forms could be assessed.

REFERENCES

1. ADAIR, G. S. The hemoglobin system. VI. The oxygen dissociation curve of hemoglobin. J. Biol. Chem. 63: 529, 1925.

2. ALTSHULER, B., E. D. PALMES, L. YARMUS and N. NELSON. Intra-pulmonary mixing of gases studied with aerosols. J. Appl. Physiol. 14: 321, 1959.

3. APTHORP, G. H. and R. MARSHALL. Pulmonary diffusing capacity: a comparison of breath-holding and steady state methods using carbon monoxide. J. Clin. Invest. 40: 1775, 1961.

4. AUSTIN, W. H., E. LACOMBE, P.W. RAND and M.CHATTERJEE. Solubility of carbon dioxide in serum from 15 to 37C. J. Appl. Physiol. 18: 301, 1963.

5. BATES, D. V. and R. V. CHRISTIE. Respiratory Function in Disease. Philadelphia: W. B. Saunders Company, 1964.

6. BATES, D. V., N. R. ANTHONISEN, H. BASS, T. HECKSCHER and A. ORIOL. Recent observations on the measurement of regional $\dot{V}/\dot{Q}$ ratios in chronic lung disease. In: Form and Function in the Human Lung. (ed) G. Cumming and L. B. Hunt. Edinburgh: E & S Livingstone Ltd.

7. BENDIXEN, H. H. The pathophysiology of chronic lung disease. In: Clinical Anesthesia, Lung Disease. (ed) D. A. Holaday. Oxford: Blackwell Scientific Publications Inc.

8. BENTIVOGLIO, L. G., F. BEEREL, P. B. STEWART, A. C. BRYAN, W. C. BALL and D. V. BATES. Studies of regional ventilation and perfusion in pulmonary emphysema using Xenon^{133}. Am. Rev. Respirat. Diseases 88: 315, 1963.

9. BOHR, C. Ueber die lungenathmug. Skand. Arch. Physiol. 2: 236, 1891.

10. BOUHUYS, A. and A. COURNAND. Distribution of inspired gas in the

lungs. Physiol. Rev. 39: 731, 1959.

11. BRINK, F., Jr. Handbook of Respiratory Data in Aviation. Washington, D.C.: Subcommittee on Oxygen and Anoxia of the Committee in Aviation Medicine, Division of Medical Sciences, National Research Council Acting for the Committee on Medical Research, Office of Scientific Research and Development, 1944.

12. BRISCOE, W. A., R. E. FORSTER and J. H. COMROE, Jr. Alveolar ventilation at very low tidal volumes. J. Appl. Physiol. 7: 27, 1956.

13. BRISCOE, W. A. and A. COURNAND. Uneven ventilation of normal and diseased lungs studied by an open circuit method. J. Appl. Physiol. 14: 284, 1959.

14. BRISCOE, W. A. A method for dealing with data concerning uneven ventilation of the lung and its effects on blood gas transfer. J. Appl. Physiol. 14: 291, 1959.

15. BRISCOE, W. A. and H. P. GURTNER. The alveolar-uninary N_2 partial pressure difference compared to other measures of the distribution of ventilation and perfusion within the lung. Fed. Proc. 19: 381, 1960.

16. BRISCOE, W. A. and A. COURNAND. The degree of variation of blood perfusion and of ventilation within the emphysematous lung, and some related considerations. In: Ciba Foundation Symposium on Pulmonary Structure and Function. London: J & A Churchill Ltd., 1962.

17. BUTLER, J. and B. H. SMITH. Pressure-volume relationships of the chest in the completely relaxed anaesthetised patient. Clin. Sci. 16: 125, 1957.

18. CALEBRISI, P. and W. H. ABELMANN. Porto-caval and porto-pulmonary anastomoses in Laennec's cirrhosis and in heart failure. J. Clin. Invest. 36: 1257, 1957.

19. CAMPBELL, E. J. M., J. B. L. HOWELL and B. W. PECKET. The pressure-volume relationships of the thorax of anaesthetized human subjects.

J. Physiol. 136: 563, 1957.

20. CANFIELD, R. E. and H. RAHN. Arterial-alveolar N_2 gas pressure differences due to ventilation-perfusion variation. J. Appl. Physiol. 10: 165, 1957.

21. COLE, R. B. and J. M. BISHOP. Effects of varying inspired oxygen tension on alveolar-arterial O_2 tension difference in man. J. Appl. Physiol. 18: 1043, 1963.

22. COMROE, J. H., Jr. Physiology of Respiration. Chicago: Year Book Medical Publishers Inc., 1966.

23. COURNAND, A., E. D. BALDWIN, R. C. DARLING and D. W. RICHARDS. Studies on the intrapulmonary mixture of gases. J. Clin. Invest. 20: 681, 1941.

24. CUDKOWICZ, L., W. H. ABELMANN, G. E. LEVINSON, G. KATZNELSON and R. M. JREISSATY. Bronchial arterial blood flow. Clin. Sci. 19: 1, 1960.

25. CUMMING, G. Gas mixing efficiency in the human lung. Resp. Physiol. 2: 213, 1967.

26. CUMMING, G., J. CRANK, K. HORSFIELD and I. PARKER. Gaseous diffusion in the airways of the human lung. Resp. Physiol. 1: 58, 1966.

27. CUMMING, G., K. HORSFIELD, J. G. JONES and D. C. F. MUIR. Inhomogeneity of ventilation in normal and abnormal lungs. In: Form and Function in the Human Lung. (ed) G. Cumming and L. B. Hunt. Edinburgh: E & S Livingstone Ltd., 1962.

28. CUMMING, G., K. HORSFIELD and S. B. PRESTON. Diffusion equilibrium in the lungs examined by nodal analysis. Resp. Physiol. 12: 329, 1971.

29. DARLING, R. C., A. COURNAND and D. W. RICHARDS. Studies on intrapulmonary mixture of gases. V. Forms of inadequate ventilation in normal and emphysematous lungs, analysed by means of breathing pure oxygen. J. Clin. Invest. 23: 55, 1944.

30. DITTMER, D. S. and R. M. GREBE (ed). Handbook of Respiration. Washington; D. C.: Natl. Acad. Sci., 1958.

31. DONALD, K. W., A. RENZETTI, R. L. RILEY and A. COURNAND. Analysis of factors affecting concentrations of O_2 and CO_2 in gas and blood of lungs; results. J. Appl. Physiol. 4: 497, 1952.

32. EGER, E. I., II. Factors affecting the rapidity of alteration of nitrous oxide concentration in a circle system. Anesthasiology 21: 348, 1960.

33. EGER, E. I., II. A mathematical model of uptake and distribution. In: Uptake and Distribution of Anesthetic Agents. New York: Mc. Graw-Hill Book Company, Inc., 1962.

34. EGER, E. I., II. Respiratory and circulatory factors in uptake and distribution of volatile anesthetic agents. Brit. J. Anaesth. 36: 155, 1964.

35. EMMANUEL, G., W. A. BRISCOE and A. COURNAND. A method for the determination of the volume of air in the lungs: Measurements in chronic pulmonary emphysema. J. Clin. Invest. 40: 329, 1961.

36. FARHI, L. E. Ventilation-perfusion relationship and its role in alveolar gas exchange. In: Advances in Respiratory Physiology. (ed) C. G. Caro, London: E. Arnold (Publishers) Ltd., 1966.

37. FARHI, L. E., A. W. T. EDWARDS and T. HOMMA. Determination of dissolved N_2 in blood by gas chromatography and $(a - A)N_2$ difference. J. Appl. Physiol. 18: 97, 1963.

38. FARHI, L. E. and A. J. OLSZOWKA. Analysis of alveolar gas exchange in the presence of soluble inert gases. Resp. Physiol. 5: 53, 1968.

39. FARHI, L. E. and H. RAHN. A theoretical analysis of the alveolar-arterial oxygen difference with special reference to the distribution effect. J. Appl. Physiol. 18: 97, 1963.

40. FENN, W. O., H. RAHN and A. B. OTIS. A theoretical study of the

composition of alveolar air at altitude. Am. J. Physiol. 146: 637, 1946.

41. FINLEY, T. N. The determination of uneven pulmonary blood flow from the arterial oxygen tension during nitrogen washout. J. Clin. Invest. 40: 1727, 1961.

42. FLETCHER, C. M. Some observations on the bronchial and emphysematous types of patient with generalised airways obstruction. In: Form and Function in the Human Lung. (ed) G. Cumming and L. B. Hunt. Edinburgh: E & S Livingstone Ltd., 1962.

43. FORSTER, R. E. Rate of gas uptake by red cells. In: Handbook of Physiology, Respiration Volume I. Washington, D. C.: American Physiological Society, 1964.

44. FRASER, R. G. and D. V. BATES. Body section roentgenography in the evaluation and differentiation of chronic hypertropic emphysema and asthma. Am. J. Roentgenol. 82: 39, 1959.

45. FRITTS, H. W., A. HARDEWIG, D. F. ROCHESTER and A. COURNAND. Estimation of pulmonary arteriovenous shunt-flow using intravenous injections of T-1824 dye and Kr^{85}. J. Clin. Invest. 39: 1841, 1960.

46. FRITTS, H. W., P. HARRIS, C. A. CHIDSEY, R. H. CLAUSS and A. COURNAND. Estimation of flow through bronchial-pulmonary vascular anastomoses with use of T-1824 dye. Circulation 23: 390, 1961.

47. FRUMIN, M. J., E. SALANITRE and H. RACKOW. Excretion of N_2O in anesthetized man. J. Appl. Physiol. 16: 720, 1961.

48. FINLEY, T. N., C. LENFANT, P. HAAB, J. PIIPER and H. RAHN. Venous admixture in the pulmonary circulation of anesthized dogs. J. Appl. Physiol. 15: 418, 1960.

49. HAGGARD, H. W. The absorption, distribution and elimination of ethyl ether. III. The relation of the concentration of ether, or any similar volatile substance in the central nervous system to the

concentration in the arterial blood, and the buffer action of the body. J. Biol. Chem. 59: 771, 1929.

50. HALDANE, J. S. Respiration (1st edition). New Haven: Yale University Press, 1922.

51. HELMHOLZ, H. E., Jr., J. B. BATEMAN and W. M. BOOTHBY. The effects of altitude anoxia on the respiratory process. J. Aviation Med. 15: 366, 1944.

52. HENDERSON, L. J. Blood, a Study in General Physiology. New Haven: Yale University Press, 1928.

53. HEPPLESTON, A. G. Lung structure in emphysema. In: Form and Function in the Human Lung. (ed) G. Cumming and L. B. Hunt. Edinburgh: E & S Livingstone Ltd., 1962.

54. HILTON, S. M. J. Physiol., London. 149: 93, 1959.

55. HIMMELBLAU, D. M. and K. B. BISCHOFF. Process Analysis and Simulation. Wiley, 1968.

56. HORSFIELD, K. In: Form and Function in the Human Lung. Page 242, discussion. (ed) G. Cumming and L. B. Hunt. Edinburgh: E & S Livingstone Ltd., 1962.

57. HORSFIELD, K. and G, CUMMING. Morphology of the bronchial tree in man. J. Appl. Physiol. 24: 373, 1968.

58. HUNTER, A. R. The group pharmacology of anaesthetic agents. I: The absorption-elimination of inhaled drugs. Brit. J. Anaesth. 28: 244, 1956.

59. International Committee for Standardisation in Haematology, 1965. (quoted by Kelman, ref. 62).

60. KELMAN, G. R. Digital computer subroutine for the conversion of oxygen tension into saturation. J. Appl. Physiol. 21: 1375, 1966.

61. KELMAN, G. R. Digital computer procedure for the conversion of P_{CO2} into CO_2 content. Resp. Physiol. 3: 111, 1967.

62. KELMAN, G. R. Computer program for the production of O_2-CO_2 diagrams. Resp. Physiol. 4: 260, 1968.

63. KELMAN, G. R. A new lung model: An investigation with the aid of a digital computer. Computers and Biomedical Research 3: 241, 1970.

64. KETY, S. S. Theory and applications of exchange of inert gases at lungs and tissues. Pharmacol. Rev. 3: 1, 1951.

65. KLOCKE, F. J. and H. RAHN. A method for determining inert gas ('N_2') solubility in urine. J. Clin. Invest. 40: 279, 1961.

66. KLOCKE, F. J. and H. RAHN. The arterial-alveolar inert gas ('N_2') difference in normal and emphysematous subjects, as indicated by the analysis of urine. J. Clin. Invest. 40: 286, 1961.

67. KROUGH, A. and J. LINDHARD. The volume of the dead space in breathing and the mixing of gases in the lungs of man. J. Physiol., London 51: 59, 1917.

68. KUO, S. S. Numerical Methods and Computers. Massachusets: Addison-Wesley Publishing Company, Inc., 1965. (pp 83-87)

69. La FORCE, R. C. and B. M. LEWIS. Diffusional transport in the human lung. J. Appl. Physiol. 28: 291, 1970.

70. LENFANT, C. and T. OKUBO. Distribution function of pulmonary blood flow and ventilation-perfusion ratio in man. J. Appl. Physiol. 24: 668, 1968.

71. LIEBOW, A. A., M. R. HALES and B. E. LINDSKOG. Enlargement of bronchial arteries and their anastomoses with pulmonary arteries in bronchiectasis. Am. J. Path. 25: 211, 1949.

72. MAPLESON, W. W. Simple analogue for the distribution of inhaled anesthetics about the body. In: Abstracts of Contributed Papers, International Biophsics Congress, Stockholm, 1961 (page 81).

73. MAPLESON, W. W. Quantitative prediction of anesthetic concentrations. In: Uptake and Distribution of Anesthetic Agents. New York:

Mc. Graw-Hill Book Company, Inc., 1962.

74. MARGARIA, R. The contribution of hemoglobin to acid-base equilbruim of the blood in health and disease. Clin. Chem. 3: 306, 1957.

75. MEAD, J. and C. COLLIER. Regulation of volume history of lungs to respiratory mechanics in anesthetized dogs. J. Appl. Physiol. 14: 699, 1959.

76. McILROY, M. B. Pulmonary shunts. In: Handbook of Physiology, Respiration Volume II. Washington, D. C., American Physiological Society, 1965.

77. NUNN, J. F. Applied Respiratory Physiology with Special Reference to Anaesthesia. London: Butterworths, 1969.

78. OGILVIE, C. M. Patterns of disrupted lung function in patients with chronic obstructive vesicular emphysema. Thorax 14: 113, 1959.

79. PAPPENHEIMER, J. R., J. COMROE, A. COURNAND, J. K. W. FERGUSON, G. F. FILLEY, W. S. FOWLER, J. S. GRAY, J. F. HELMHOLTZ, A. B. OTIS, H. RAHN and R. L. RILEY. Standardization of definition and symbols in respiratory physiology. Fedn. Proc. 9: 602, 1950.

80. PRICE, H. L., P. J. KOVNAT, J. N. SAFER, E. H. CONNER and M. L. PRICE. Uptake of thiopental by body tissues and its relation to duration of narcosis. Clin. Pharmacol. & Therap. 1: 16, 1960.

81. RAHN, H. A concept of mean alveolar air and the ventilation-bloodflow relationships during pulmonary gas exchange. Am. J. Physiol. 158: 21, 1949.

82. RAUWERDA, P. E. Unequal Ventilation of Diffrent Parts of the Lung and the Determination of Cardiac Output. (Thesis) Groningen, The Netherlands: Univ. of Groningen, 1946.

83. RAVIN, M. B., R. M. EPSTEIN and J. R. MALM. Contribution of thebesian veins to the physiological shunt in anesthetized man.

J. Appl. Physiol. 20: 1148, 1965.

84. RILEY, R. L. and A. COURNAND. 'Ideal' alveolar air and the analysis of ventilation-perfusion relationships in the lungs. J. Appl. Physiol. 1: 825, 1949.

85. RILEY, R. L. and A. COURNAND. Analysis of factors affecting partial pressure of oxygen and carbon dioxide in gas and blood of lungs: theory. J. Appl. Physiol. 4: 77, 1951.

86. RILEY, R. L. and S. PERMUTT. The four-quadrant diagram for analyzing the distribution of gas and blood in the lung. In: Handbook of Physiology, Respiration Volume II. Washington, D. C., American Physiological Society, 1965.

87. ROBERTSON, J. S., W. E. SIRI and H. B. JONES. Lung ventilation patterns determined by analysis of nitrogen elimination rates. J. Clin. Invest. 29: 577, 1950.

88. ROELSEN, E. Fractional analysis of alveolar air after inspiration of hydrogen as a method for the determination of the distribution of inspired air in the lungs. Acta. Med. Scand. 95: 452, 1938.

89. ROSS, B. B. and L. E. FARHI. Dead space ventilation as a determinant in the ventilation-perfusion concept. J. Appl. Physiol. 15: 363, 1960.

90. ROUGHTON, F. J. W. Transport of oxygen and carbon dioxide. In: Handbook of Physiology, Respiration Volume I. Washington, D. C., American Physiological Society, 1964.

91. SAID, S. I. and C. M. BANERJEE. Venous admixture to the pulmonary circulation in human subjects breathing 100 per cent oxygen. J. Clin Invest. 42: 507, 1963.

92. SAIDEL, G. M., T. C. MILITANO and E. H. CHESTER. Pulmonary gas transport characterization by a dynamic model. Resp. Physiol. 12: 305, 1971.

93. SAUNDERS, P. An analysis of inhalation anesthesia by graphic means. Anesthesiology 5: 274, 1944.

94. SCRIMSHIRE, D. A., P. J. TOMLIN and R. A. ETHERIDGE. Computer simulation of gas exchange in the human lungs. J. Appl. Physiol. (in press), 1973.

95. SCRIMSHIRE, D. A. and P. J. TOMLIN. Gas exchange during the initial stages of N_2O uptake and elimination in a lung model. J. Appl. Physiol. (in press), 1973.

96. SECHER, O. (ed) Physical and Chemical Data on Anaesthetics. Acta Anaesthesiologica Scandinavica, p.53, Supplementum XLII, 1971.

97. SEVERINGHAUS, J. H. The rate of uptake of nitrous oxide in man. J. Clin. Invest. 33: 1183, 1954.

98. SEVERINGHAUS, J. H. Oxyhemoglobin dissociation curve. Correction for temperature and pH variation in human blood. J. Appl. Physiol. 12: 485, 1958.

99. SEVERINGHAUS, J. W. Role of lung factors. In: Uptake and Distribution of Anesthetic Agents. New York: Mc. Graw-Hill Book Company, Inc., 1962.

100. SEVERINGHAUS, J. W. Blood gas calculator. J. Appl. Physiol. 21: 1108, 1966.

101. SHAH, J., J. G. JONES, J. GALVIN and P. J. TOMLIN. Pulmonary gas exchange during induction of anaesthesia with nitrous oxide in seated subjects. Brit. J. Anaesth. 43: 1013, 1971.

102. SIGGAARD ANDERSEN, O. The pH-log P_{CO_2} blood acid - base nomogram revised. Scandinav. J. Clin. & Lab. Invest. 14:598, 1962.

103. SONNE, C. On the possibilty of mixing the air in the lungs with foreign air, especially as it is used in Krough and Lindhard's nitrous oxide method. J. Physiol., London 52: 75, 1918.

104. STAUB, N. C. The interdependence of pulmonary structure and function. Anesthesiology 24: 831, 1963.

105. SUWA, K. and H. H. BENDIXEN. A mathematical analysis of physiological dead space in a lung model. J. Appl. Physiol. 24: 549, 1968.

106. van SLYKE, D. D. and J. SENDROY, Jr. Studies of gas electrolyte equilibria in blood. XV. Line charts for graphic calculation by the Henderson-Hasselbalch equation, and for calculating plasma carbon dioxide content from whole blood content. J. Biol. Chem 79: 781, 1928.

107. WEIBEL, E. R. Morphometry of the Human Lung. Berlin: Springer, 1963.

108. WEIBEL, E. R. and D. M. GOMEZ. Architecture of the human lung. Science 137: 577, 1962.

109. WIDDICOMBE, J. G. Respiratory reflexes in man and other mammalian species. Clin. Sci. 21: 163, 1961.

110. WILDHACK, W. A. Oxygen requirements at high altitudes. J. Aeron. Sci. 9: 543, 1942.

111. WEST, J. B. Regional differences in gas exchange in the lung of erect man. J. Appl. Physiol. 17: 893, 1962.

112. WEST, J. B. Topographical distribution of blood flow in the lung. In: Handbook of Physiology, Respiration Volume II. American Physiological Society, Washington, D. C., 1965.

113. WEST, J. B. Ventilation-perfusion inequality and overall gas exchange in computer models of the lung. Resp. Physiol. 7: 88, 1969.

114. WEST, J. B. Ventilation/blood flow and gas exchange. 2nd ed. Oxford: Blackwell Scientific Publications, 1970.

TABLE 1

Classification of chronic pulmonary emphysema according to the airways affected*

1. Respiratory bronchioles
   - (a) Focal emphysema due to dust.
   - (b) Centrilobular emphysema.

2. Alveolar sacs and alveolar ducts
   - (a) Distal-acinar emphysema.

3. Alveolar sacs, alveolar ducts and respiratory bronchioles
   - (a) Pan-acina emphysema.

4. Irregular
   - (a) Coarse scarring.
   - (b) Fine scarring, mature or incipient (chronic bronchiolo-alveolitis).
   - (c) Linear emphysema.
   - (d) Bullae.

*Reproduced from Heppleston (53).

TABLE 2

Comparison of changes in arterial P_{O_2} during uptake and elimination in a homogeneous lung model (inert gas solubility = 10).

Breath number	Uptake ΔP_{aO_2}	Elimination ΔP_{aO_2}
1	10.0	10.2
2	23.4	24.6
3	37.0	38.2
4	49.0	48.7
5	62.9	55.5
10	127.5	67.5
15	183.0	68.8
20	230.6	68.9

TABLE 3

$\dot{Q}s/\dot{Q}t$ x 100 Per cent.	End capillary		Mixed arterial		Venous	
	C_{O_2}	C_{CO_2}	C_{O_2}	C_{CO_2}	C_{O_2}	C_{CO_2}
10	20.54	41.69	19.99	42.13	14.99	46.13
20	20.54	41.68	19.29	42.69	14.29	46.69
40	20.54	41.68	17.21	44.35	12.21	48.35
60	20.54	41.67	13.04	47.68	8.04	51.68

Arterio-venous C_{O_2} difference = 5 ml/100 ml.

Arterio-venous C_{CO_2} difference = 4 ml/100 ml.

TABLE 4 (a)

Results obtained from the analysis of Farhi (36)

Uneven ventilation		L	M
	Ventilation %	20.21	79.79
Parameter b = .5			
	Blood flow %	62.24	37.76
		L	M
	Ventilation %	12.09	87.91
Parameter b = 1.0			
	Blood flow %	74.00	26.00
		L	M
	Ventilation %	9.71	90.29
Parameter b = 1.5			
	Blood flow %	80.68	19.32
Uneven blood flow		L	M
	Ventilation %	34.73	65.27
Parameter b = 0.5			
	Blood flow %	79.72	20.28
		L	M
	Ventilation %	29.20	70.80
Parameter b = 1.0			
	Blood flow %	91.37	28.63
		L	M
	Ventilation %	24.99	75.01
Parameter b = 1.5			
	Blood flow %	96.21	3.79

TABLE 4 (b)

Actual distributions existing in models lumped into two compartments

Uneven Ventilation

		L	M
	Ventilation %	22.60	77.40
Parameter b = 0.5			
	Blood flow %	60.00	40.00
		L	M
	Ventilation %	12.43	87.57
Parameter b = 1.0			
	Blood flow %	70.00	30.00
		L	M
	Ventilation %	4.42	95.58
Parameter b = 1.5			
	Blood flow %	70.00	30.00

Uneven blood flow

		L	M
	Ventilation %	40.00	60.00
Parameter b = 0.5			
	Blood flow %	77,40	22.60
		L	M
	Ventilation %	30.00	70.00
Parameter b = 1.0			
	Blood flow %	87.57	12.43
		L	M
	Ventilation %	30.00	70.00
Parameter b = 1.5			
	Blood flow %	95.58	4.42

TABLE 5

	TISSUE GROUP			
	VRG	MG	FG	VPG
Tissue/blood partition coefficients for nitrous oxide	1.06	1.13	2.30	1.00
Tissue/blood partition coefficients for nitrogen	1.1	1.0	5.2	1.0
Volume of tissue group, ml.	6000.0	33,000.0	14,500.0	12,500.0
%systemic blood flow to tissue group	75.0	18.1	5.4	1.5

Parameter values in the simulation of tissue exchange of nitrous oxide and nitrogen.

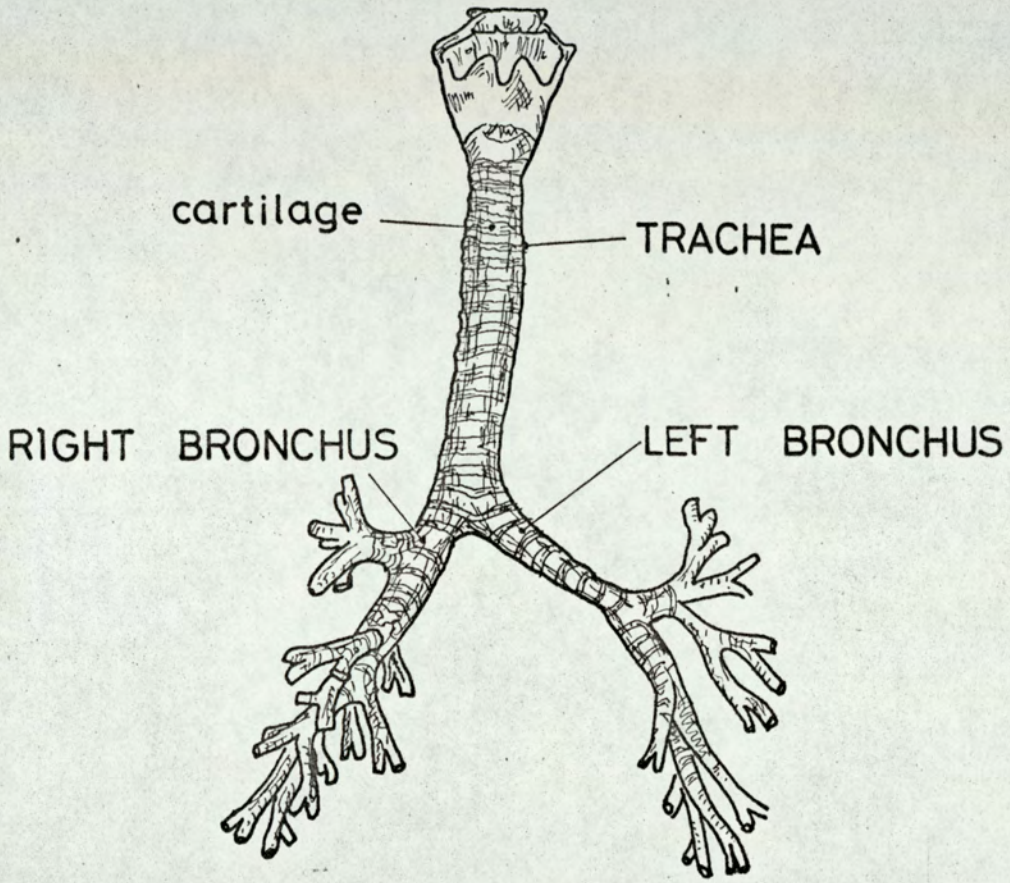

FIGURE 1

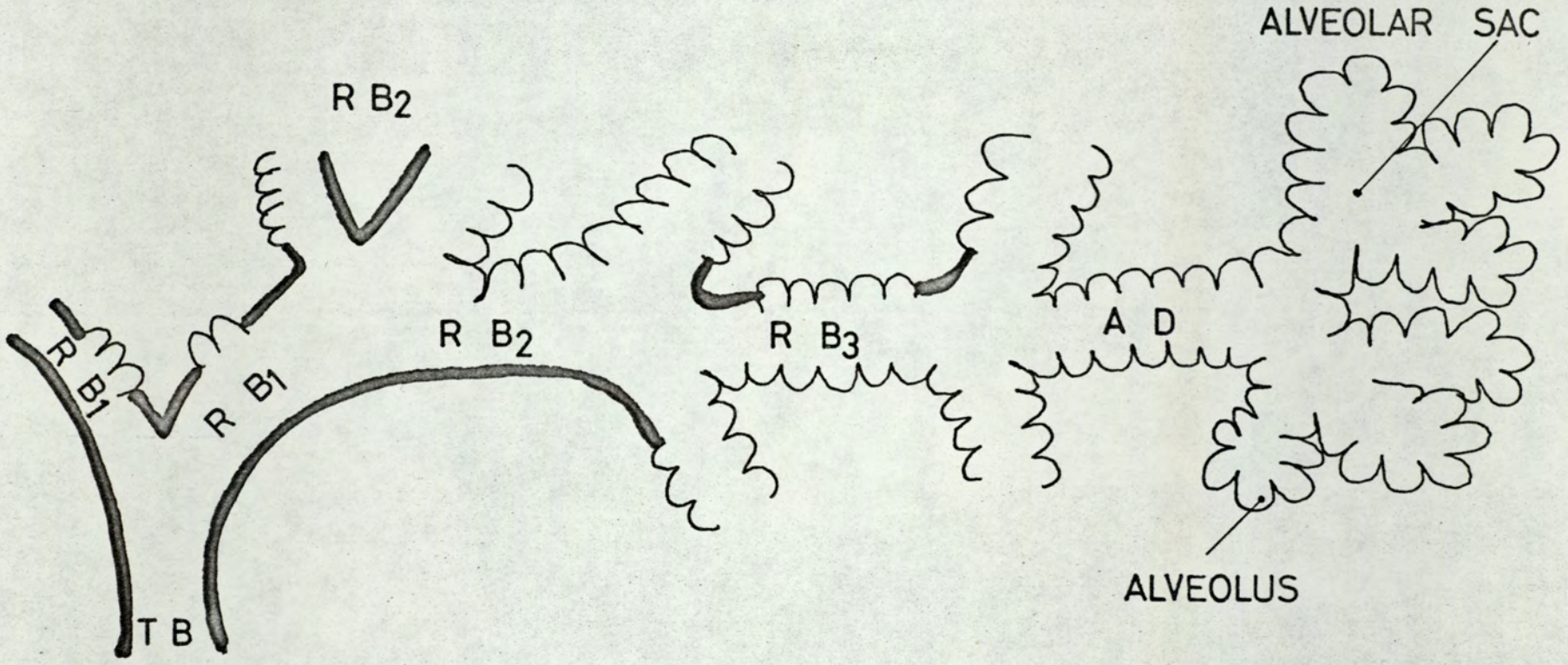

FIGURE 2

FIGURE 3

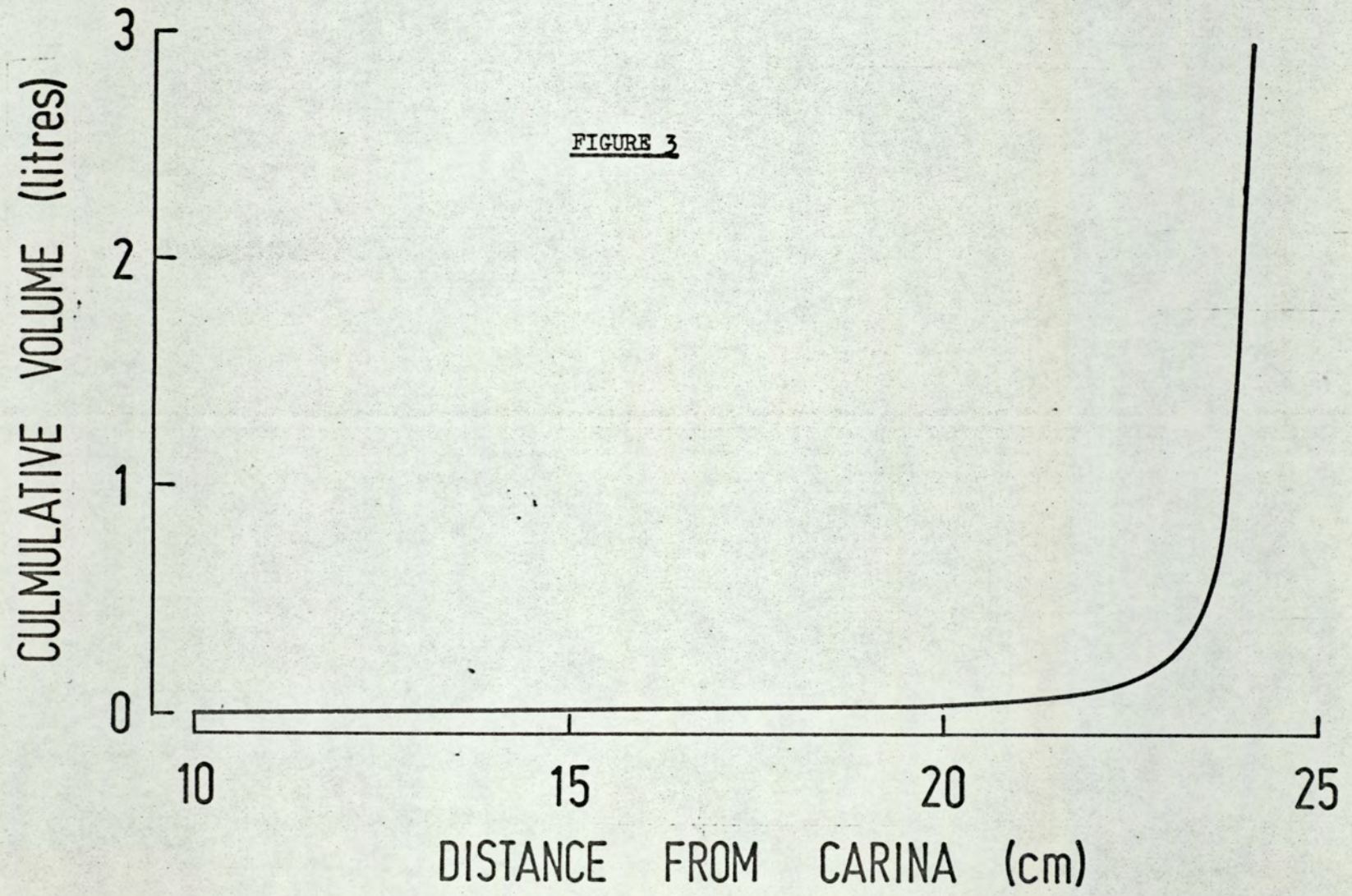
CULMULATIVE VOLUME (litres)
3
2
1
0
10
15
20
25
DISTANCE FROM CARINA (cm)

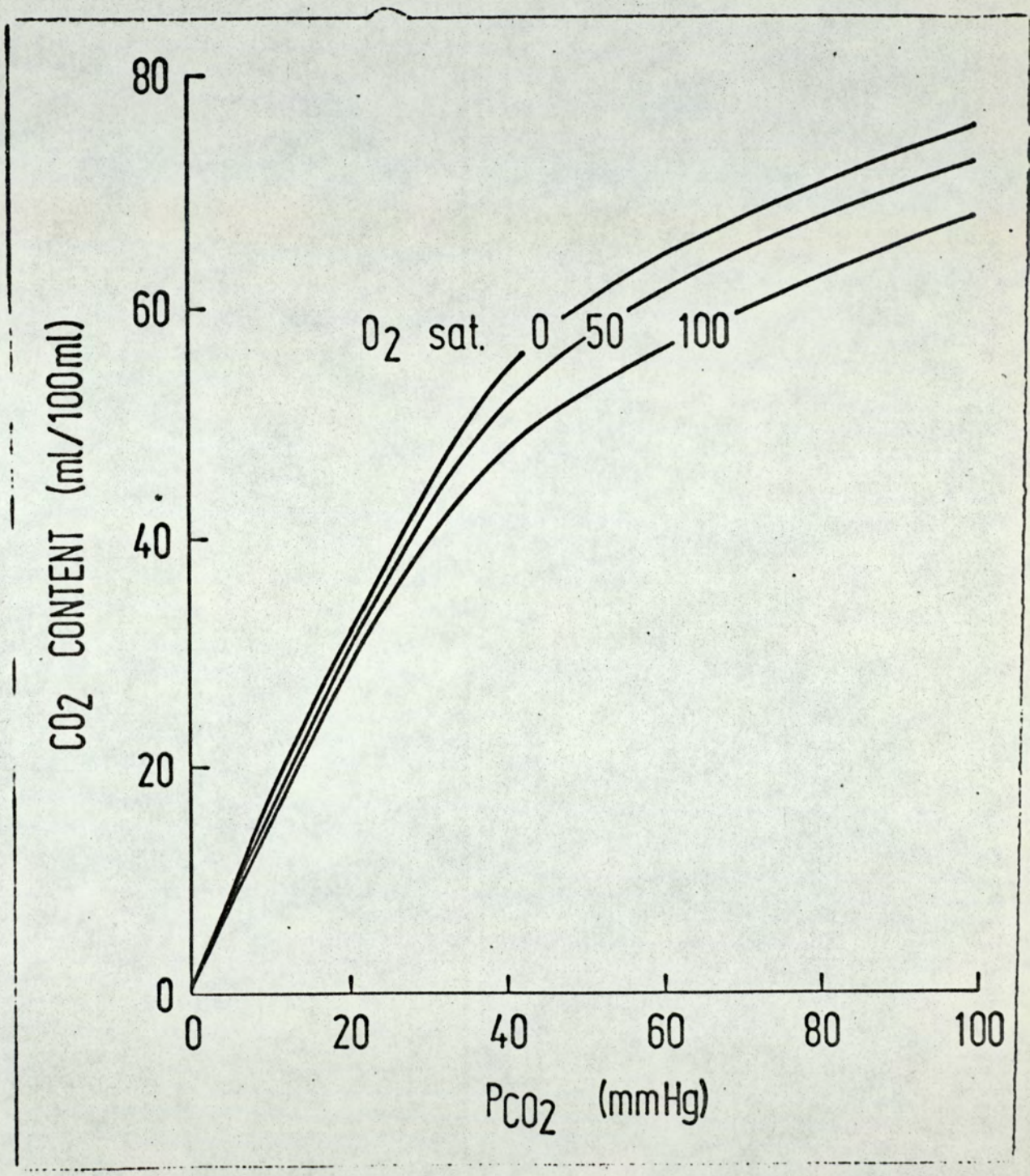
80
60
40
20
0
CO_2 CONTENT (ml/100ml)
O_2 sat. 0 50 100
0
20
40
60
80
100
P_{CO_2} (mmHg)

FIGURE 4

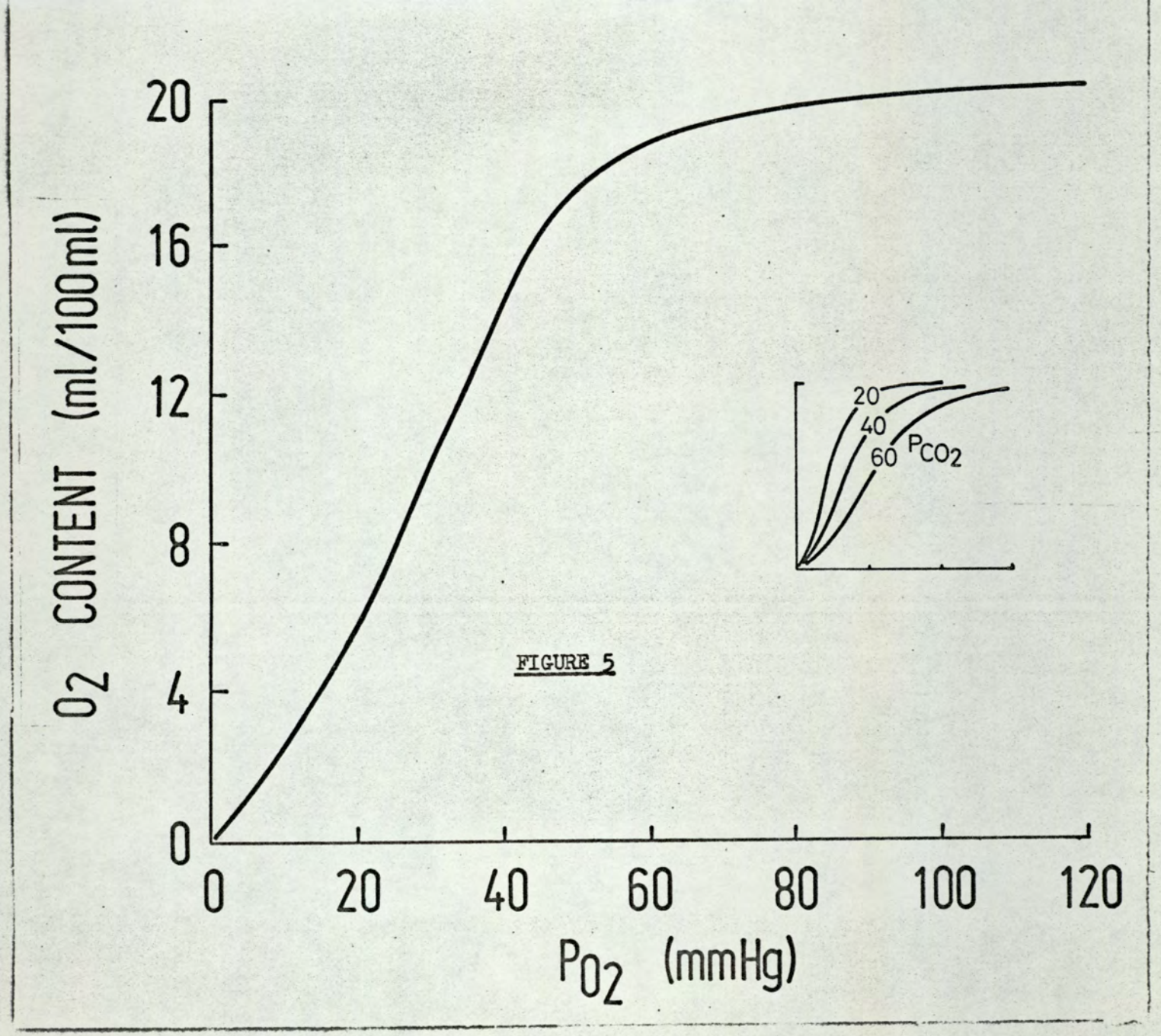
20
16
12
8
4
0
O_2 CONTENT (ml/100ml)
0
20
40
60
80
100
120
P_{O_2} (mmHg)
20
40
60
P_{CO_2}

FIGURE 5

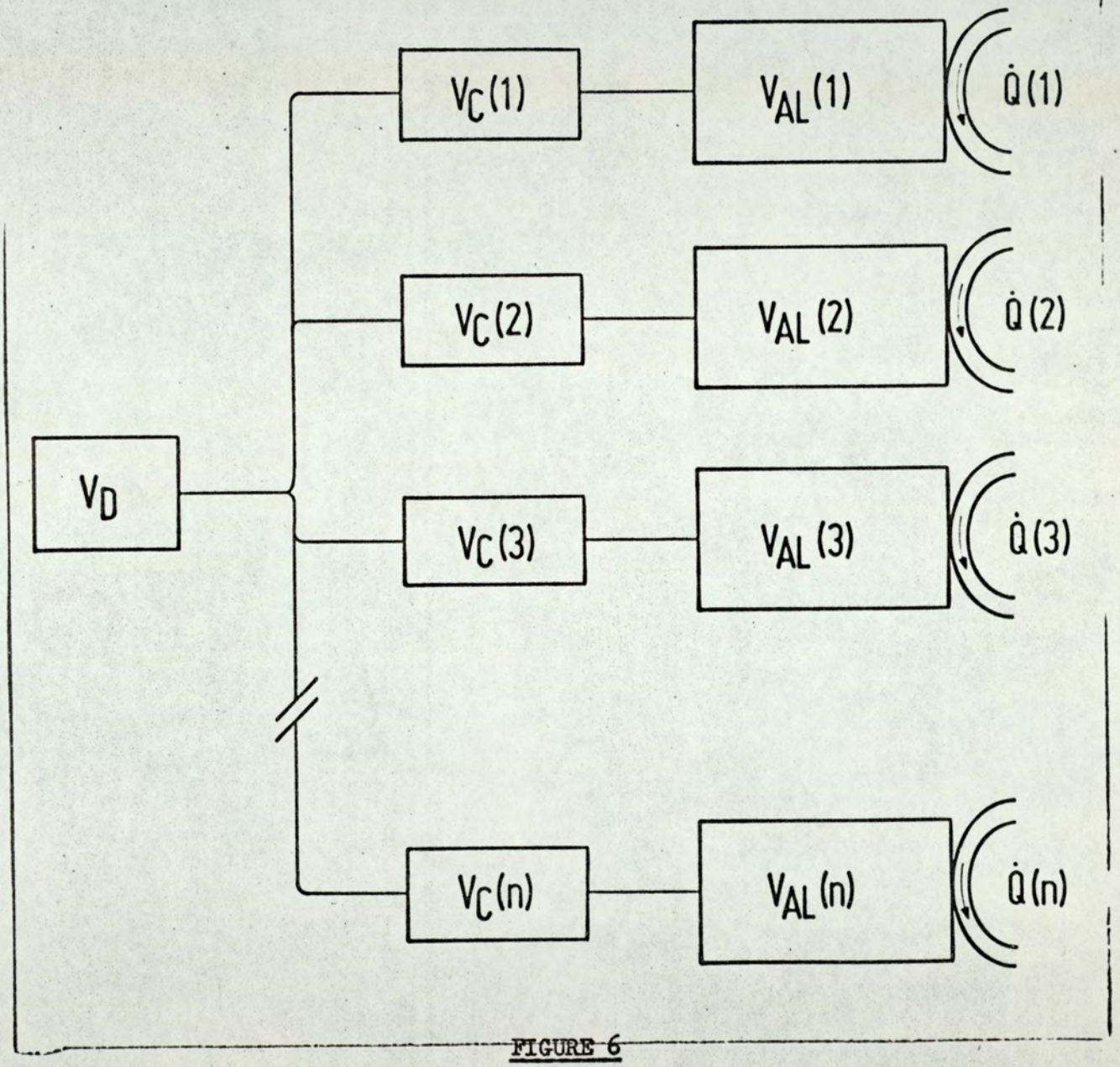
V_D
$V_C(1)$
$V_C(2)$
$V_C(3)$
$V_C(n)$
$V_{AL}(1)$
$V_{AL}(2)$
$V_{AL}(3)$
$V_{AL}(n)$
$\dot{Q}(1)$
$\dot{Q}(2)$
$\dot{Q}(3)$
$\dot{Q}(n)$

FIGURE 6

FIGURE 7

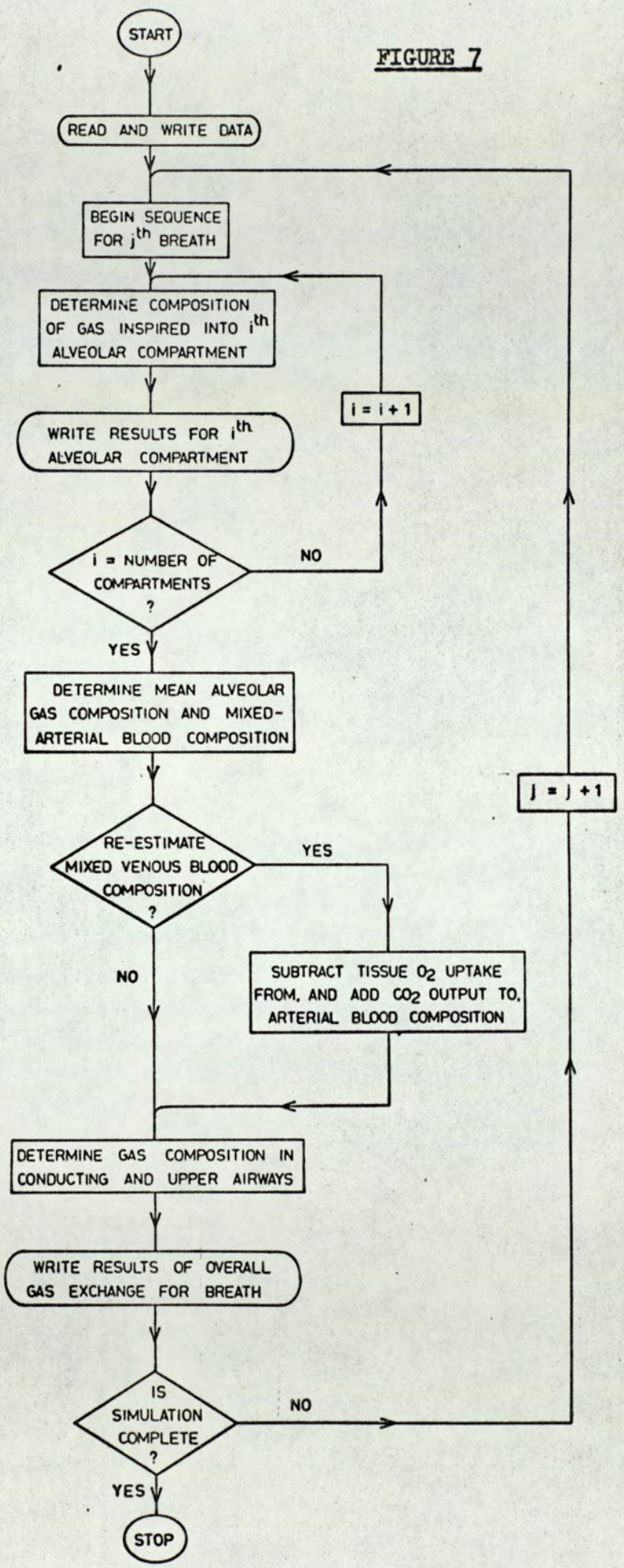
START
READ AND WRITE DATA
BEGIN SEQUENCE FOR j^th BREATH
DETERMINE COMPOSITION OF GAS INSPIRED INTO i^th ALVEOLAR COMPARTMENT
WRITE RESULTS FOR i^th ALVEOLAR COMPARTMENT
i = i + 1
i = NUMBER OF COMPARTMENTS ?
NO
YES
DETERMINE MEAN ALVEOLAR GAS COMPOSITION AND MIXED-ARTERIAL BLOOD COMPOSITION
j = j + 1
RE-ESTIMATE MIXED VENOUS BLOOD COMPOSITION ?
YES
NO
SUBTRACT TISSUE O2 UPTAKE FROM, AND ADD CO2 OUTPUT TO, ARTERIAL BLOOD COMPOSITION
DETERMINE GAS COMPOSITION IN CONDUCTING AND UPPER AIRWAYS
WRITE RESULTS OF OVERALL GAS EXCHANGE FOR BREATH
IS SIMULATION COMPLETE ?
NO
YES
STOP

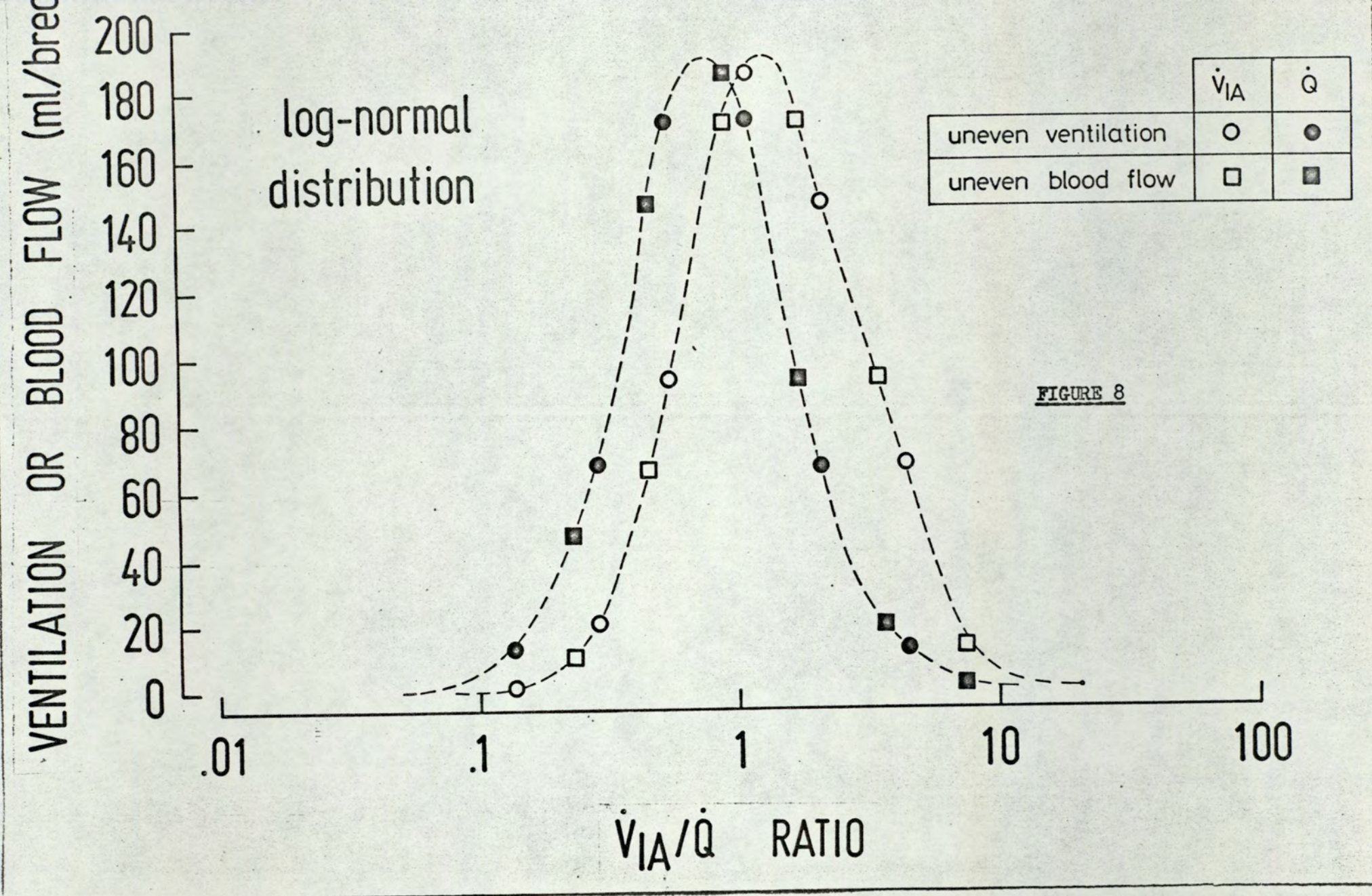
log-normal
distribution
$\dot{V}_{IA}$
$\dot{Q}$
uneven ventilation
uneven blood flow
VENTILATION OR BLOOD FLOW (ml/breath)
200
180
160
140
120
100
80
60
40
20
0
.01
.1
1
10
100
$\dot{V}_{IA}/\dot{Q}$ RATIO

FIGURE 8

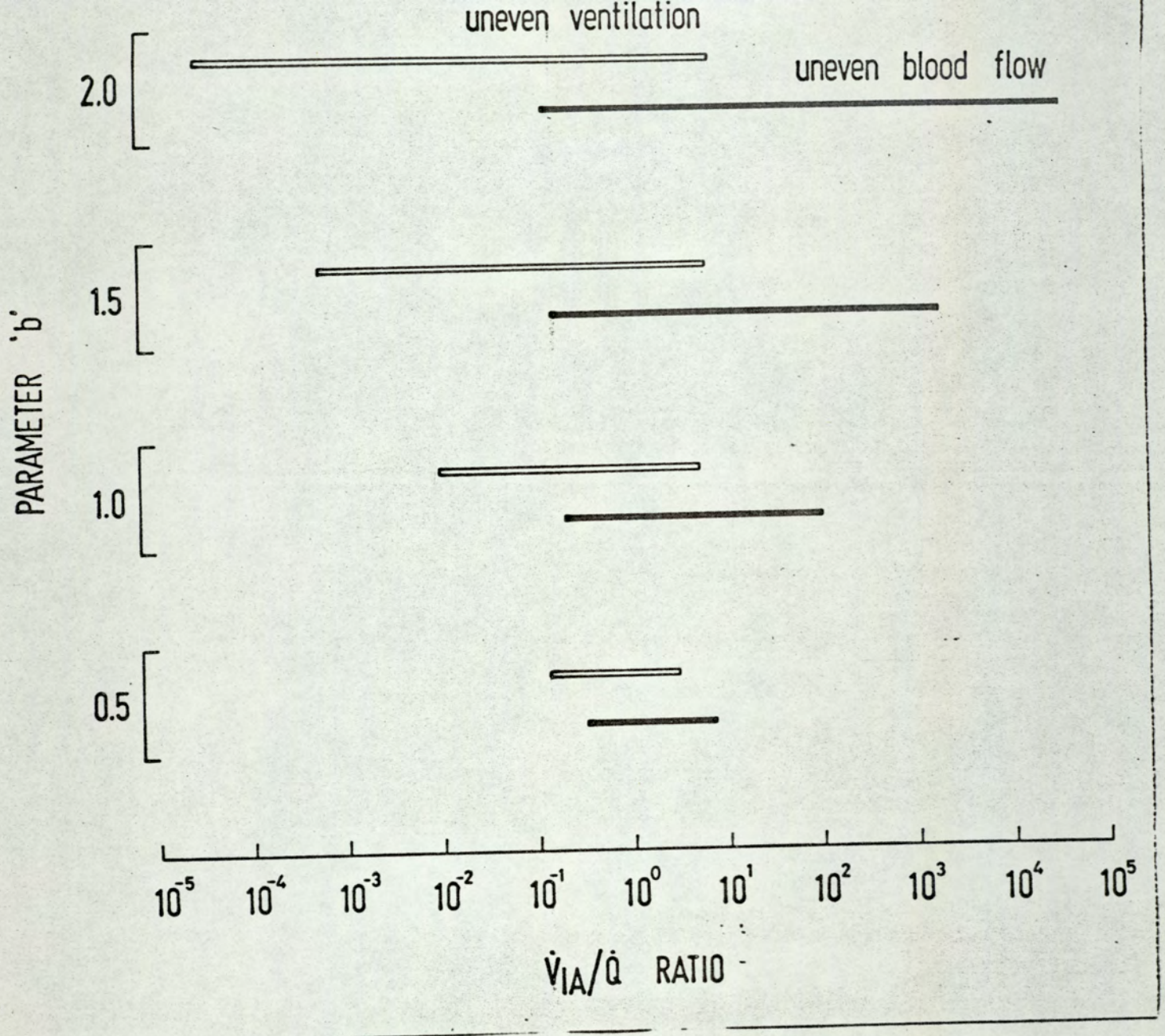
uneven ventilation
uneven blood flow
2.0
1.5
1.0
0.5
PARAMETER 'b'
10^{-5} 10^{-4} 10^{-3} 10^{-2} 10^{-1} 10^{0} 10^{1} 10^{2} 10^{3} 10^{4} 10^{5}
$\dot{V}_{IA}/\dot{Q}$ RATIO

FIGURE 9

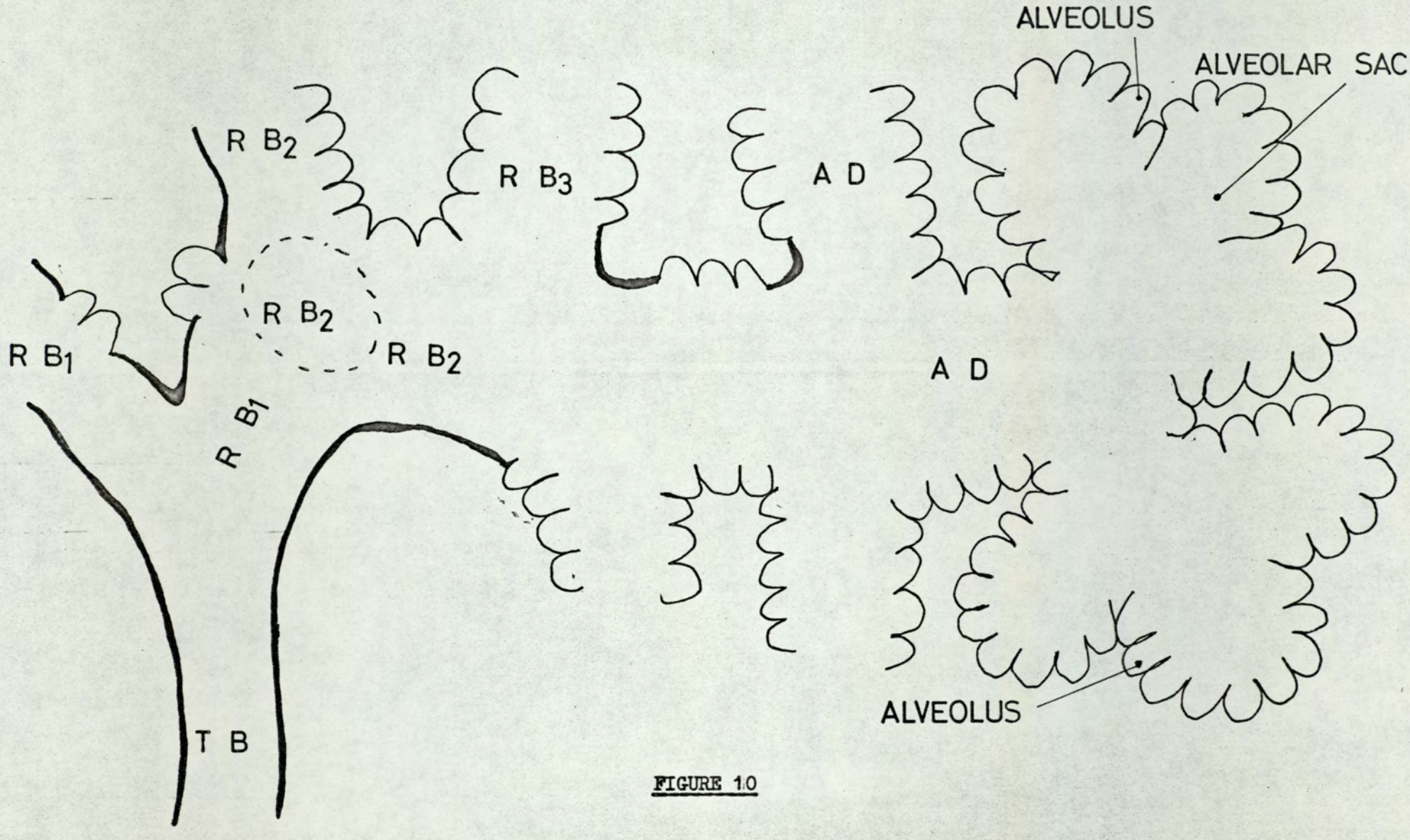
ALVEOLUS
ALVEOLAR SAC
R B2
R B3
A D
R B2
R B1
R B2
R B1
A D
ALVEOLUS
T B

FIGURE 10

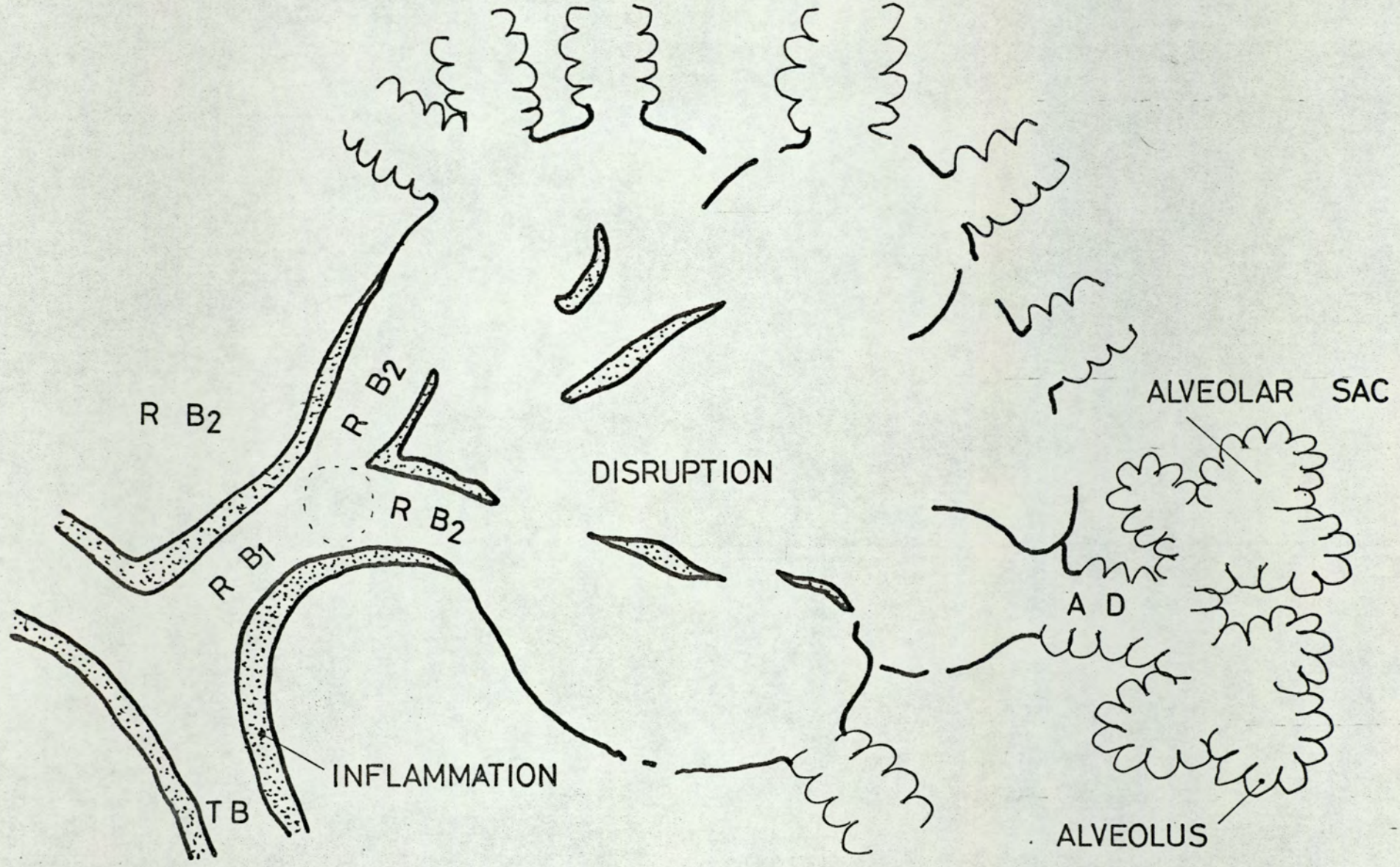
R B2
R B2
R B2
R B1
DISRUPTION
ALVEOLAR SAC
A D
INFLAMMATION
T B
ALVEOLUS

FIGURE 11

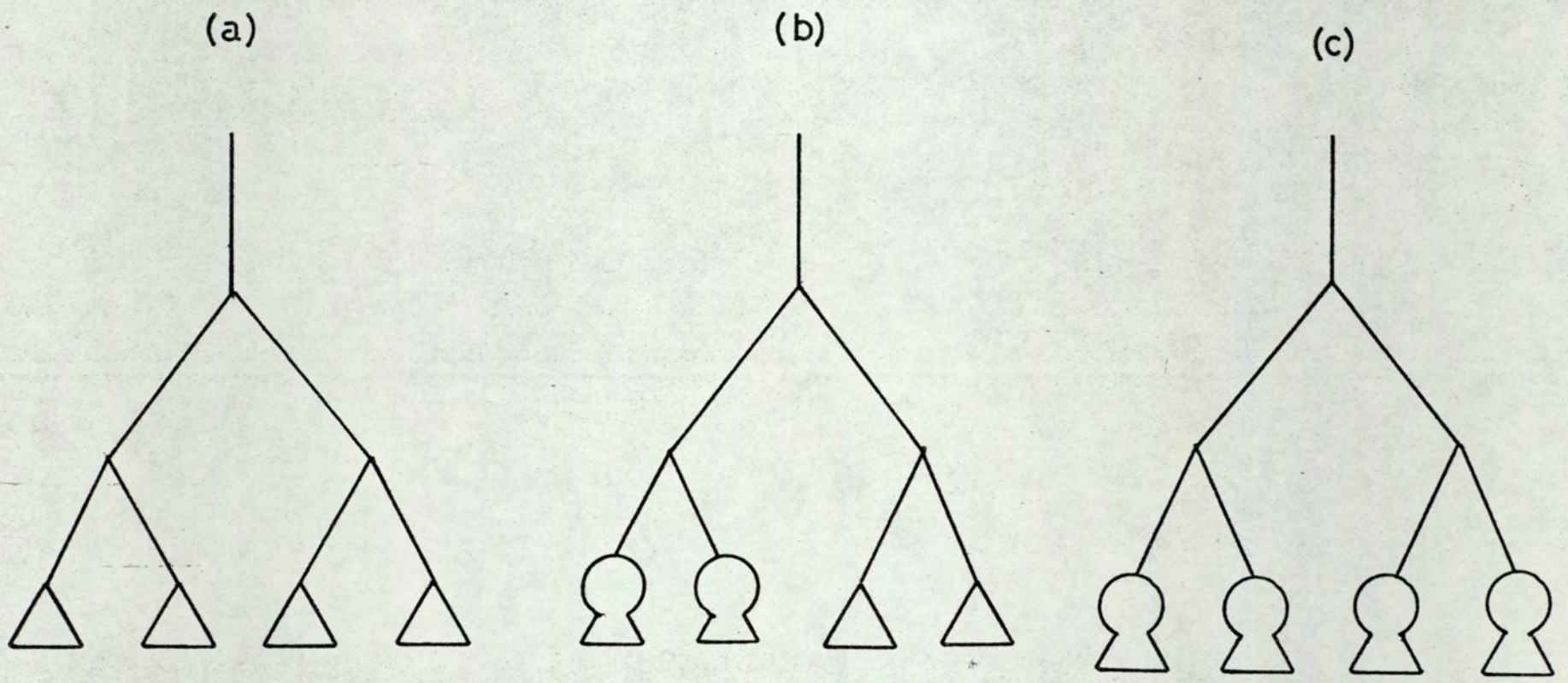

FIGURE 12

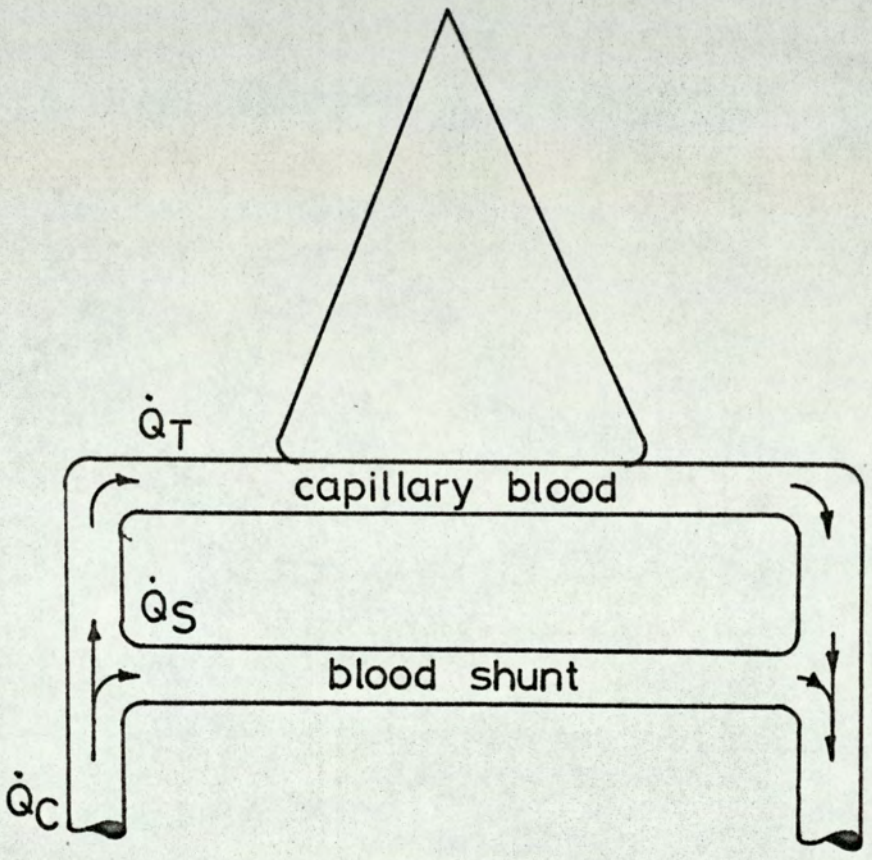

FIGURE 13

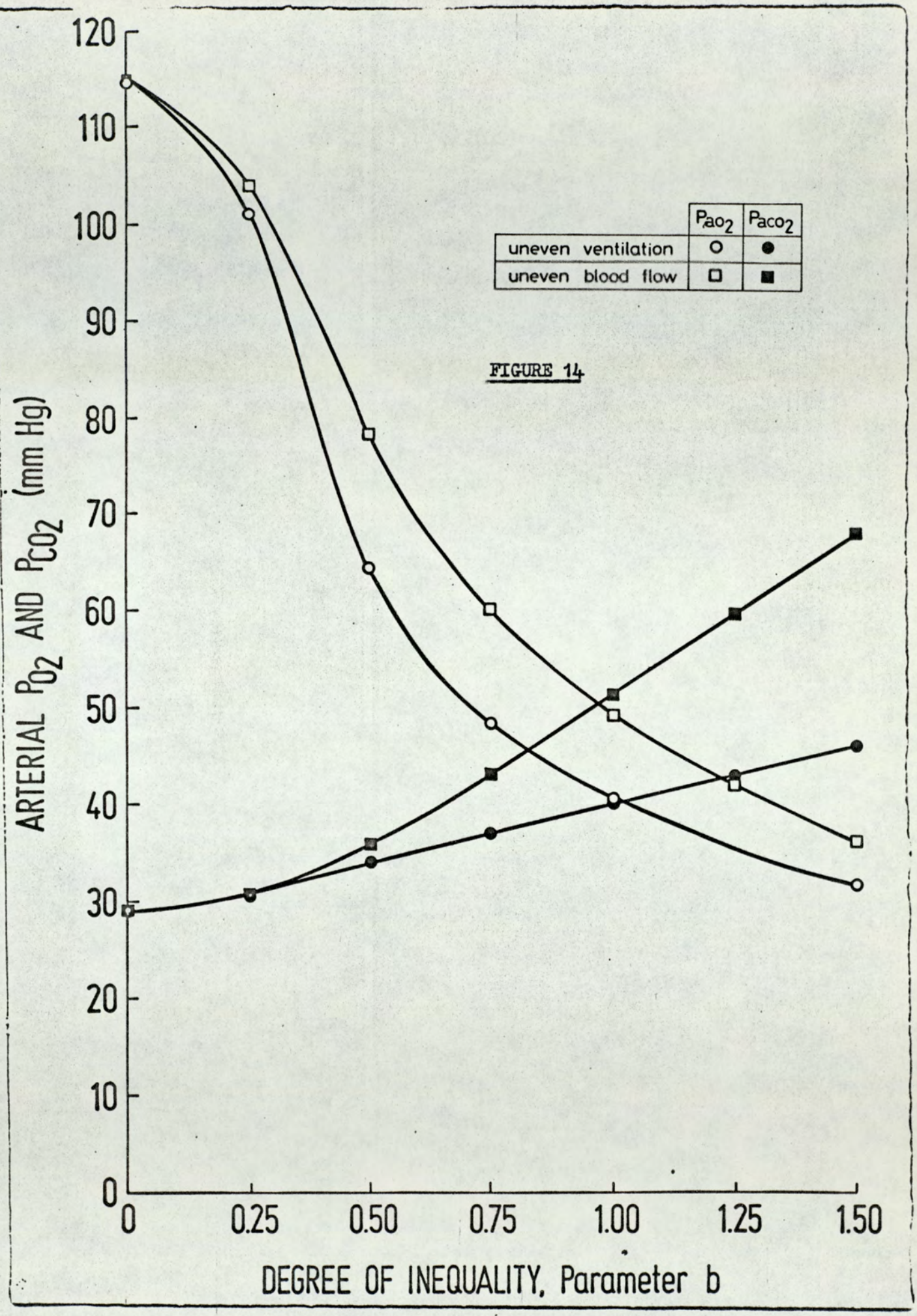
120
110
100
90
80
70
60
50
40
30
20
10
0
0
0.25
0.50
0.75
1.00
1.25
1.50
ARTERIAL P_{O_2} AND P_{CO_2} (mm Hg)
DEGREE OF INEQUALITY, Parameter b
P_{ao_2}
P_{aco_2}
uneven ventilation
uneven blood flow

FIGURE 14

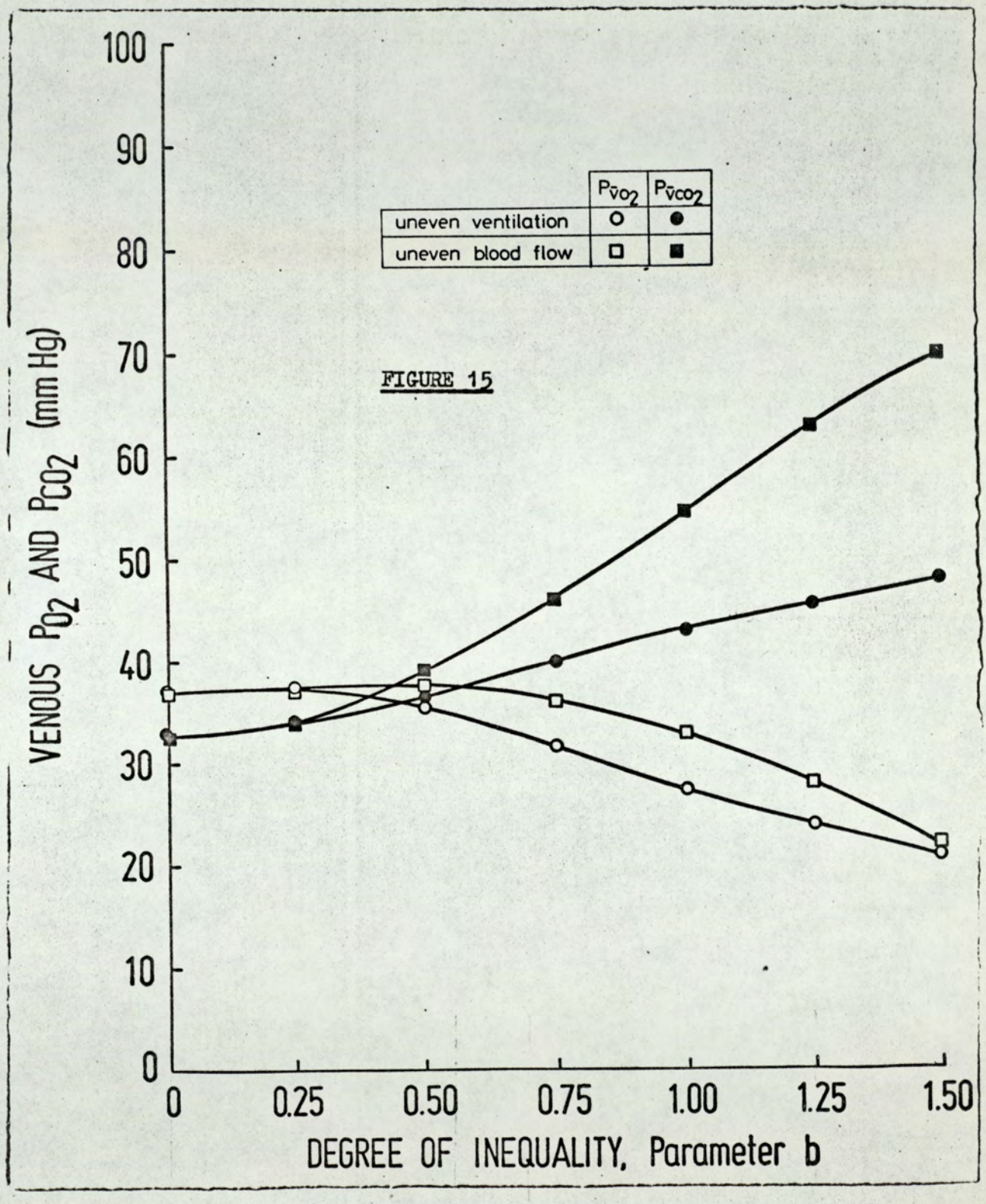
100
90
80
70
60
50
40
30
20
10
0
VENOUS P_{O_2} AND P_{CO_2} (mm Hg)
$P_{\bar{v}O_2}$
$P_{\bar{v}CO_2}$
uneven ventilation
uneven blood flow
0
0.25
0.50
0.75
1.00
1.25
1.50
DEGREE OF INEQUALITY, Parameter b

FIGURE 15

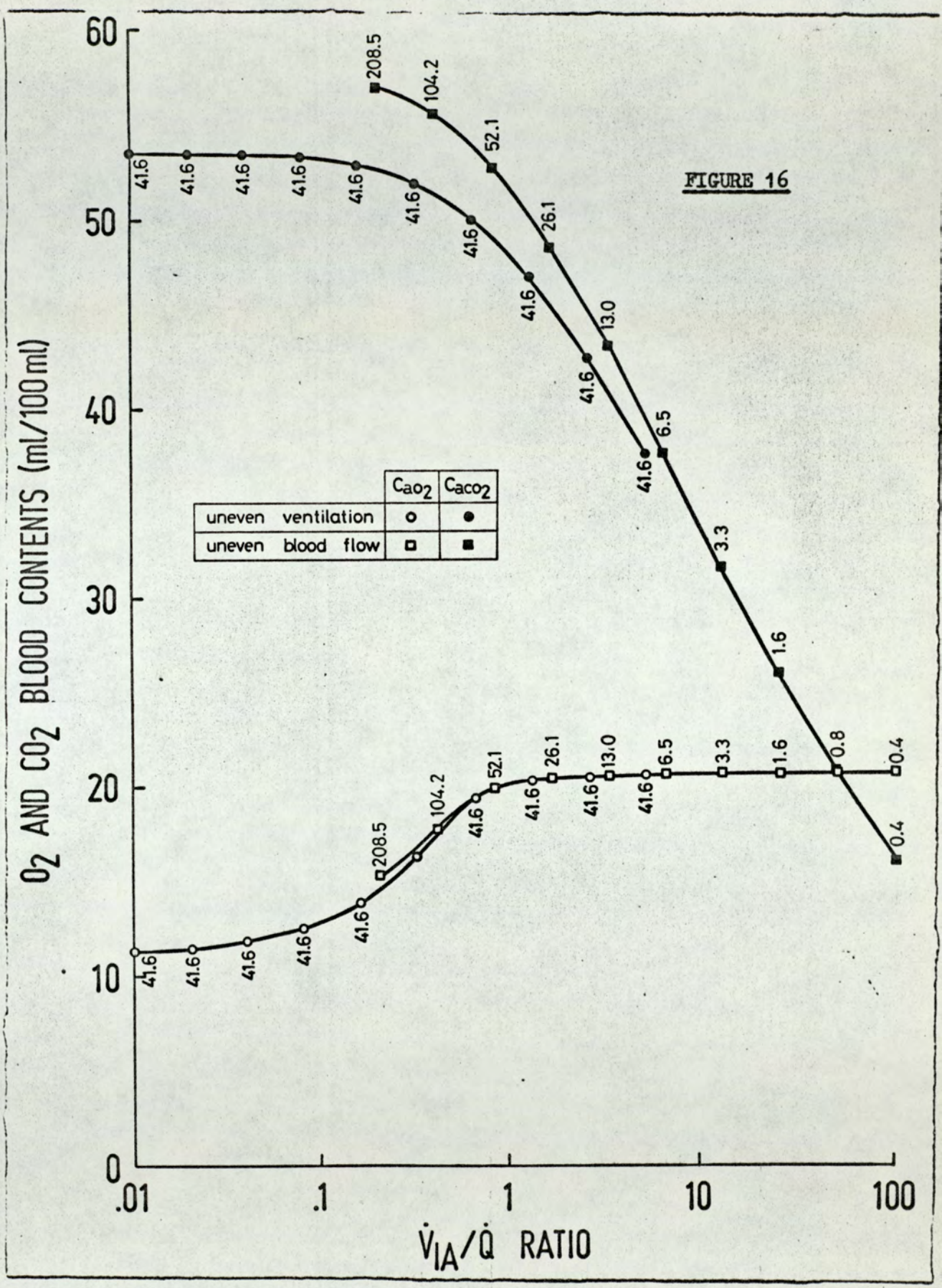
FIGURE 16
O_2 AND CO_2 BLOOD CONTENTS (ml/100 ml)
$\dot{V}_{IA}/\dot{Q}$ RATIO
60
50
40
30
20
10
0
.01
.1
1
10
100
C_{aO_2}
C_{aCO_2}
uneven ventilation
uneven blood flow
41.6
208.5
104.2
52.1
26.1
13.0
6.5
3.3
1.6
0.8
0.4

FIGURE 17

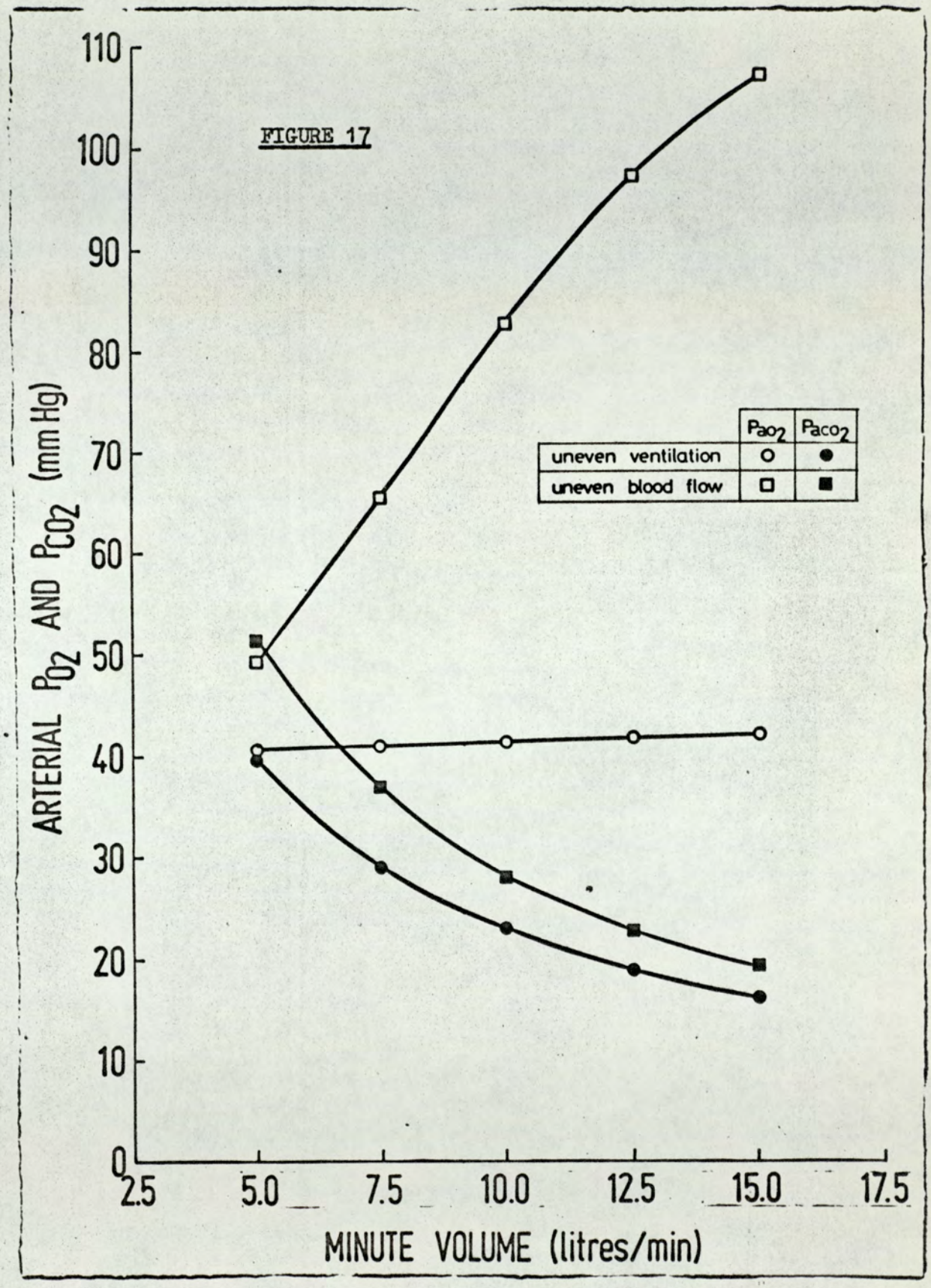
110
100
90
80
70
60
50
40
30
20
10
0
ARTERIAL P_{O_2} AND P_{CO_2} (mm Hg)
2.5
5.0
7.5
10.0
12.5
15.0
17.5
MINUTE VOLUME (litres/min)
P_{ao_2}
P_{aco_2}
uneven ventilation
uneven blood flow

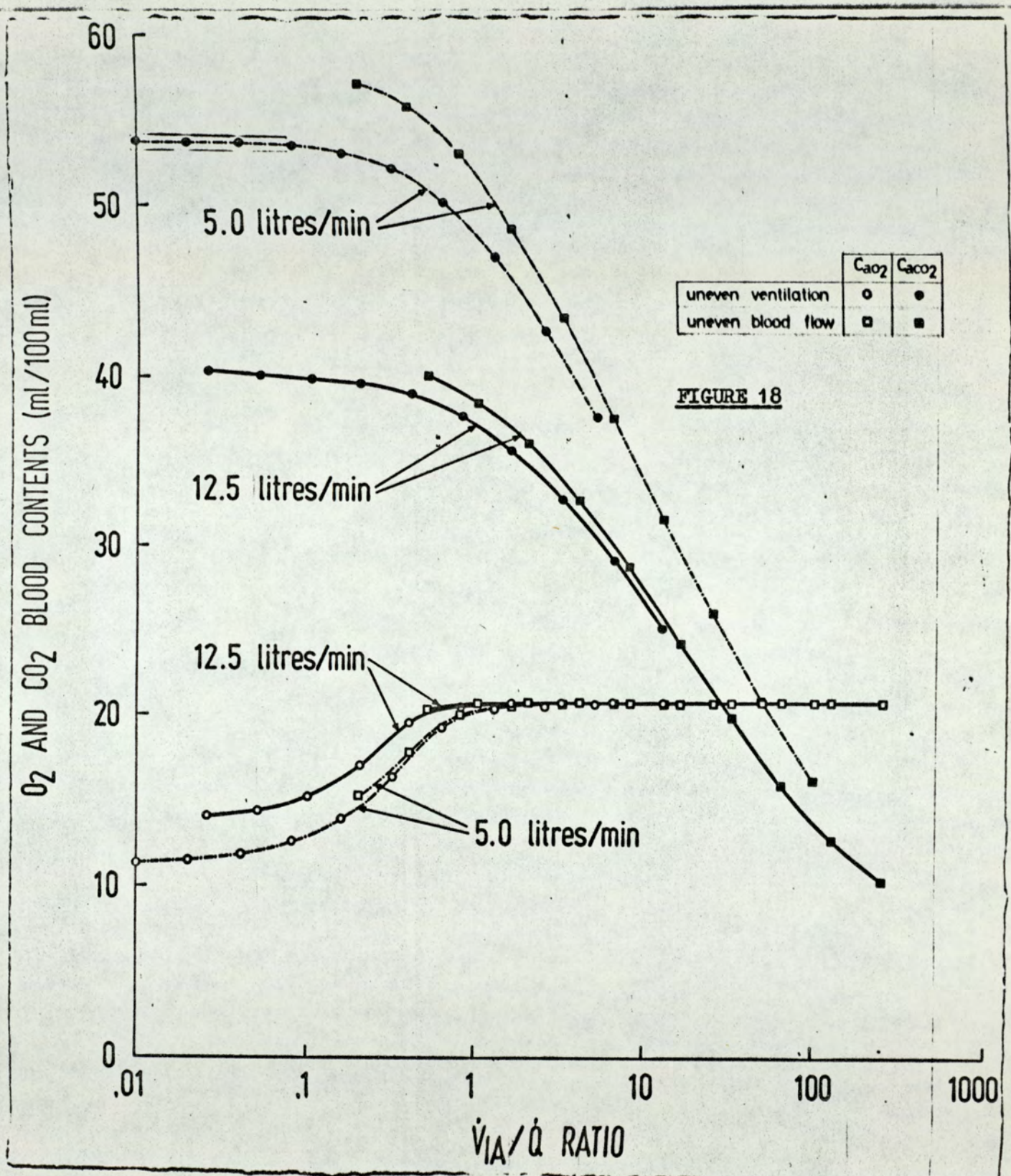
60
50
40
30
20
10
0
O_2 AND CO_2 BLOOD CONTENTS (ml/100ml)
5.0 litres/min
12.5 litres/min
12.5 litres/min
5.0 litres/min
C_{aO_2}
C_{aCO_2}
uneven ventilation
uneven blood flow
.01
.1
1
10
100
1000
$\dot{V}_{IA}/\dot{Q}$ RATIO

FIGURE 18

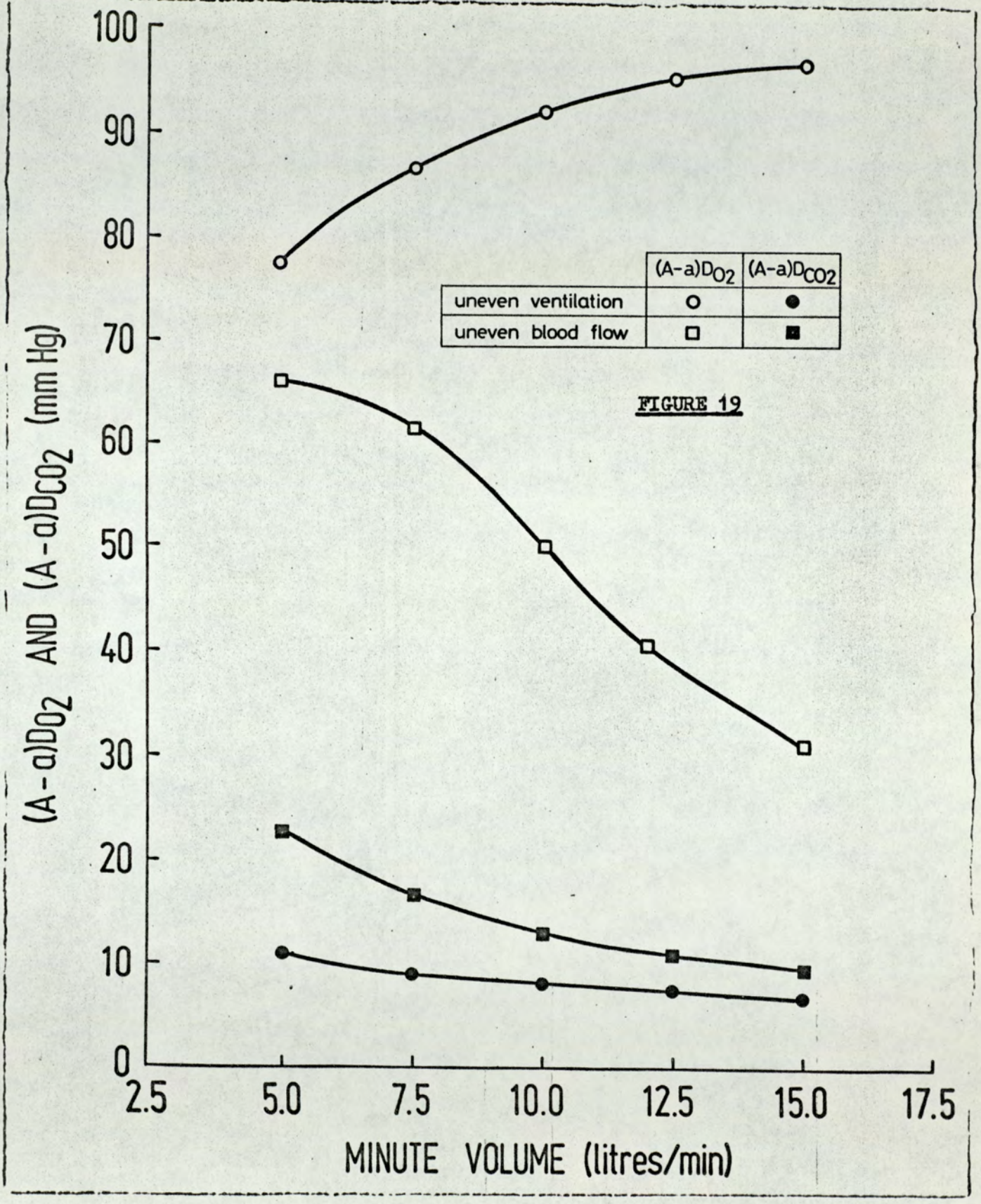
100
90
80
70
60
50
40
30
20
10
0
2.5
5.0
7.5
10.0
12.5
15.0
17.5
(A-a)D$_{O_2}$ AND (A-a)D$_{CO_2}$ (mm Hg)
MINUTE VOLUME (litres/min)
(A-a)D$_{O_2}$
(A-a)D$_{CO_2}$
uneven ventilation
uneven blood flow

FIGURE 19

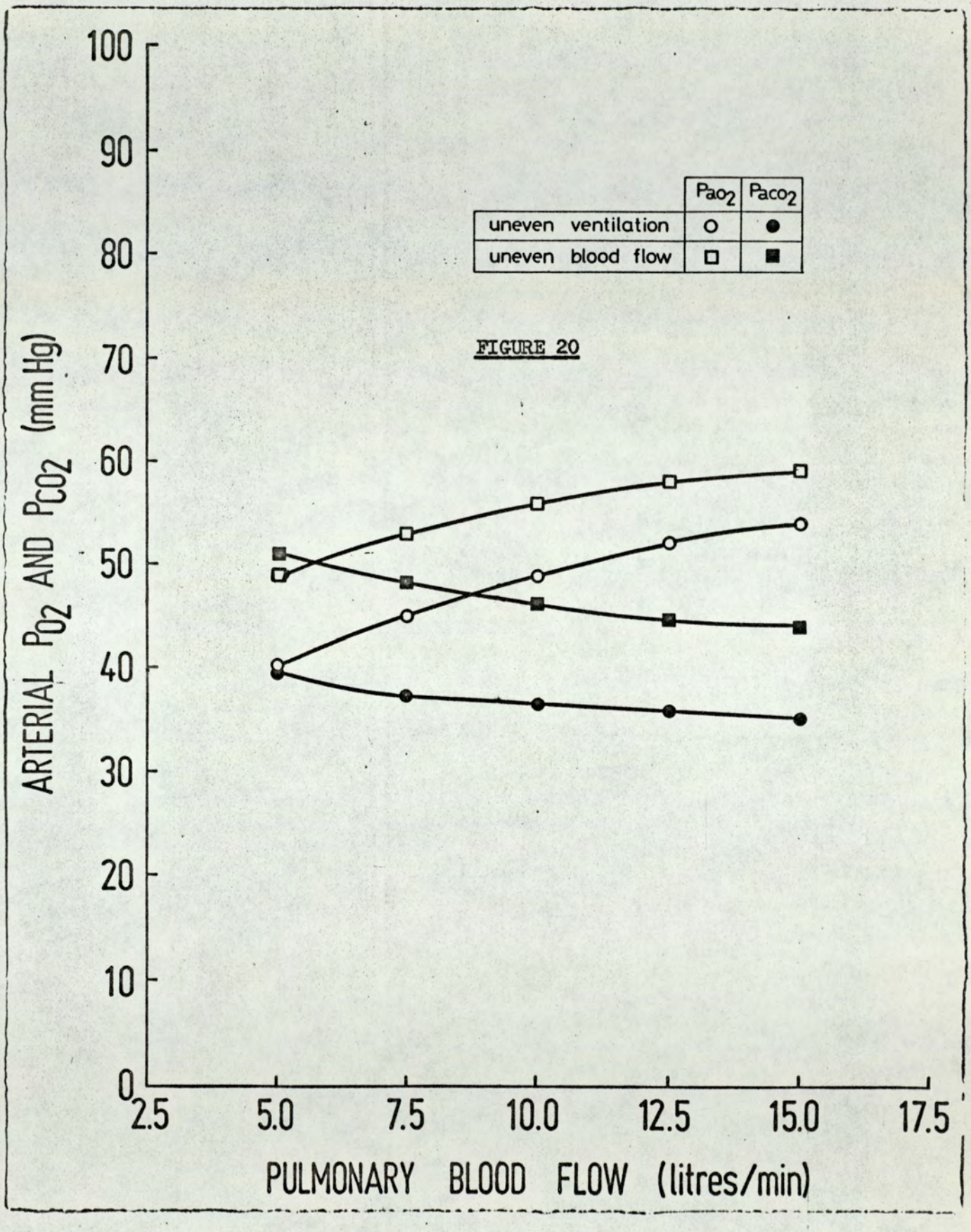
100
90
80
70
60
50
40
30
20
10
0
ARTERIAL P_{O_2} AND P_{CO_2} (mm Hg)
2.5
5.0
7.5
10.0
12.5
15.0
17.5
PULMONARY BLOOD FLOW (litres/min)
P_{ao_2}
P_{aco_2}
uneven ventilation
uneven blood flow

FIGURE 20

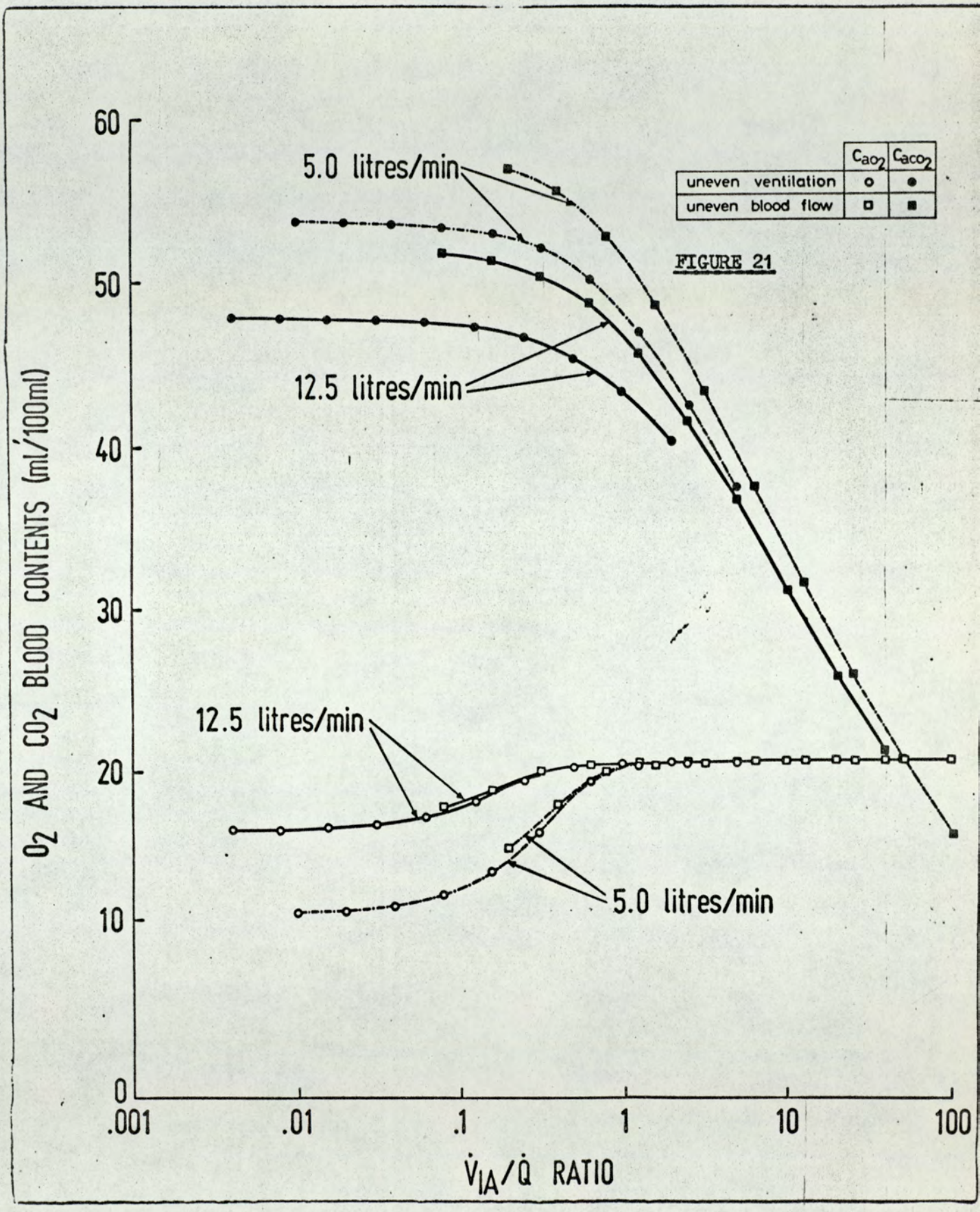
60
50
40
30
20
10
0
.001
.01
.1
1
10
100
O_2 AND CO_2 BLOOD CONTENTS (ml/100ml)
$\dot{V}_{IA}/\dot{Q}$ RATIO
5.0 litres/min
12.5 litres/min
12.5 litres/min
5.0 litres/min
C_{ao_2}
C_{aco_2}
uneven ventilation
uneven blood flow

FIGURE 21

FIGURE 22

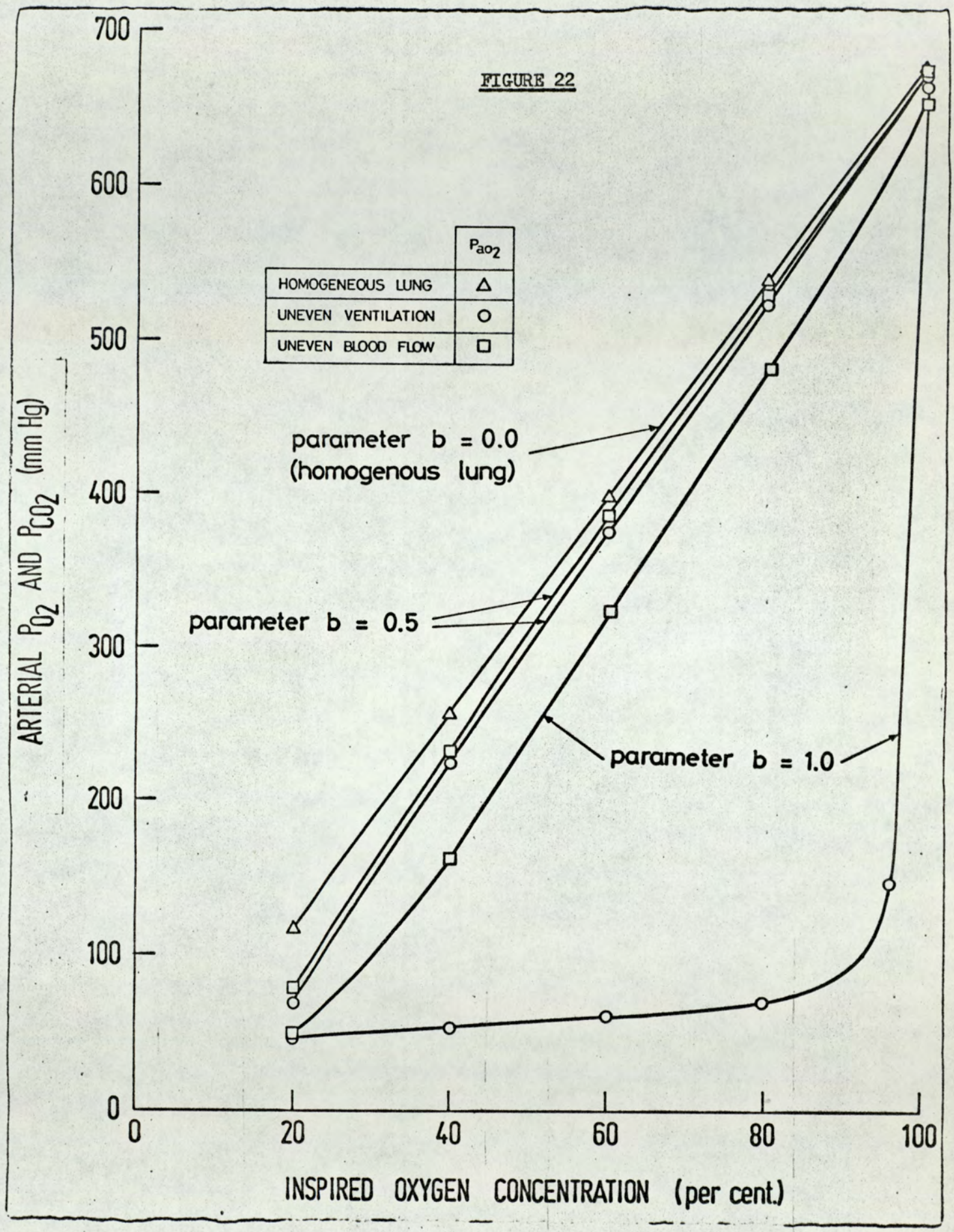
700
600
500
400
300
200
100
0
0
20
40
60
80
100
ARTERIAL P_{O_2} AND P_{CO_2} (mm Hg)
INSPIRED OXYGEN CONCENTRATION (per cent.)
P_{ao_2}
HOMOGENEOUS LUNG
UNEVEN VENTILATION
UNEVEN BLOOD FLOW
parameter b = 0.0
(homogenous lung)
parameter b = 0.5
parameter b = 1.0

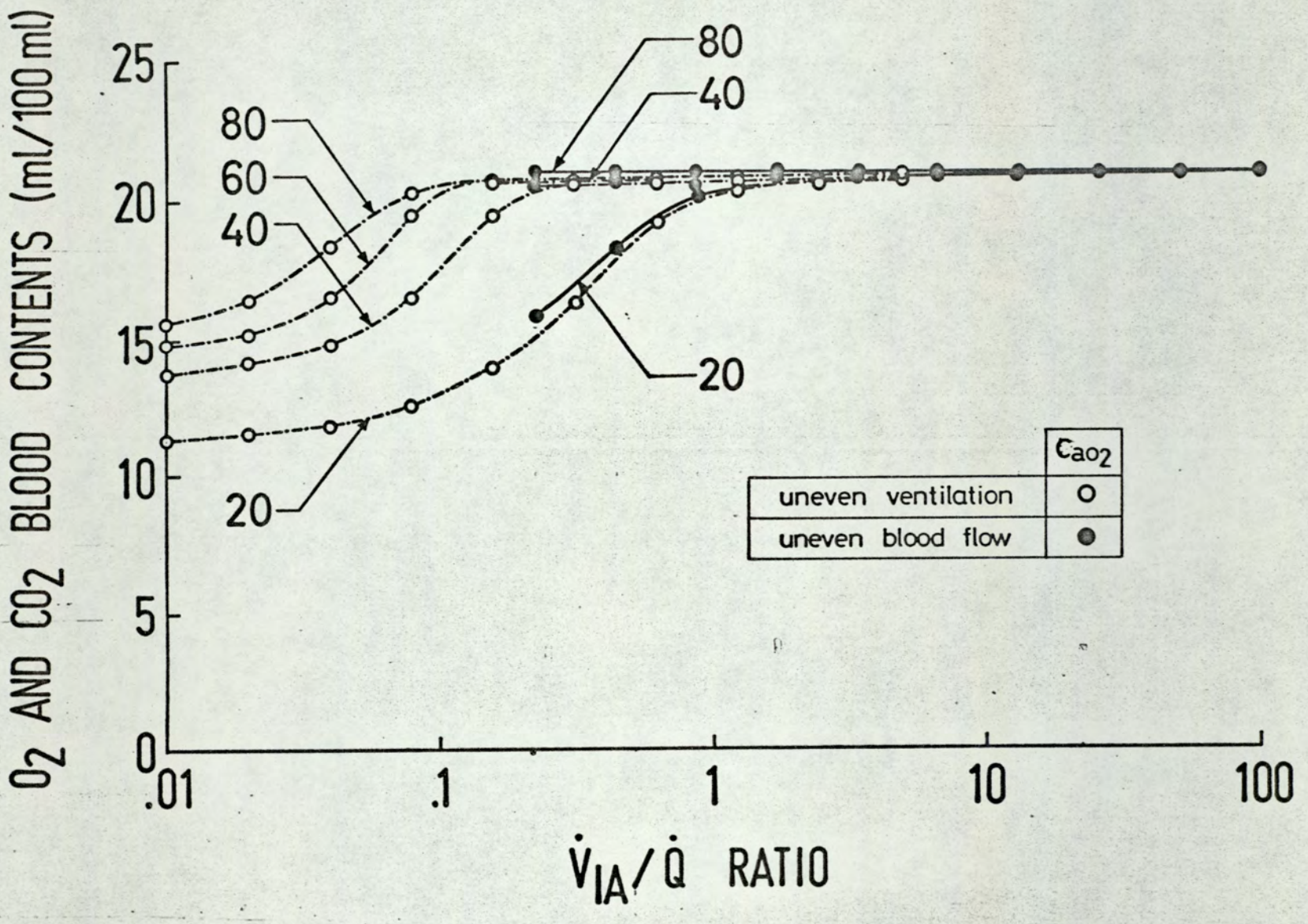
O_2 AND CO_2 BLOOD CONTENTS (ml/100 ml)
25
20
15
10
5
0
.01
.1
1
10
100
$\dot{V}_{IA}/\dot{Q}$ RATIO
80
60
40
20
80
40
20
C_{aO_2}
uneven ventilation
uneven blood flow

FIGURE 23

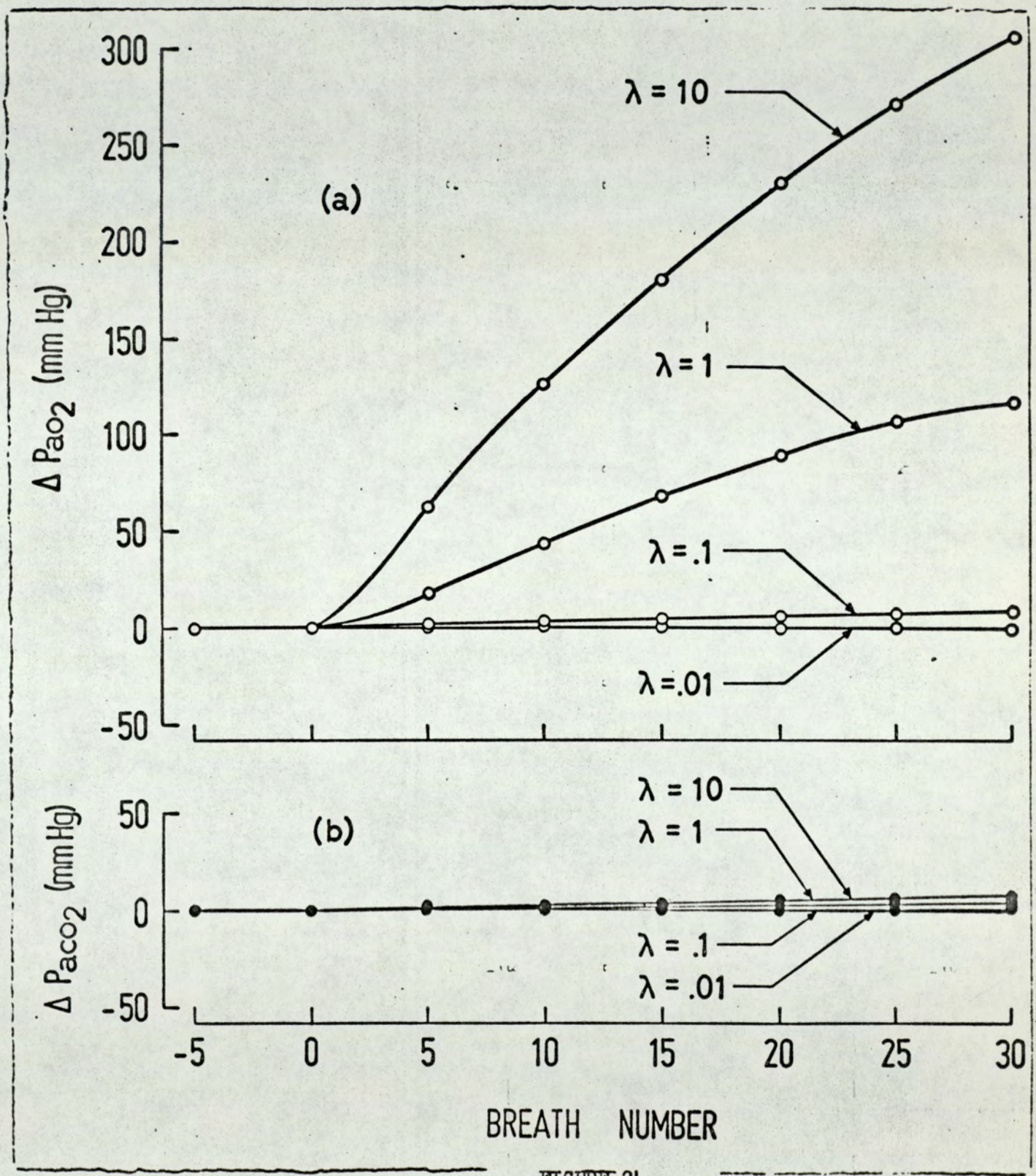
300
250
200
150
100
50
0
-50
Δ Pao2 (mm Hg)
(a)
λ = 10
λ = 1
λ = .1
λ = .01
50
0
-50
Δ Paco2 (mm Hg)
(b)
λ = 10
λ = 1
λ = .1
λ = .01
-5
0
5
10
15
20
25
30
BREATH NUMBER

FIGURE 24

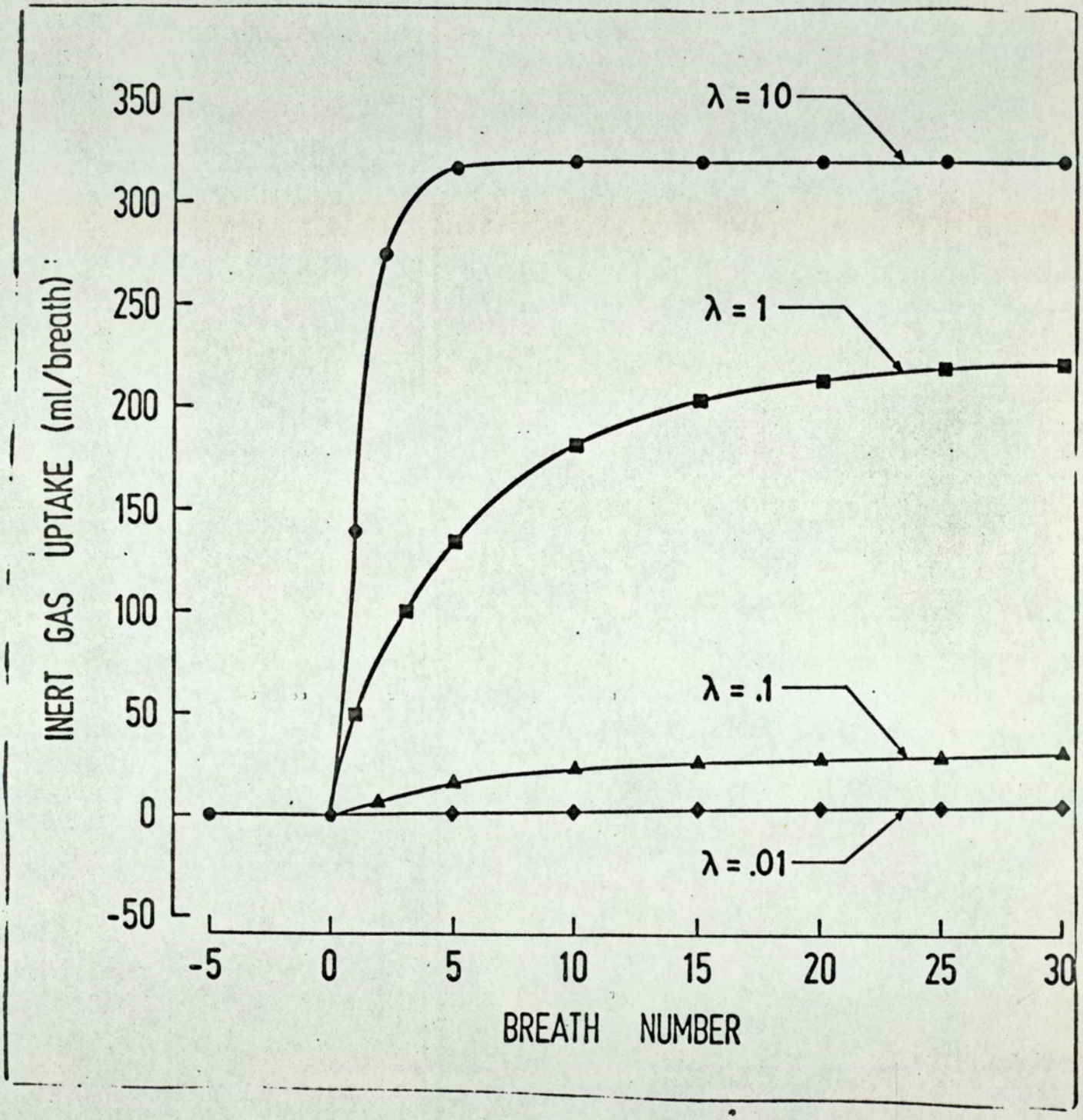
350
300
250
200
150
100
50
0
-50
INERT GAS UPTAKE (ml/breath)
λ = 10
λ = 1
λ = .1
λ = .01
-5
0
5
10
15
20
25
30
BREATH NUMBER

FIGURE 25

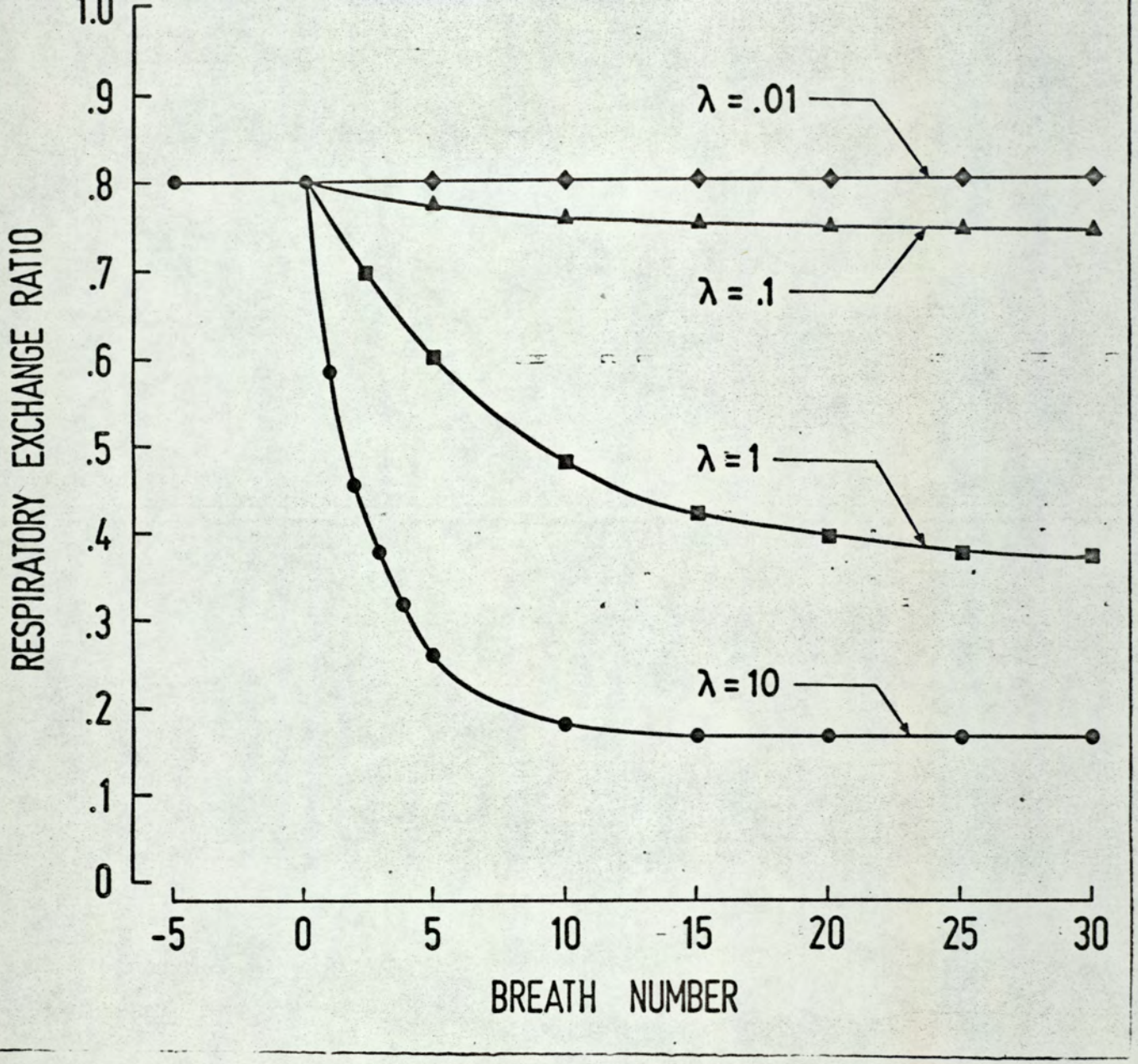
RESPIRATORY EXCHANGE RATIO
1.0
.9
.8
.7
.6
.5
.4
.3
.2
.1
0
λ = .01
λ = .1
λ = 1
λ = 10
-5
0
5
10
15
20
25
30
BREATH NUMBER

FIGURE 26

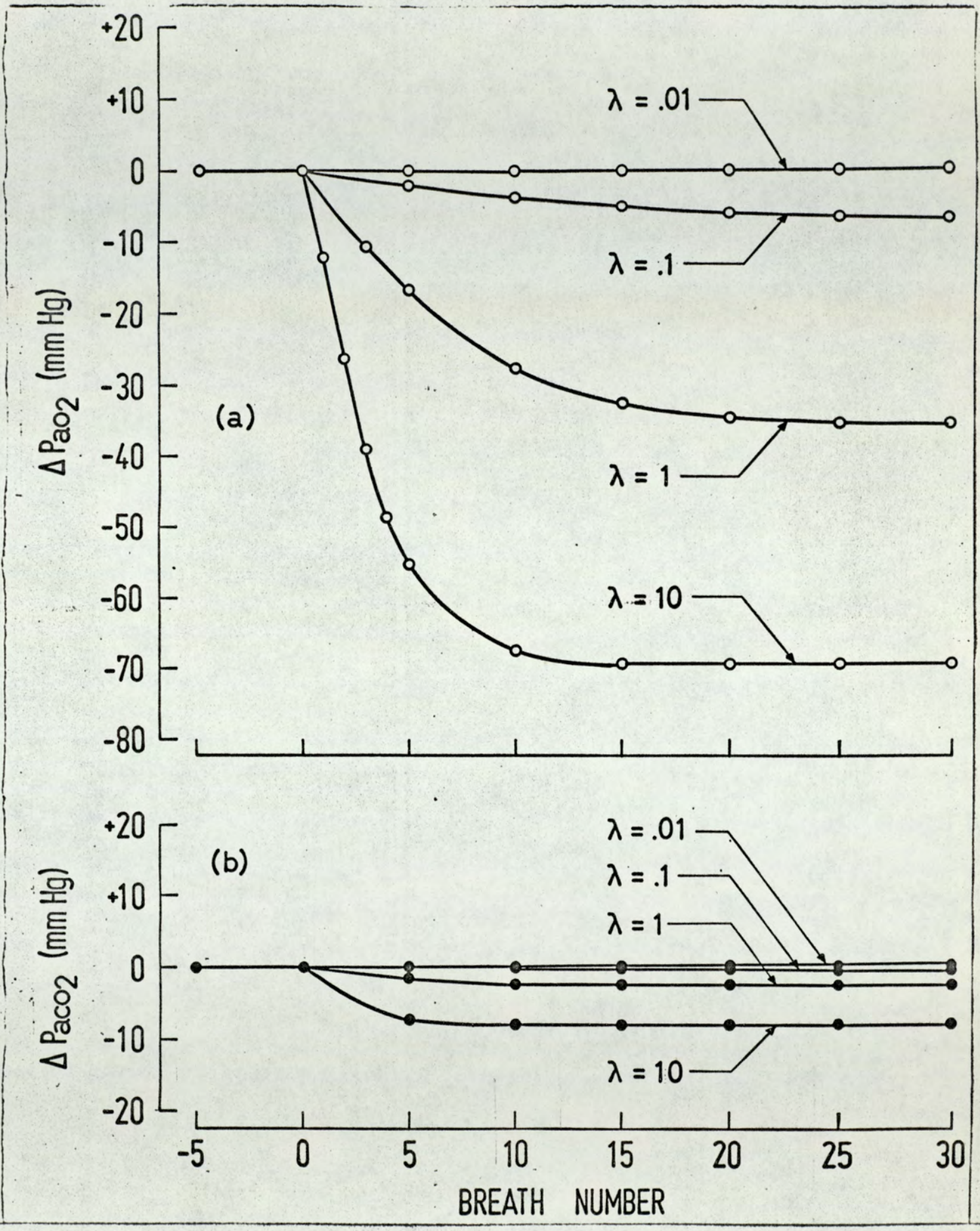
+20
+10
0
-10
-20
-30
-40
-50
-60
-70
-80
ΔPao2 (mm Hg)
(a)
λ = .01
λ = .1
λ = 1
λ = 10
+20
+10
0
-10
-20
ΔPaco2 (mm Hg)
(b)
λ = .01
λ = .1
λ = 1
λ = 10
-5
0
5
10
15
20
25
30
BREATH NUMBER

FIGURE 27

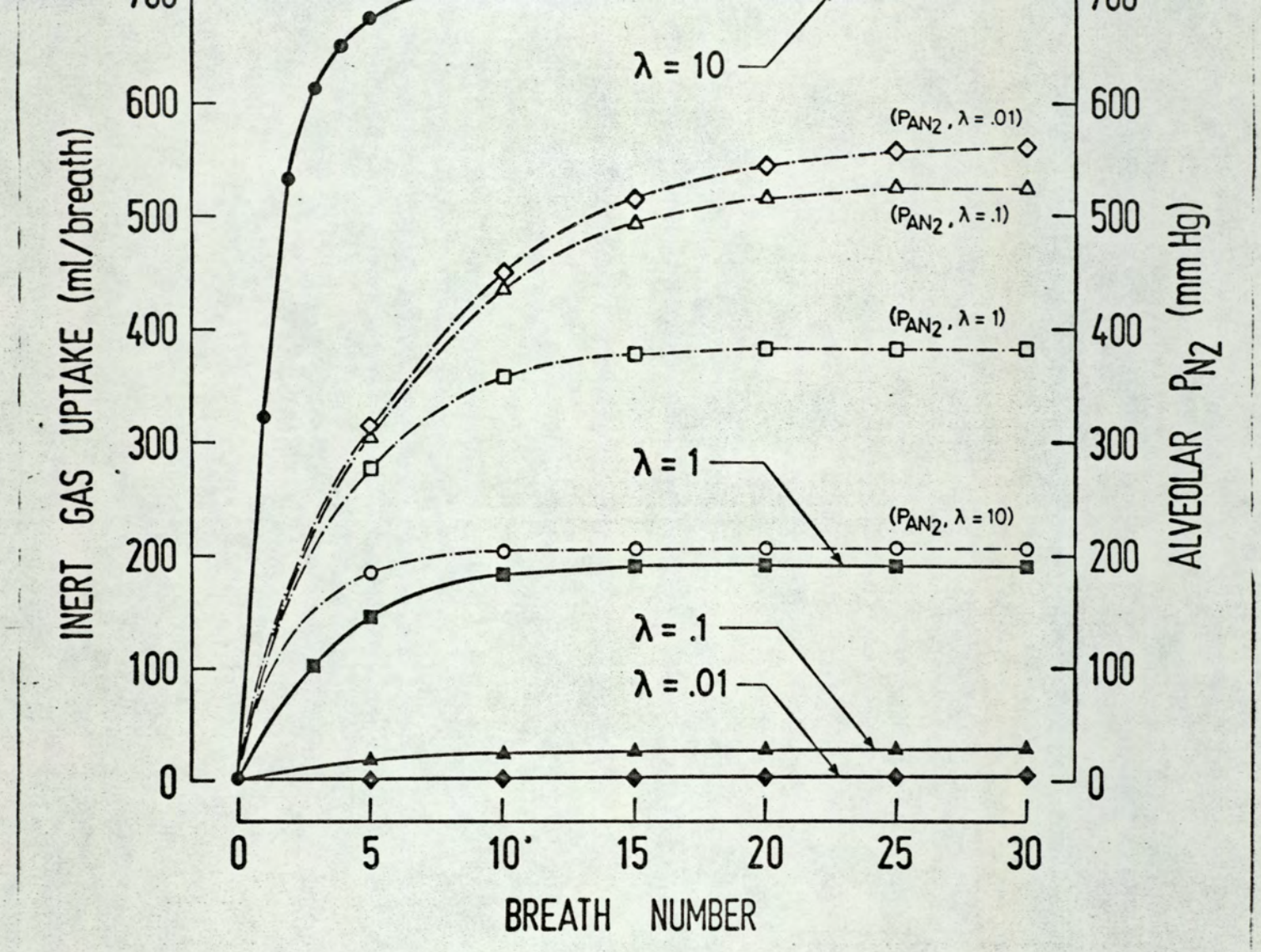
INERT GAS UPTAKE (ml/breath)
ALVEOLAR P_{N_2} (mm Hg)
BREATH NUMBER
0
5
10
15
20
25
30
100
200
300
400
500
600
λ = 10
λ = 1
λ = .1
λ = .01
(P_{AN_2}, λ = .01)
(P_{AN_2}, λ = .1)
(P_{AN_2}, λ = 1)
(P_{AN_2}, λ = 10)

FIGURE 28

FIGURE 29

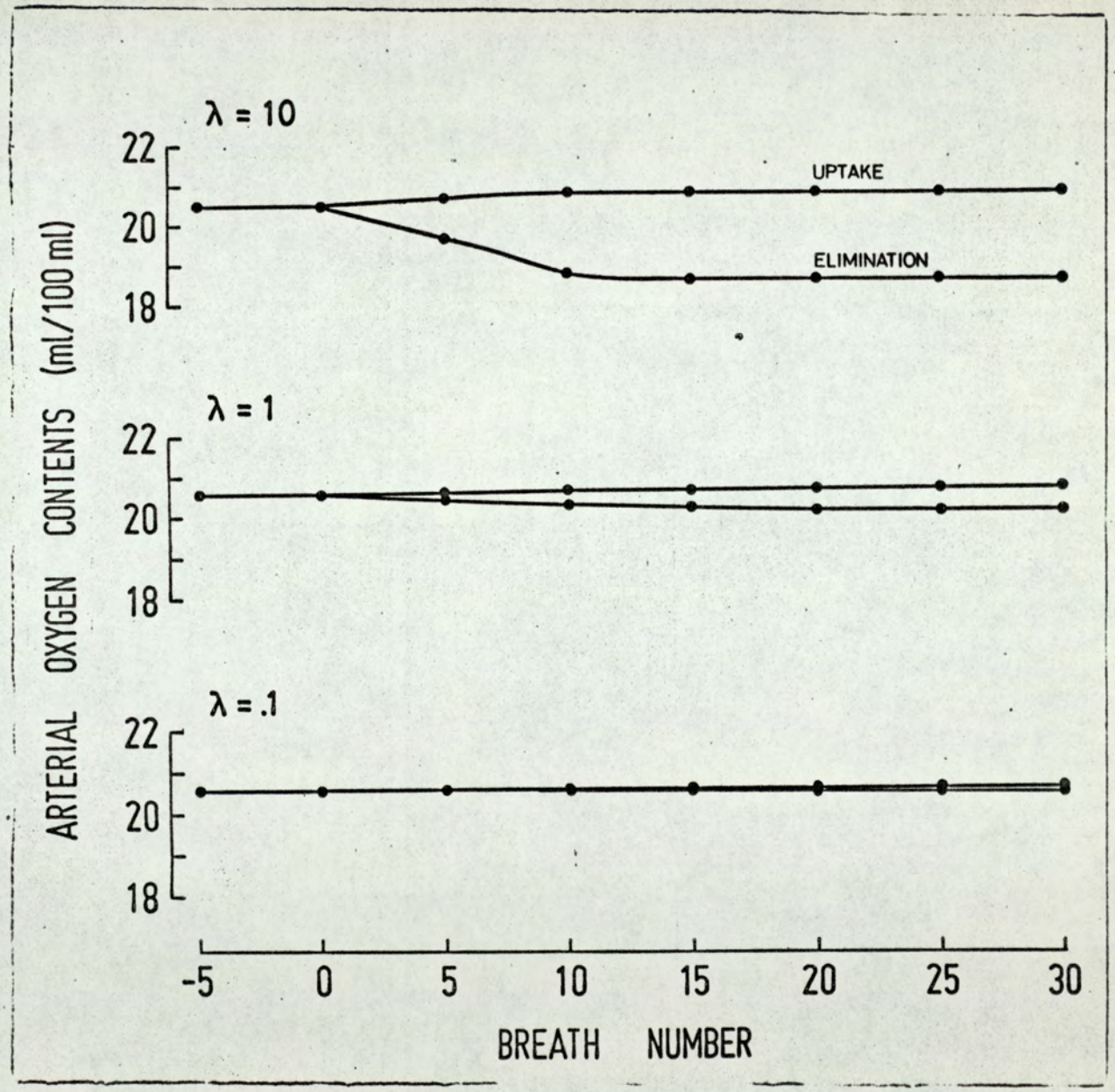
λ = 10
22
20
18
UPTAKE
ELIMINATION
λ = 1
22
20
18
λ = .1
22
20
18
ARTERIAL OXYGEN CONTENTS (ml/100 ml)
-5
0
5
10
15
20
25
30
BREATH NUMBER

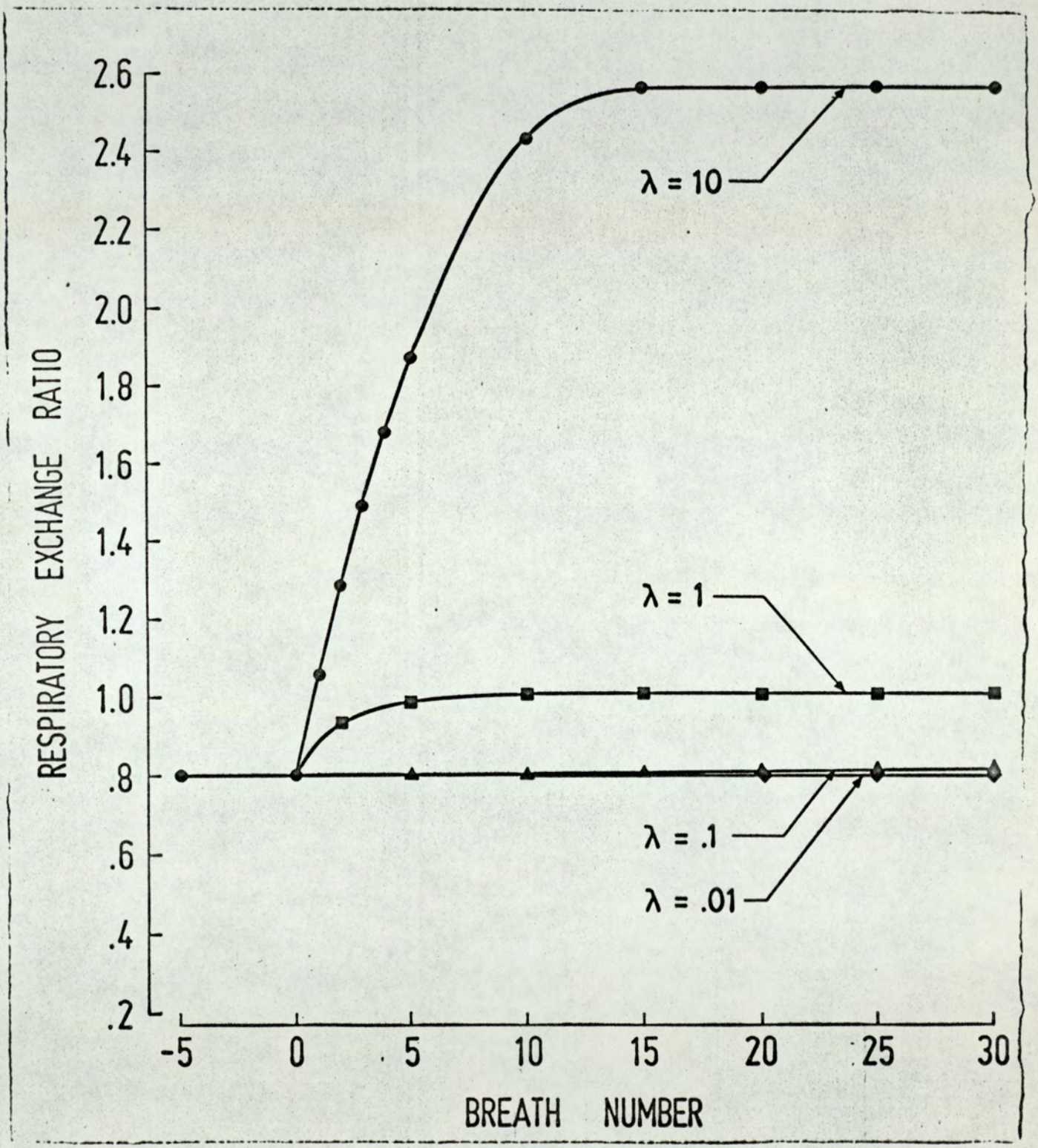
RESPIRATORY EXCHANGE RATIO
2.6
2.4
2.2
2.0
1.8
1.6
1.4
1.2
1.0
.8
.6
.4
.2
λ = 10
λ = 1
λ = .1
λ = .01
-5
0
5
10
15
20
25
30
BREATH NUMBER

FIGURE 30

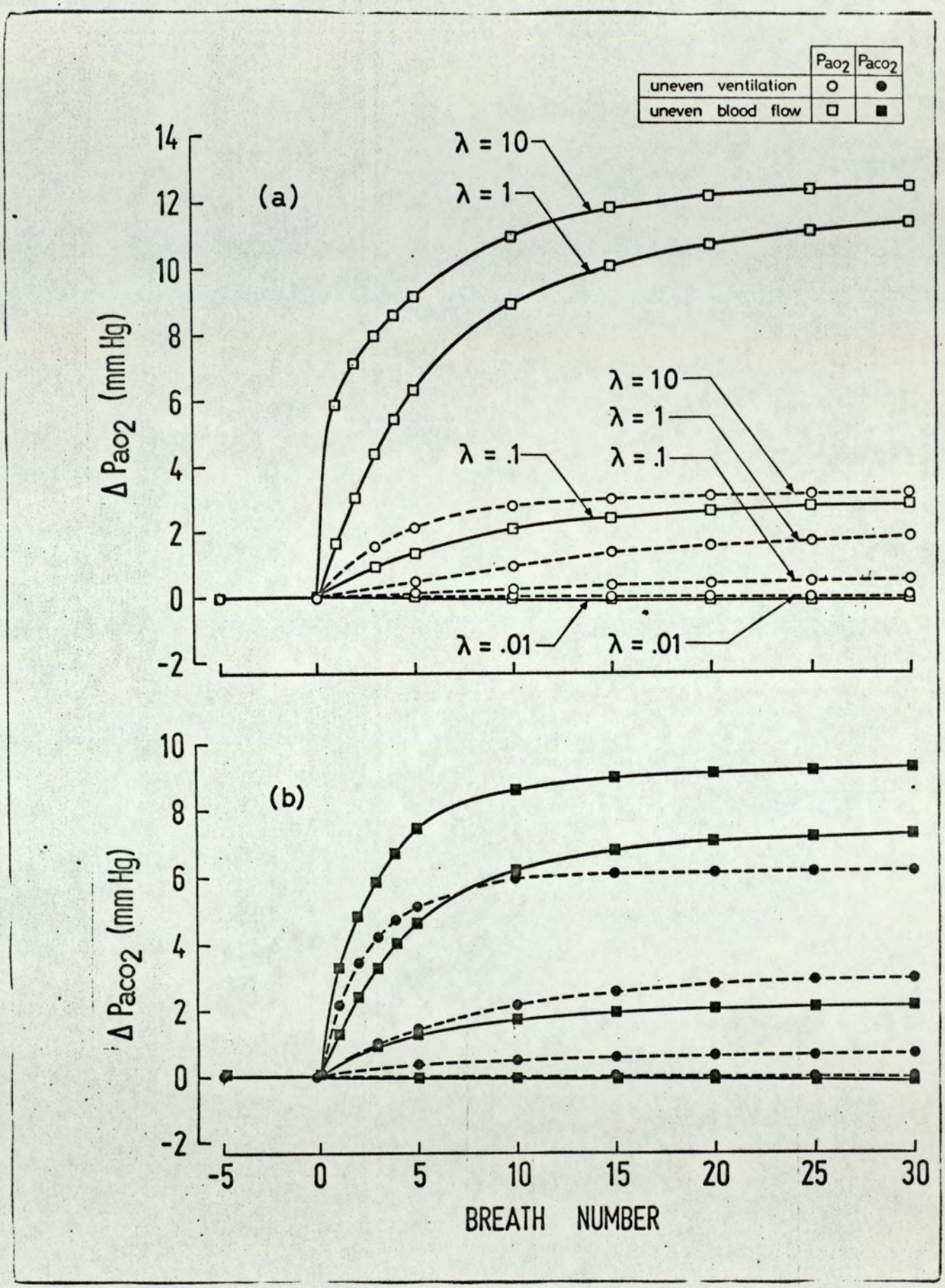
P_{ao_2} P_{aco_2}
uneven ventilation
uneven blood flow
(a)
λ = 10
λ = 1
λ = .1
λ = .01
λ = 10
λ = 1
λ = .1
λ = .01
Δ P_{ao_2} (mm Hg)
14
12
10
8
6
4
2
0
-2
(b)
Δ P_{aco_2} (mm Hg)
10
8
6
4
2
0
-2
-5
0
5
10
15
20
25
30
BREATH NUMBER

FIGURE 31

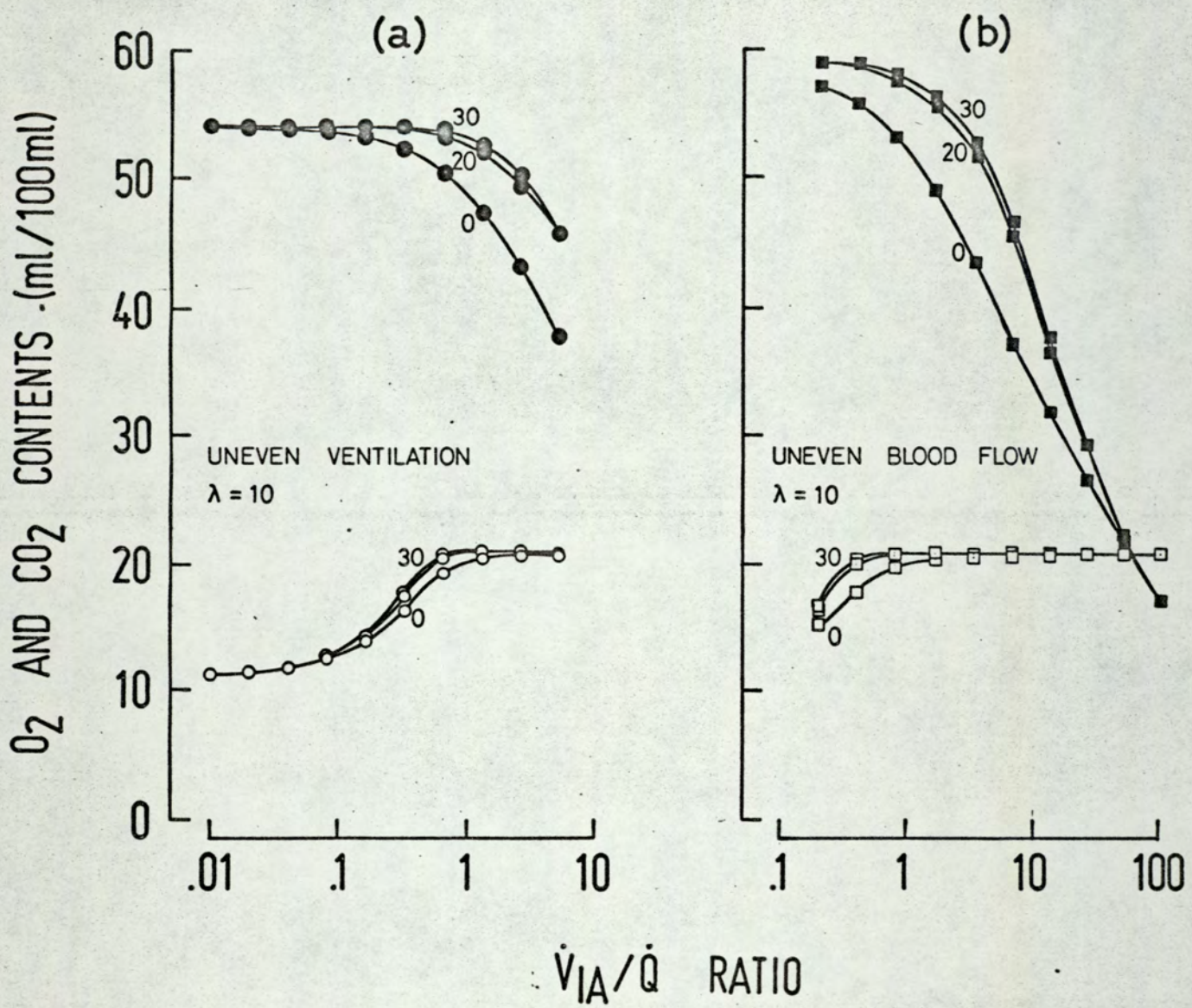
(a)
(b)
60
50
40
30
20
10
0
O_2 AND CO_2 CONTENTS -(ml/100ml)
30
20
0
UNEVEN VENTILATION
λ = 10
UNEVEN BLOOD FLOW
λ = 10
.01
.1
1
10
100
$\dot{V}_{IA}/\dot{Q}$ RATIO

FIGURE 32

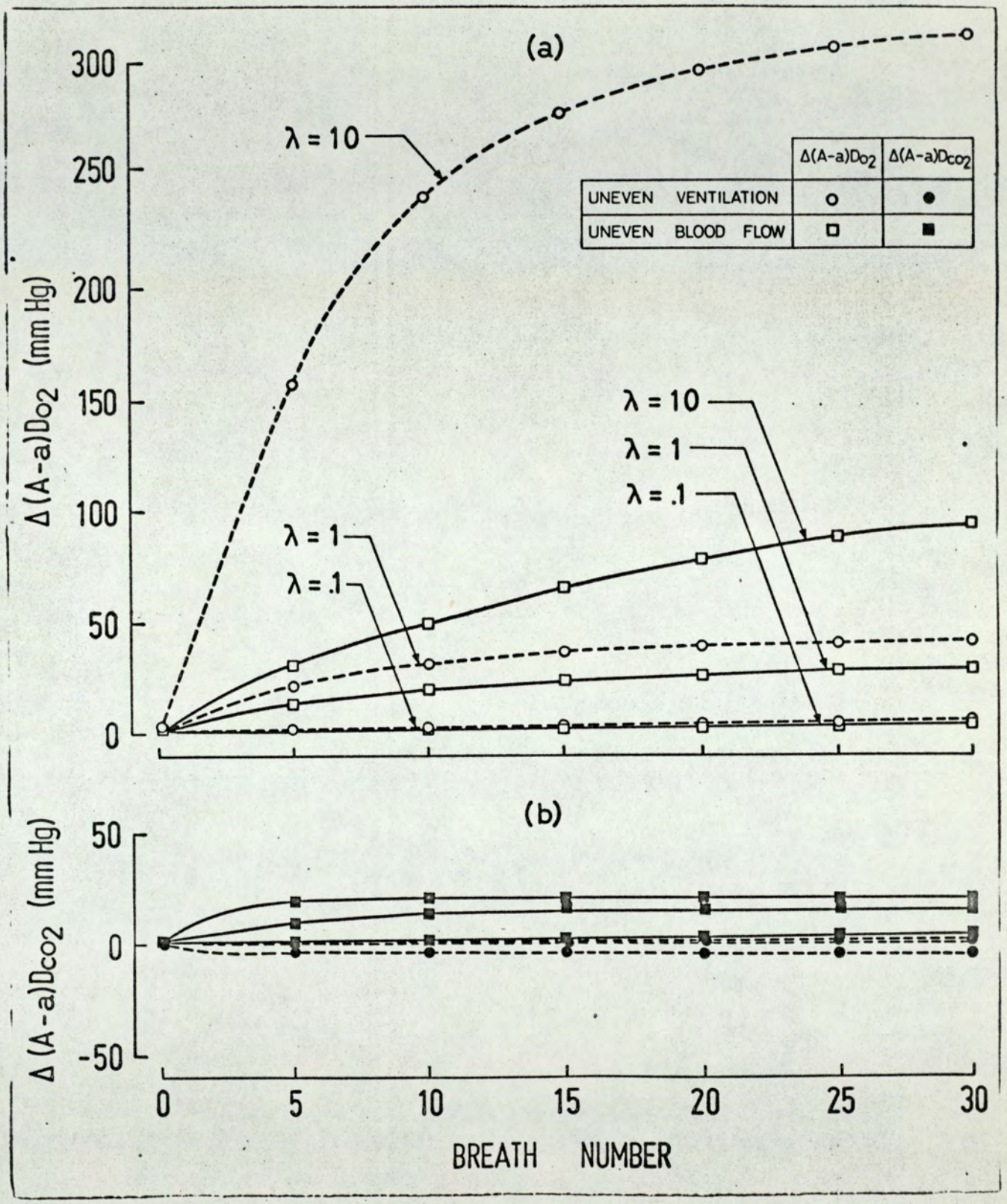
(a)
300
250
200
150
100
50
0
Δ (A-a)Do2 (mm Hg)
λ = 10
λ = 1
λ = .1
λ = 10
λ = 1
λ = .1
Δ(A-a)Do2
Δ(A-a)Dco2
UNEVEN VENTILATION
UNEVEN BLOOD FLOW
(b)
50
0
-50
Δ (A-a)Dco2 (mm Hg)
0
5
10
15
20
25
30
BREATH NUMBER

FIGURE 33

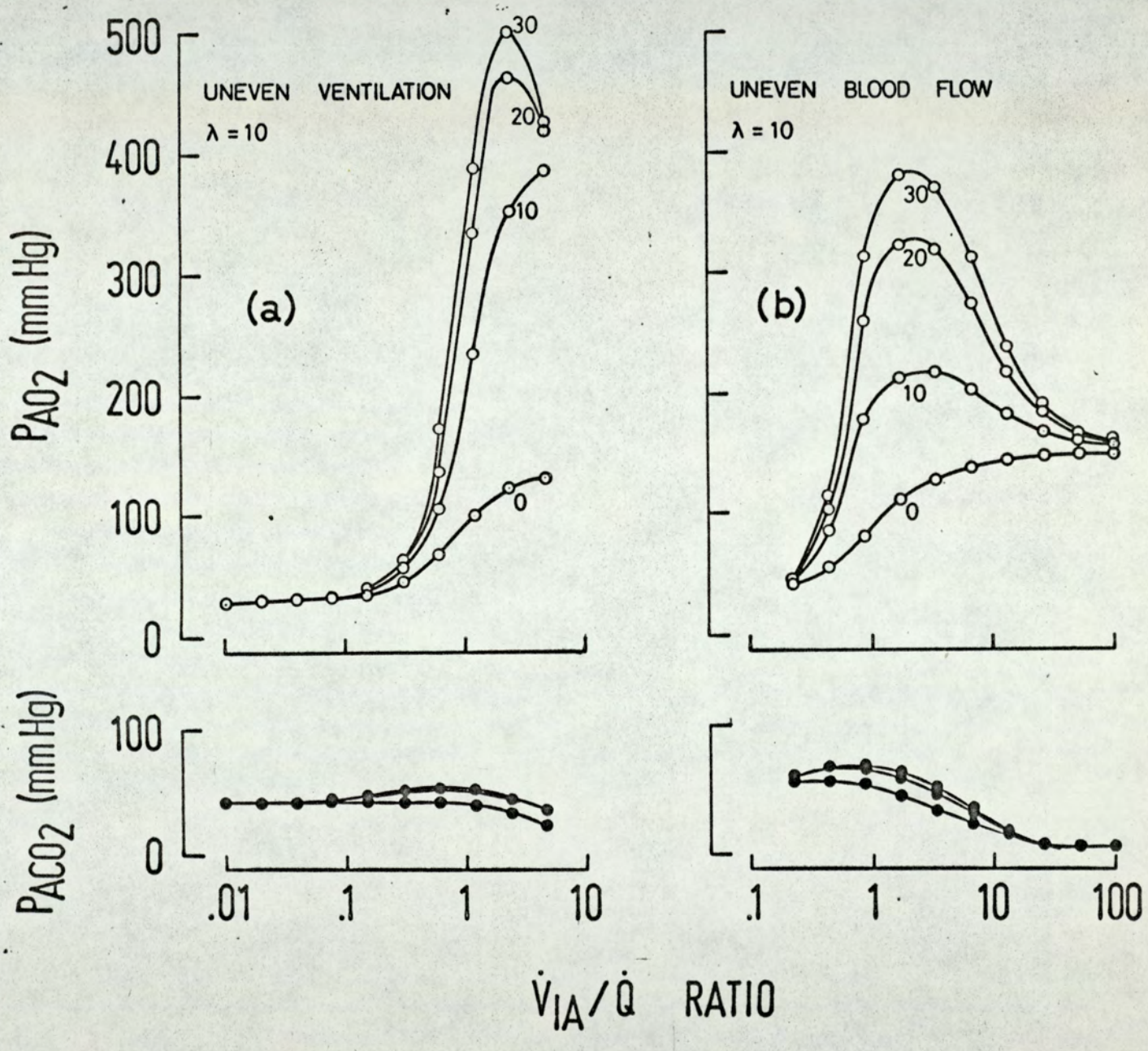
UNEVEN VENTILATION
λ = 10
(a)
UNEVEN BLOOD FLOW
λ = 10
(b)
30
20
10
0
500
400
300
200
100
0
P_{AO_2} (mm Hg)
P_{ACO_2} (mm Hg)
.01
.1
1
10
100
$\dot{V}_{IA}/\dot{Q}$ RATIO

FIGURE 34

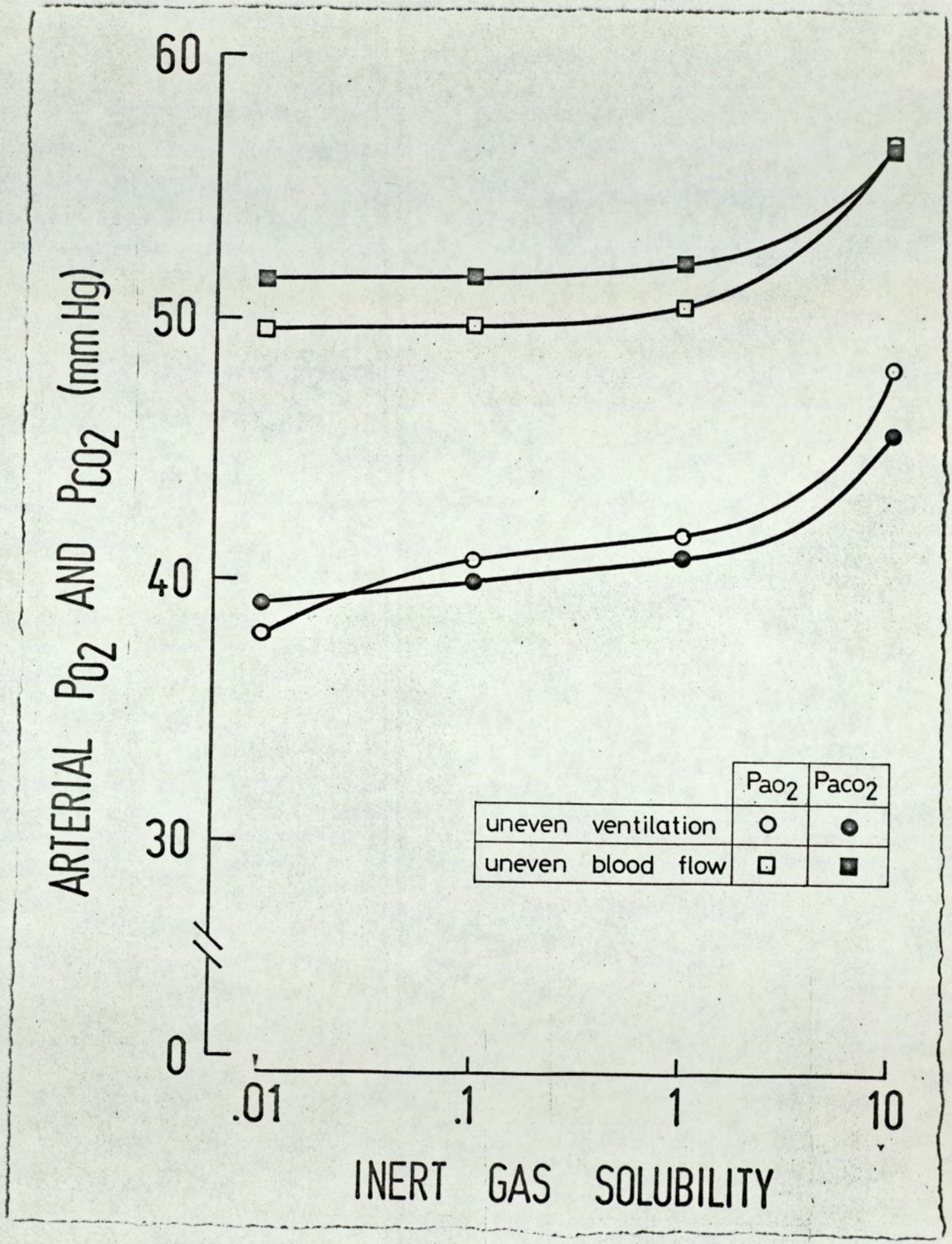
60
50
40
30
0
ARTERIAL P_{O_2} AND P_{CO_2} (mm Hg)
Pao_2
$Paco_2$
uneven ventilation
uneven blood flow
.01
.1
1
10
INERT GAS SOLUBILITY

FIGURE 35

FIGURE 36

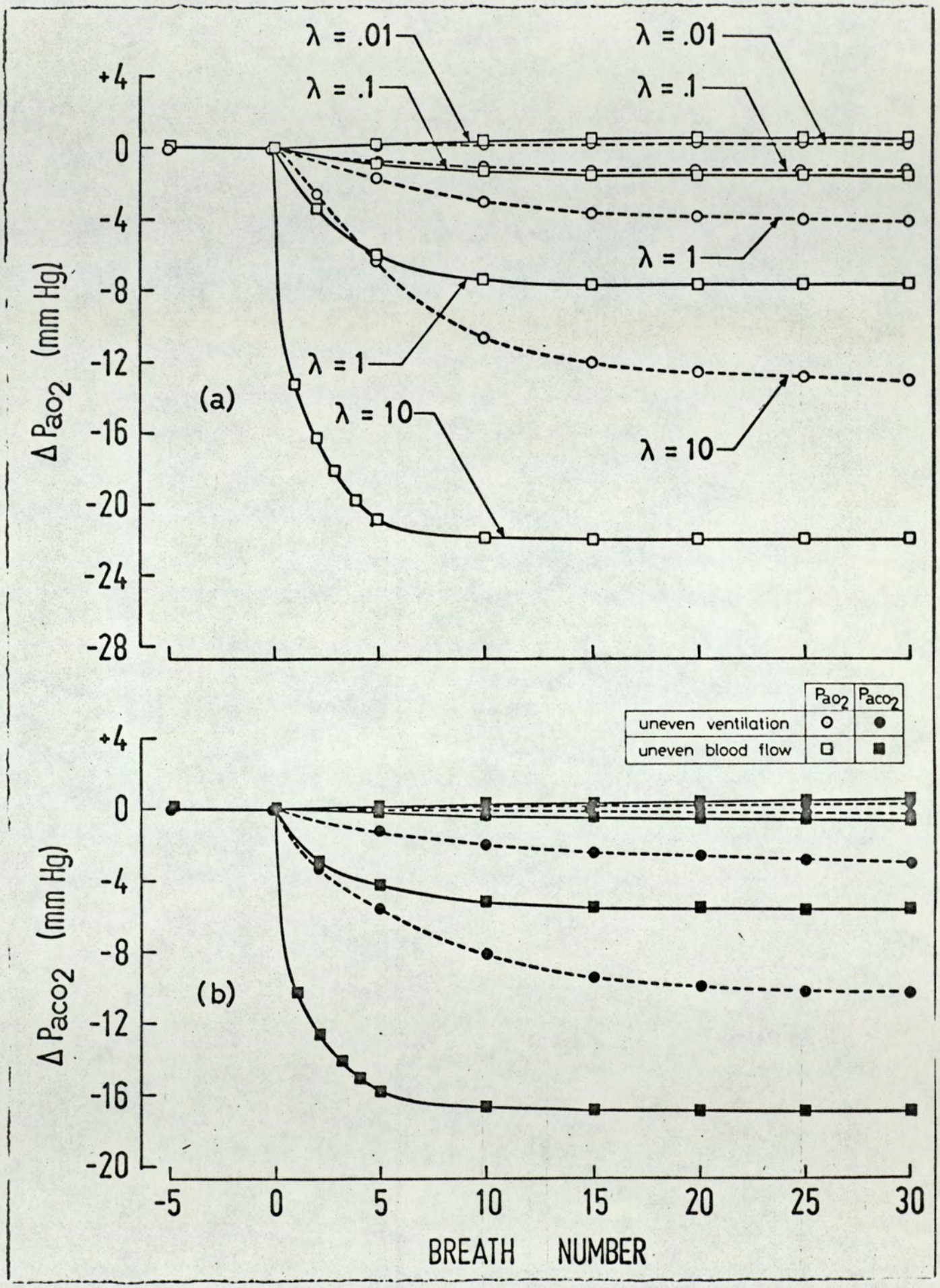
λ = .01
λ = .1
λ = 1
λ = 10
(a)
(b)
+4
0
-4
-8
-12
-16
-20
-24
-28
ΔPao2 (mm Hg)
ΔPaco2 (mm Hg)
Pao2
Paco2
uneven ventilation
uneven blood flow
-5
0
5
10
15
20
25
30
BREATH NUMBER

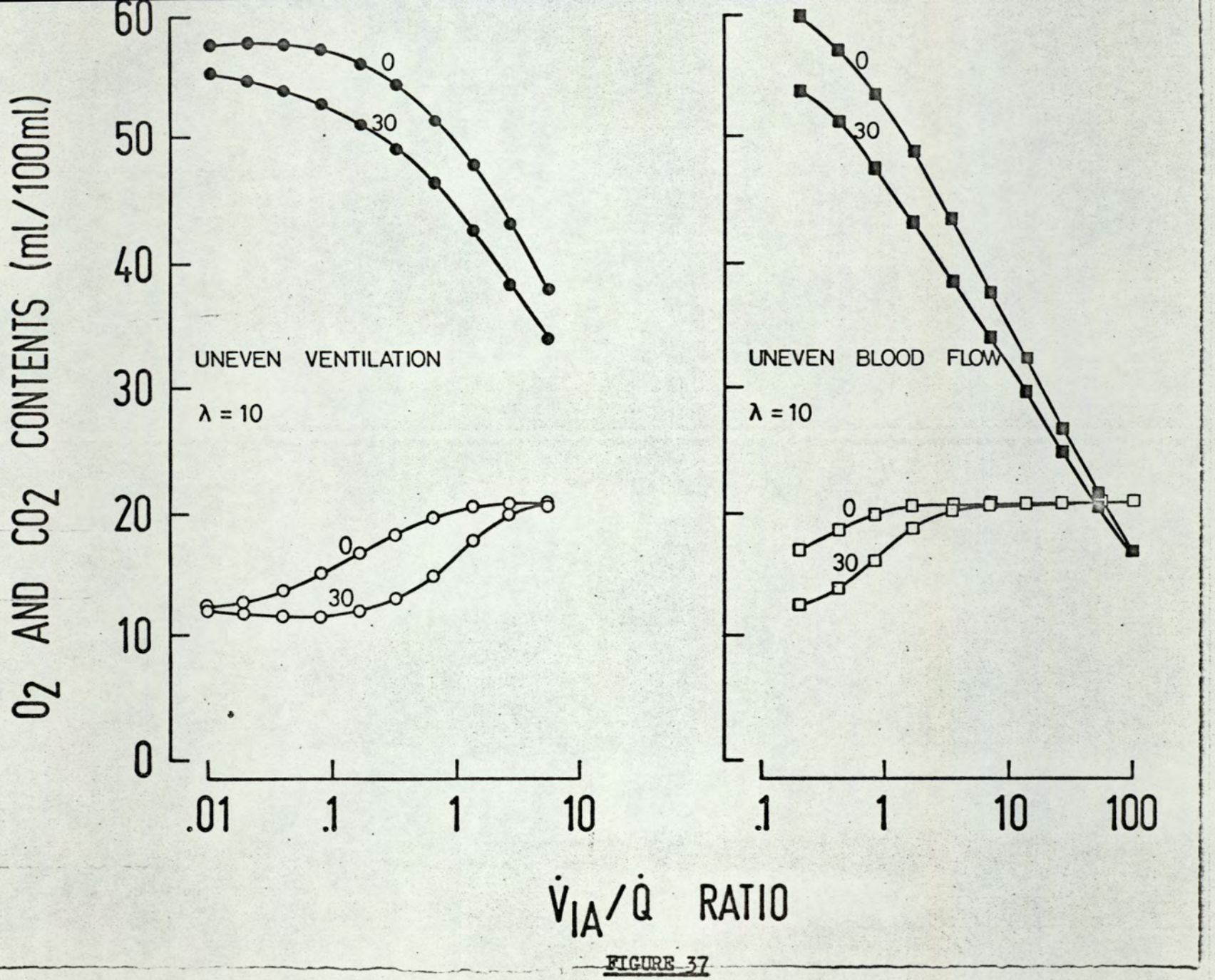
O_2 AND CO_2 CONTENTS (ml/100ml)
60
50
40
30
20
10
0
UNEVEN VENTILATION
λ = 10
0
30
0
30
.01
.1
1
10
UNEVEN BLOOD FLOW
λ = 10
0
30
0
30
.1
1
10
100
$\dot{V}_{IA}/\dot{Q}$ RATIO

FIGURE 37

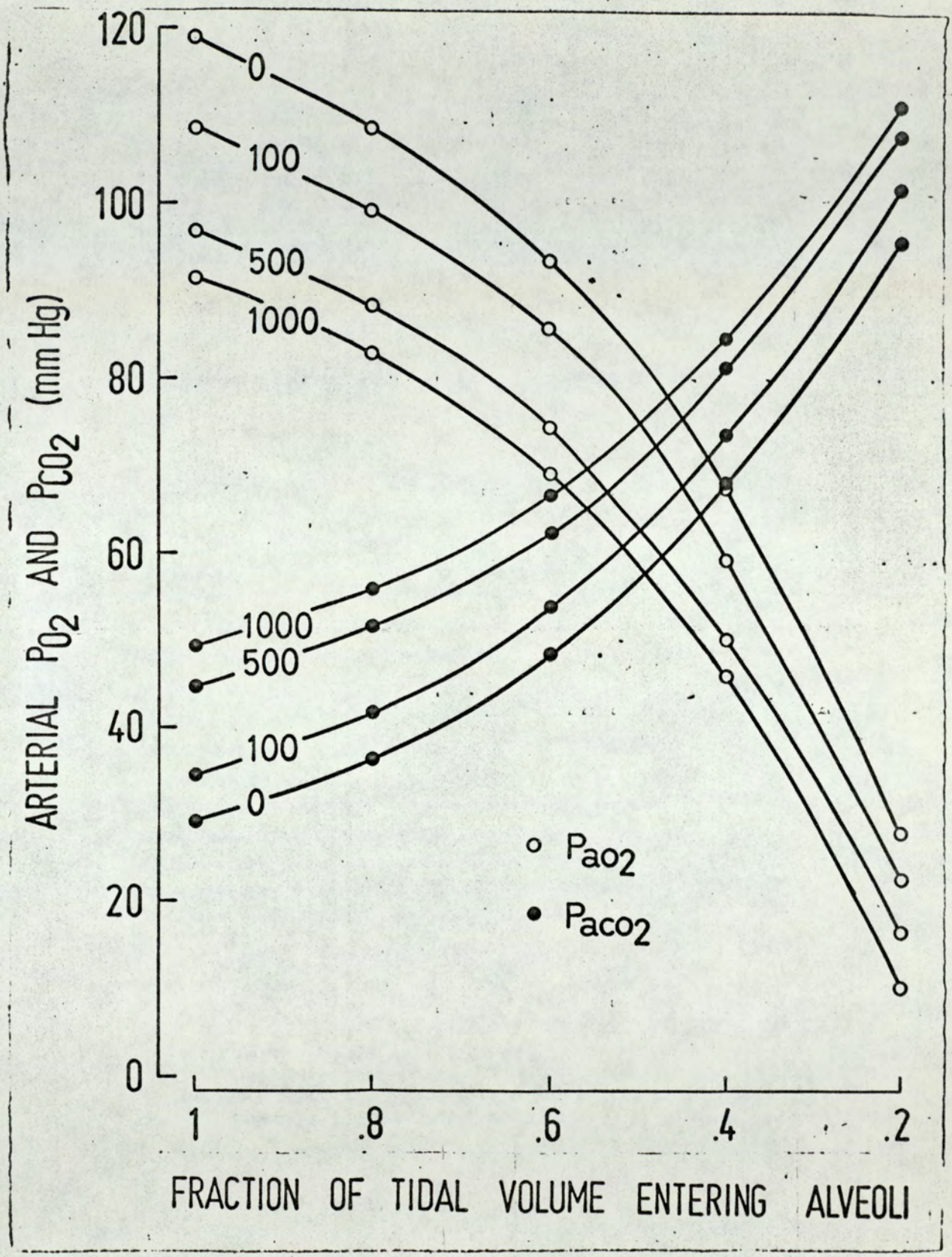
120
100
80
60
40
20
0
ARTERIAL P_{O_2} AND P_{CO_2} (mm Hg)
0
100
500
1000
1000
500
100
0
P_{ao_2}
P_{aco_2}
1
.8
.6
.4
.2
FRACTION OF TIDAL VOLUME ENTERING ALVEOLI

FIGURE 38

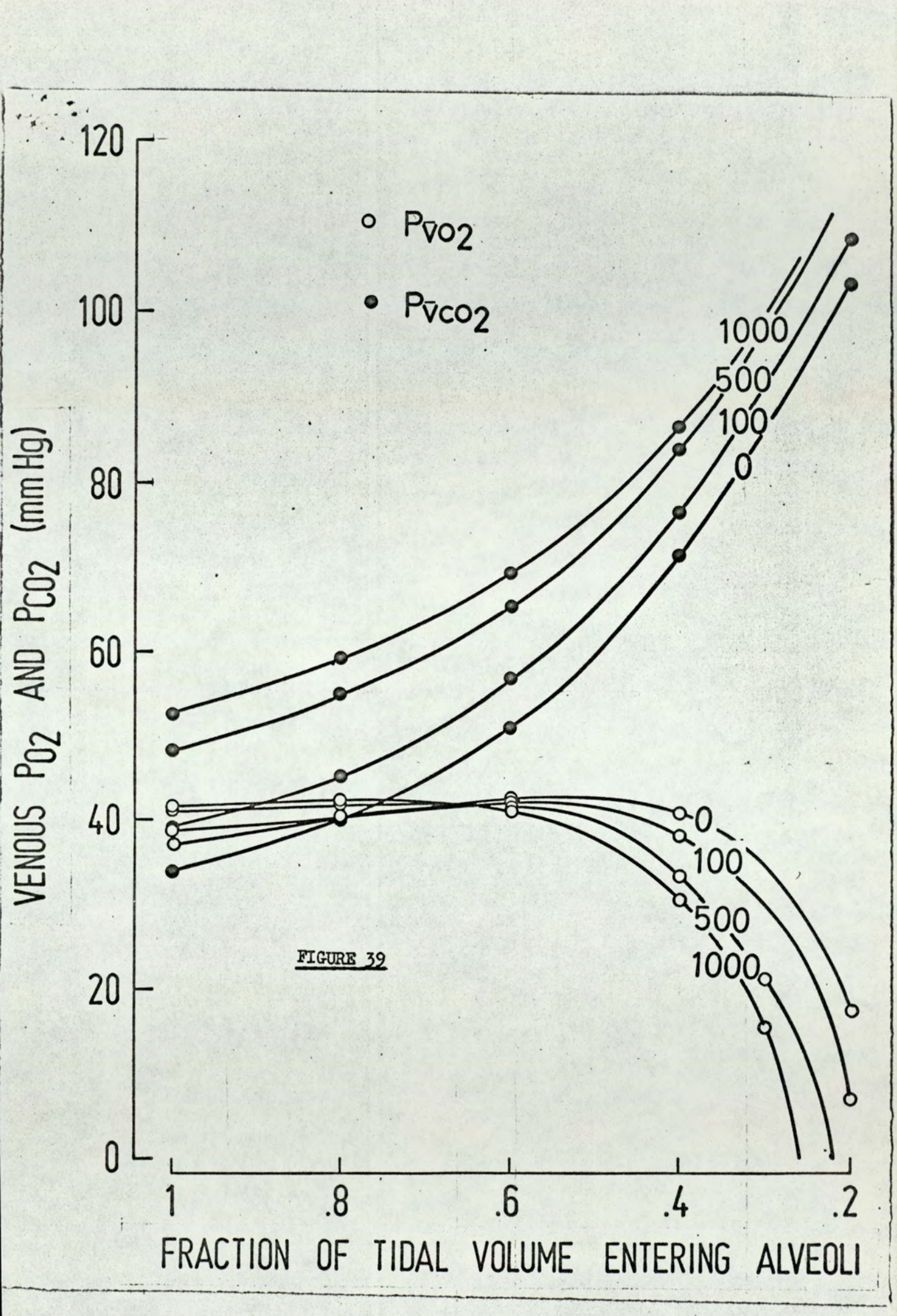
120
100
80
60
40
20
0
VENOUS P_{O_2} AND P_{CO_2} (mm Hg)
$P_{\bar{v}O_2}$
$P_{\bar{v}CO_2}$
1000
500
100
0
0
100
500
1000
1
.8
.6
.4
.2
FRACTION OF TIDAL VOLUME ENTERING ALVEOLI

FIGURE 39

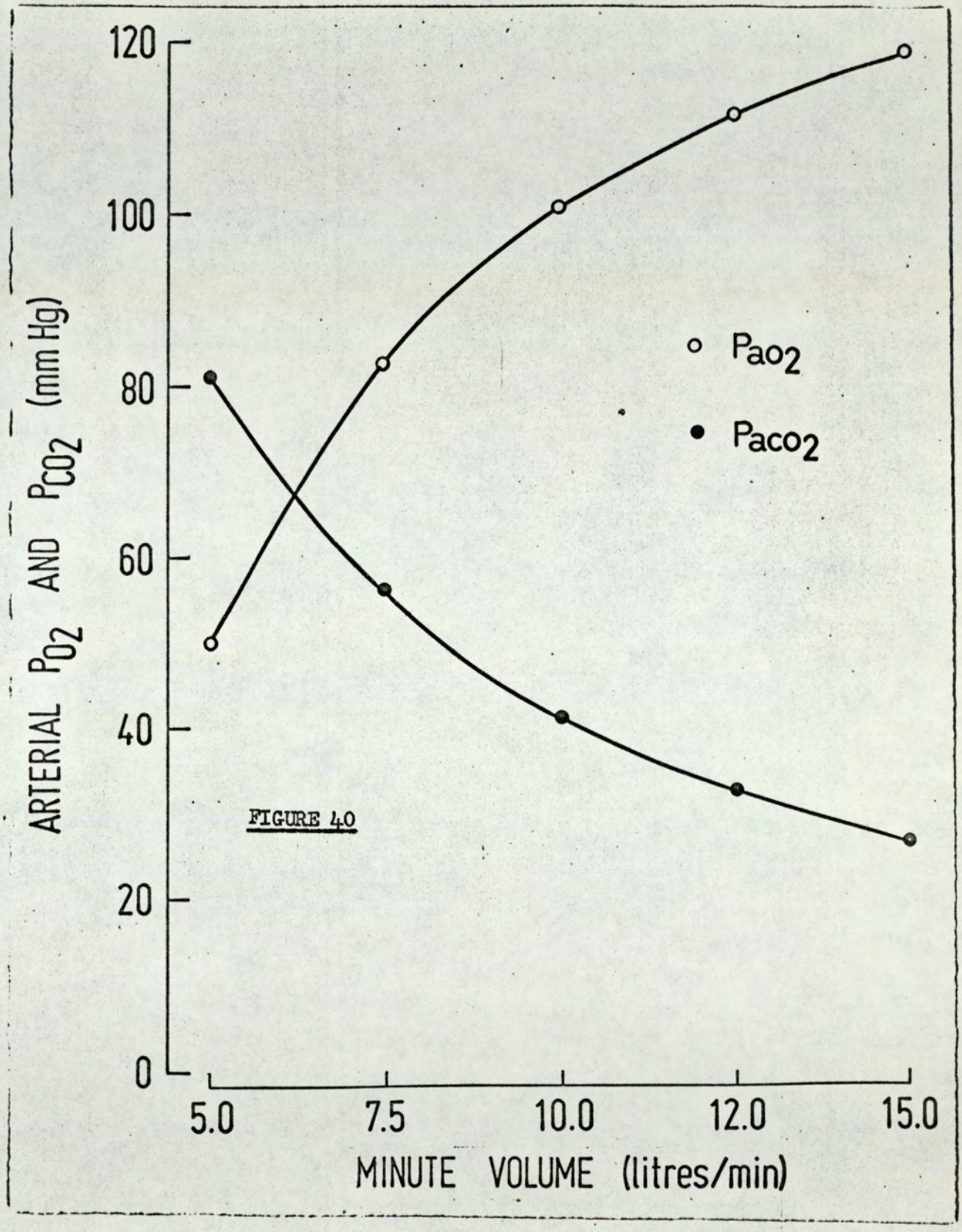
120
100
80
60
40
20
0
ARTERIAL P_{O_2} AND P_{CO_2} (mm Hg)
P_{ao_2}
P_{aco_2}
5.0
7.5
10.0
12.0
15.0
MINUTE VOLUME (litres/min)

FIGURE 4.0

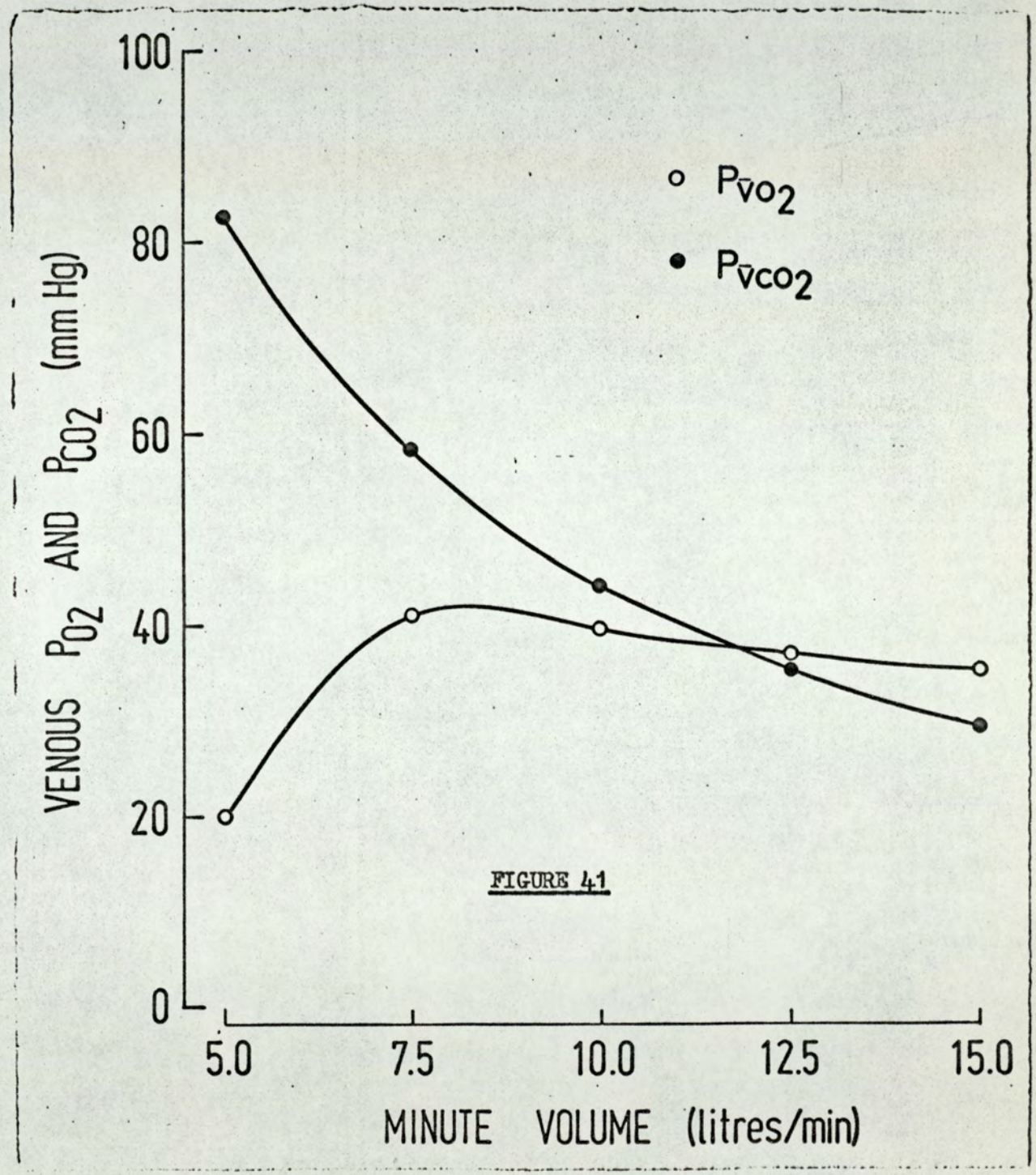
100
80
60
40
20
0
VENOUS P_{O_2} AND P_{CO_2} (mm Hg)
$P_{\bar{v}O_2}$
$P_{\bar{v}CO_2}$
5.0
7.5
10.0
12.5
15.0
MINUTE VOLUME (litres/min)

FIGURE 41

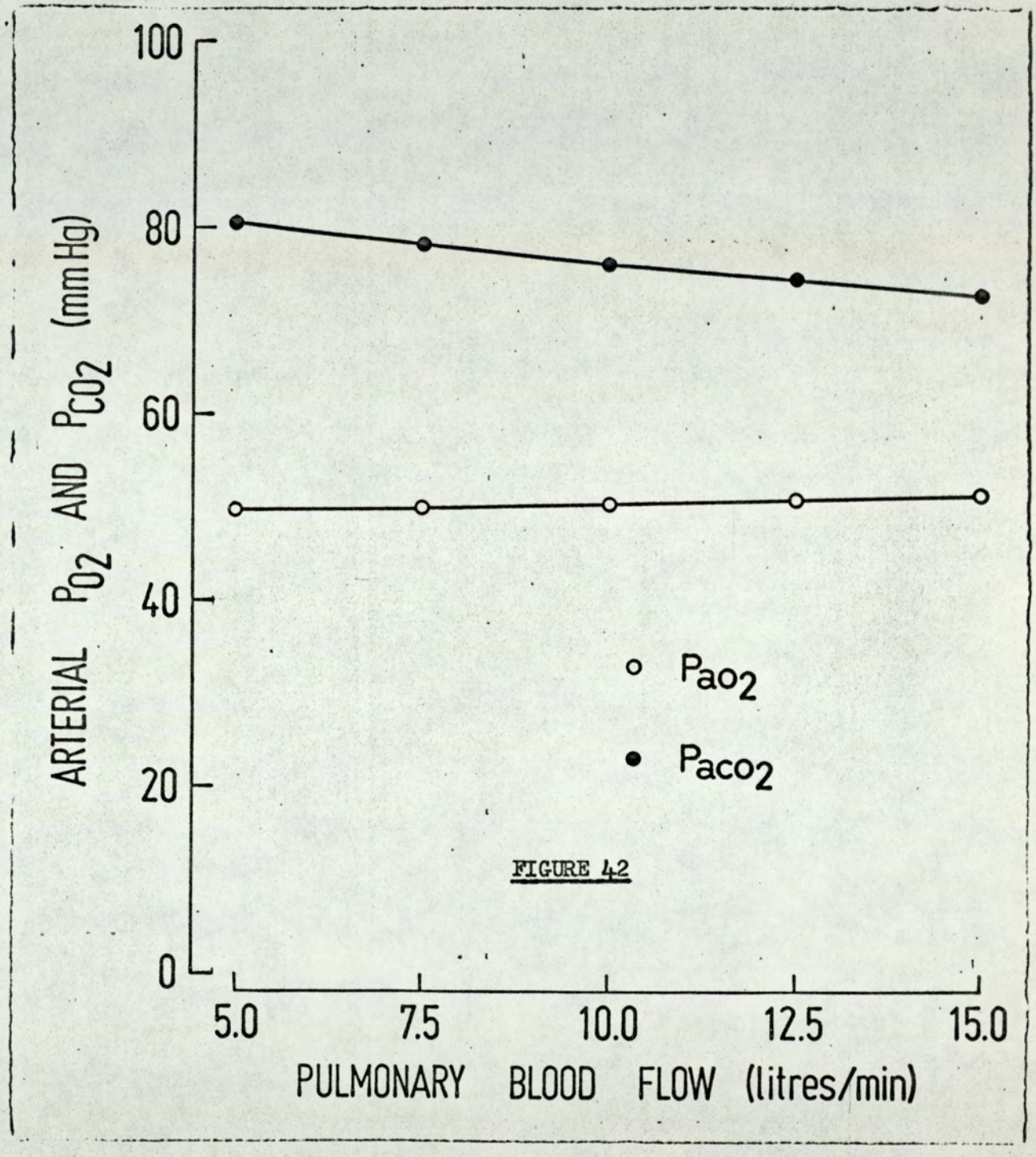
100
80
60
40
20
0
ARTERIAL P_{O_2} AND P_{CO_2} (mm Hg)
P_{ao_2}
P_{aco_2}
5.0
7.5
10.0
12.5
15.0
PULMONARY BLOOD FLOW (litres/min)

FIGURE 42

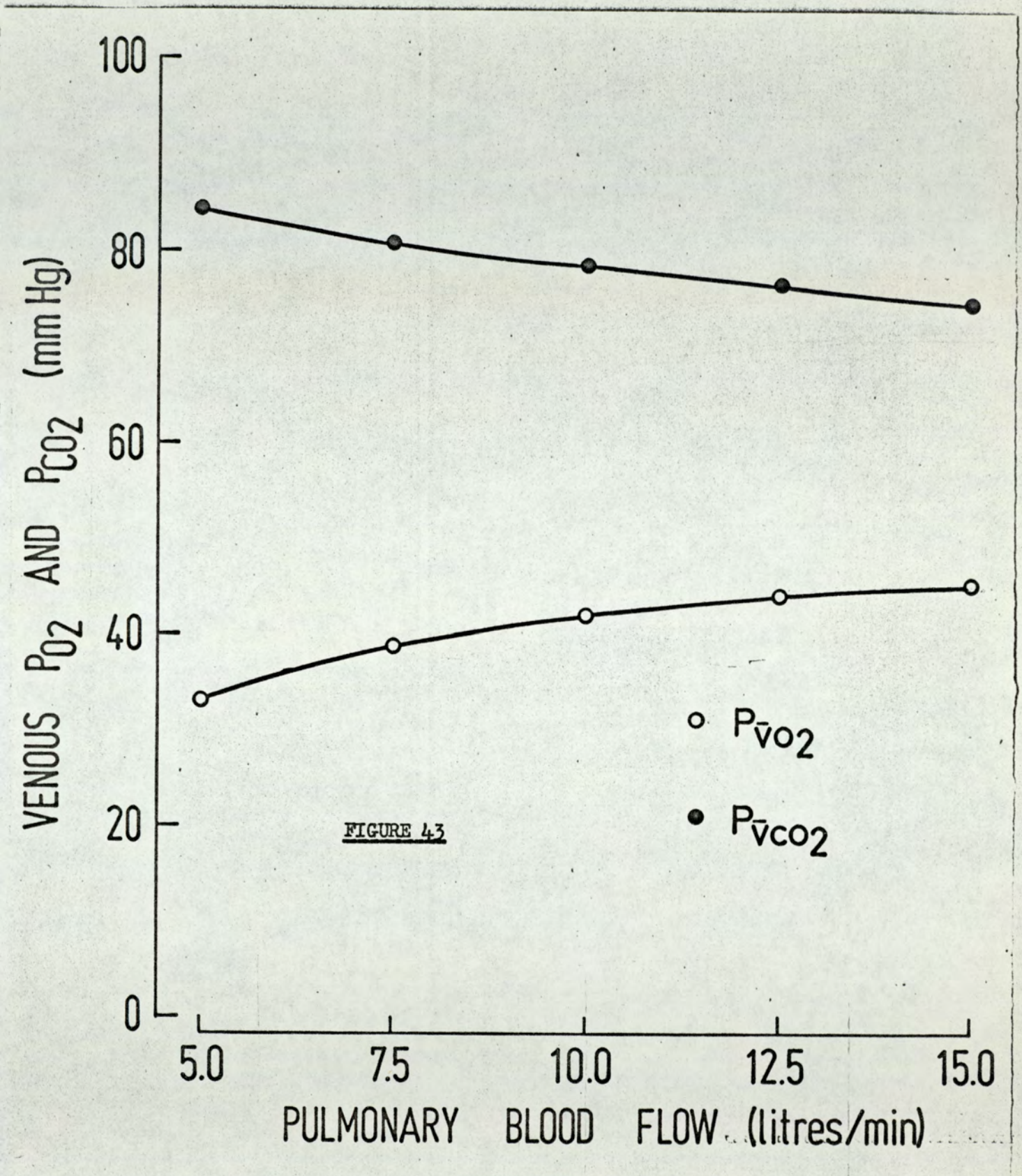
100
80
60
40
20
0
VENOUS P_{O_2} AND P_{CO_2} (mm Hg)
$P_{\bar{v}O_2}$
$P_{\bar{v}CO_2}$
5.0
7.5
10.0
12.5
15.0
PULMONARY BLOOD FLOW (litres/min)

FIGURE 43

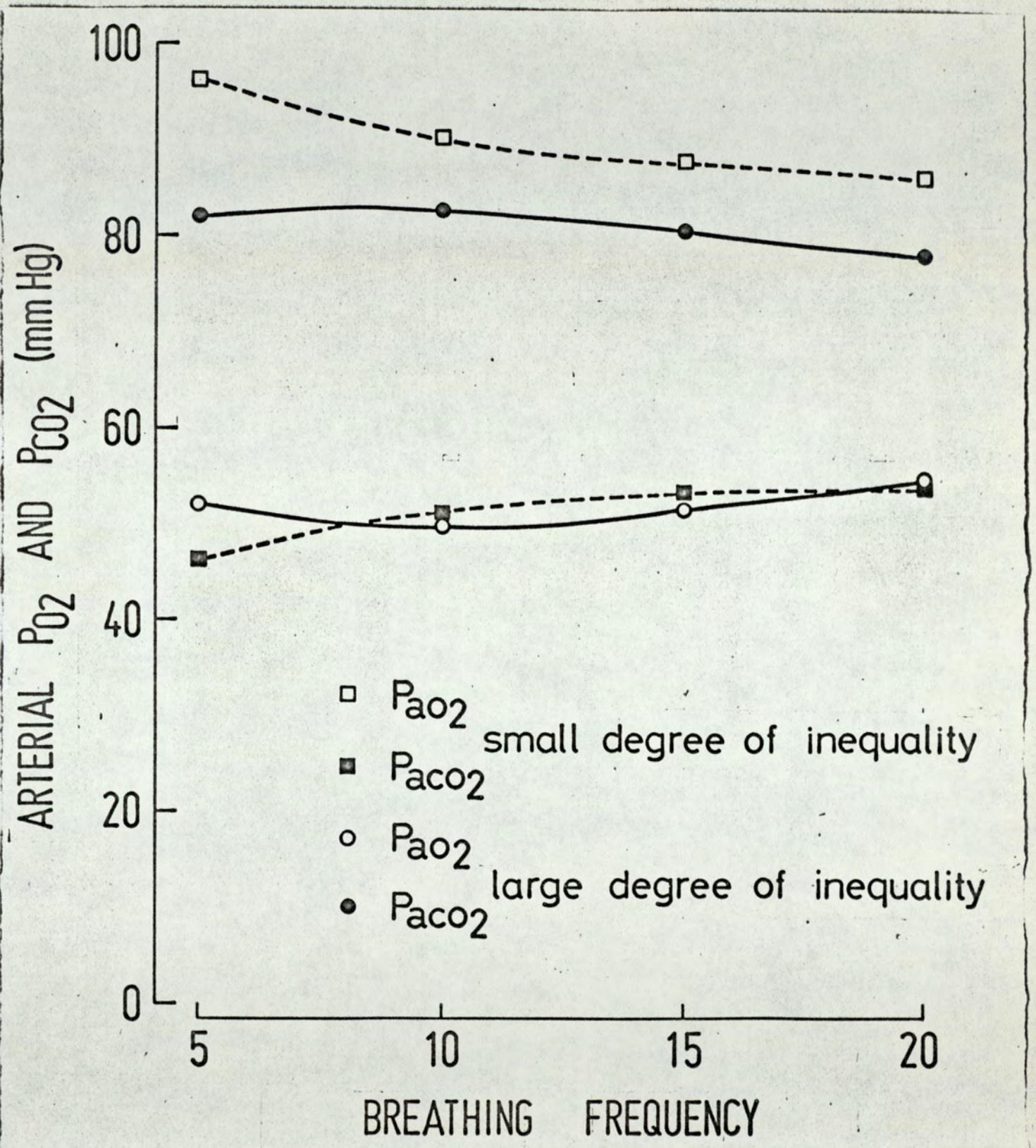
100
80
60
40
20
0
ARTERIAL P_{O_2} AND P_{CO_2} (mm Hg)
P_{ao_2}
P_{aco_2}
small degree of inequality
P_{ao_2}
P_{aco_2}
large degree of inequality
5
10
15
20
BREATHING FREQUENCY

FIGURE 44

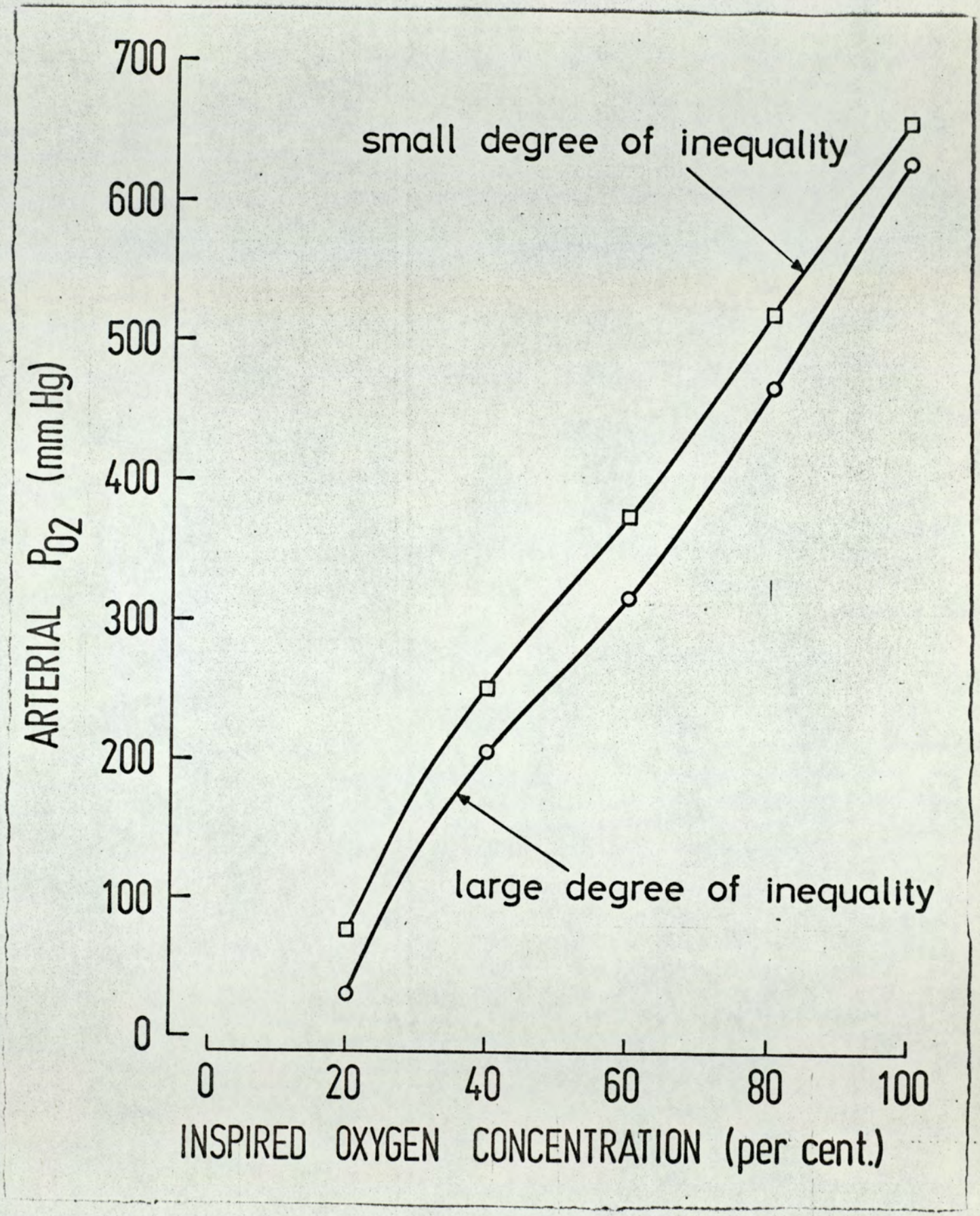
700
600
500
400
300
200
100
0
ARTERIAL P_{O2} (mm Hg)
small degree of inequality
large degree of inequality
0
20
40
60
80
100
INSPIRED OXYGEN CONCENTRATION (per cent.)

FIGURE 45

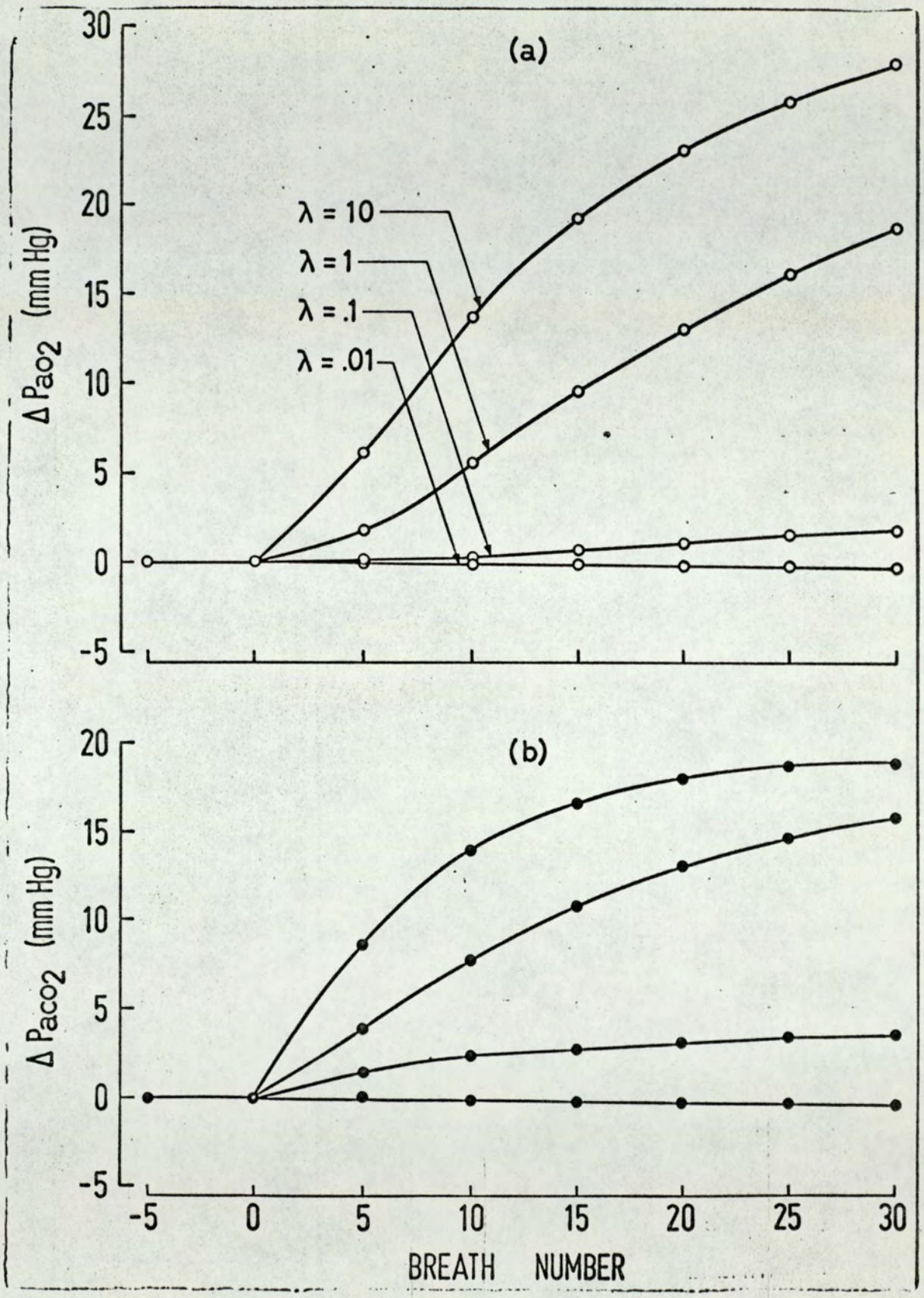
(a)
λ = 10
λ = 1
λ = .1
λ = .01
Δ Pao2 (mm Hg)
30
25
20
15
10
5
0
-5
(b)
Δ Paco2 (mm Hg)
20
15
10
5
0
-5
-5
0
5
10
15
20
25
30
BREATH NUMBER

FIGURE 46

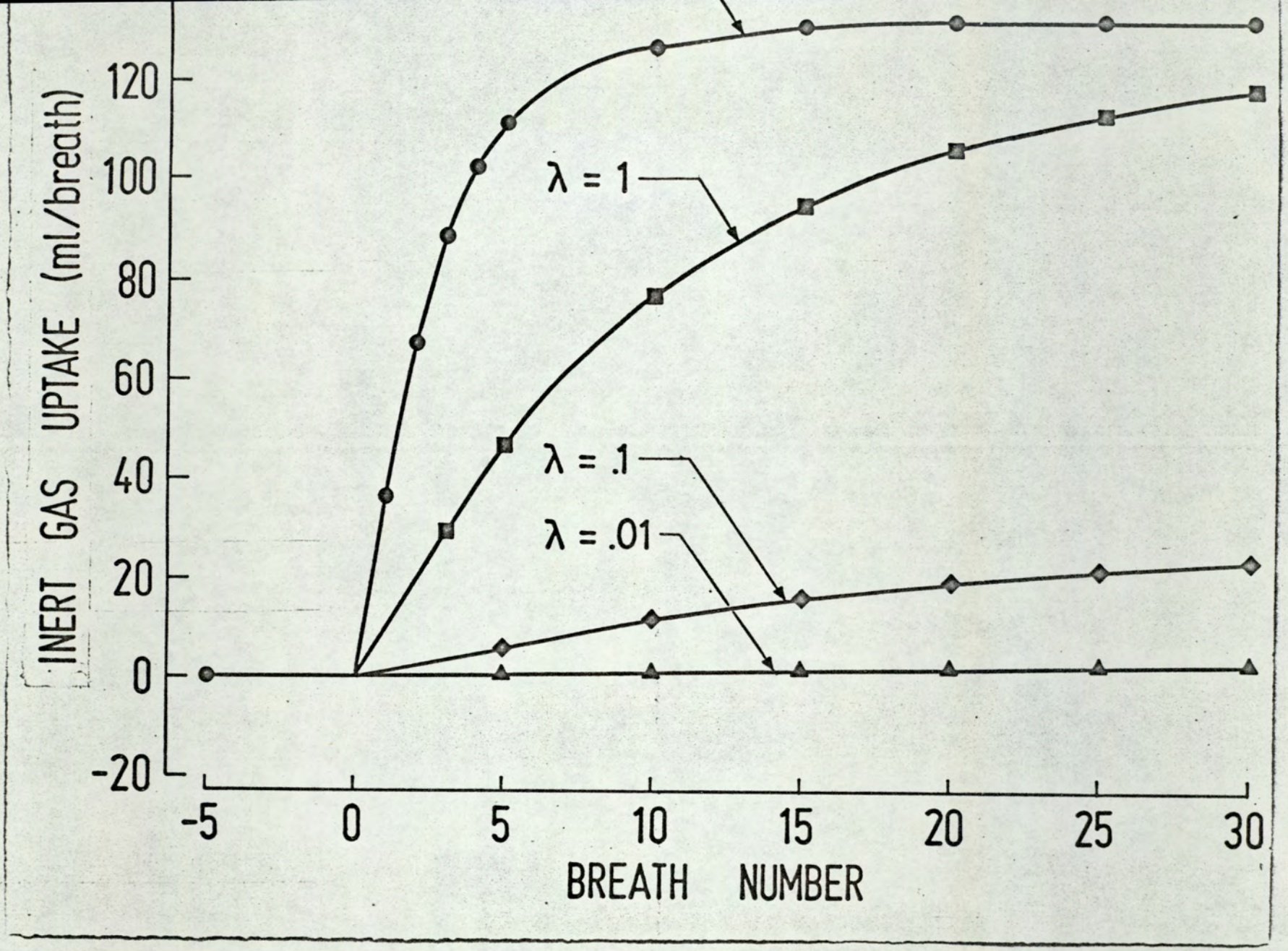
INERT GAS UPTAKE (ml/breath)
120
100
80
60
40
20
0
-20
λ = 1
λ = .1
λ = .01
-5
0
5
10
15
20
25
30
BREATH NUMBER

FIGURE 47

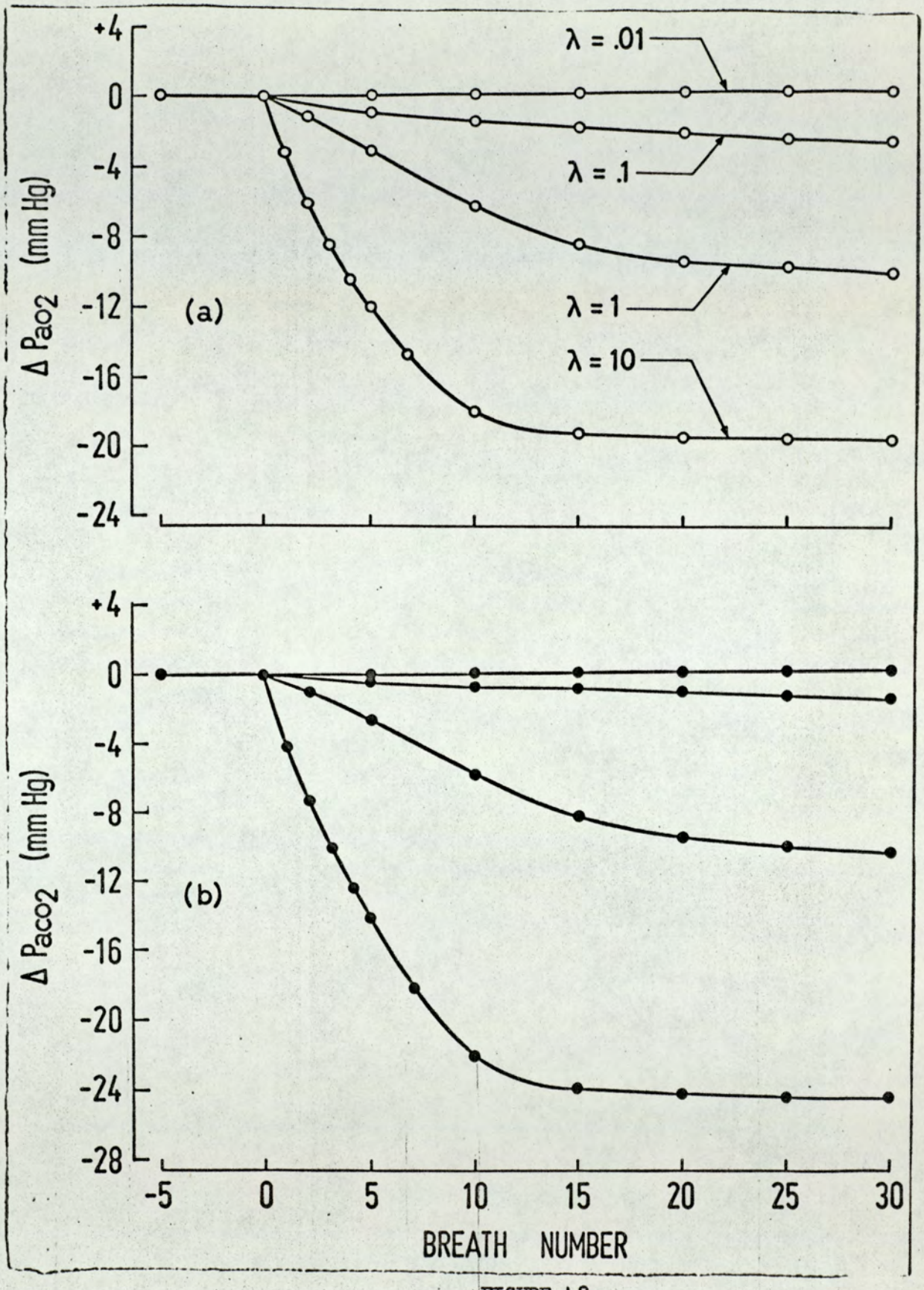
+4
0
-4
-8
-12
-16
-20
-24
Δ Pao2 (mm Hg)
(a)
λ = .01
λ = .1
λ = 1
λ = 10
+4
0
-4
-8
-12
-16
-20
-24
-28
Δ Paco2 (mm Hg)
(b)
-5
0
5
10
15
20
25
30
BREATH NUMBER

FIGURE 48

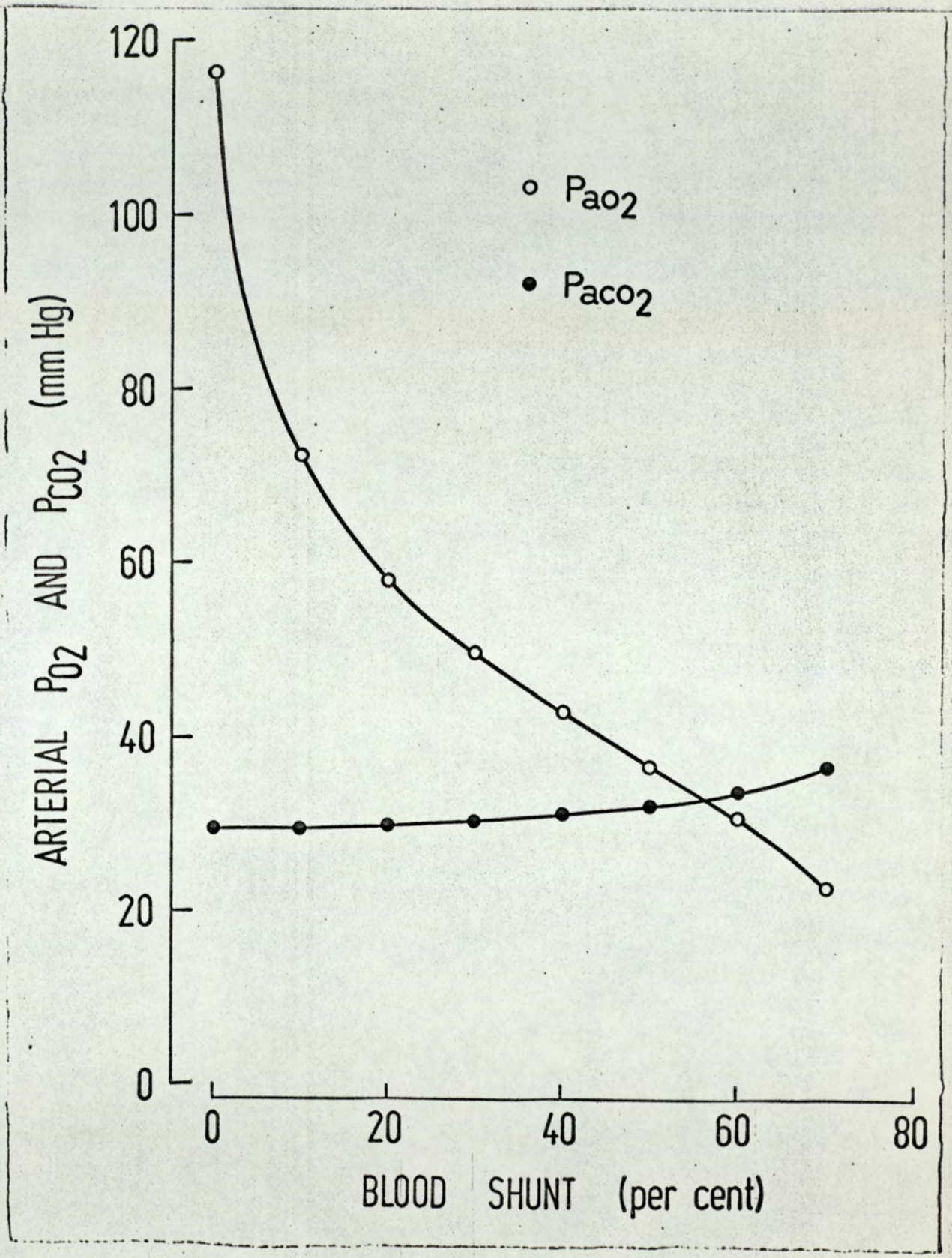
120
100
80
60
40
20
0
ARTERIAL P_{O_2} AND P_{CO_2} (mm Hg)
P_{ao_2}
P_{aco_2}
0
20
40
60
80
BLOOD SHUNT (per cent)

FIGURE 49

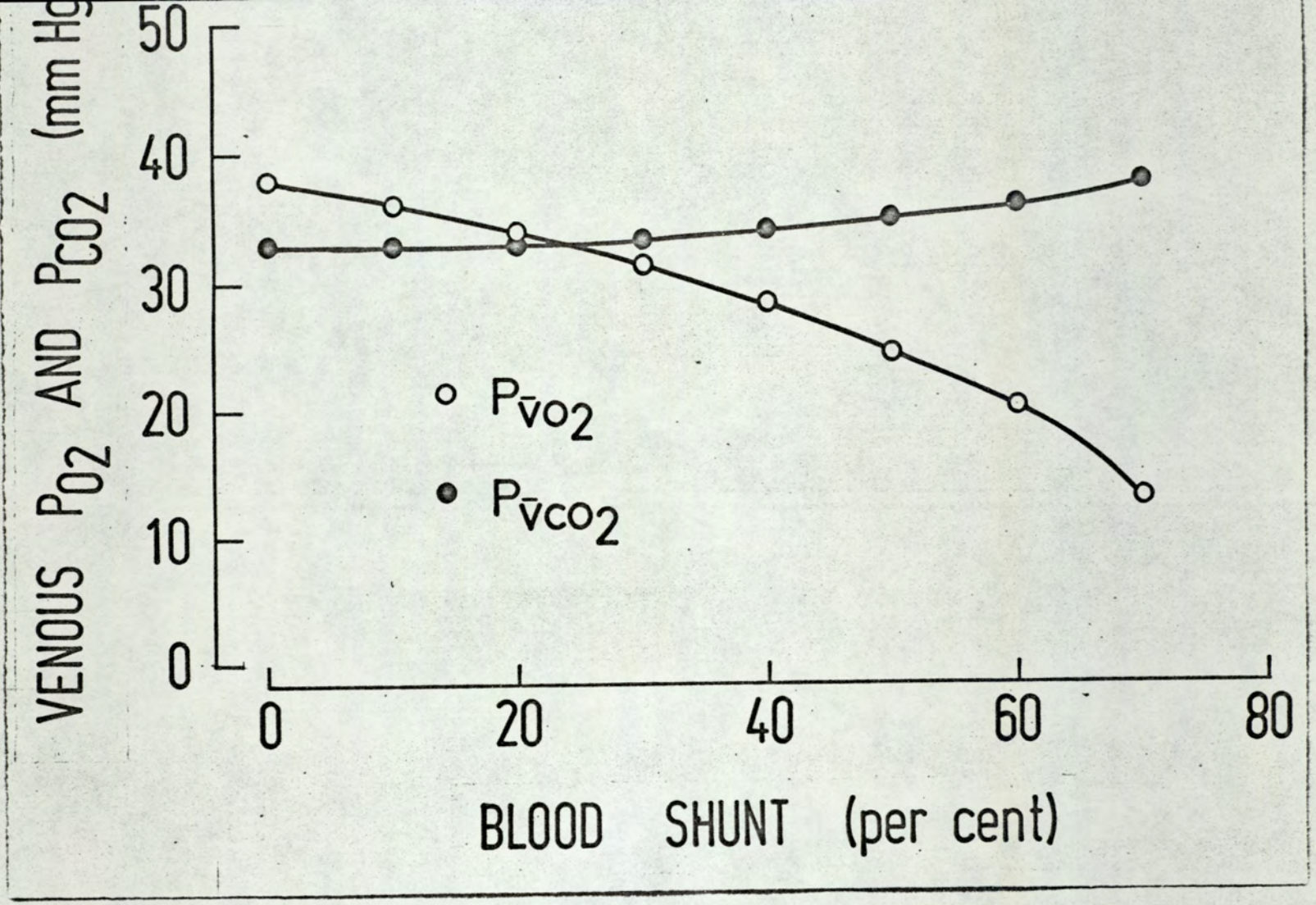
VENOUS P_{O_2} AND P_{CO_2} (mm Hg
50
40
30
20
10
0
$P_{\bar{v}O_2}$
$P_{\bar{v}CO_2}$
0
20
40
60
80
BLOOD SHUNT (per cent)

FIGURE 50

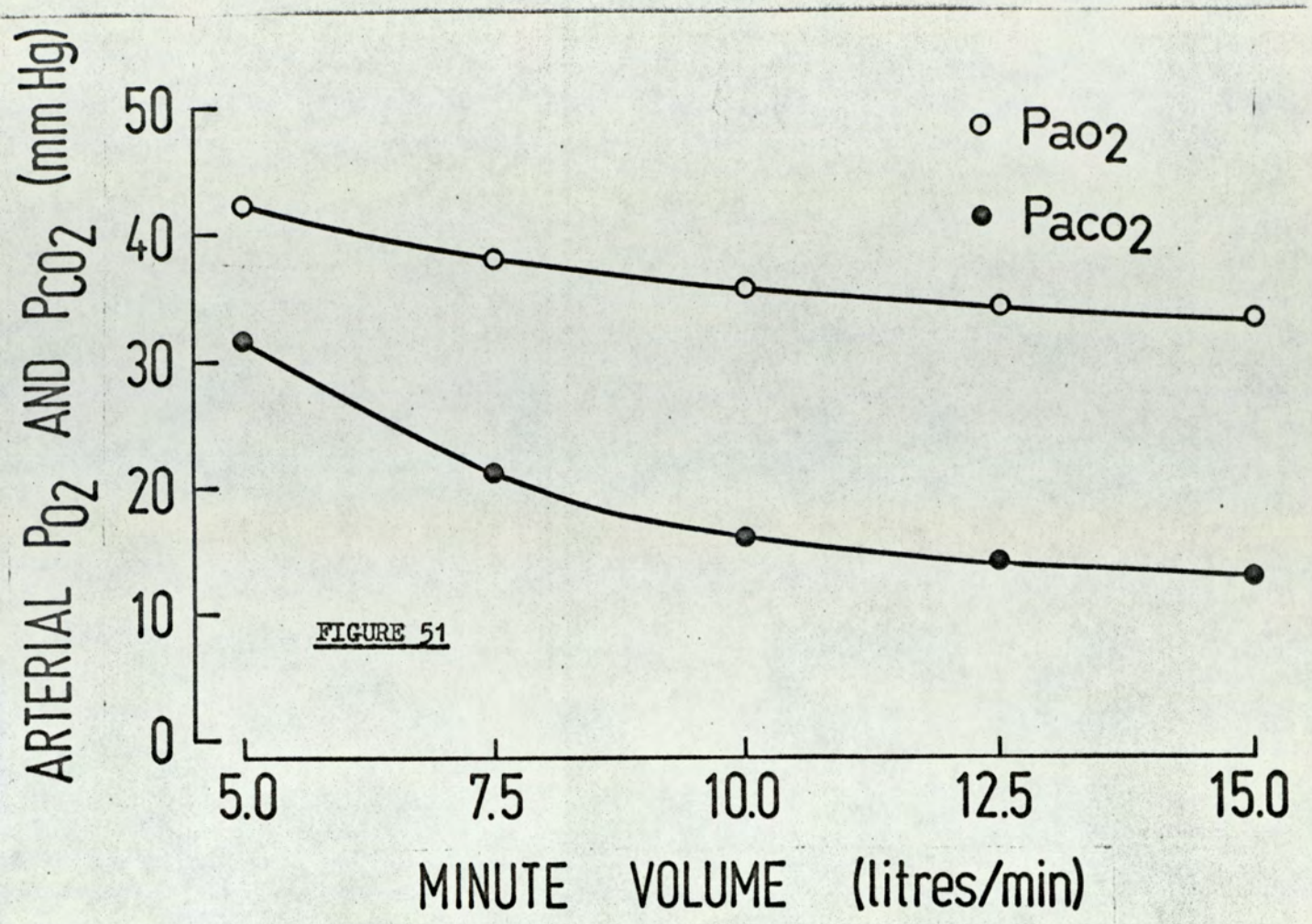

FIGURE 51

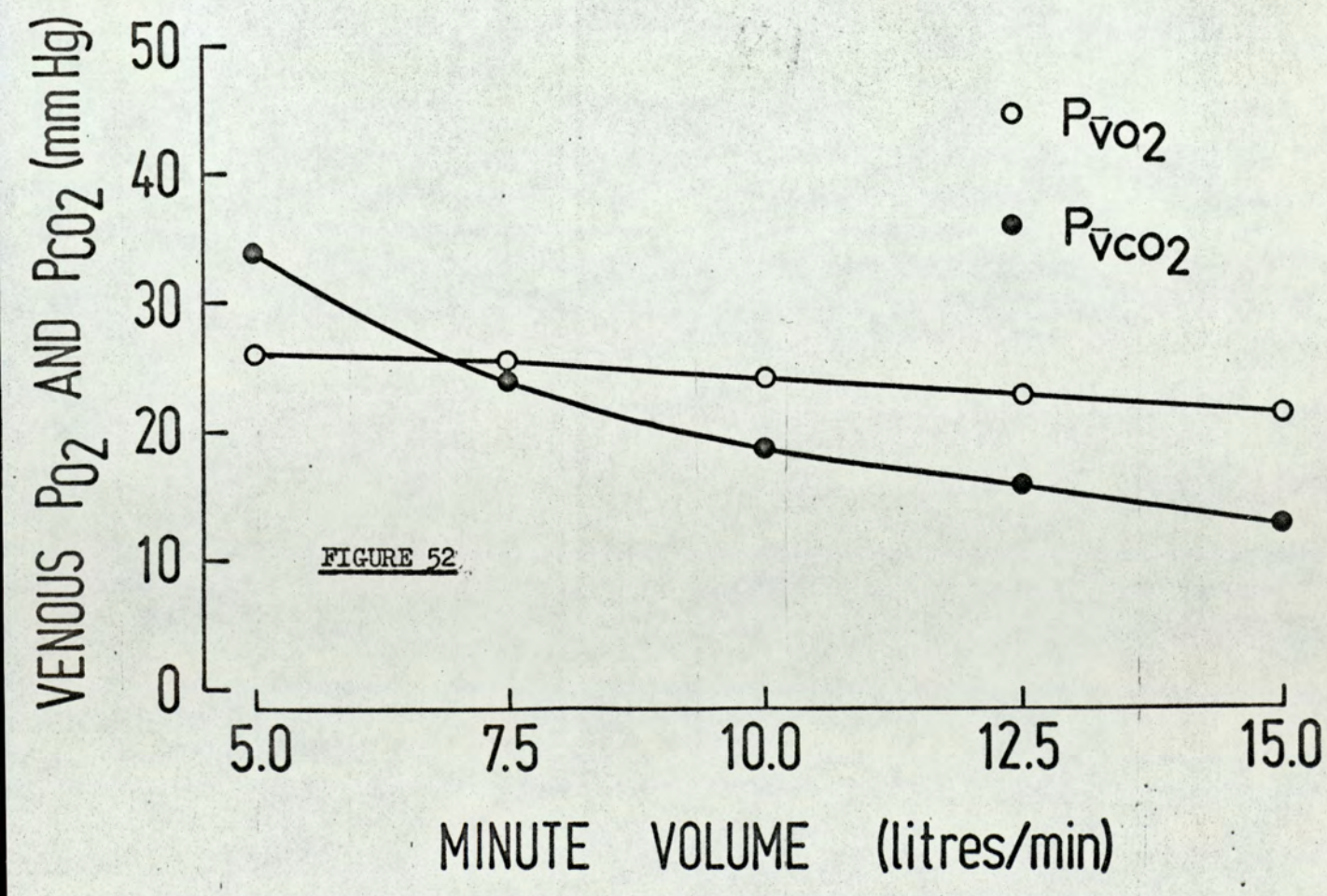

FIGURE 52

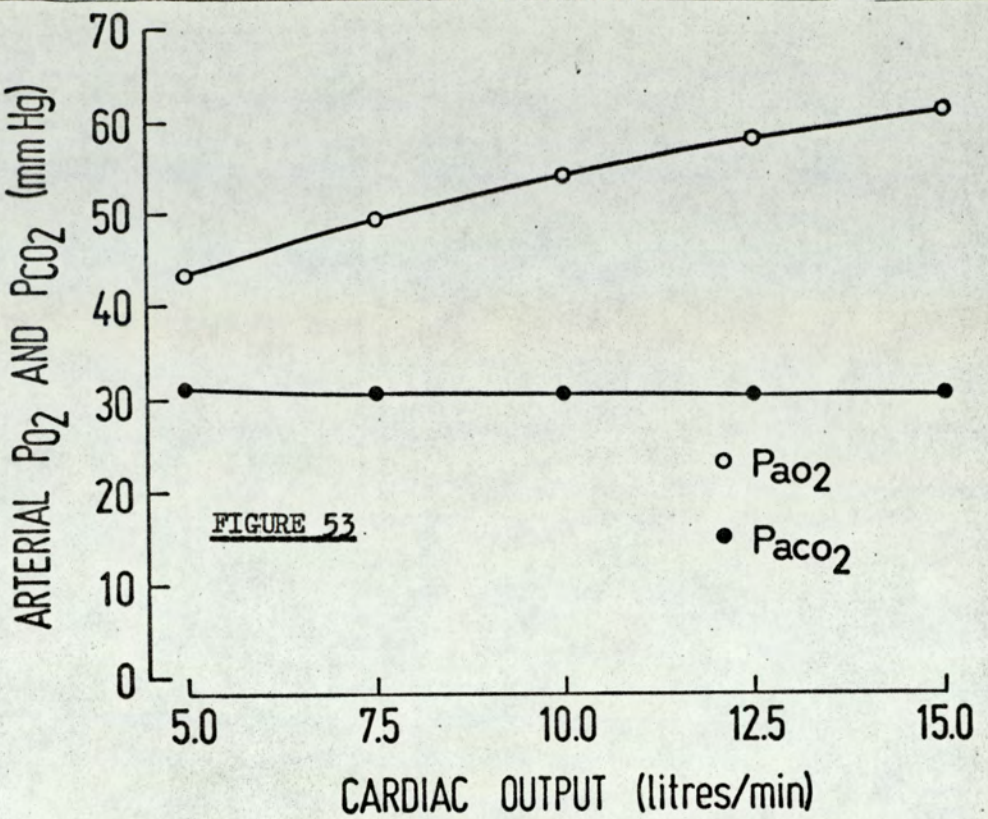

FIGURE 53

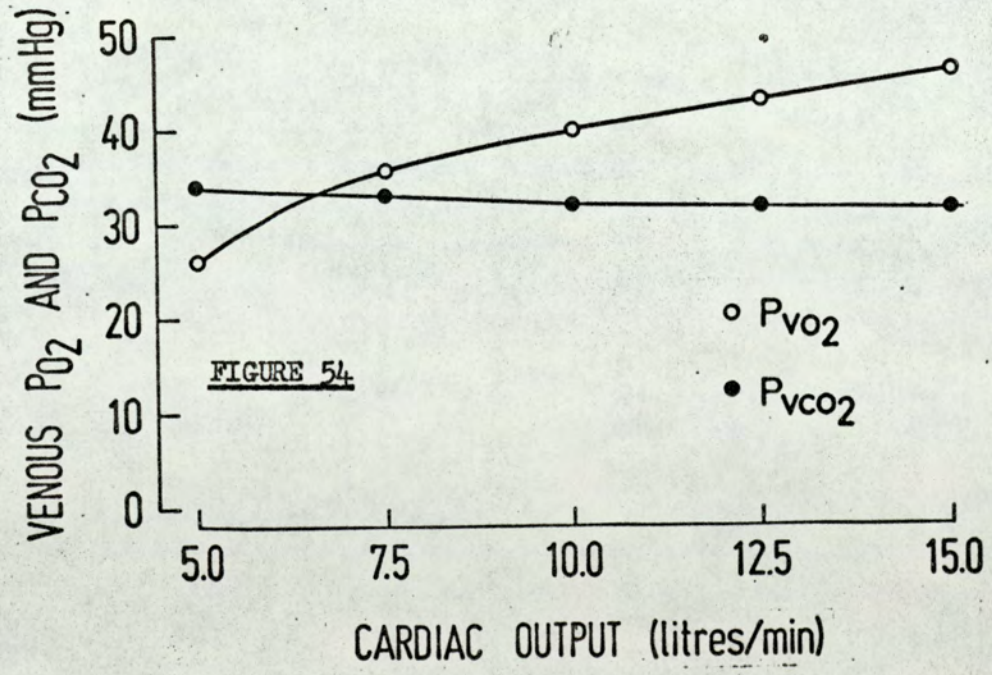

FIGURE 54

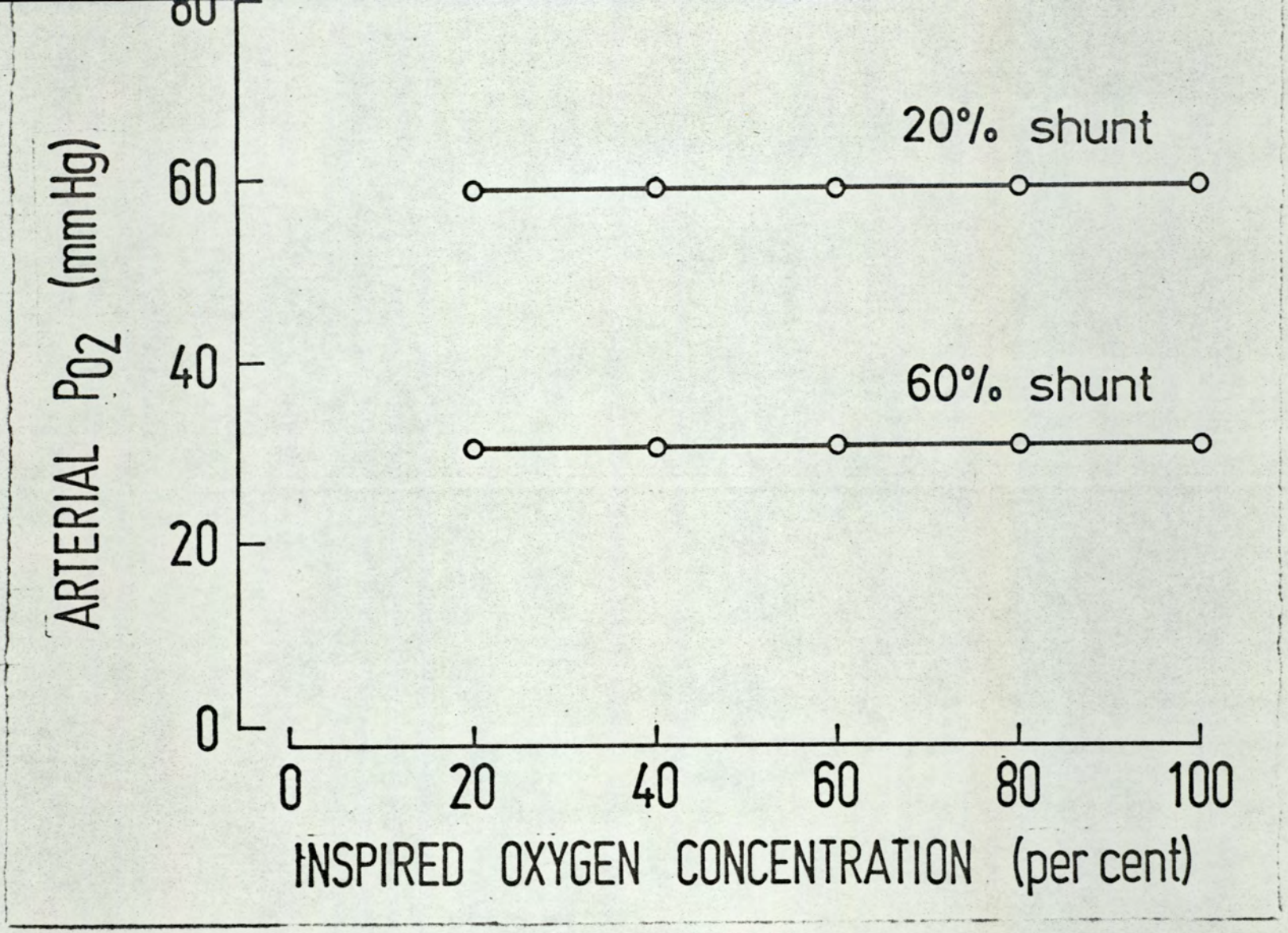
ARTERIAL P_{O_2} (mm Hg)
0
20
40
60
20% shunt
60% shunt
0
20
40
60
80
100
INSPIRED OXYGEN CONCENTRATION (per cent)

FIGURE 55

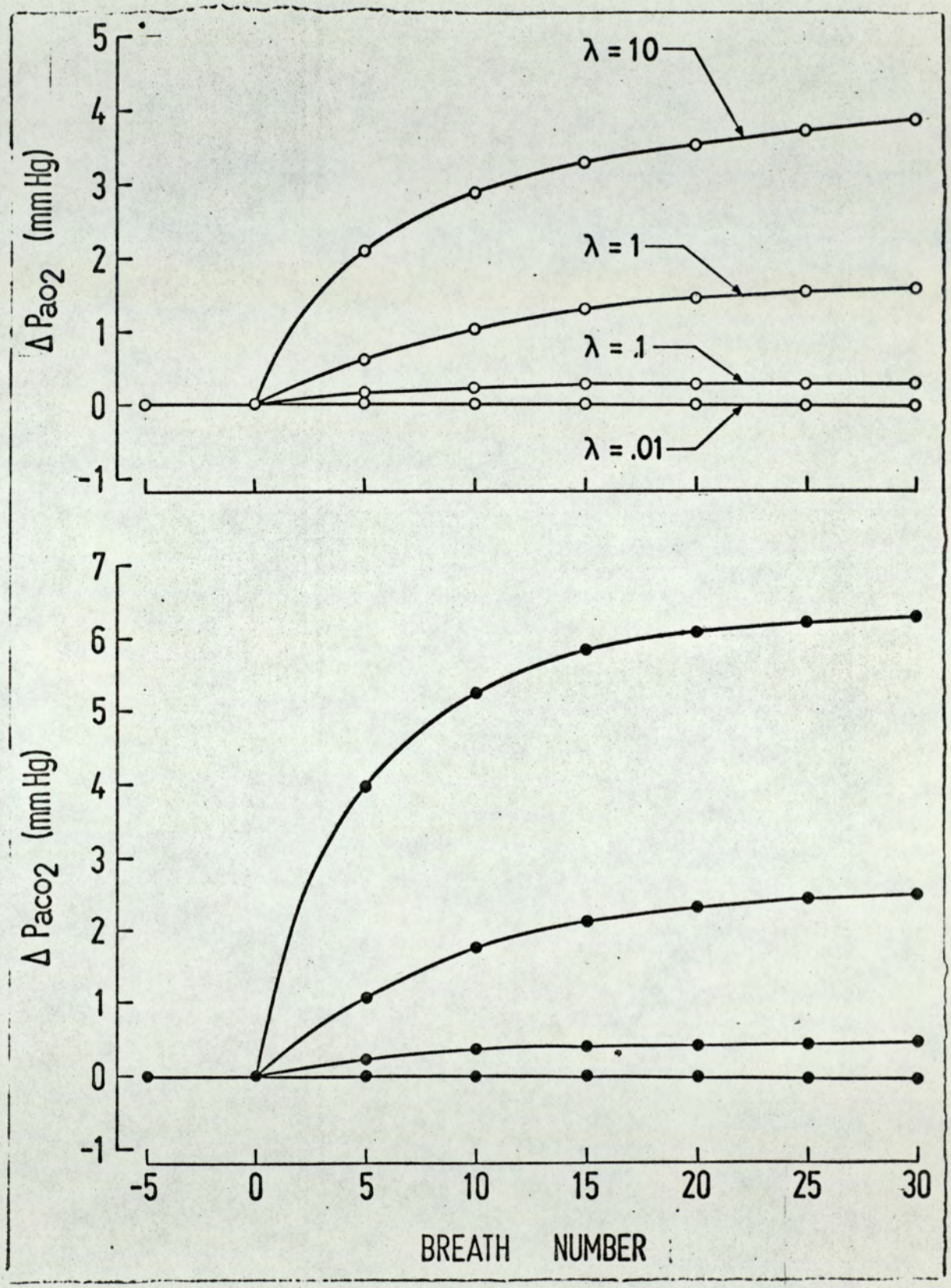
λ = 10
λ = 1
λ = .1
λ = .01
Δ Pao2 (mmHg)
Δ Paco2 (mmHg)
BREATH NUMBER
-5
0
5
10
15
20
25
30

FIGURE 56

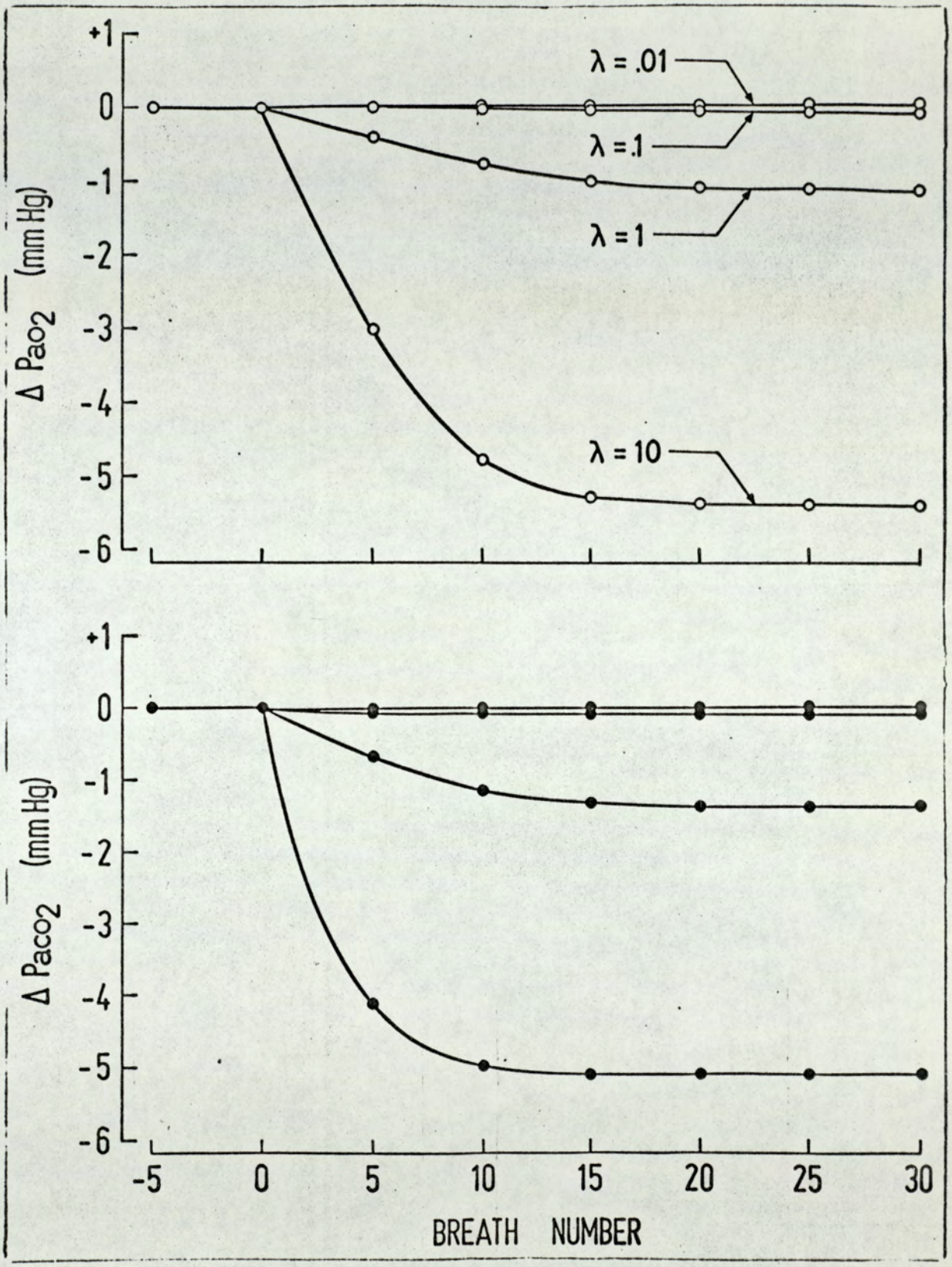
+1
0
-1
-2
-3
-4
-5
-6
Δ Pao2 (mm Hg)
λ = .01
λ = .1
λ = 1
λ = 10
Δ Paco2 (mm Hg)
-5
0
5
10
15
20
25
30
BREATH NUMBER

FIGURE 57

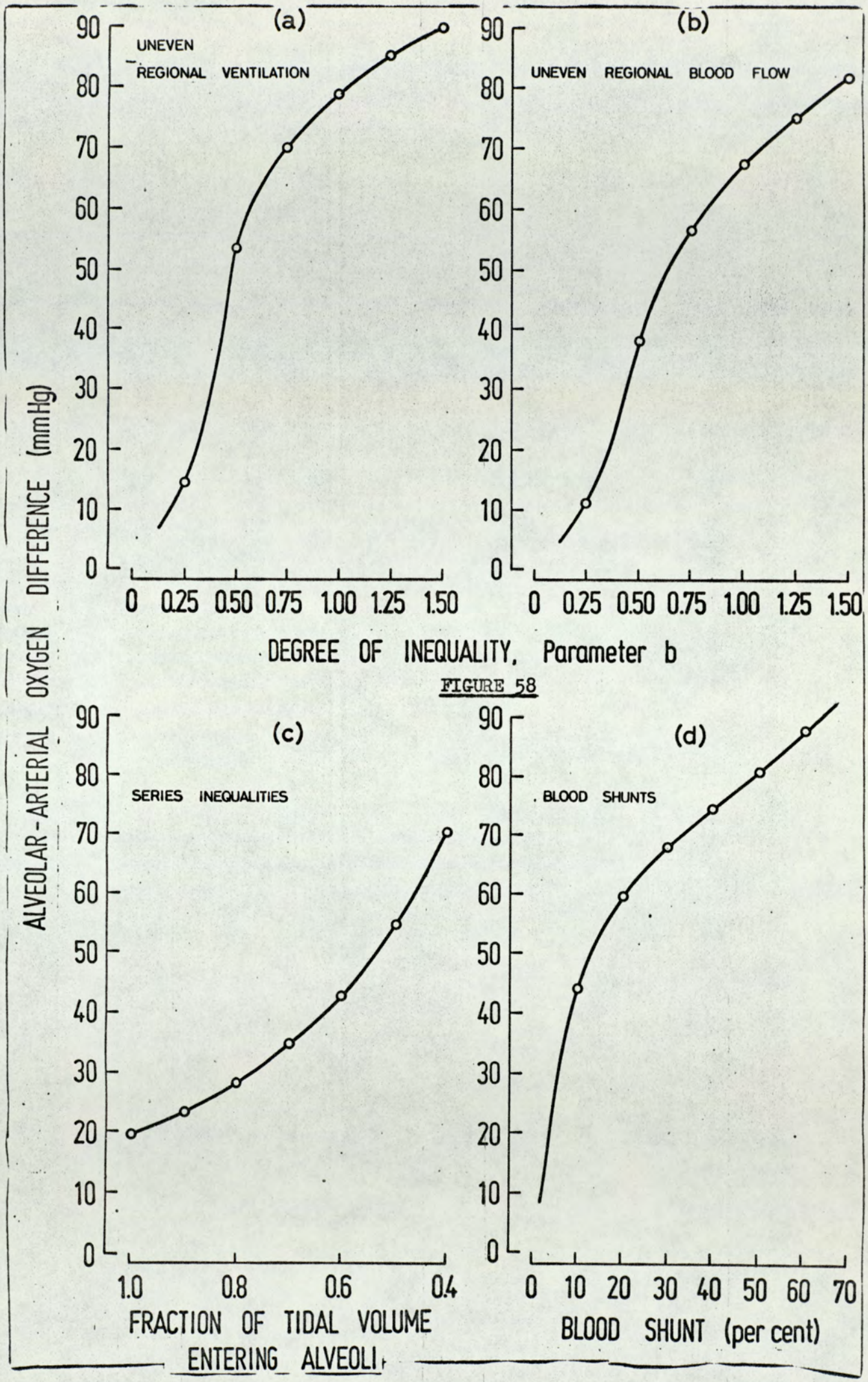
(a)
UNEVEN
REGIONAL VENTILATION
(b)
UNEVEN REGIONAL BLOOD FLOW
ALVEOLAR-ARTERIAL OXYGEN DIFFERENCE (mmHg)
0 10 20 30 40 50 60 70 80 90
0 0.25 0.50 0.75 1.00 1.25 1.50
DEGREE OF INEQUALITY, Parameter b
(c)
SERIES INEQUALITIES
(d)
BLOOD SHUNTS
1.0 0.8 0.6 0.4
FRACTION OF TIDAL VOLUME ENTERING ALVEOLI
0 10 20 30 40 50 60 70
BLOOD SHUNT (per cent)

FIGURE 58

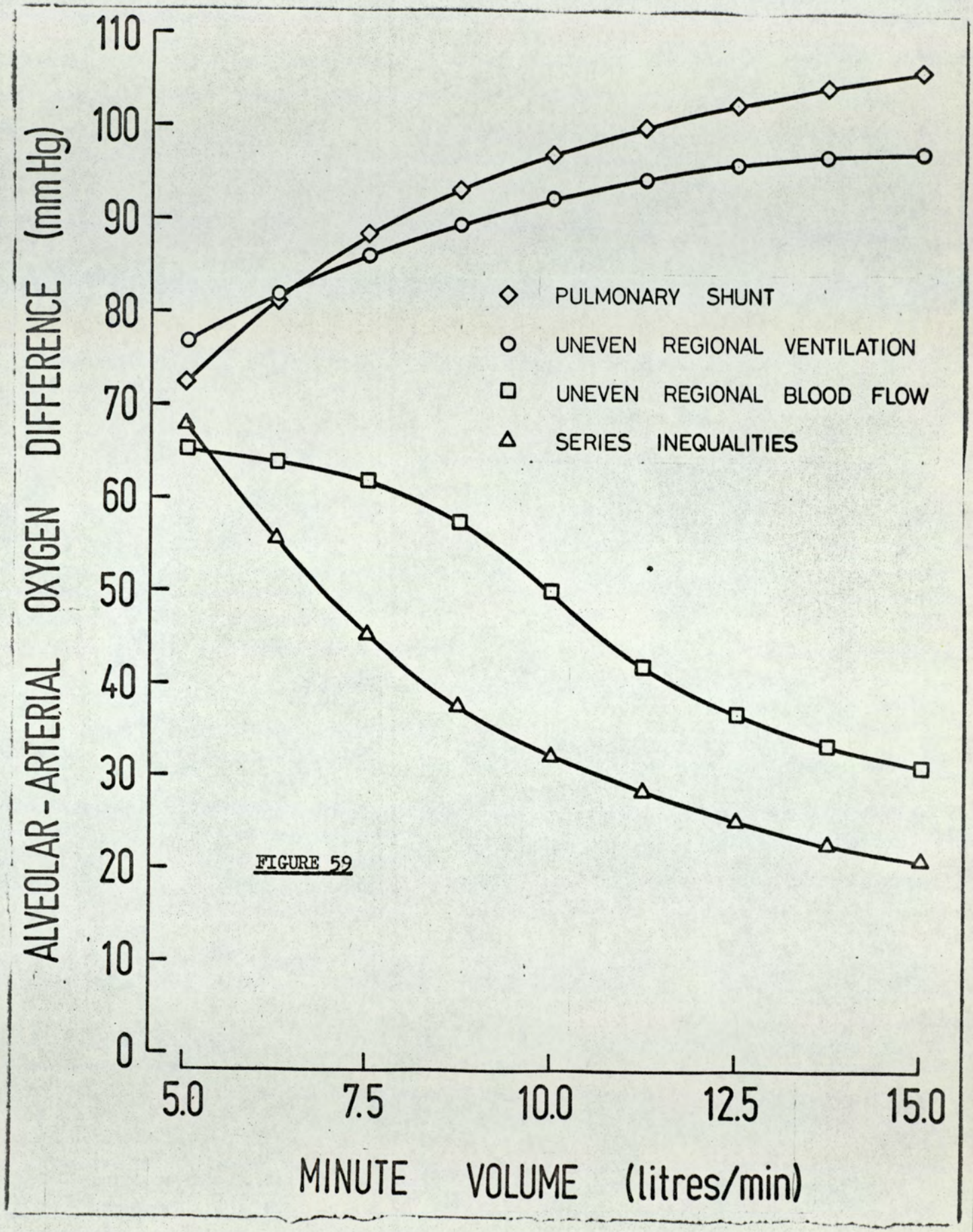
ALVEOLAR-ARTERIAL OXYGEN DIFFERENCE (mm Hg)
110
100
90
80
70
60
50
40
30
20
10
0
5.0
7.5
10.0
12.5
15.0
MINUTE VOLUME (litres/min)
PULMONARY SHUNT
UNEVEN REGIONAL VENTILATION
UNEVEN REGIONAL BLOOD FLOW
SERIES INEQUALITIES

FIGURE 59

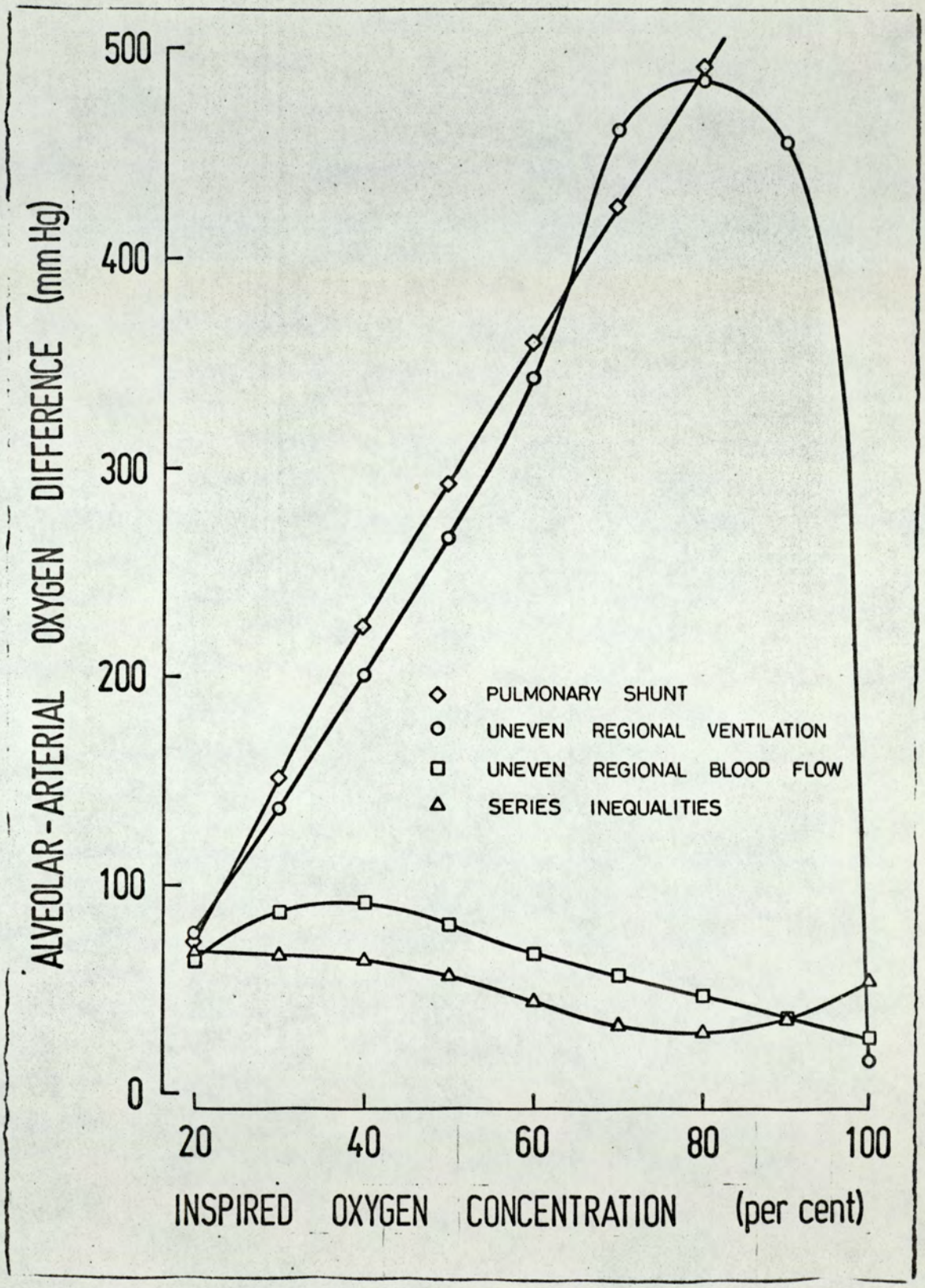
ALVEOLAR-ARTERIAL OXYGEN DIFFERENCE (mm Hg)
500
400
300
200
100
0
20
40
60
80
100
INSPIRED OXYGEN CONCENTRATION (per cent)
PULMONARY SHUNT
UNEVEN REGIONAL VENTILATION
UNEVEN REGIONAL BLOOD FLOW
SERIES INEQUALITIES

FIGURE 60

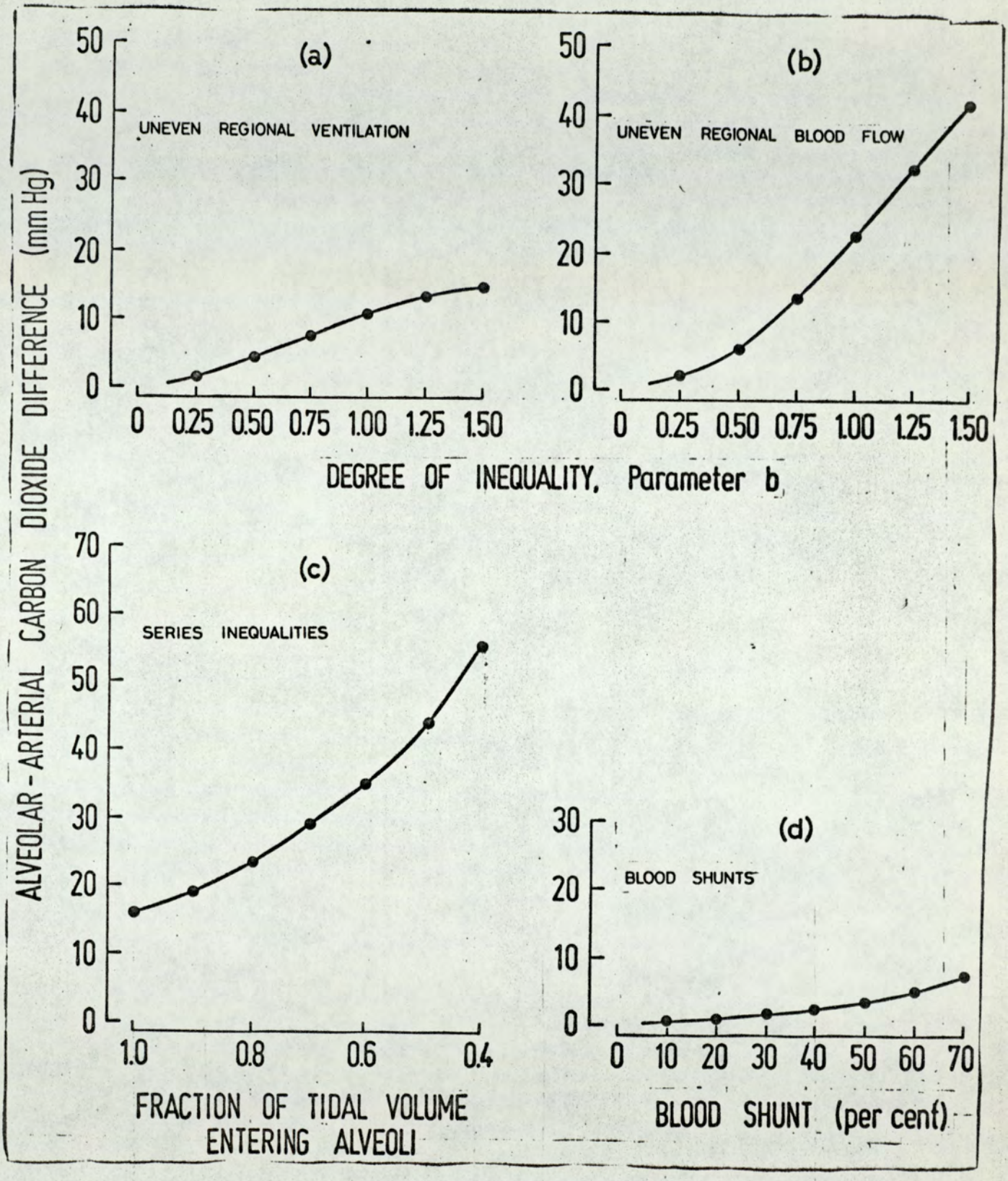
ALVEOLAR - ARTERIAL CARBON DIOXIDE DIFFERENCE (mm Hg)
(a)
UNEVEN REGIONAL VENTILATION
(b)
UNEVEN REGIONAL BLOOD FLOW
DEGREE OF INEQUALITY, Parameter b
(c)
SERIES INEQUALITIES
FRACTION OF TIDAL VOLUME ENTERING ALVEOLI
(d)
BLOOD SHUNTS
BLOOD SHUNT (per cent)

FIGURE 61

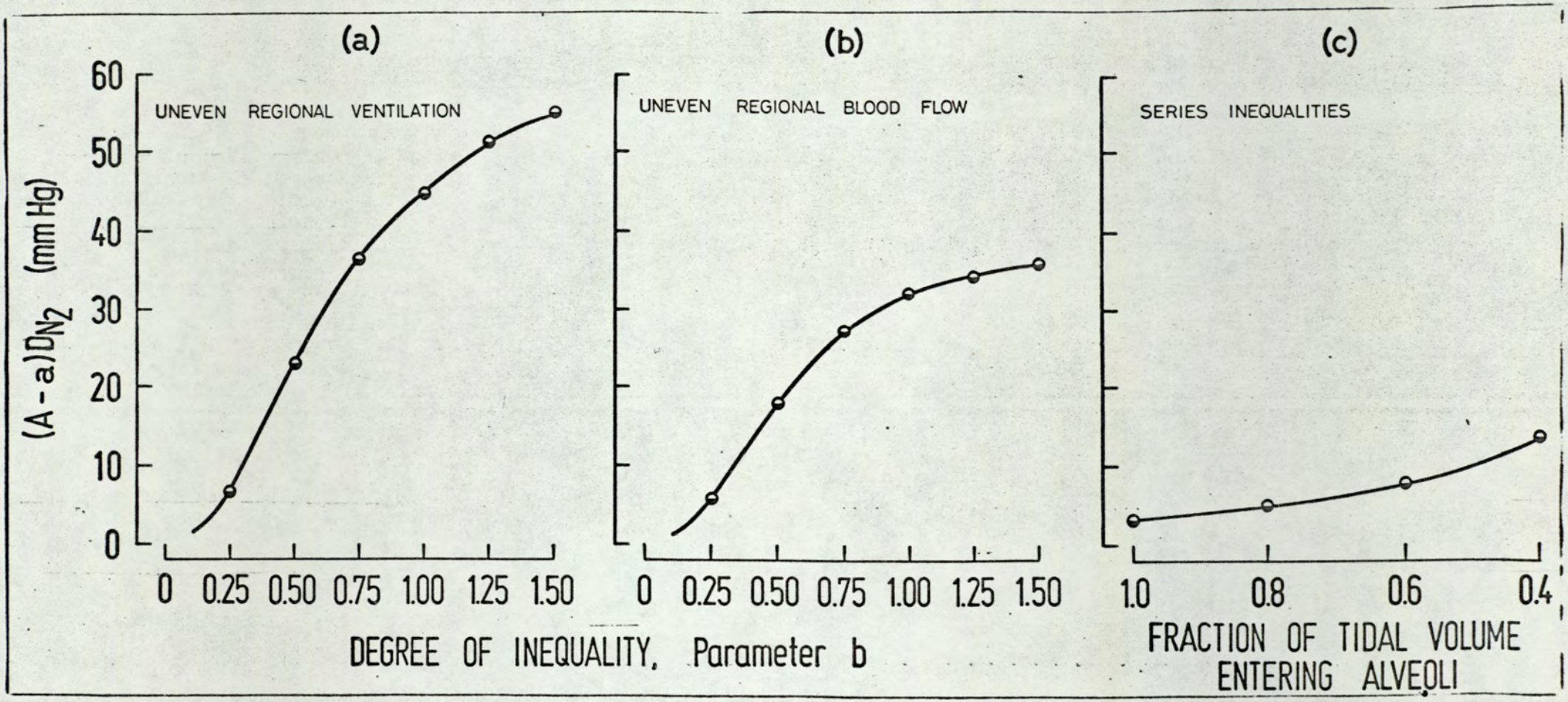
(a)
(b)
(c)
UNEVEN REGIONAL VENTILATION
UNEVEN REGIONAL BLOOD FLOW
SERIES INEQUALITIES
(A - a)D_{N_2} (mm Hg)
60
50
40
30
20
10
0
0 0.25 0.50 0.75 1.00 1.25 1.50
0 0.25 0.50 0.75 1.00 1.25 1.50
1.0 0.8 0.6 0.4
DEGREE OF INEQUALITY, Parameter b
FRACTION OF TIDAL VOLUME ENTERING ALVEOLI

FIGURE 62

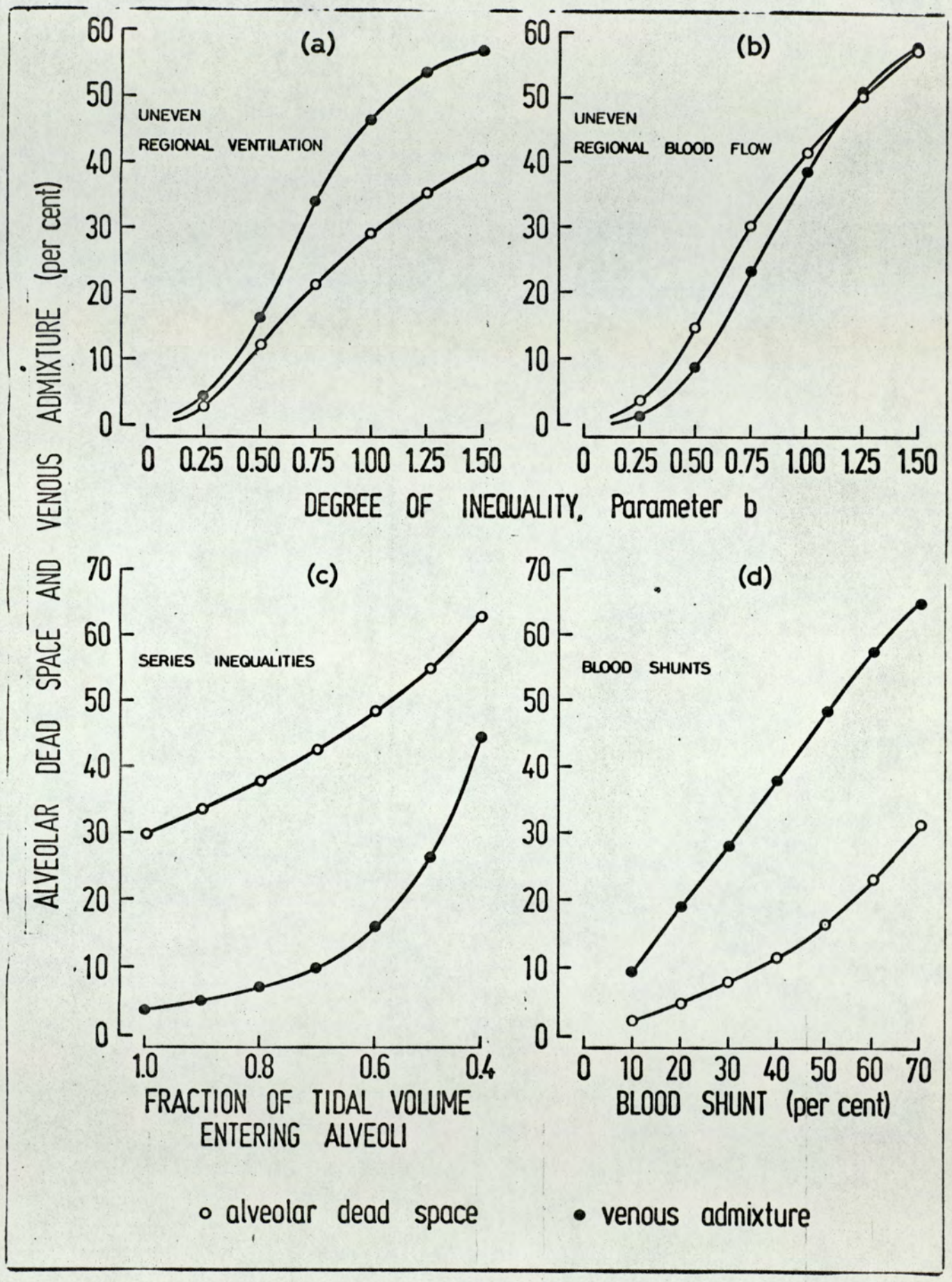
(a)
UNEVEN
REGIONAL VENTILATION
(b)
UNEVEN
REGIONAL BLOOD FLOW
ALVEOLAR DEAD SPACE AND VENOUS ADMIXTURE (per cent)
0 10 20 30 40 50 60
0 0.25 0.50 0.75 1.00 1.25 1.50
DEGREE OF INEQUALITY, Parameter b
(c)
SERIES INEQUALITIES
(d)
BLOOD SHUNTS
0 10 20 30 40 50 60 70
1.0 0.8 0.6 0.4
FRACTION OF TIDAL VOLUME ENTERING ALVEOLI
0 10 20 30 40 50 60 70
BLOOD SHUNT (per cent)
o alveolar dead space
• venous admixture

FIGURE 63

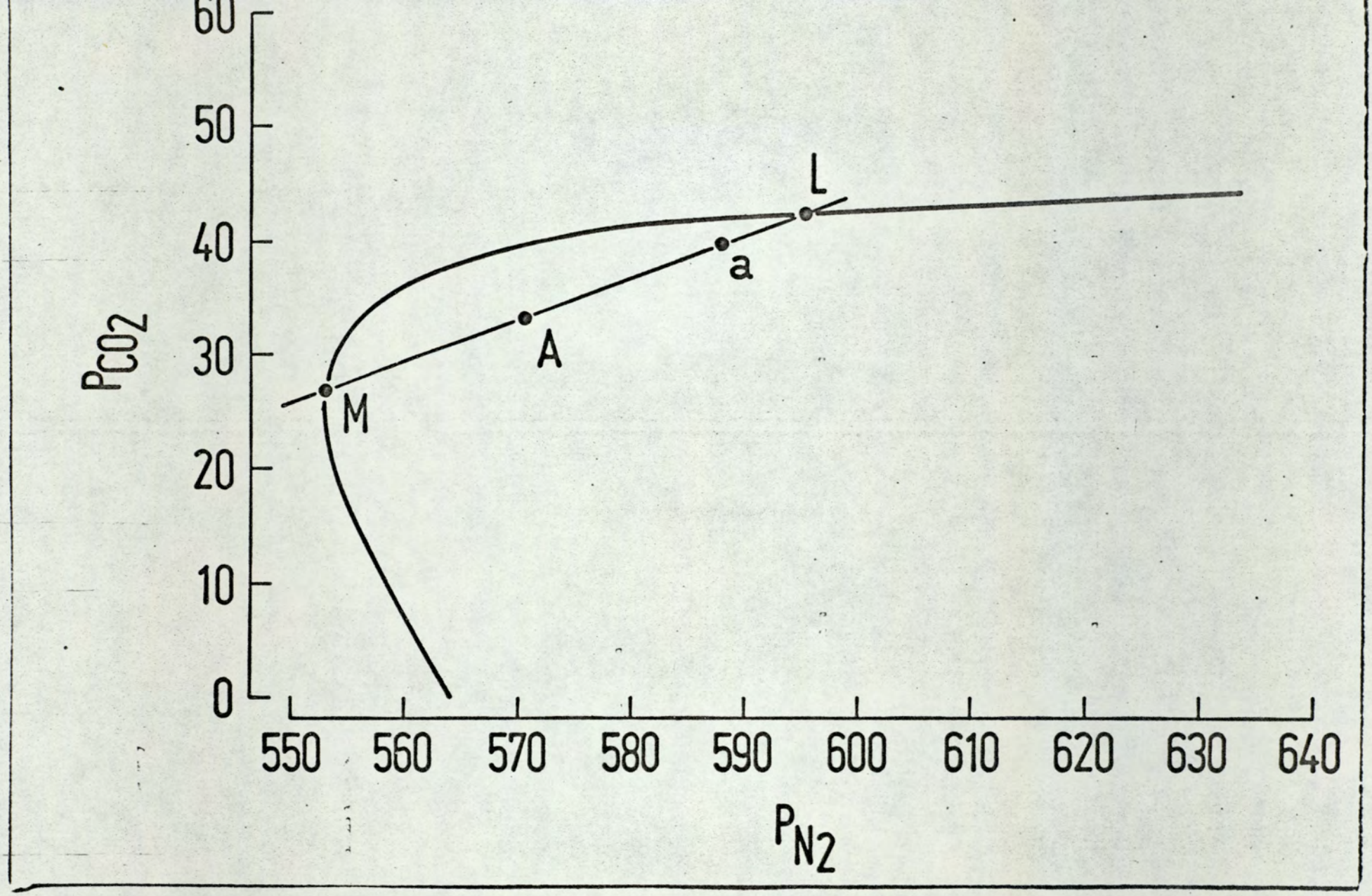
60
50
40
30
20
10
0
P_{CO_2}
L
a
A
M
550
560
570
580
590
600
610
620
630
640
P_{N_2}

FIGURE 64

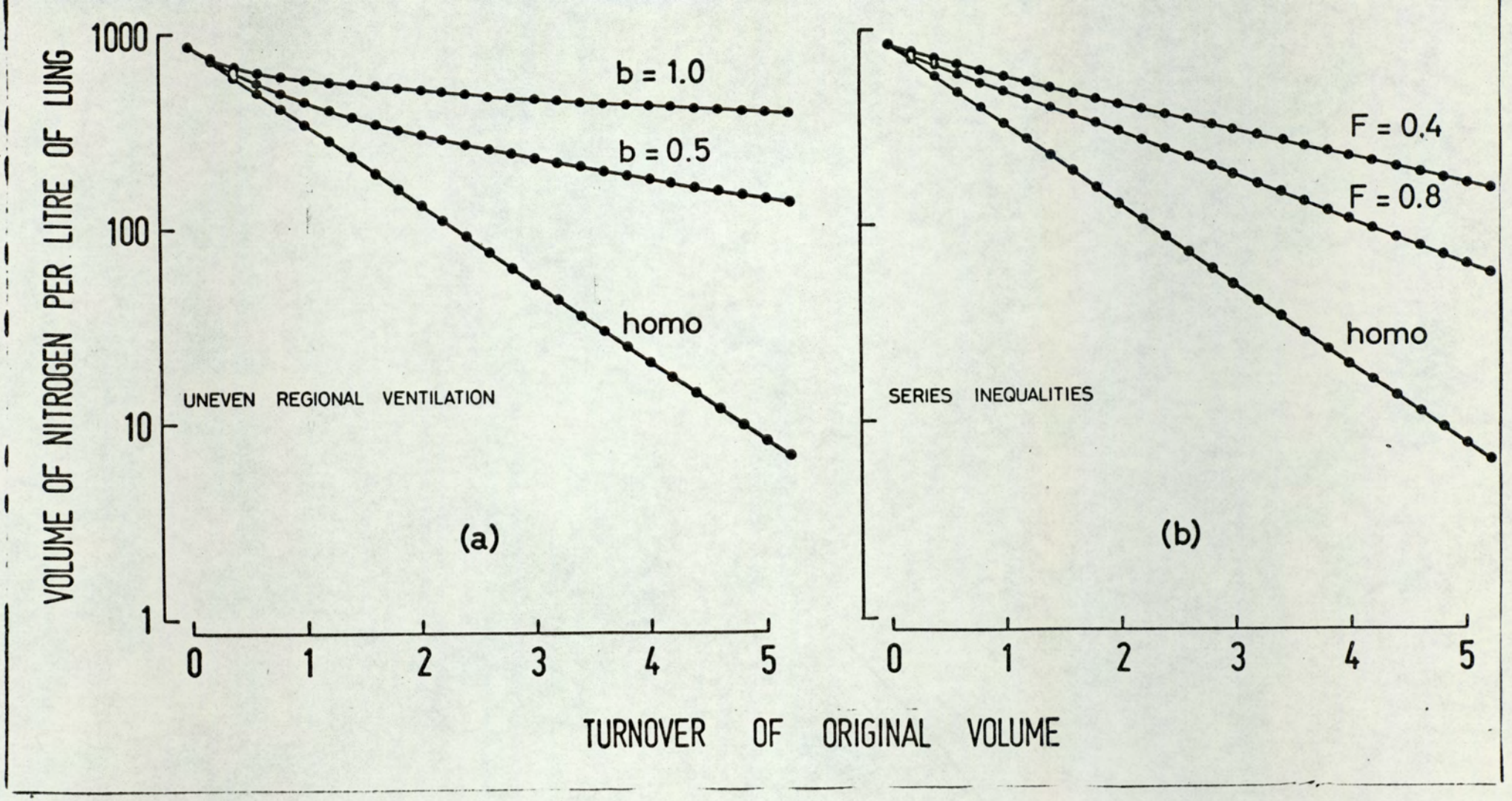
VOLUME OF NITROGEN PER LITRE OF LUNG
1000
100
10
1
b = 1.0
b = 0.5
homo
UNEVEN REGIONAL VENTILATION
(a)
0
1
2
3
4
5
F = 0.4
F = 0.8
homo
SERIES INEQUALITIES
(b)
0
1
2
3
4
5
TURNOVER OF ORIGINAL VOLUME

FIGURE 65

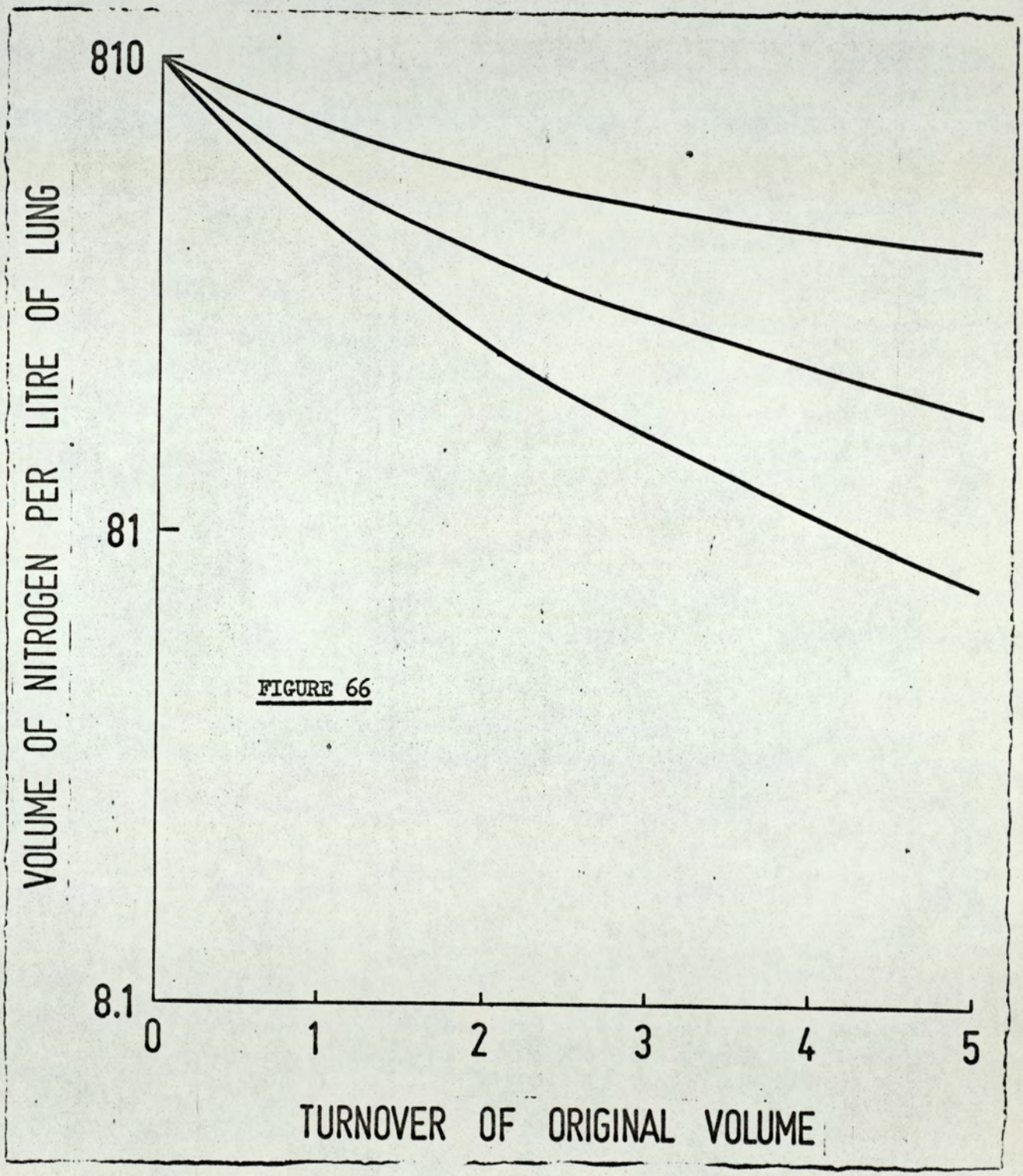
810
81
8.1
0
1
2
3
4
5
VOLUME OF NITROGEN PER LITRE OF LUNG
TURNOVER OF ORIGINAL VOLUME

FIGURE 66

FIGURE 67

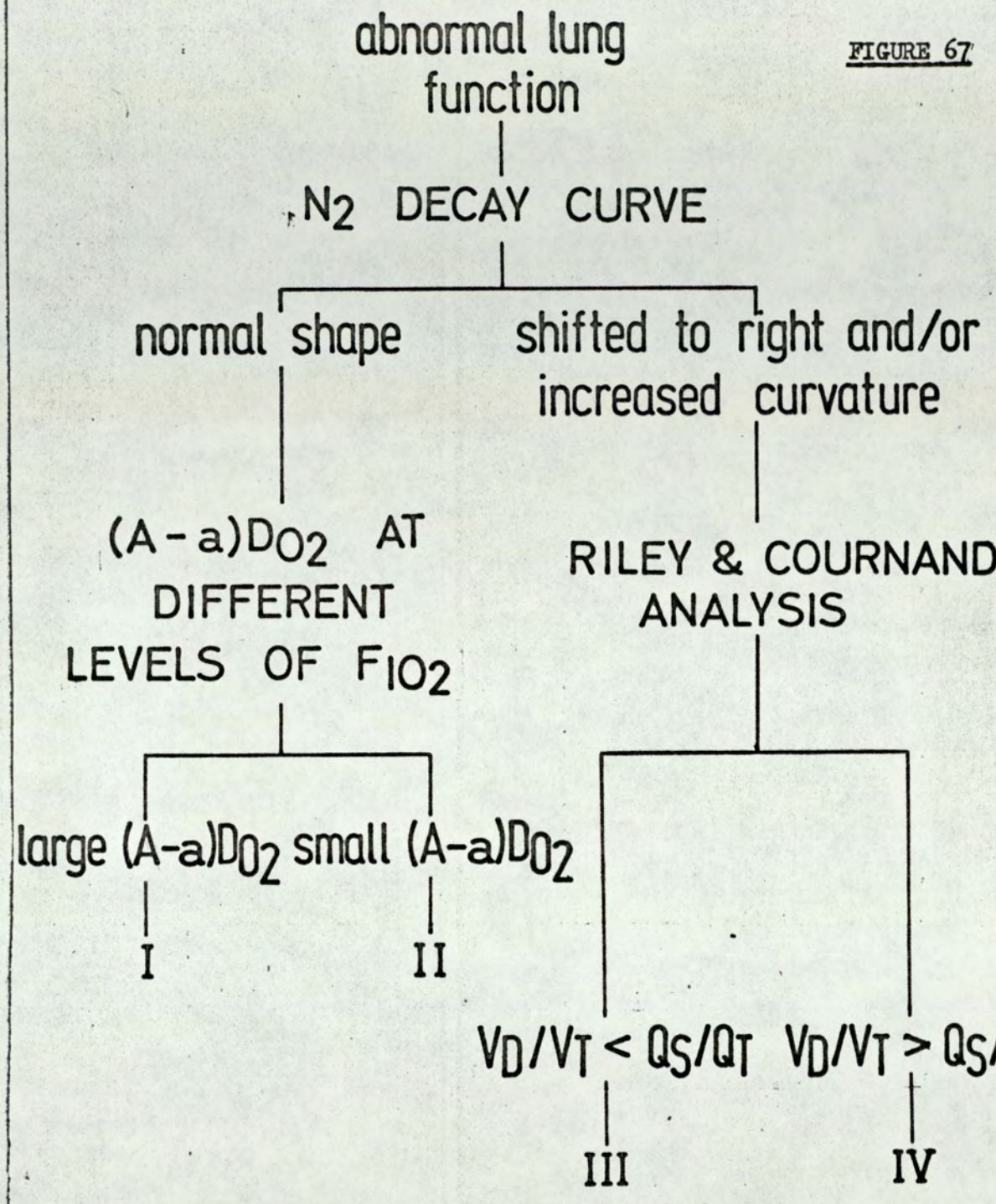

I BLOOD SHUNTS

II UNEVEN REGIONAL DISTRIBUTION OF BLOOD FLOW

III UNEVEN REGIONAL DISTRIBUTION OF VENTILATION

IV SERIES INEQUALITIES

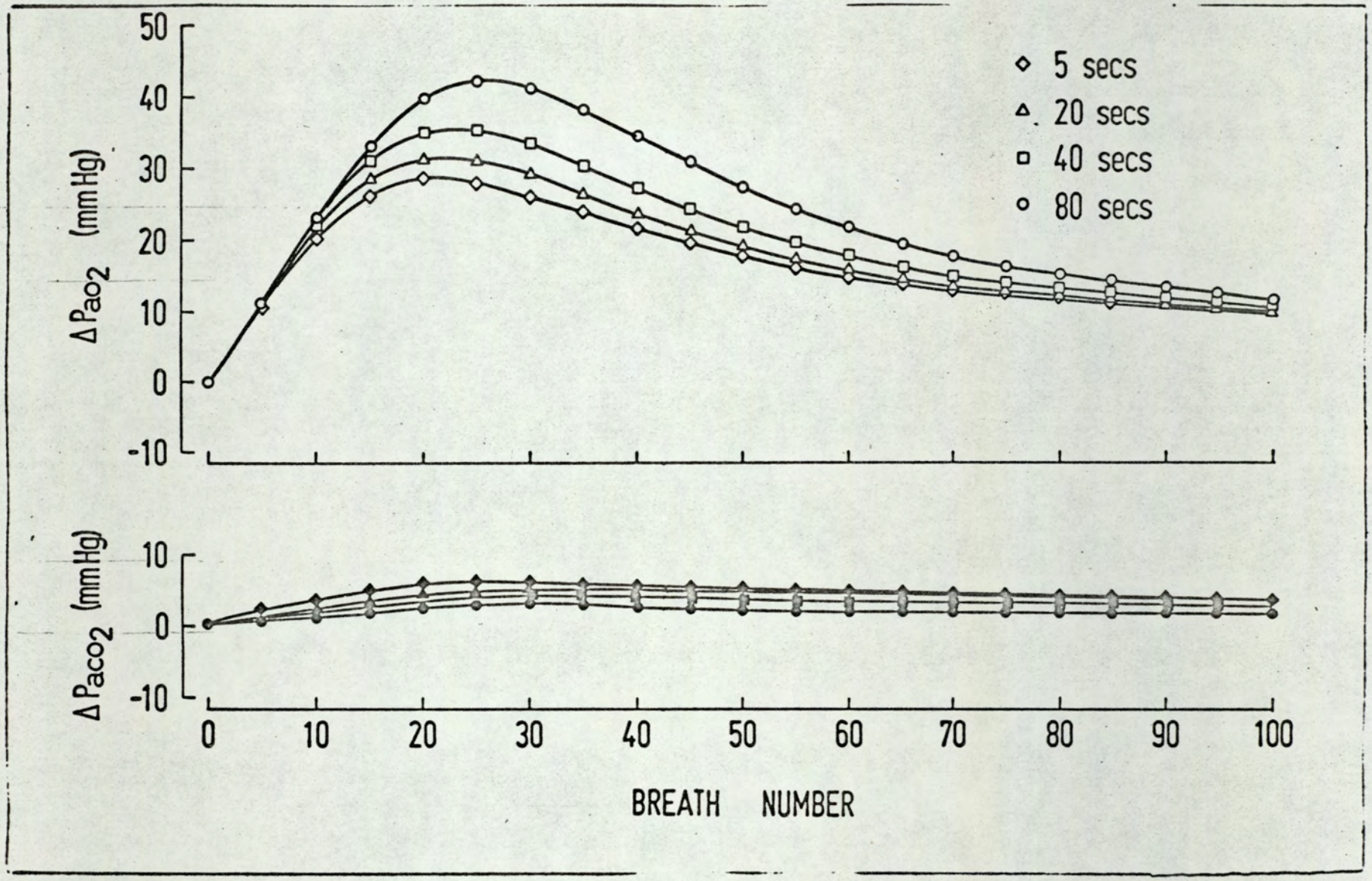
50
40
30
20
10
0
-10
ΔP_{ao_2} (mmHg)
5 secs
20 secs
40 secs
80 secs
10
0
-10
ΔP_{aco_2} (mmHg)
0
10
20
30
40
50
60
70
80
90
100
BREATH NUMBER

FIGURE 68

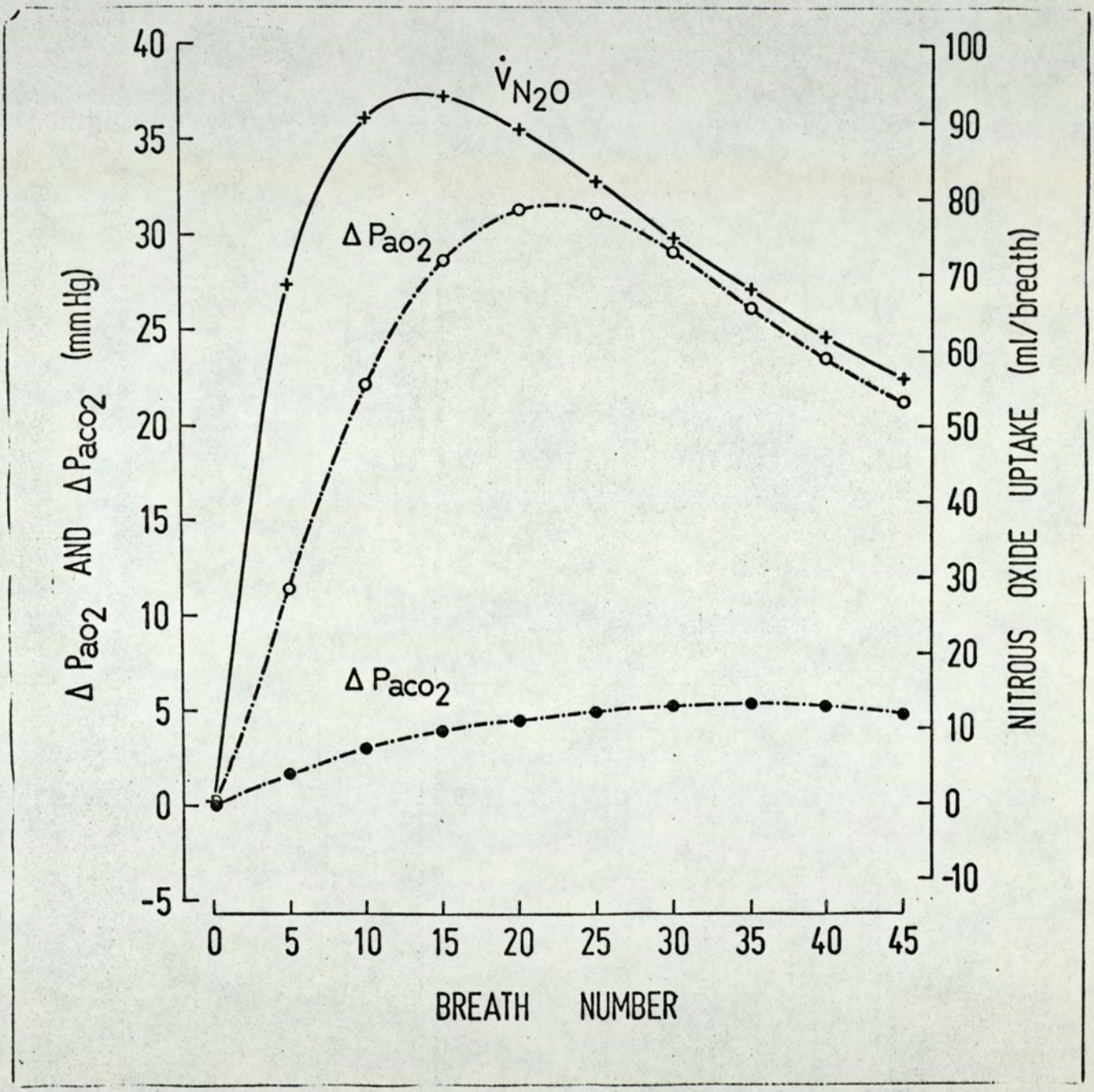
40
35
30
25
20
15
10
5
0
-5
100
90
80
70
60
50
40
30
20
10
0
-10
$\dot{V}_{N_2O}$
ΔP_{ao_2}
ΔP_{aco_2}
ΔP_{ao_2} AND ΔP_{aco_2} (mmHg)
NITROUS OXIDE UPTAKE (ml/breath)
0 5 10 15 20 25 30 35 40 45
BREATH NUMBER

FIGURE 69

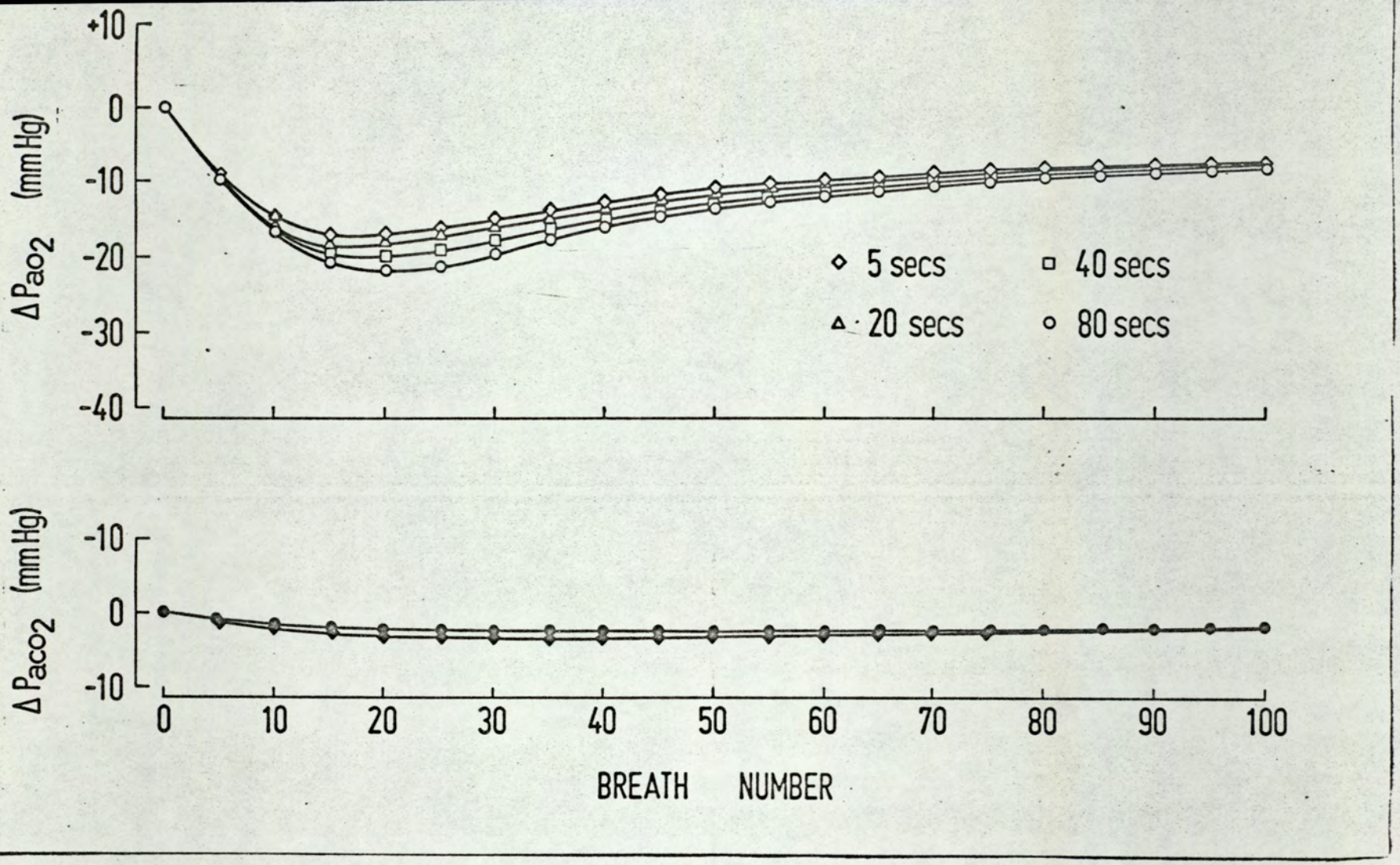
+10
0
-10
-20
-30
-40
ΔPao2 (mmHg)
5 secs
40 secs
20 secs
80 secs
-10
0
-10
ΔPaco2 (mmHg)
0
10
20
30
40
50
60
70
80
90
100
BREATH NUMBER

FIGURE 70

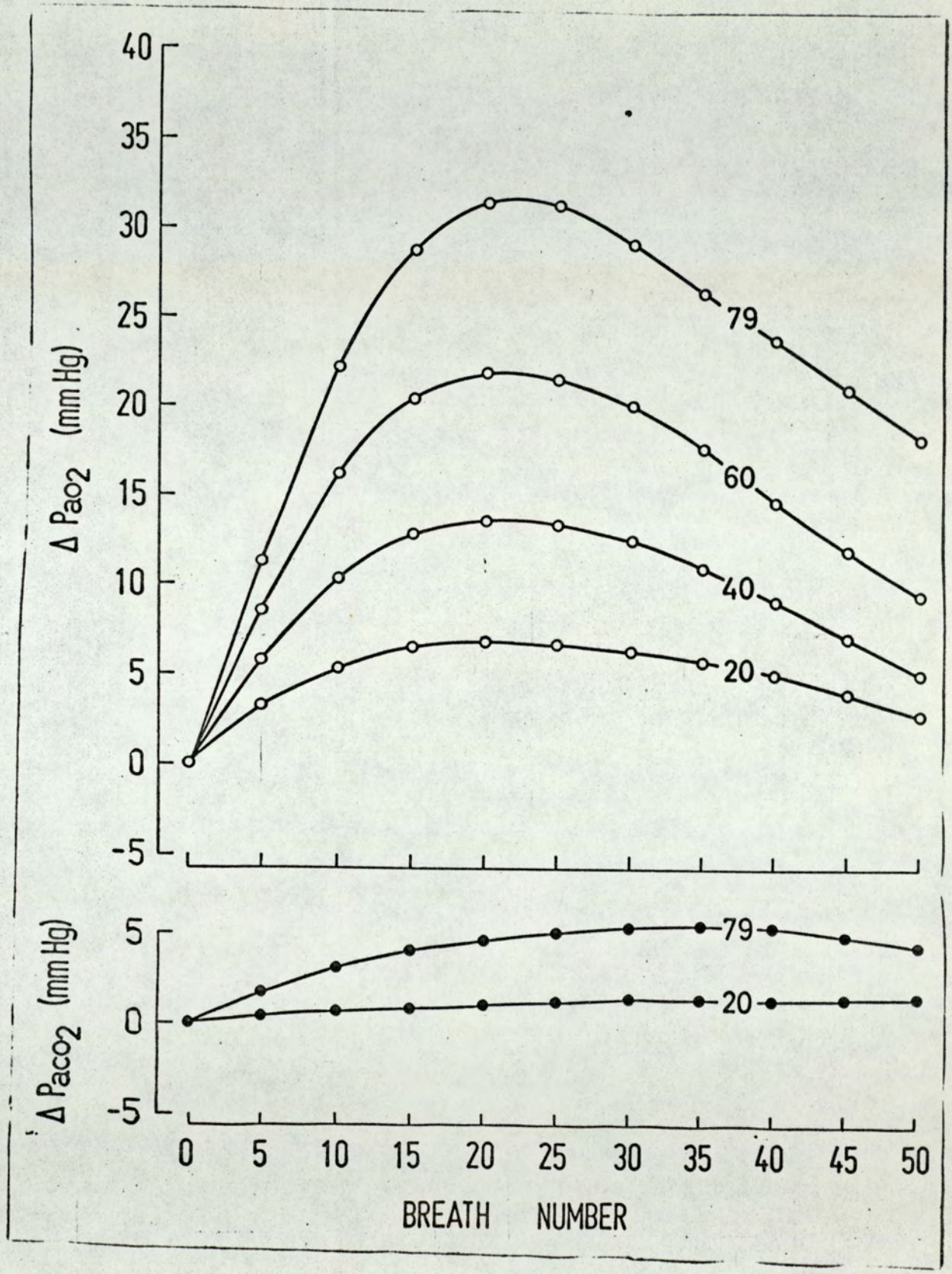
40
35
30
25
20
15
10
5
0
-5
Δ Pao2 (mm Hg)
79
60
40
20
5
0
-5
Δ Paco2 (mm Hg)
79
20
0
5
10
15
20
25
30
35
40
45
50
BREATH NUMBER

FIGURE 71

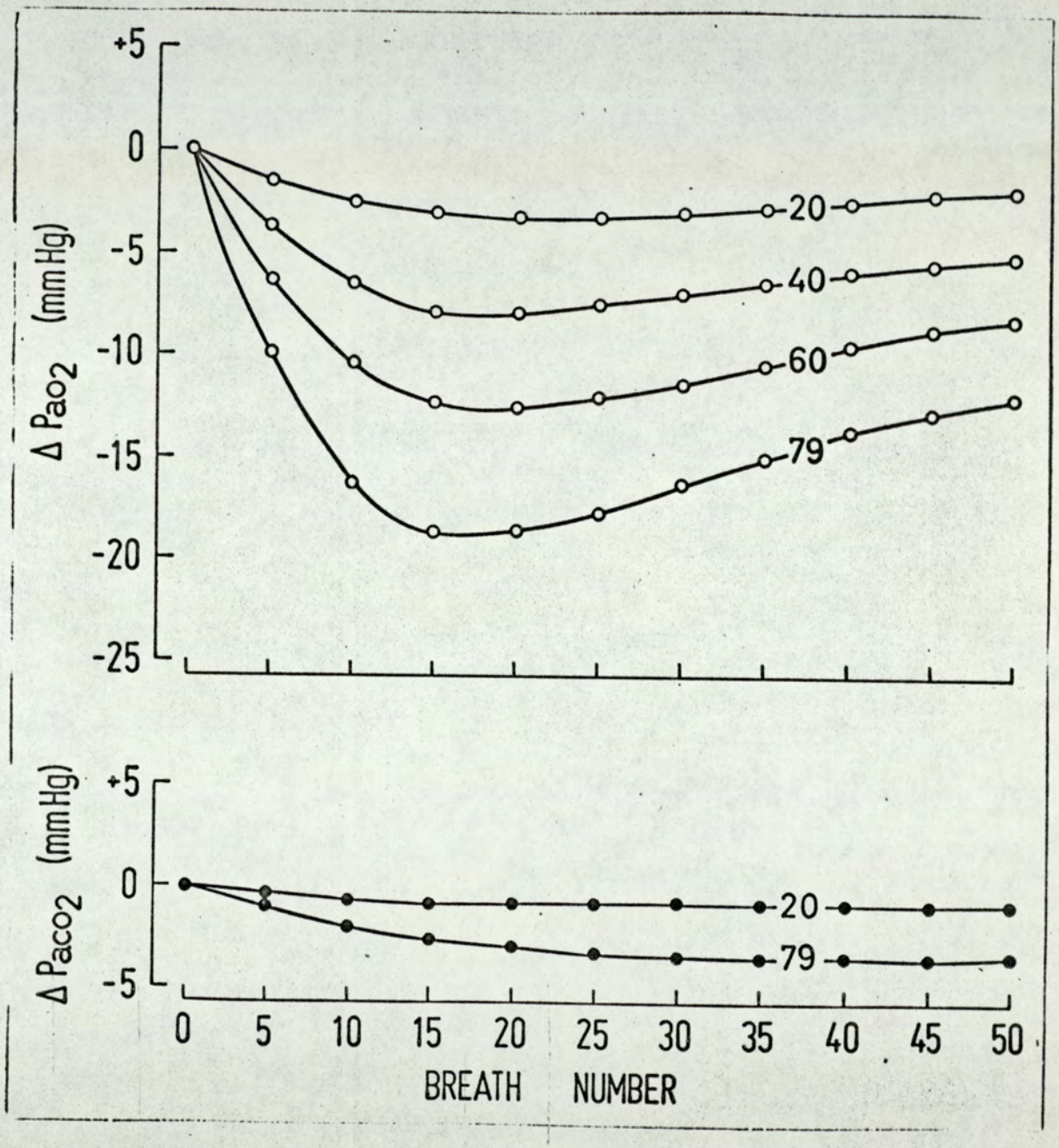
+5
0
-5
-10
-15
-20
-25
Δ Pao2 (mmHg)
20
40
60
79
+5
0
-5
Δ Paco2 (mmHg)
20
79
0
5
10
15
20
25
30
35
40
45
50
BREATH NUMBER

FIGURE 72

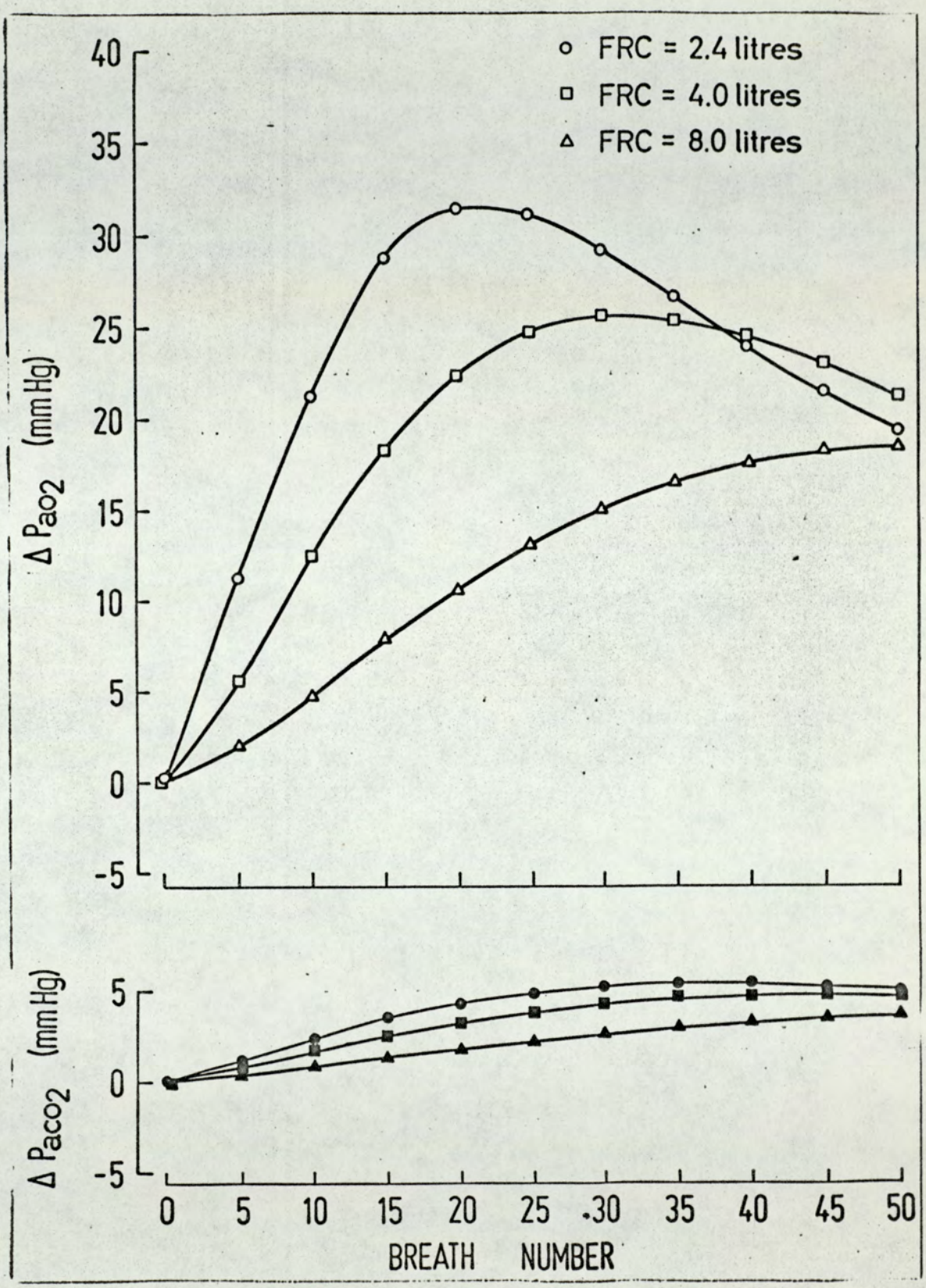
FRC = 2.4 litres
FRC = 4.0 litres
FRC = 8.0 litres
40
35
30
25
20
15
10
5
0
-5
Δ Pao2 (mmHg)
5
0
-5
Δ Paco2 (mmHg)
0
5
10
15
20
25
30
35
40
45
50
BREATH NUMBER

FIGURE 73

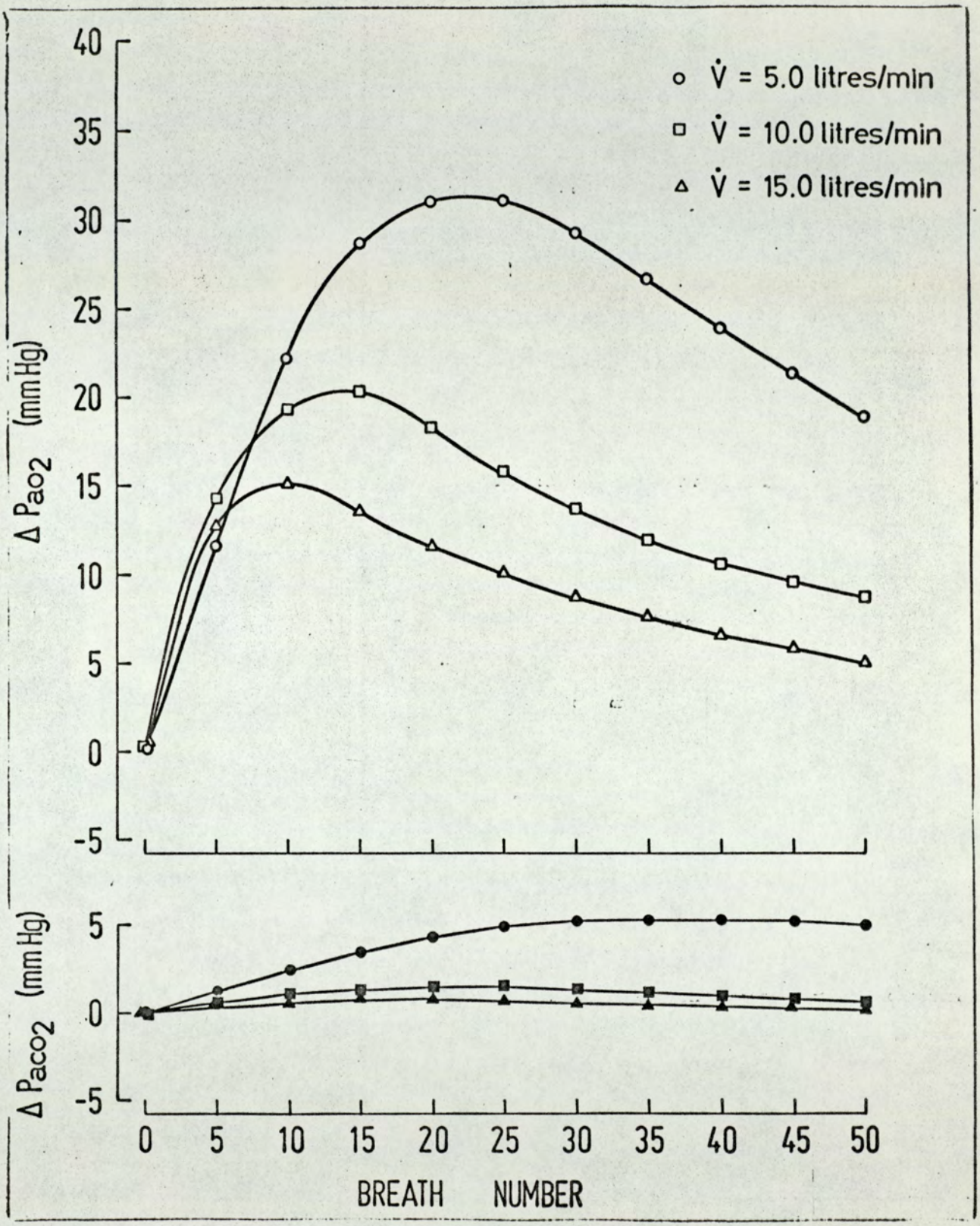
40
35
30
25
20
15
10
5
0
-5
Δ Pao2 (mmHg)
o V̇ = 5.0 litres/min
□ V̇ = 10.0 litres/min
△ V̇ = 15.0 litres/min
5
0
-5
Δ Paco2 (mmHg)
0 5 10 15 20 25 30 35 40 45 50
BREATH NUMBER

FIGURE 74

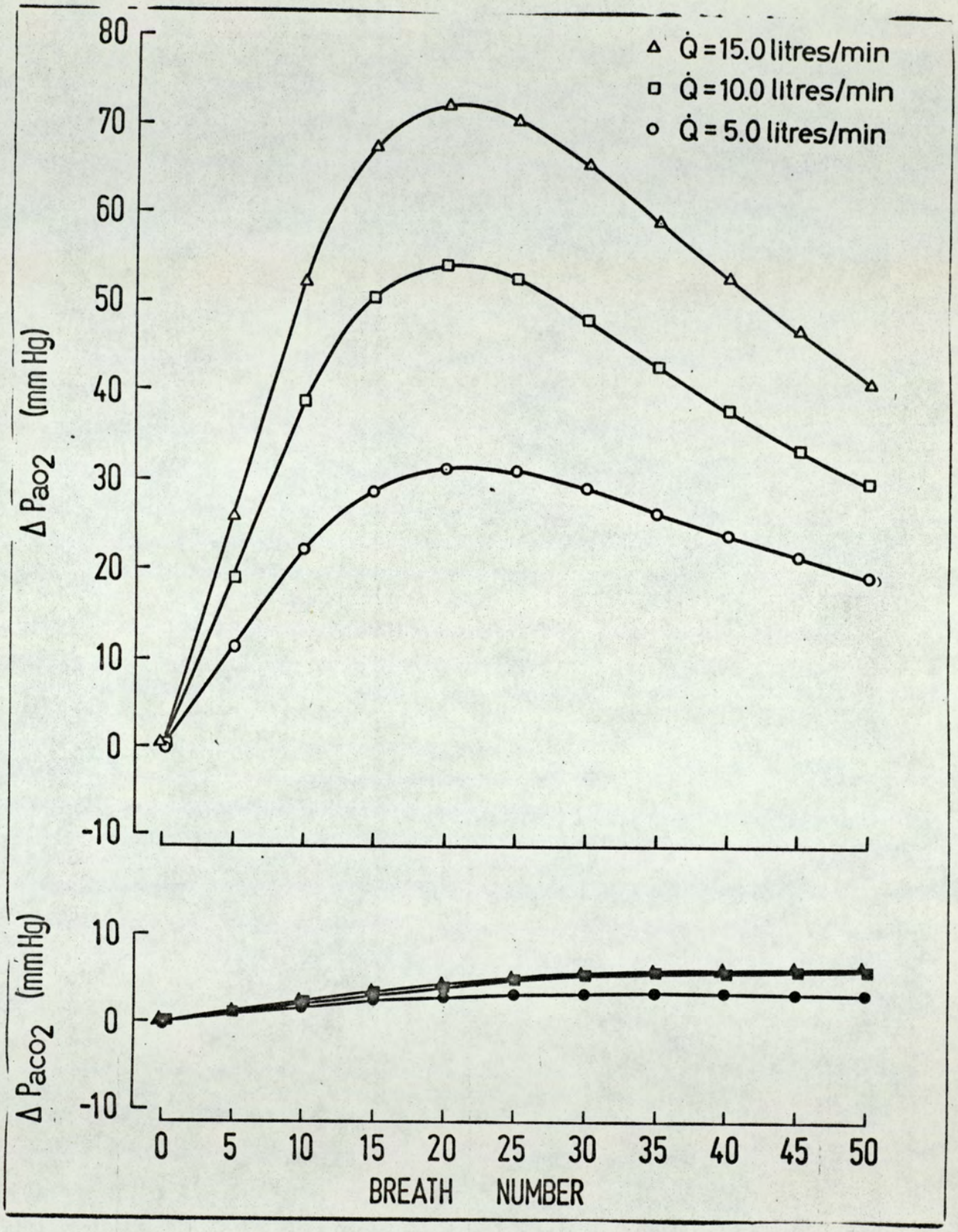
Q̇ = 15.0 litres/min
Q̇ = 10.0 litres/min
Q̇ = 5.0 litres/min
Δ Pao2 (mm Hg)
80
70
60
50
40
30
20
10
0
-10
Δ Paco2 (mm Hg)
10
0
-10
0
5
10
15
20
25
30
35
40
45
50
BREATH NUMBER

FIGURE 75

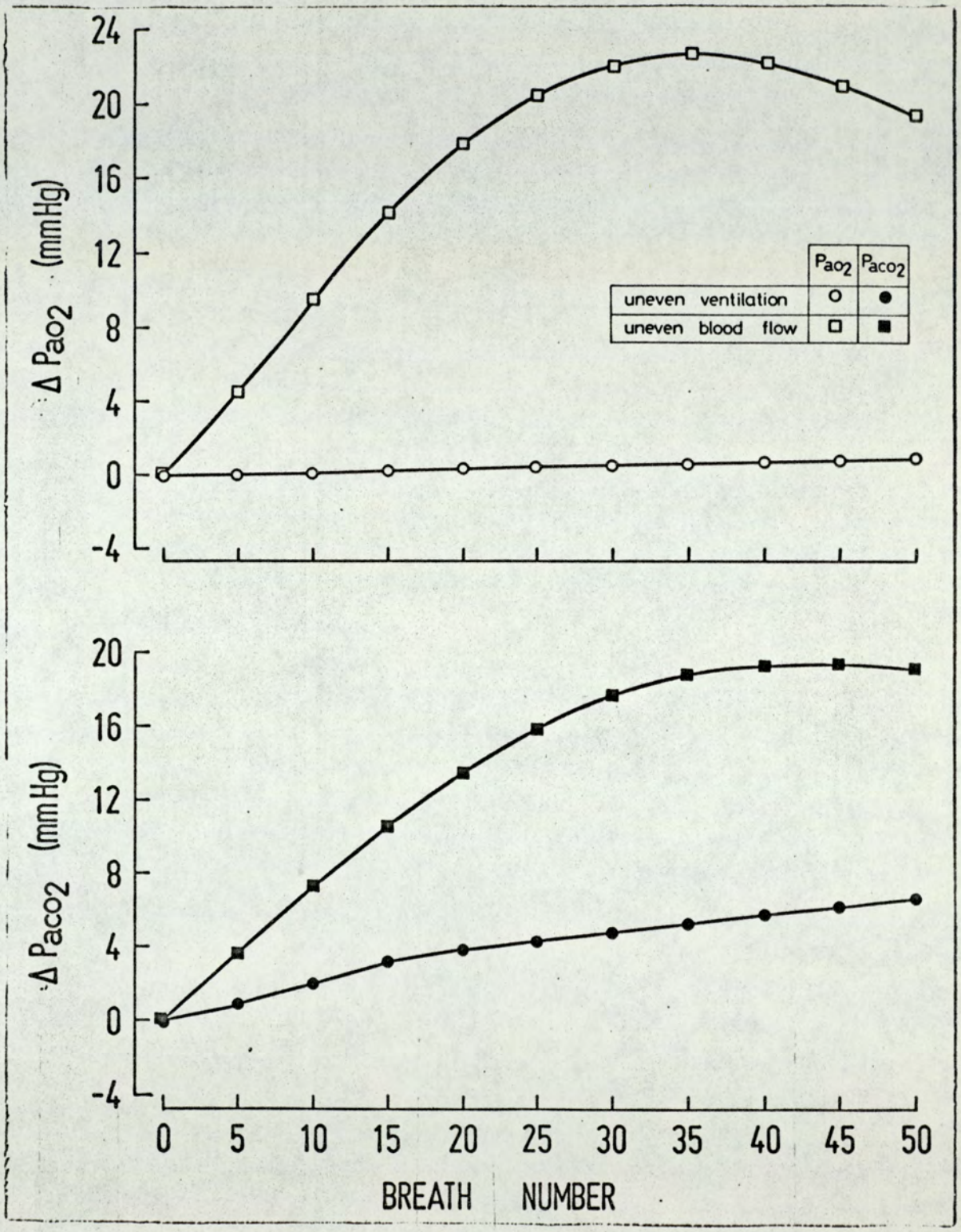
24
20
16
12
8
4
0
-4
Δ Pao2 (mmHg)
Pao2
Paco2
uneven ventilation
uneven blood flow
20
16
12
8
4
0
-4
Δ Paco2 (mmHg)
0
5
10
15
20
25
30
35
40
45
50
BREATH NUMBER

FIGURE 76

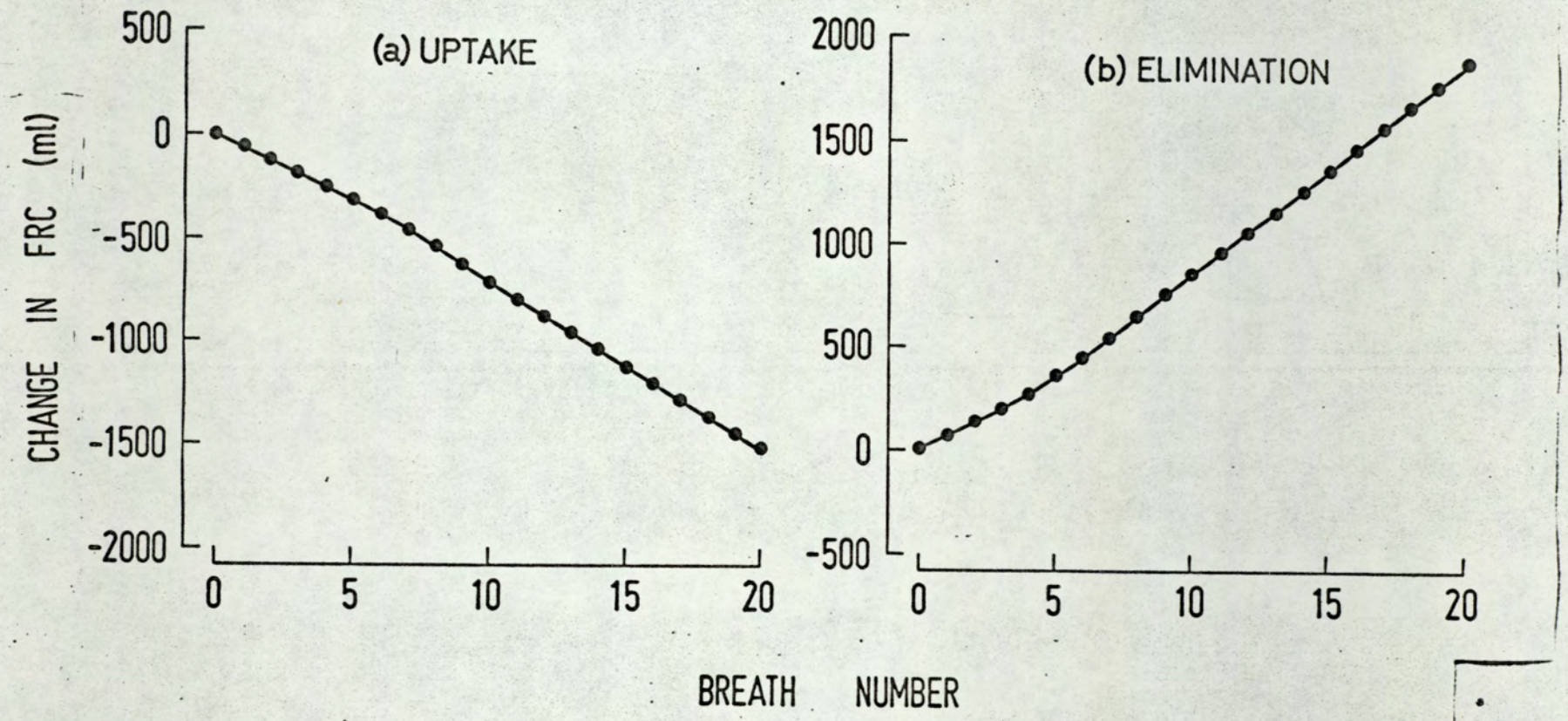
(a) UPTAKE
(b) ELIMINATION
CHANGE IN FRC (ml)
500
0
-500
-1000
-1500
-2000
2000
1500
1000
500
0
-500
0
5
10
15
20
BREATH NUMBER

FIGURE 77

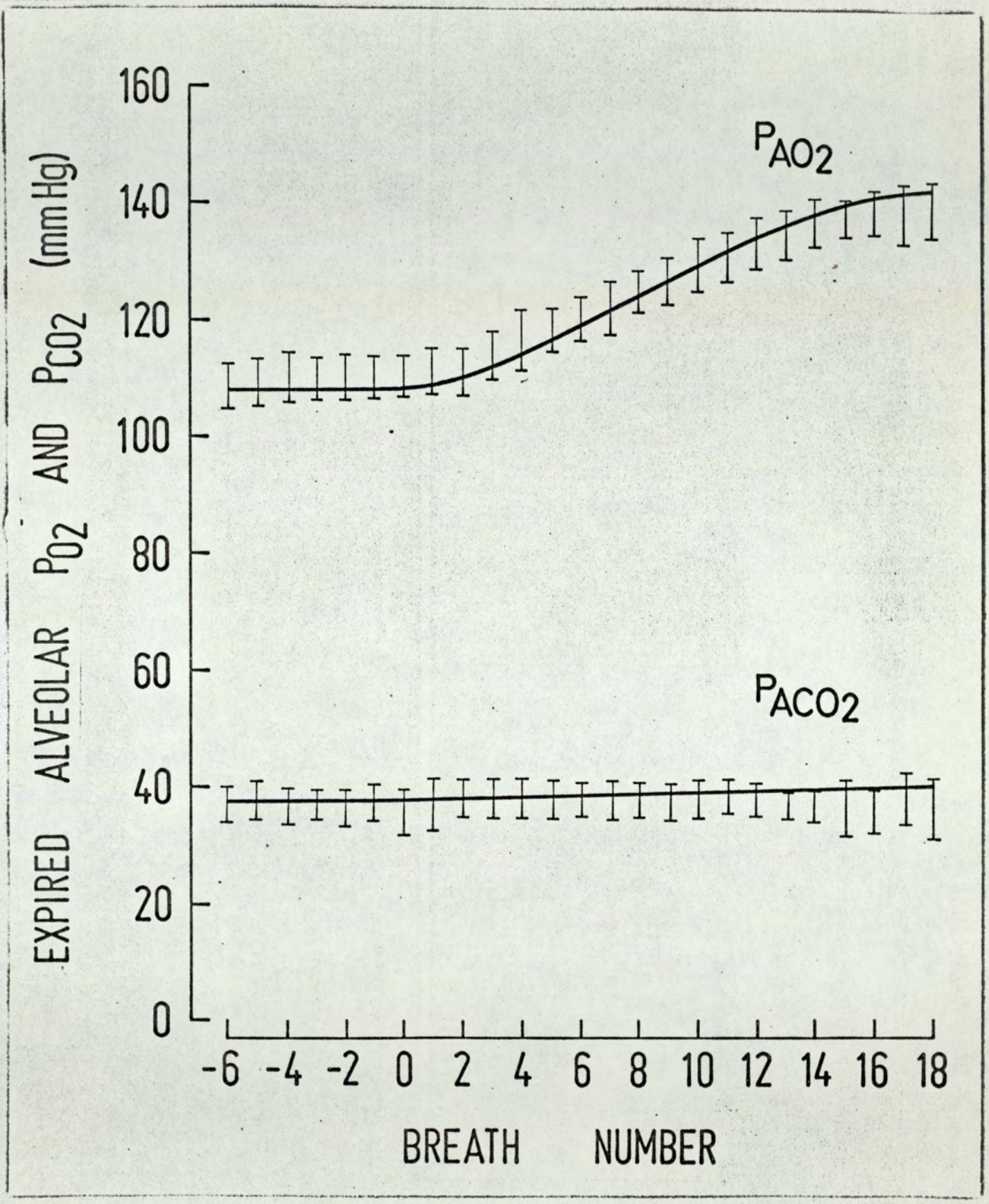
EXPIRED ALVEOLAR P_{O_2} AND P_{CO_2} (mm Hg)
160
140
120
100
80
60
40
20
0
P_{AO_2}
P_{ACO_2}
-6 -4 -2 0 2 4 6 8 10 12 14 16 18
BREATH NUMBER

FIGURE 78

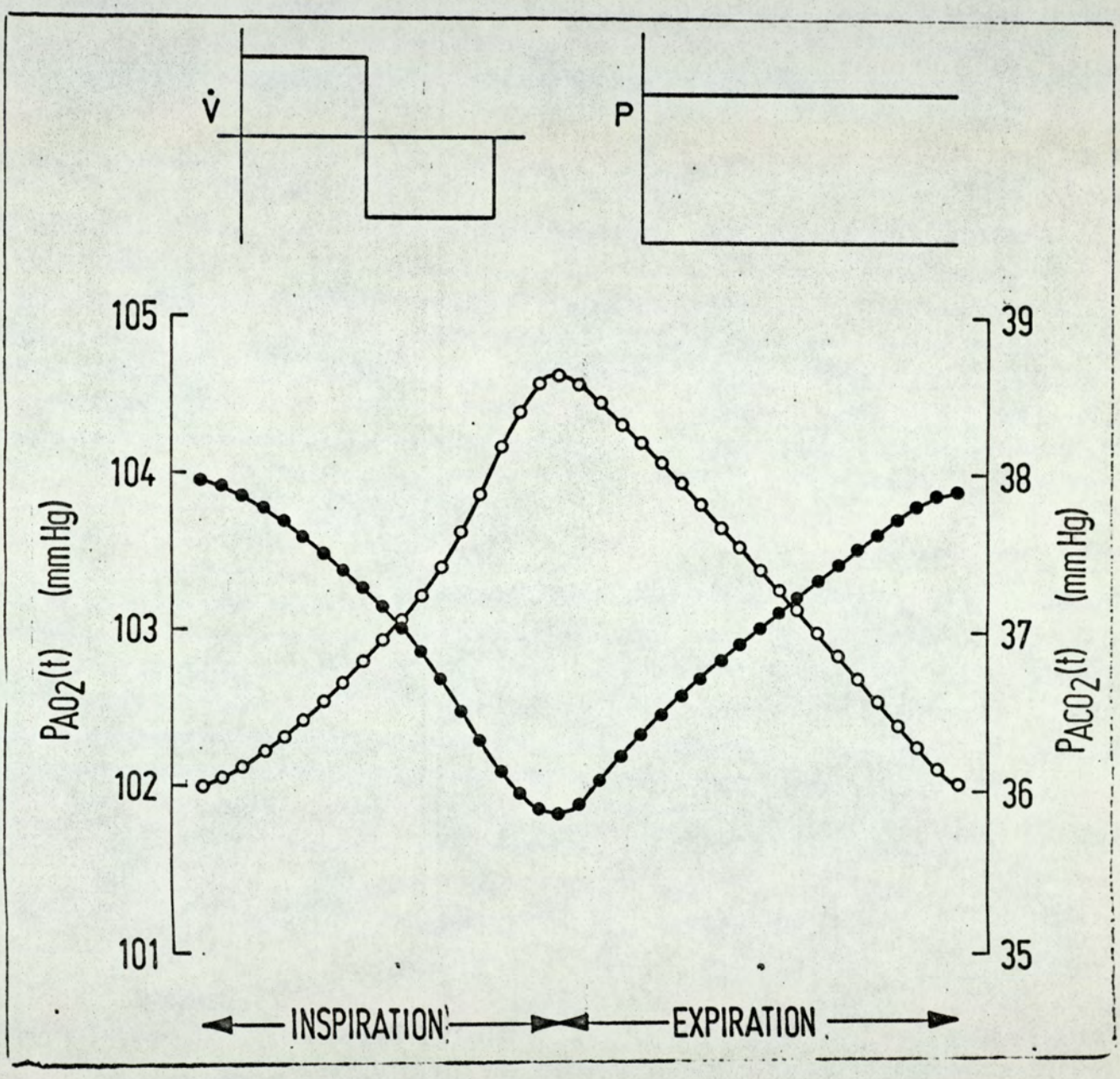
V̇
P
105
104
103
102
101
39
38
37
36
35
PAO2(t) (mm Hg)
PACO2(t) (mm Hg)
INSPIRATION
EXPIRATION

FIGURE 79